



UNIVERSITY OF
LEICESTER

**A Pre-Clinical Investigation of the Anti-Cancer Effects
of the Frankincense Constituent AKBA on Ovarian
Cancer Cells**

Thesis submitted for the degree of

Doctor of Philosophy

at the University of Leicester

by

Kamla Khalfan Said Al-Salmani BSc (Hons), MSc

Department of Cancer Studies

University of Leicester

2016

Abstract

A pre-clinical investigation of the anti-cancer effects of the frankincense constituent AKBA on ovarian cancer cells

This study examines the biologically active component of frankincense, 3-O-acetyl-11-keto- β -boswellic acid (AKBA), in ovarian cancer cells to evaluate its potential cytotoxicity towards high grade serous ovarian cancer and its potential ability to address the cancer's known resistance to cisplatin.

Ovarian cancer causes significant mortality, the five-year survival rate being very low compared to other cancers as most of the cases are diagnosed late, typically at stages IIIa-IIIc and IV. Most of these cases relapse and develop resistance to first line chemotherapy; therefore, new strategies are urgently needed to overcome resistance. Extracts from *Boswellia* sp., used for centuries as herbal medicine in Asia, have known anti-inflammatory properties and anti-cancer potential alone or in combination with other chemotherapies. The active ingredients of *Boswellia* sp., boswellic acids, have many effects on various cancer cells including induction of apoptosis.

In this study, several approaches and analyses were performed in examining the effect of AKBA on four ovarian cancer cell lines, including a cisplatin resistant line. These investigations included analysis of cell proliferation and viability, cell cycle distribution, apoptosis, DNA damage formation, production of reactive oxygen species and gene expression. The results obtained from this work suggest that AKBA induces apoptosis in ovarian cancer cell lines either directly through extrinsic and intrinsic pathways, or indirectly by affecting other cellular mechanisms such as inhibiting cell proliferation/viability, inducing DNA damage and decreasing production of reactive oxygen species. Furthermore, AKBA exposure alters the expression of multiple genes, potentially impacting on several cellular processes.

The key findings of this project are that AKBA is cytotoxic to ovarian cancer cells, at pharmacologically achievable concentrations. AKBA exposure also induces multiple gene expression changes that would impact on many different biological pathways in ovarian cancer cells including genes related to DNA damage and repair, cell cycle, cell metabolism, and cell adhesion and metastasis. Consequently, AKBA may form the basis of a novel anticancer treatment for ovarian cancer potentially alongside conventional therapy.

Acknowledgements

Firstly, I would like to express my thanks to the University of Leicester for accepting this project proposal for my PhD. I would like to express my gratitude to my supervisors, Prof George DD Jones, Dr Mark Evans and Dr Esther Moss for their guidance, advice, support, and encouragement during this project. I also thank Dr Raj Patel for his advice and support during this project and I thank Dr Salvador Macip for his help in using the flow cytometry machine.

I would like to thank my co-supervisor Dr Ikram Burney from Sultan Qaboos University for all his support throughout the project time.

My thanks also extends to our departmental postgraduate tutor Dr Don Jones for his support, encouragement and overseeing of this project and also to Dr Nicolas Sylvius of Nucleus Genomics, Genetics Department for running the microarray samples and for his assistance in analysing the results.

I would like to thank all the people in other laboratories who gave me help and who allowed me to use their facilities.

I am grateful to the Ministry of Health, Ministry of Higher Education and my colleagues and staff at the National genetic centre in Oman.

Lastly, huge thanks to my family, words cannot express how grateful I am to my parents, my in-laws for their support and encouragement.

Finally, I would like to acknowledge my deepest gratitude to my beloved husband and my children.

List of contents

Abstract	I
Acknowledgements.....	II
List of table's and figures	VII
List of Equations	X
List of Abbreviations:	XI
Chapter one	15
Thesis Introduction	15
1.1 Frankincense	16
1.1.1 Boswellic acids	18
1.1.2 Medicinal uses of Frankincense.....	20
1.1.3 Acetyl-11-keto-beta-boswellic acid (AKBA):.....	22
1.1.4 Cytotoxic properties of Boswellic acid and mainly AKBA:	23
1.1.5 Cell line studies and cytotoxicity.....	23
1.1.6 Metabolic activity of Boswellic acids and AKBA.....	30
1.2 Ovarian Cancer	31
1.2.1 Ovarian cancer subtype.....	33
1.2.2 Aetiology and Pathophysiology of Ovarian Cancer	33
1.2.3 Current treatment of ovarian cancer.	35
1.2.4 Ovarian cancer cell-lines for in vitro studies	37
1.2.4.1 A2780 and A2780cis	37
1.2.4.2 OVCAR-4	38
1.2.4.3 UWB1.289	39
1.3 DNA damage & repair	40
1.4 The Cell Cycle.	41
1.5 Aims and objectives.....	42
1.5.1 Hypothesis	43

Chapter 2	44
Materials and Methods.....	44
2. Materials and Methods:	45
2.1 Cell-lines for in vitro studies	45
2.2 Cell lines used in this research.....	45
2.4 Summary of the techniques/approach.....	46
2.5 Cell culture medium and supplements.....	46
2.6 Chemicals and Reagents	46
2.7 Kits and antibodies.....	47
2.8 Preparation of buffers and working reagents	48
2.8.1 The test compound AKBA	49
2.9 Cell culture.....	49
2.10 Cell Culture:.....	50
2.11 Methods	51
2.11.9 Gene expression	66
2.11.10 Quantitative-PCR (Q-PCR)	70
2.11.11 Statistical Analysis.....	73
Chapter 3	74
Investigations for the ability of AKBA to address cisplatin resistance in ovarian cancer cell lines.....	74
3.1 Introduction.....	75
3.1.1 Ovarian Cancer:	75
3.1.2 AKBA therapeutic effect in cisplatin resistant cell line	76
3.2 Results.....	78
3.2.1 The effect of AKBA on cell growth and proliferation.....	78
3.2.2 The effect of AKBA on the cell cycle	82
3.2.3 AKBA induces apoptosis.....	86

3.2.4 AKBA induces DNA damage and ROS generation	90
3.2.5 Proteins expression analysis by western blotting	94
3.3 Discussion	99
3.3.1 The effect of AKBA in A2780 and A2780cis	99
3.3.2 Protein expression in the ovarian cancer cell lines following AKBA treatment	100
3.3.3 The anti-ovarian cancer potential of AKBA	102
3.3.4 Concluding remarks	105
Chapter 4	106
Effect of AKBA on a known BRCA1 mutated ovarian cancer cell line and a high grade serous ovarian cancer cell line	106
4.1 Introduction.....	107
4.2 Results.....	110
4.2.1 AKBA effect in BRCA1 mutant ovarian cancer cells and OVCAR4 cells.....	110
4.3 Discussion.....	138
4.3.1 AKBA induces DNA damage in UWB1.289 cells	138
4.3.2 The effect of AKBA in OVCAR 4 cells	140
4.3.3 Anti-ovarian cancer potential of AKBA	141
4.3.4 Conclusion	143
Chapter 5	144
A preliminary examination for mechanisms of action and the genes involved in the actions of AKBA in ovarian cancer cell lines	144
5.1 Introduction:.....	145
5.2 Gene expression results	146
5.2.1 Gene functions and pathways:	147
5.2.2 Gene percentage of OVCAR 4 gene affected after AKBA treatments....	147

5.2.3 The Molecular function and the biological mechanism of the genes expression changes affected by AKBA exposure of OVCAR 4 cells	149
5.2.4 Apoptosis Pathway confirmation:.....	159
5.3 QPCR analysis	160
5.4 Discussion	165
5.4.1 Potential clinical applications from this research	167
5.4.2 Conclusion	168
Chapter 6	169
General Discussion and Thesis Summary	169
6.1 Discussion	170
6.1.1 AKBA as anticancer Therapy	172
6.1.2 Gene expression data	174
6.1.3 Cell proliferation.....	175
6.1.4 DNA damage and repair	176
6.1.5 Cell metabolism and DNA damage	176
6.1.6 Apoptosis	177
6.1.7 AKBA as potential anti-cancer agent	179
6.2 Summary of the results obtained in all cell lines	180
6.2.1 Method of choice to assess the effect of AKBA in ovarian cancer cell line	180
6.3 Conclusion	182
6.4 Future work.....	182
6.5 Thesis related work:.....	184
Appendix.....	185
Appendix.....	186
References.....	189

List of table's and figures

Figure 1. 1 Boswellia trees producing Omani Frankincense. Photograph taken by the candidate in the Dhofar region, Oman.....	16
Figure 1. 2 Different grads of Omani frankincense compared with Indian and Somalian frankincense.	18
Figure 1. 3 Chemical structures of 3-O-acetyl-11-keto- β -boswellic acid (AKBA).	19
Table 1. 1 Chemical structures of the major boswellic acids:	19
Figure 1. 4 Apoptotic pathways (intrinsic and extrinsic).....	24
Table 1. 2 Published anti-tumour activity of AKBA:	29
Figure 1. 5 Ovarian cancer statistics by age in Females 2012.....	32
Figure 1. 6 Ovarian cancer.....	35
Table 2. 1 The TargetAmp™- Nano Labeling Kit for Illumina® Expression BeadChip kit content:	48
Figure 2. 1 The principle of the AlamarBlue® Assay (Rampersad, 2012).	52
Figure 2. 2 Comet Assay procedure.....	54
Figure 2.3 The Olympus meta-system microscope.	57
Figure 2. 4 ROS production measured by BD FACSCanto™ II Flow Cytometer shows the shift in FITC gating in the + positive control.	58
Figure 2. 5 An illustration of the gating of each phase of the cell cycle.	60
Figure 2. 6 The plotted 4-quadrant gate.....	61
Figure 2. 7 Annexin V/PI apoptosis assay.....	61
Table 2. 2 Standard dilution scheme:.....	64
Table 2. 3 Summary of the composition of 12% SDS-PAGE gels:	65
Figure 2. 8 The cDNA synthetisationusing TargetAmp™-Nano Labeling Kit for Illumina® Expression BeadChip steps.	67
Figure 2. 9 The total RNA analysis in ng using Aglient 2100 bioanalyser. Nanoseries II.	68
Figure 2. 10 Direct Hybridization Assay Workflow from ILLUMINA Whole-Genome Gene Expression Direct Hybridization Assay Guide.....	69
Figure 2. 11 TaqMan® Gene Expression Cells-to-CT™ Procedure Overview	71
Figure 2. 12 TaqMan® Gene Expression Array plate work flow.	72
Table 2. 4 QPCR conditions for TaqMan® Array Plates run on QPCR 7300:	73
Figure 3.1. 1 Microscopic images of A2780 cell line cells exposed to AKBA.....	79
Figure 3.1. 2 AKBA-induced cell growth inhibition in A2780 & A2780cis.....	80

Figure 3.1. 3 AKBA induced cell growth inhibition in A2780 & A2780cis cells.....	81
Figure 3.2. 1 Immediate exposure with AKBA to assess cell cycle arrest in A2780 and A2780cis cells.....	83
Figure 3.2. 2 AKBA exposure for different time points, to assess cell cycle arrest in A2780 cells at a range of concentrations.	84
Figure 3.2. 3 AKBA exposure for different time points, to assess cell cycle arrest in A2780cis cells at a range of concentrations.....	85
Figure 3.3. 1 Immediate exposure with AKBA to assess cell death in A2780 and A2780cis cells.....	86
Figure 3.3. 2 AKBA exposure for different time points (6 h, 16 h, 24 h & 48 h) to assess cell death in A2780 cells at a range of concentrations.	88
Figure 3.3. 3 AKBA exposure for different time points (6 h, 16 h, 24 h & 48 h) to assess cell death in A2780cis cells at a range of concentrations.	89
Figure 3.4. 1 AKBA-induced DNA damage in A2780 and A2780cis cells for different time and at a range of concentrations.	91
Figure 3.4. 2 AKBA-induced ROS generation in A2780 and A2780cis cells for different time and at a range of concentrations.	92
Figure 3.4.2 AKBA-induced Double strand DNA damage using Gamma-H2AX Assay in A2780 and A2780cis cells.....	93
Figure 3.5. 1 Quantification of apoptotic protein expression in A2780 cells.....	95
Figure 3.5. 2 Quantification of apoptotic protein expression in A2780 cells.....	96
Figure 3.5. 3 Quantification of apoptotic protein expression in A2780cis.....	97
Figure 3.5. 4 Quantification of apoptotic protein expression in A2780cis.....	98
Figure 4.2. 1 Microscopic images of UWB1.289 cells exposed to AKBA.....	111
Figure 4.2. 2 Microscopic images of OVCAR-4 cells exposed to AKBA.....	113
Figure 4.2. 3 AKBA-induced cell growth inhibition in UWB 1.289 and OVCAR 4 cells at different concentrations over time.	115
Figure 4.2. 4 AKBA-induced cell growth inhibition in UWB 1.289 and OVCAR4 cells using different concentrations over time.	116
Figure 4.2. 5 AKBA-induced cell growth inhibition after 24 hours in UWB 1.289 (IC ₅₀ = 20.07) and OVCAR4 (IC ₅₀ = 17.80).	117
Table 4. 1 cell growth inhibition IC ₅₀ after 24 hours of treatment.....	117

Figure 4.2.6 AKBA-induced cell growth inhibition after 24 hours in A2780 (IC50= 21.78), A2780cis (IC50= 18.58), UWB 1.289 (IC50 = 20.07) and OVCAR4 (IC50 = 17.80).....	118
Figure 4.3. 1 Effect of AKBA on cell cycle of UWB1.289 cells.	120
Figure 4.3. 2 Effect of AKBA on cell death of UWB1.289 cells using Annexin V/PI. Effect of AKBA	124
Figure 4.3. 3Effect of AKBA on cell cycle of OVCAR4 cells.....	126
Figure 4.3. 4 Effect of AKBA on cell death of OVCAR4 using Annexin V/PI.....	129
Figure 4.4. 1 AKBA-induced DNA damage in UWB1.289 and OVCAR4.	130
Figure 4.4. 2 AKBA-induced DNA double strand breaks presented by the number of foci per cell in Both UWB1.289 and OVCAR4 cells.	131
Figure 4.4. 3 ROS generation in UWB1.289 and OVCAR4 cell lines after treatment with AKBA.....	132
Figure 4.4. 4 Quantification of apoptotic protein expression in UWB 1.289 cells.	134
Figure 4.4. 5 Quantification of apoptotic protein expression in UWB 1.289 cells.	135
Figure 4.4.6 Quantification of apoptotic protein expression in OVCAR4 cells.....	136
Figure 4.4.7 Quantification of apoptotic protein expression in OVCAR4 cells.....	137
Figure 5.2. 1 Affected genes percentage of OVCAR4 cell lines gene expression (described in table 5.2.3).....	148
Table 5.2. 1Number of genes affected by 50 μ M of AKBA in different molecular functions and biological process of OVCAR 4 cells after 6 h of exposure.....	149
Figure 5.2.2 Molecular function classifications determined by gene ontology analysis.	150
Figure 5.2. 3 Biological processes classification as determined by gene ontology analysis.....	151
Table 5.2. 2Total number of Genes up regulated and down regulated as determined using array track.....	151
Table 5.2. 3 6h treatments with AKBA using a cut off p value of <0.05 and fold change of >1.8.....	152
Table 5.2. 4 16h treatments with AKBA using cut off p value of< 0.05 and fold change of 1.8	153
Table 5.2. 5 24h treatments with AKBA using cut off p value of <0.05 and fold change of 1.8	154
Table 5.2. 6 The most common genes affected after filtering.	155

Figure 5.2. 4 Effect of AKBA on pathways impacting on apoptosis.	156
Figure 5.2. 5 Apoptotic genes affected by AKBA treatments from the microarray analysis.....	158
Table 5.3. 1 QPCR Assay plate.	160
Figure 5.3.1 Quantitative real time PCR Amplification Plot results using the Applied Biosystems 7300 Q PCR System.....	160
Figure 5.3. 2(A-F) Apoptotic genes expression in OVCAR4 cell lines.	162
Figure 5.3.3 The most common apoptotic genes affected in OVCAR4 cells.....	163
Figure 5.3.4 Apoptotic pathways in OVCAR4 cell lines affected byAKBA.	164
Figure 7. 1 RNA concentrations and purity for the control samples 1&2 using Nano DE 72901367	186
Figure 7. 2 RNA concentrations and purity for the 6 h treatment with 25 μ M samples 1&2 using Nano DE 72901367.....	187
Figure 7. 3 Gel image with Total RNA concentrations using Nano DE 72901367	188
Figure 7. 4 Gel image with Total RNA concentrations using Nano DE 72901367	188

List of equations

Equation 2. 1 Cell counting formula.....	51
Equation 2. 2 The mathematical formula for the calculation of % tail DNA damage using the comet assay scoring software.....	55
Equation 2. 3 Formula for calculating DNA concentration.	71

List of Abbreviations

AD	Latin phrase anno domini means “in the year of our Lord” (1 ST Century)
AEB	Alkaline electrophoresis buffer
AKT1\2	Alpha serine/threonine-protein kinase
ALS	Alkali labile sites
ATF3	Activating Transcription Factor 3
ATP	Adenosine triphosphate
BAK	BCL2 Antagonist/Killer
BAX	BCL2-associated X protein
BCL2	B-cell CLL/lymphoma 2
BER	Base excision repair
BRCA1&2	Breast cancer 1&2
BRAF	Serine/threonine protein kinase B-raf
BSA	Bovine serum albumin
Caspase	Cysteine aspartic acid-specific protease
CCD	Charge-coupled device camera
CCNE1	Cyclin E1
CD133	PROM1 gene (member of pentaspan trans membrane glycoproteins)
CDKN1A	Cyclin-dependent kinase inhibitor 1A (p21)
Cdks	Cyclin-dependant kinases
cDNA	Complementary deoxyribonucleic acid
cRNA	Complementary ribonucleic acid
Ct	Cycle Threshold
CXCR4	Protein Coding gene (C-X-C Motif Chemokine Receptor 4)
DCFHDA	2',7'-Dichlorofluorescin
DDIT3	DNA Damage Inducible Transcript 3
DMEM	Dulbecco's Modified Eagle Medium
DMSO	Dimethyl sulfoxide
DNA	Deoxyribonucleic acid
DR5	Death receptor 5
DSBs	Double strand breaks

DUTP	Deoxyuridine 5-triphosphate
EDTA	Ethylenediaminetetraacetic acid
ERCC1	Excision Repair Cross-Complementing (Excision Repair 1) gene
Erk-1/2	Extracellular Signal-Regulated Kinase 1\2
ETO	Etoposide
Fas	TNF receptor superfamily, member 6
FC	Fold change
FCS	Fetal calf serum
FDA	Food and Drug Administration
FITC	Fluorescein-5-isothiocyanate
FL2-A	Area of the fluorescence peak
FL2-W	Width of the fluorescence peak
FSC	Forward-angle light scatter
Gadd45A	Growth arrest and DNA-damage-inducible alpha
G0 phase	Quiescent or Gap phase 0
G1 Phase	Gap 1 phase
G2 phase	Gap 2 phase
GO	Gene ontology
h	Hour
H2O2	Hydrogen peroxide
HR	Homologous recombination repair
IGF-IR	Insulin Like Growth Factor 1 Receptor
kDa	Kilodaltons
LMA	LMA Low-melting-point agarose
5-LO	5-lipoxygenase
MFI	Mean Fluorescence Intensity
mg	Milligram
min	Minute
mL	Millilitre
mm	Millimetre
MMR	Mismatch repair
M phase	Mitosis phase

mRNA	Messenger ribonucleic acid
MS	Methylated Sprit
MTT assay	[3-(4,5-dimethylthiazol-2-yl)-2,5-diphenyltetrazolium bromide]
NADPH	Nicotinamide Adenine Dinucleotide Phosphate-oxidase
NACT	Neoadjuvant chemotherapy
NER	Nucleotide excision repair
NF-κB	Nuclear factor kappaB
NRU	Neutral red uptake (NRU) assay
ng	Nanogram
nm	Nanometer
PBS	Phosphate buffered saline
PCR	Polymerase chain reaction
PHH3	Mitosis-Specific Antibody Anti-Phosphohistone-H3
PI	Propidium iodide
PI3K	Phosphatidylinositol 3-kinase
poly(dT)	Polydeoxythymidylic acid oligonucleotide
PS	Phospholipid phosphatidylserine
PVDF	Immobilon®-P transfer membrane
QRT-PCR	Quantitative reverse transcription PCR
ROS	Reactive oxygen species
RNase	Ribonuclease
rpm	Revolutions per minute
RPMI	Roswell Park Memorial Institute medium
S	Seconds
SD	Standard deviation
SEM	Standard error of the mean
siRNAs	Small interfering RNAs
S phase	Synthesis phase
SSB	Single strand break
SSC	Side-angle light scatter
SDS-PAGE	SDS-polyacrylamide gel electrophoresis
TNF	Tumour necrosis factor
T-RNA	Total ribonucleic acid

TUNEL	Terminal deoxyribonucleotidyl transferase (TDT)-mediated dUTP-digoxigenin nick end labeling assay
U	Unit
μg	Microgram
μL	Microliter
μM	Micromolar
VEGF	Vascular endothelial growth factor
v/v	Volume/volume
WHO	World health organization
w/v	Weight/volume

Chapter one

Thesis Introduction

1.1 Frankincense

Frankincense is the gum resin produced by trees of the *Boswellia* species. The genus *Boswellia* comprises at least 25 species, including *B. serrata*, *B. carterii*, *B. frereana*, *B. papyrifera* and *B. socotrana* (Frank and Unger, 2006, Henkel, 2011). Trees of the *Boswellia* species are typically 5-10 meters in height and have small dark leaves (Fig 1.1). *Boswellia* trees vary in size, shape and type, depending on the pH of growing soil (with the optimal pH being between 7.9& 8.5) and climate, and start producing frankincense at the age of 5-10 years. These trees require a high temperature to grow with specific humidity (80 to 90 %) in order to produce good quality frankincense. Oman has been known for many years as a major producer of high grade frankincense (Al-Salmi, 2006). Frankincense was one of the most important commercial products of Middle Eastern countries and it has been used in different cultures and religions for different purposes but the highest grade of frankincense is produced in southern Oman (Dhofar) and in Yemen.



Figure 1. 1 *Boswellia* trees producing Omani Frankincense. Photograph taken by the candidate in the Dhofar region, Oman.

The earliest use of frankincense dates back to the Egyptian Queen Hathsepsut from the 15th century BC who favoured the use of the aromatic extract for her personal care (Badria, 2015). Early Egyptian uses of frankincense also range from use in incense for religious rituals and ceremonies, embalming, mummification and for beautification. (Dharmananda, 2003, Grieve, 2014, Badria, 2015). The use of frankincense spread throughout the Middle East and was used by the Assyrians, Romans, Babylonians and the Greeks (Badria, 2015). Frankincense was so prized for many years that it was considered a gift worthy of Kings. According to academic researchers, frankincense was originally grown in the Arabian Peninsula (Evershed et al., 1997, Dharmananda, 2003, Cotton, 2014) as documented by Herodotus in the 5th century BC, however the Old Testament includes a scripture reference to frankincense in Exodus 30:34, written in approximately 1440 BC (DeCanio, 2012).

Frankincense is harvested 2 to 3 times/year, from May through to September, via incisions made in the tree trunk following a specific procedure using a specific knife. Firstly, the hard cover of the trunk is cut to allow the milky, sticky fluid to follow out of the trunk of the tree (Al-Salmi, 2006). Secondly, after three to five days, the accumulated frankincense is collected and new cuts created in the trunk. Next, 2 weeks after the second step, the farmers create deeper cuts which allows the gum resin to bleed out of the trunk till the harvesting ends (Al-Salmi, 2006). The frankincense is categorized according to colour and purity (Fig 1.2); Grade 1 is white with a mild greenish colour and is considered the highest quality; it is known as 'luban thaker' and is used mostly for treatments (Al-Salmi, 2006). Grade 2 is yellow/white and highly aromatic and is called 'Al hogery'; it is also considered a high quality. Grade 3, called 'Al-najdi', is a yellow/slightly brownish colour and may contain some tree bark and is considered to be of a good quality (Al-Salmi, 2006). Finally grade 4, which is more of a yellow/dark brown colour contains a lot of tree bark and this used primarily for fumigation including the killing of mosquitos and flies (Badria, 2015, Gebrehiwot et al., 2003). The poorer quality of Grade 3 frankincense, coupled with its finer texture and low price means this grade is used predominantly to make highly volatile frankincense oil (Badria, 2015).

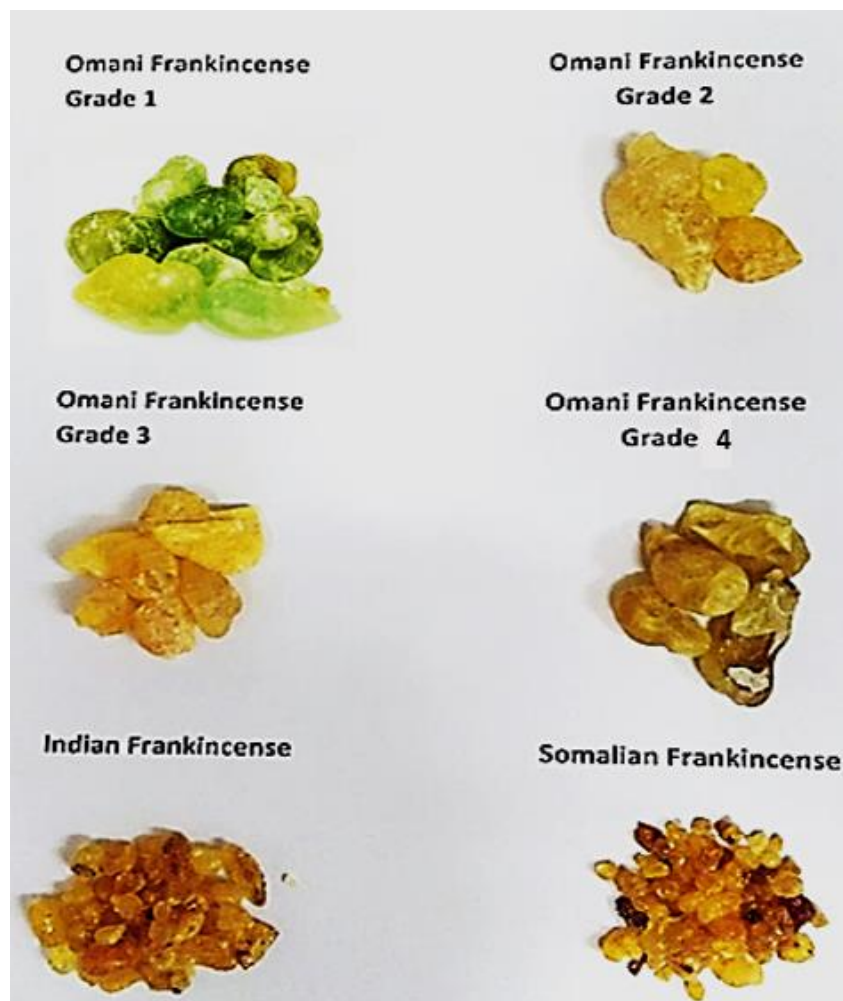


Figure 1. 2 Different grads of Omani frankincense compared with Indian and Somalian frankincense.

1.1.1 Boswellic acids

Frankincense has been used for centuries to treat a variety of chronic inflammatory diseases (Frank et al., 2009). The major constituents of the gum resin are a volatile oil, mucous and a lipophilic fraction containing triterpenes compounds present as di-, tetra- and pentacyclic triterpenes (Bücheler and Simmet, 2003). Boswellic acids in the gum resin are the most active components and they have the molecular formula $C_{32}H_{52}O_4$. They make up the majority of pentacyclic triterpenes (Bücheler et al., 2003), although the relative concentrations of individual boswellic acids vary depending on the species of *Boswellia*. Boswellic acids can exist in either acetyl-alpha-boswellic acid or acetyl-beta-boswellic acid depending on the position of the C-19 and C-20 methyl groups. Most boswellic acids are present in the β -configurations (e.g. β -boswellic acid (β -BA), 11-keto- β -boswellic acid (KBA), 3-O-acetyl- β -boswellic acid (ABA) and 3-O-acetyl-11-keto- β -boswellic acid

(AKBA) and further classification can be performed based on the presence or absence of a ketone group (RCOR') on C-11 and an acetoxy group on C-3 (Fig 1.3).

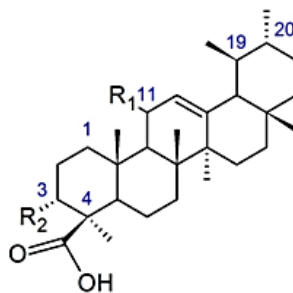


Figure 1. 3 Chemical structures of 3-O-acetyl-11-keto-β-boswellic acid (AKBA).

Table 1. 1 Chemical structures of the major boswellic acids:

R ₁	R ₂	Name
-H	-OH	β-boswellic acid (β-BA)
=O		11-keto-β-boswellic acid (KBA)
-H		3-O-acetyl-β-boswellic acid (ABA)
=O		3-O-acetyl-11-keto-β-boswellic acid (AKBA)

Boswellic acid types are classified by their R₁ and R₂ groups, Boswellic acids exist in α- and β-configurations, depending on the position of two methyl groups on C-19 and C-20 the β-configuration, as described in the table (1.1).

Boswellic acids are thought to be responsible for the anti-inflammatory effects of Boswellia extracts (Safayhi and Sailer, 1997), an effect demonstrated by Singh and Atal (1986) in rat and mouse models. These important experiments revealed that a mixture of boswellic acids led to a 25-46% inhibition of paw oedema in rodents and a 45-67% decrease in arthritic effect. Furthermore, oral Boswellic acids did not manifest any toxic effects in mice and rats (LD₅₀ greater than 2 g/kg) and did not cause the formation of ulcers (Singh and Atal, 1986). Boswellic acids are the primary bioactive compounds in frankincense which block leukotriene biosynthesis via inhibition of 5-lipoxygenase and exert potent anti-inflammatory effects in various pathologies (Sailer et al., 1996). Apart from the immunosuppressive activity of boswellic acids, several studies have reported that boswellic acids activate pro-apoptotic as well as anti-proliferative activity

against malignant cells (Glaser et al., 1999). The anti-proliferative action of different pentacyclic triterpenes has been previously demonstrated and some lipoxygenase (LO) inhibitors have been shown to induce cell death in various cell types (Hoernlein et al., 1999a).

1.1.2 Medicinal uses of Frankincense

Whilst many herbs have contraindications, Badria reports that frankincense is one of the safest herbs with only negligible toxicity when used in large amounts (400 mg) (Badria., 2015). The earliest medicinal uses of frankincense date back to ancient texts as recorded by Pliny the Elder in the 1st century AD as an effective antidote for hemlock poisoning and as recorded by the 10th century physician Avicenna as a cure for tumours, gastrointestinal distress and fever (Badria, 2015). Historically, frankincense derived from *B. carterii* was used extensively throughout China for virtually all illnesses and in traditional Indian (Ayurvedic) medicine frankincense is documented as effective for the treatment of illnesses including but not limited to: chronic lung diseases, diarrhoea, dysentery, pulmonary diseases, menorrhoea, dysmenorrhoea, syphilis, piles, liver disorders, gonorrhoea and ulcers (Badria, 2015). Cotton (2014) highlights frankincense as possessing a psychoactive molecule, incensole acetate, which behaves as a TRPV3 channel agonist, which suggests frankincense may be beneficial in the treatment of depression, whereas Grieve (2014) suggests frankincense is a stimulant.

More recently, boswellic acids have proven themselves to be effective treatment options for a variety of illnesses and diseases. For example, in 2003 Badria and co-workers demonstrated hepato-protective effects of boswellic acids from *B. carterii* when coupled with glycyrrhizin in rats presenting with liver injury (Badria et al., 2003a). Another study demonstrated reduced herpes activity in using purified compounds of boswellic acid (Badria et al., 2003b) whereas another group demonstrated boswellic acids strong effectivities as an immune system modulator (Mikhaeil et al., 2003). Similarly, boswellic acids extracted from gum resin have demonstrated efficacy in studies of inflammatory bowel disease (Badria, 2015, Sayed and El Sayed, 2016), demonstrating enhanced benefits with significantly less risk to the patient than the prescription drug mesalazine (Gerhardt et al., 2001). In a randomised trial of 44 patients with brain cancer receiving radiation treatment, AKBA demonstrated a reduction of greater than 75% in cerebral oedema in upwards of 60% of the intervention group suggesting AKBA is a safe alternative to steroid pharmaceuticals (Kirste et al., 2011). Further, Huan et al (2000)

reports β -boswellic acids as being effective as both anti-hyperlipidemic and anti-tumour agents, whereas Mikhaeil et al (2003) determined boswellic acids in frankincense oil to foster upwards of 90% lymphocyte transformation to lymphoblast's, thus suggesting boswellic acid offers enhanced immunological protection through the oil's immune stimulant properties.

The primary anti-inflammatory effect is due to the 5-lipoxygenase (5-LO) inhibitory activity of the boswellic acids (Frank et al., 2006), with AKBA being the most effective inhibitor, with an IC₅₀ value of 1.2 μ M; Lalithakumari et al. also suggest a similar value of 1.5 μ M (Lalithakumari et al., 2006). Further, research using liquid chromatography-electrospray ionisation-mass spectrometry/mass spectrometry (LC-ESI-MS/MS) identified AKBA as an inhibitory agent of several CYP enzymes (1A2, 2C8, 2C9, 2C19, 2D6 and 3A4) (Frank et al., 2006) whilst Siemoneit and co-workers determined the anti-inflammatory properties of boswellic acids and their ability to inhibit microsomal prostaglandin E₂ synthase-1 (Siemoneit et al., 2011).

When boswellic acids were combined with curcumin, significant improvements (reduced oedema, musculoskeletal pain and tenderness) was found in 50 patients with osteoarthritis of the knee, this study also demonstrated superior efficacy in treating osteoarthritic symptoms with both boswellic acid and curcumin compared to 50 mg of diclofenac when followed up at three to seven weeks post-treatment (F. et al., 2004). Additionally, the boswellic acid/curcumin combination negated the negative side effects evidenced in the control group treated with diclofenace. Another study also conducted a randomised controlled trial on the effectiveness of boswellic acid on osteoarthritis of the knee and determined that the use of this combination significantly reduced joint swelling and pain, whilst increasing flexibility and the ability to walk; however, radiographic imaging demonstrated no change in disease progression (Kimmatkar, 2003).

Boswellic acid has also been demonstrated as being effective against bronchial asthma. For instance, in a double-blind study, the incidence of asthmatic attacks was reduced during the six-week trial to 0.3 attacks/week in the intervention group compared to an average 1.2 attacks/week in the control group (Gupta et al., 1998). Furthermore, when examining the leukotriene inhibitory effect of boswellic acids, Badria et al (2004) identified increases in both total lung capacity using forced expiratory volume in 1 second (FEV₁), and performance compared to those receiving a placebo, leading researchers to believe that the anti-inflammatory effect of boswellic acids is a result of additional mechanisms of action, not solely isolated to the inhibition of leukotriene synthesis.

In a randomised controlled trial by Madisch et al (2007), 26 patients diagnosed with collagenous colitis were treated either with a placebo (control group) or with a *B. serrata* extract (which contains boswellic acids and other boswellia compounds). Following a six-week treatment protocol, those in the *B. serrata* intervention group were more likely to achieve complete remission of their disorder (Madisch et al., 2007). This is consistent with findings from Kiela et al (2005) who conducted similar research on chemically-induced colitis in mice. However, additional assessments, including quality of life and histo-pathological examination of collagen thickness, showed that there were no statistically significant differences in either of these factors between the placebo and the *B. serrata* extract intervention group (Madisch et al., 2007). Anthoni et al (2006) also determined that a semi-synthetic version of AKBA, AKBA, is also an effective anti-inflammatory agent for successfully mitigating the inflammatory effects of colitis.

Although there is significant literature identifying the medicinal benefits of boswellic acids, and in particular AKBA, a systematic review conducted by Ernst (2008) of the seven randomised controlled trials from India using oral administration of boswellic extracts for treating asthma, osteoarthritis, rheumatoid arthritis, Crohn's disease and collagenous colitis yielded only "suggestive" rather than "compelling" results, probably due to the limitations of sample size (the largest trial of the seven had a maximum sample size of 102 patients).

Although frankincense offers a wide variety of health benefits, less commonly known is the effective pest control properties of frankincense. For example, when the oil is ignited a variety of flying insects, including mosquitoes, are naturally repelled, thereby reducing the threat of malaria (Richardson and Dorr, 2015). Additionally, in medieval times, frankincense was used as a fumigant in religious ceremonies and churches (Hamidpour et al., 2013, Crow, 2004).

1.1.3 Acetyl-11-keto-beta-boswellic acid (AKBA):

Acetyl-11-keto- β -boswellic acid (AKBA) is a pentacyclic triterpene that inhibits 5-LO and its potential antitumor effects have been studied in detail. Importantly, AKBA has been investigated in models of gastrointestinal (gastric and colorectal), prostate and pancreatic cancers, leukaemia cell lines and brain tumours. One recent study conducted a small prospective, randomized, placebo-controlled, double-blind clinical trial of boswellia supplementation in patients with primary or secondary malignant cerebral tumours treated with radiotherapy plus either boswellia supplementation (4.2 g/day) or

placebo. Boswellia supplementation significantly reduced cerebral oedema measured by MRI in the patient cohort. Different authors speculate that this could be due to the anti-inflammatory effect of boswellic acids and/or an additional anti-tumour effect (Kirste et al., 2011, Sayed et al., 2016). Importantly for the work in this dissertation, the role of AKBA or any other boswellic acid derivatives in ovarian cancer has not been reported in peer-reviewed scientific literature thus far, but the study of other cancers can offer useful insights as to the potential relevance of AKBA treatment in ovarian cancer.

1.1.4 Cytotoxic properties of Boswellic acid and mainly AKBA:

Several researchers have reported the benefits of frankincense (Bone, 2006) and most specifically *Boswellia serrata* in treating brain cancer patients, as the herb demonstrates efficacy in reducing oedema surrounding the brain in cancer patients. However, Bone (2006) continued to report on the cytotoxic properties, highlighting the role of AKBA as a cancer cell growth inhibitor, as a promoter of apoptosis in many cell lines, and as an inhibitor of DNA synthesis.

There are numerous positive findings of AKBA's anti-cancer effects *in vitro* using various cell-model systems (Bone, 2006, Hostanska et al., 2002), ranging from myeloid leukaemia, melanomas, and colon cancer cells to liver and brain cancer cells. Park et al. (2002a; 2002c) also evidenced AKBA as being effective in the treatment of meningioma cells at low concentrations (2 – 8 μ M). Park et al (2002a) determined that AKBA inhibited phosphorylation of Erk-1/2 whilst impairing cancer cell motility, as mediated through the Erk pathway. These two studies demonstrate the effectiveness of AKBA treatment in cell culture. The following section will highlight the various cell lines studied and published studies evidencing the cytotoxic effectiveness of AKBA.

1.1.5 Cell line studies and cytotoxicity

Pang et al (2009) conducted research on the use of AKBA to suppress angiogenesis, specifically as it relates to prostate cancer. Xenograft mouse assays were used, with five mice being injected with PC-3 cells (Pang et al., 2009). When the tumours were $\sim 10 \text{ mm}^3$, treatment in the AKBA intervention group commenced for a period of one month (Pang et al., 2009). The mice were then sacrificed, and a variety of processes were performed, including histological staining, a Matrigel plug assay, rat aortic ring assay, cell viability assay, endothelial cell migration assay, endothelial cell Transwell migration assay, endothelial cell capillary-like tube formation assay, western blot analysis and *in vitro* vascular endothelial growth factor receptor 2 (VEGFR2) kinase inhibition assay (Pang et

al., 2009). Results concluded that AKBA administered at a dosage of 10 mg/kg/d was effective at suppressing the weight and volume of tumours (Pang et al., 2009). Further, anti-angiogenesis was evident when comparing blood vessel numbers from treated rats microscope [high-power field (HPF)] (2.83 ± 1.17 blood vessels/HPF) to the control group (13.50 ± 2.43 blood vessels/HPF) (Pang et al., 2009). The same anti-angiogenic effect was also found for AKBA when treating tumour endothelial cells (Pang et al., 2009).

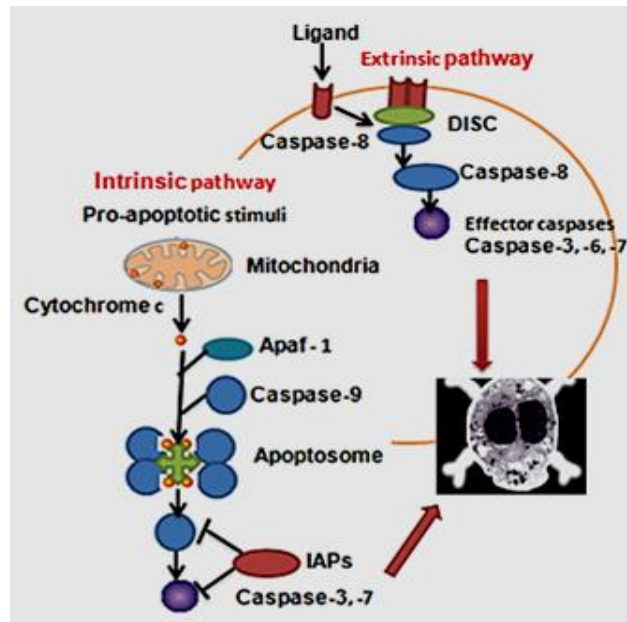


Figure 1.4 Apoptotic pathways (intrinsic and extrinsic)

Finally, AKBA demonstrated apoptosis in both tumour and endothelial cells, highlighting the positive impact of AKBA on both the VEGFR2 and mTOR pathways (Pang et al., 2009). Lu *et al.* also investigated the impact of AKBA on prostate cancer in cell lines, specifically comparing AKBA's action on the androgen-dependent (LNCaP) and androgen-independent (PC-3) prostate cell lines (Lu et al., 2008). A variety of assays were performed on the cell lines before and after treatment with AKBA, including an MMT assay and an apoptosis assay (fragmented DNA) (Lu et al., 2008). Twenty-four hours prior to AKBA treatment, a mitochondrial membrane potential assay was performed (Lu et al., 2008). Finally, cells were either treated with 10 $\mu\text{g/mL}$ AKBA or left untreated, followed by a luciferase assay and reverse transcription-PCR analysis to analyse death receptor DR5 expressions (Lu et al., 2008). The results determined that AKBA promotes apoptosis (Fig 1.4) and, is also a cell-growth inhibitor for androgen-independent cell lines (Lu et al., 2008). Additionally, it was demonstrated that caspase-8 and caspase-3 pathways are activated by AKBA, whilst AKBA also activates DR5 levels

and promoters via the CHOP-mediated pathway (Lu et al., 2008).

Park *et al.* (2011a) conducted research on the cytotoxic properties of AKBA in relation to pancreatic cancer, however, a wider variety of cancer cell lines were investigated, including pancreatic cancer cells, human leukemic cell lines, myeloma and human breast cancer cells. Cell lines were then subject to western blotting, electrophoretic mobility shift assay, RNA analysis and reverse transcription-PCR, quantitative real-time polymerase chain reaction, chromatin immune-precipitation assay and an invasion assay following treatment with AKBA (Park et al., 2011a). After that, cells were implanted orthotopically in nude mice (Park et al., 2011a). Following tumour growth and excision, the tumours were processed for histological analysis (Park et al., 2011a). Results determined that AKBA suppresses chemokine receptor (CXCR4) signalling in pancreatic cancer cells (PANC-28), down-modulates CXCR4 in human leukemic cells (KBM-5), kidney cancer cells (A293), myeloma cells (U266), breast cell lines (MDA-MB-231, MCF7/Neo, MCF7/HER2, and SKBR3), and four pancreatic cell lines (AsPC-1, BxPC-3, MIA PaCa-2, and PANC-28) (Park et al., 2011a). It was interesting to note the down-regulation of CXCR4 due to AKBA was not mediated by degradation of CXCR4 protein but actually occurs at the transcription level, involving the NF- κ B pathway (Park et al., 2011a). These results were corroborated by additional research conducted by Park et al, which further showed the effectiveness of AKBA treatment as matching that found with the traditional chemotherapy pharmaceutical gemcitabine (Park et al., 2011a). Ni and co-workers also researched the role of AKBA in pancreatic cell lines, including PaCa-2, Panc-28, and MIA but they included the additional pancreatic cell lines BXPC-3 and DANG in their investigation. The cells were treated with frankincense essential oils of different dilutions ranging from 1:200 – 1:2,700 dilutions (Ni et al., 2012). A cell cytotoxicity assay was performed to identify the percentage of damaged cells due to frankincense essential oil, as was a cell viability assay (Ni et al., 2012). Other assessments included genomic DNA fragmentation to measure apoptosis from pancreatic cancer cells seeded in culture plates and then treated with an AKBA dilution of 1:1,200 (Ni et al., 2012). Western blot analysis was also performed to assess the effect of AKBA in impacting the caspase signalling pathway (Ni et al., 2012). Xenografts were performed on mice using MIA PaCa-2 cancer cells; seven days later the mice were randomly assigned to a control or treatment group, with the treatment group receiving 3 injections of frankincense essential oil spaced four days apart (Ni et al., 2012). Tumours were removed from euthanised mice and then analysed via immune-histo-chemistry to assess

cytostatic activity, ultimately yielding the numbers of immuno-reactive cells from control mice compared to treated mice (Ni et al., 2012). Results demonstrated frankincense essential oil as being effective at suppressing pancreatic cancer cell growth and viability in the cell lines studied, and leading to tumour cell apoptosis via the caspase pathway (Ni et al., 2012). Ni et al. also determined that AKBA acts as a cell cycle modulator in the pancreatic cell lines studied (Ni et al., 2012). When tumour sizes were compared in control versus AKBA treated mice, tumour growth was significantly retarded in the mice treated with AKBA (Ni et al., 2012). Finally, immuno-histochemical analysis determined that PHH3 stained cells were fewer in number in tumours excised from AKBA treated mice compared to those from control mice, with terminal deoxy-nucleotidyl transferase dUTP nick end labelling (TUNEL) quantitative analysis determining that AKBA causes apoptosis (Ni et al., 2012).

Two studies were performed using colon cancer cell lines. Lui, and co-authors in 2006 built upon the known anti-inflammatory and anticancer benefits associated with AKBA in their investigation of the cellular growth inhibitory capabilities for HCT-116, HT-29, and LS174T cell lines. In a prior study, Liu, and co-authors in 2002 had already determined AKBA as effective in engaging the caspase-8 pathway to induce colon cancer cell apoptosis; notably, the study reported in this thesis investigates a similar set of parameters, however utilises a lower AKBA dosage. Similar to the above studies by Ni and his group and Park and co-authors, different assessment protocols were performed on cancer cells treated with AKBA including, DNA synthesis, cell viability testing and cell cycle assessment (Park et al., 2011a, Liu et al., 2006, Ni et al., 2012). Additionally, tumour cells were assayed to identify apoptosis by staining with annexin V (Liu et al., 2006). Results confirmed increased dosage levels enhanced the extent to which AKBA inhibited the growth of HCT-116 cancer cells (Liu et al., 2006). The same result was found for HCT-116 cell viability, which demonstrated a reduction in viability to a level half of the untreated control group with a dosage of 5 μM of AKBA, whilst cell growth decreased to 45% of that of the untreated control with a dosage of 20 μM of AKBA (Liu et al., 2006). When cell lines HT-29 and LS174T were tested, reductions and inhibitory responses were also identified at levels ranging from 40 – 50% compared with those of untreated controls for dosages between 20 – 30 μM of AKBA (Liu et al., 2006). Further, results confirmed that at doses lower than 20 μM AKBA, inhibited cell growth, with little evidence of apoptosis; however, when the dosage was increased to 50 μM of AKBA, evidence of apoptosis increased from 2% to 30% in a dose dependent manner (Liu et al.,

2006). Further, p21 pathway regulators were shown to be altered due to AKBA. For example, a 4-5 fold up regulation of p21, which inhibits cyclin-dependent kinases required for cell cycle progression, is seen following AKBA treatment, but there were no direct effect on p53 pathway mediated growth inhibition (Liu et al., 2006).

Following on from the studies by Liu and co-workers (Liu et al., 2006) on the HCT116 cell line, Yadav *et al.* conducted research on the same cell line investigating the effect of AKBA on cancer cell growth, proliferation, angiogenesis and metastasis using both colorectal cancer cell lines and xenographs (Yadav et al., 2012). HCT116 cancer cells were transferred to six four-week old athymic mice, who were then randomly assigned to a control group, or one of three AKBA treatment groups who received varying oral dose levels of AKBA: 50 mg/kg, 100 mg/kg, or 200 mg/kg (Yadav et al., 2012). Mice were euthanized at 28 days following treatment, at which time tumours were excised and assayed (Yadav et al., 2012). Results of the xenograft demonstrated significantly reduced cell tumour volume in all three of the treatment groups compared to the untreated control, with the reduction in tumour volume correlating the level of AKBA received (Yadav et al., 2012). Similarly, metastasis was inhibited on a dose-dependent basis in those mice treated with AKBA (Yadav et al., 2012). Those mice treated with 100 mg/kg presented with minimal metastasis, whereas those receiving 200 mg/kg presented with even lower levels of metastatic disease (Yadav et al., 2012). Additionally, Yadav *et al.* (2012) determined that metastasis to other organs was prevented with AKBA administration when compared to controls. AKBA also evidenced a decrease in angiogenesis as measured by CD31 micro-vessel density analysis, most notably at a dosage of 200 mg/kg (Yadav et al., 2012). Finally, Yadav *et al.* determined that the major signalling pathway affected in their AKBA trial was the NF- κ B pathway, known to be responsible for cell growth and metastatic activity; this pathway was inhibited in a dose dependent manner, with a treatment dose of 200 mg/kg providing the greatest inhibitory effect.

Examining the effect of AKBA on breast cell lines, Suhail *et al.* (2011) conducted research on T47D, MCF7, MDA-MB-231, and MCF10-2A. A key feature of the study was the multifaceted use of both oestrogen-receptive and non-oestrogen-receptive cell lines (Suhail et al., 2011). Whilst the studies conducted by Liu *et al.* (2006) and Yadav *et al.* (2012) used xenografts, Suhail *et al.* (2011) conducted all research using cell culture. Various assays, including the XTT assay to assess cell proliferation and western blot analysis to determine protein expression, demonstrated a variety of pathway expressions, including: Caspase-3, 8 and 9, phosphor Akt, PARP, cyclin D1, phosphor-ERK1/2, β -

actin and cdk4. The various breast cancer cell lines responded with different levels of sensitivity to AKBA; however, all cell lines exhibited a suppression of viability, increased apoptosis and an effect on gene expression proteins based upon pathway expression (Suhail et al., 2011). Suhail et al (2011) also demonstrated anti-angiogenesis properties of AKBA.

Zhao et al (2003) used the MTT assay to investigate the cell growth inhibitory properties of boswellic acid in the mouse melanoma cell line B16F10 and upon HT-1080, a human fibro-sarcoma cell line. Results determined AKBA to be effective in inhibiting cell growth of the mouse melanoma cells in a dose dependent fashion; this was particularly evident in cells with an increased melanin content treated with 50 μ M AKBA (Zhao et al., 2003). Results also determined that boswellic acids could effectively induce apoptosis in HT-1080 cells, with results similar to those for mouse melanoma cells, being time and dose dependent (Zhao et al., 2003). Many of the above studies have concluded that the safety associated with boswellic acids, makes these compounds a potentially effective cancer treatment. Whilst these studies are preliminary, if the results were replicated, this would strongly suggest the AKBA as an effective intervention to promote apoptosis in cancer cells (Zhao et al., 2003).

More recently, (Burlando et al., 2008) investigated the effectiveness of AKBA on skin normal cell lines HaCaT, NCTC 2544, and HFFF2. The cell lines were treated and examined *in vitro* by both DNA and MTT assays with the cancer cells being exposed to increasing concentrations of AKBA (Burlando et al., 2008). Results demonstrated aggressive cytotoxic activity on cancer cell membranes for all the cell lines, as evidenced by NRU assay (Burlando et al., 2008). The same results were found for HaCaT cells, however the observation was more pronounced for the HFFF2 and NCTC 2544 cells (Burlando et al., 2008). HaCaT's has a unique highly differentiated phenotype which could be responsible for the lower rates of cytotoxicity noted (Burlando et al., 2008).

In investigating the cytotoxic role of frankincense on bladder cancer cell lines, researchers examined the effect of frankincense oil on J82 and UROtsa cell lines (normal) *in vitro* using the XTT cell viability assay, trypan blue exclusion and TUNEL analysis (Frank et al., 2009). Results determined that frankincense oil inhibited cancer cell line viability and fostered apoptosis (Frank et al., 2009). Imaging demonstrated that J82 cancer cells shrank following treatment with frankincense oil, whereas UROtsa cells did not exhibit the same behaviour, despite treatment with increasing concentrations of frankincense oil (Frank et al., 2009). Results of TUNEL analysis also revealed apoptosis in J82 cancer cells treated

with frankincense oil. Researchers provided a detailed genetic analysis of up- and down-regulator genetic profiling in J82 bladder cancer cell line modulated by frankincense oil, suggesting that the DDIT3, ATF3 pathways are most likely responsible for induction of apoptosis and inhibitory responses (Frank et al., 2009).

Table 1. 2 Published anti-tumour activity of AKBA:

Author /year	Cancer investigated	Cell line/Mouse model	Type of BA & Con	Anti-tumour effect	Pathway affected
Catanzaro et al 2015	Colon cancer	LoVo and HT29 cell lines	BSE & AKBA (0.1-10 µg/ml BSE & 0.27 µg/ml	Cell viability & NO ROS generation	NF-κB phosphorylation
Zhang et al, 2013	Gastric/Colonic	SGC-7901/MN-45 xenograft cells& Polyplasia (APC mice)	AKBA (2.5, 5, 10, 20, & 40 µM)	Apoptosis& Reduced polyp formation	WNT, p21, p53& NFκB
Al Salmani et al., 2013	Ovarian	UWB1.298, A2780, A2780cis (cell lines)	AKBA (5, 10, 15, 25, &50 µM)	Apoptosis	DNA damage
Takahashi et al., 2012	Colorectal	Primary lines (cell lines)& mice	AKBA (5,10,15,20, 25, 40, 50, 60 µM) & (50, 100, 200 mg/ kg/ day)	Inhibits cancer growth	Let-7, mrR-200
Shen et al., 2012	Colorectal	RKO, SW48 and SW480 cell lines	AKBA (20 & 40 µM)	Activate Tumour suppressor& demethylation	SAMD14, SMPD3
Yadav et al., 2012	Colorectal	HCT116 (mouse model)	AKBA (50, 100 & 200 mg/ kg)	Inhibition growth, invasive, angiogenic & metastasis	NF-κB, apoptosis
Ni et al., 2012	Pancreatic	MIA, PaCa-2, Panc-28, BXPC-3 cell lines	BA in oil (19.6 & 30.1 mg/ml)	Apoptosis, Proliferation	Caspase, ErK1 / 2, AKt
Park et al 2011 (a & b)	Pancreatic	AsPC-1, PANC-28 cell lines and MIA PaCa-2 mice	AKBA (10, 25 & 50 µM) 100 mg/kg/ day	Growth inhibition and apoptosis	NF-κB
Suhail et al., 2011	Breast	T47D, MCF7, MDA-MB-231, MCF10-2A cell lines	BA in oil (19.6 & 30.1 mg/ml)	Apoptosis	Caspase-3-independent & PARP

Pang et al 2009	Prostate	HUVEC, PC-3 cells and Xenograft	AKBA (0.5,1,5,10,20, 50, 100, 200 μ M) & (10 mg/kg/d)	Anti-angiogenic	VEGFR2, VEGF and mTOR
Frank et al., 2009	Bladder	J82, UROtsa cells	1:1000 frankincense oil	Cell growth inhibition, apoptosis	DDIT3, ATF3
Lu et al., 2008	Prostate	LNCaP, PC-3 cells	AKBA (5, 10, 15 & 20 μ M)	Apoptosis	DR-5, CHOP-mediated
Burlando et al, 2008	Skin	Normal cell lines (HaCaT, NCYTC2544, HFFF2 cells)	AKBA rang of high conc. (0.5 – 500 μ M)	No toxicity	NOT IDENTIFIED
Singh et al 2007	-	plug assay (mice)	AKBA (10 mg/kg/d)	Anti-angiogenic	AKT/mTOR TNF α
Liu et al., 2006	Colon	HCT-116, HT-29, LS174T cells	AKBA (5, 15, 20, 25, 30 & 50 μ M)	Apoptosis& cell cycle	P21
Takada et al., 2006	Bone	Osteoclasts (RAW264.7 cells)	AKBA (10, 20, 30, 40 & 50 μ M)	Inhibited survival and invation	NF κ B, MAPK
Zhao et al., 2003	Melanoma, Fibrosarcoma	B16F10 (mouse - melanoma) cells; HT-1080 (human-fibro-sarcoma) cells	AKBA (12.5, 25, 50 & 75 μ M)	Apoptosis, invasion	DNA topological isomerization & cell cycle
Park et al, 2002	Meningioma	Primary cells	AKBA (2 – 8 μ M)	Growth arrest	Erk1/2
Hoernlein et al., 1999	Leukaemia	HL-60/CCRF cells	AKBA (10, 20, 30, 40, & 50 μ M)	Growth inhibition/G1 arrest	Topoisomerase 1

1.1.6 Metabolic activity of Boswellic acids and AKBA

According to Sharma (2010), one of the primary metabolic actions that lead to cell death is aerobic glucose oxidation that yields increased oxidative phosphorylation of mitochondrial membranes, which has effects both anti-proliferation and apoptotic proteins when oxygen is present. This leads to increased levels of CO₂ that leads to cell death, which when combined with anaerobic glucose oxidation serves to significantly decrease mitochondrial levels of energy and energy production.

Sharma (2010) explains how this impacts cancer cells by highlighting the profile of cancer cells as presenting with “high glucose consumption, high glycolytic rate, rapid cell

proliferation, lactic acid accumulation, extracellular acidic low pH, low glucose availability and oxygen deprivation.” Although the mechanism of action of boswellic acids, and more specifically AKBA, is unknown (Liu et al., 2006), this suggests that cancer cell lines are starved when anaerobic glucose utility blocks cell aerobic metabolic activity and leads to cell apoptosis(Sharma, 2010).

Other researchers suggest that AKBA leads to cell apoptosis via the NF- κ B pathway in a similar manner to chemotherapy, by inhibiting TNF and inhibited receptor activation of NF- κ B ligand-induced apoptosis. AKBA leads to apoptosis through inhibiting NF- κ B signalling and inhibiting invasion(Takada et al., 2006). There are a number of cancer cell lines which have been studied specifically with AKBA (detailed more in the section1.1.5).

1.2 Ovarian Cancer

Ovarian cancer is the 5th most common malignancy in women and despite intensive efforts to improve diagnosis and treatment, most diagnosed women eventually die from their disease. The vast majority of ovarian cancers are actually tubal in origin not ovarian(Mills and Fuh, 2017). Consequently, it is now being referred to as pelvic serous cancer because it is not possible to differentiate between the sites of origin and not only does it arise in the epithelial layer (Moss et al., 2015). The symptoms of this cancer include frequent urination, difficulty eating, an abdominal mass, tiredness and pelvic pain (Coleman et al., 2011a). Ovarian cancer is the leading cause of death amongst the gynaecological cancers (Jemal A et al., 2010). The vast majority of patients (>80%) have high grade serous but <15% are mucinous ovarian tumours (60-80%) and present with stage III and IV disease (Cannistra, 2004). The relative five-year survival for invasive epithelial ovarian cancer decreases dramatically with the stage of disease at diagnosis; with 92.0% survival outcome reported for stage I cancers; this is because mucinous tumours, which have a good prognosis, typically present with stage I disease. But as the stage increases, survival decreases: stage II (55.1%), stage III (21.9%) and stage IV (5.6%) (Cancer Research UK., 2012). Despite the high mortality rate, the incidence of ovarian cancer is low, making up around two percent of total cancers in the UK(Cancer Research UK., 2013).

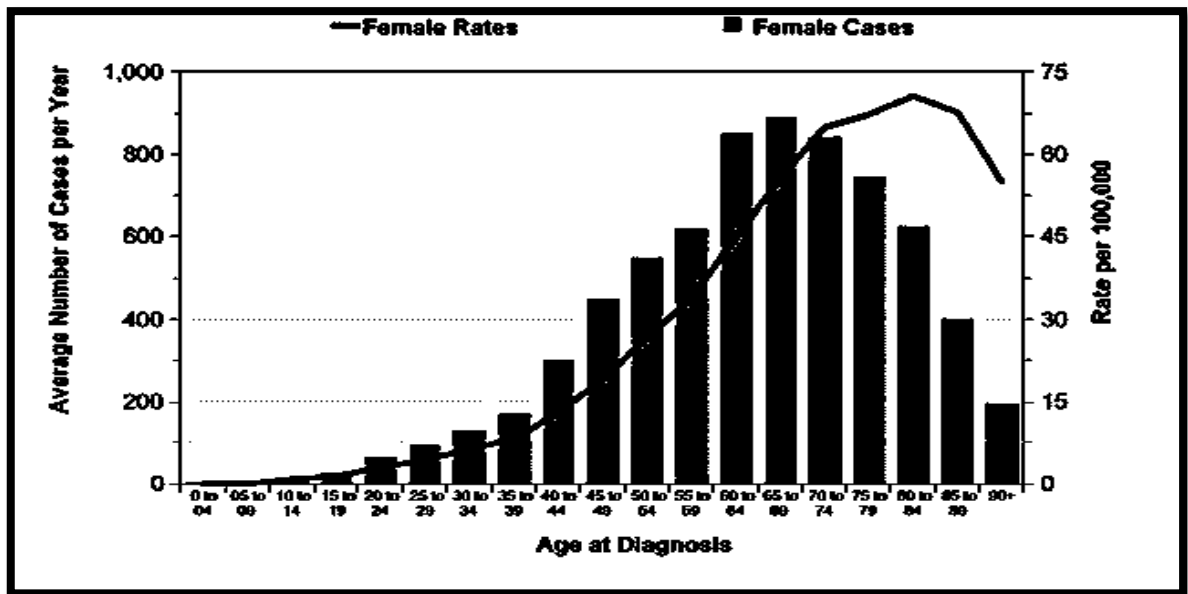


Figure 1. 5 Ovarian cancer statistics by age in Females 2012.

Taken from Cancer Research UK (<http://www.cancerresearchuk.org/health-professional/cancer-statistics/statistics-by-cancer-type/ovarian-cancer/incidence#heading-One>).

According to the most recent statistics from Cancer Research UK, over 7,100 women were diagnosed with ovarian cancer in 2012 resulting in 4,300 deaths (Cancer Research UK., 2013). In Europe ~65,500 new cases were reported in 2012 and ~239,000 new cases reported worldwide with an average prevalence of 12 in 100,000 of women.

The disease becomes more common with increasing age and most frequently diagnosed women are between 55 to 64 years of age (Cancer Research UK., 2012). Nonetheless, ovarian cancer is the 6th most common female cancer in Arab countries and so is regarded as moderately frequent in the Middle East. According to Arab Cancer Epidemiology 2010, presented by Salim and co-authors, 6.2% of all gynaecological cancers in Oman are ovarian cancer, which makes it the 2nd highest gynaecological cancer in the Arab world (Salim E et al., 2009). Furthermore, a report by the Omani Ministry of Health concerning the incidence of cancer in Oman for 2010, states that ovarian cancer is present as one of the highest cancer types amongst all types of cancer in females, accounting for 15% of all gynaecological cancers.

Chemotherapy represents the standard treatment for patients with ovarian cancer. The chemotherapy that has been shown to be the most active in ovarian cancer are the platinum based drugs cisplatin and carboplatin. These drugs are typically used in combination with another cytotoxic agent in order to improve the outcome of the patients. In the UK carboplatin is used because it is less toxic than cisplatin and has the same

efficacy as cisplatin. Many trials have been conducted over the past 20 years trying to improve on the standard regimen of intravenous carboplatin and paclitaxel however, to date, the results have been disappointing. However, advances have been made in the delivery route of chemotherapy with administration intraperitoneally rather than intravenously. This has been shown to increase survival in patients with stage IIIc epithelial ovarian adenocarcinomas (Armstrong et al., 2006) and this treatment regime was being further evaluated in international clinical trials in order to determine the optimum protocol (Armstrong et al., 2006).

The majority of ovarian cancer patients relapse and develop resistance to first line chemotherapy (Ledermann, 2010). Cisplatin resistance significantly reduces the effectiveness of the treatments and the cellular mechanisms which determine resistance are not well-understood (Zhu et al., 2005). Therefore, an urgent need to understand mechanisms of chemo-resistance in ovarian cancer and the design of strategies to overcome this resistance are required.

1.2.1 Ovarian cancer subtype

Ovarian, fallopian, and peritoneal cancers are all been presented as ovarian cancer, which is mostly epithelial origin cancers, and the most common OC is the high grade serous (HGSC), then the endometrioid and followed by mucinous (Mills et al., 2017, Koshiyama et al., 2017).

They are divided into 2 sub types; Type I which is originally from endometrioid, mucinous (benign serous cystadenoma) commonly present the low grade serous cancer with mutation in BRAF and KRAS. Type II which commonly includes the High Grade Serous and these patients progress very badly, and mostly present with mutation in BRCA1, BRCA1, TP53, BARD1, BRIP1, CHEK2, NBN, PALB2, RAD50 family, and NF1 which mostly found to be resistant to the first line chemotherapy (Mills et al., 2017, Koshiyama et al., 2017).

1.2.2 Aetiology and Pathophysiology of Ovarian Cancer

The exact etiology of ovarian cancer is not well understood mainly because the disease only becomes symptomatic at an advanced stage. As a result, the initiating and progressing biological mechanisms of carcinogenesis in the ovarian epithelium, which accounts for ~90% of cases, are unclear (Menon et al., 2014). The most popular hypothesis is that carcinogenesis takes place in ovarian epithelium cell-lined inclusion cysts (Hunn and Rodriguez, 2012). Cells are entrapped in the tissue stroma and receive

constant stimulation from stromal growth factors eventually leading to neoplasia. This hypothesis has been supported by previous pathological findings describing ovarian intraepithelial neoplasia with demonstrable histological cellular and atypical nuclei in stage I ovarian cancer (Plaxe et al., 1990). In addition, premalignant dysplastic alterations in the ovarian epithelium, as well as an association between neoplastic changes and an up-regulation of cyclooxygenase-2 and down regulation of tumor suppressor activity in epithelial cells, also indicate epithelial involvement in ovarian cancer (Yang et al., 2002). More recently, it has been suggested that ovarian carcinogenesis may involve cells from the fallopian tube. Indeed, ovarian cancer has a similar histopathological appearance to the fallopian tube, while classic pathological evidence of premalignant dysplasia has been identified in the fimbriated end of the fallopian tube in subjects undergoing prophylactic oophorectomy. Studies of serous pelvic carcinoma have shown involvement of tubal carcinomas with similar changes in p53 expression and activity in pelvic and fallopian tumors, indicating a common molecular origin (Chivukula et al., 2011). Family history of the disease is clearly an important risk factor. It appears that 10-12% of affected women carry germline mutations in the BRCA1/2 genes and a 20% - 40% lifetime risk of developing tubal cancer (King et al., 2003), while an additional fraction comes from a genetic background of other mutations in DNA repair genes which may confer an additional 10% risk of developing ovarian cancer (Yi et al., 2014).

Carcinogenesis is a very complex multifactorial process and different molecular mechanisms including hereditary, biological or environmental parameters participate in the neoplastic transformation of healthy tissues. In ovarian cancer the established dogma proposes that ovulation, characterized by repeated tissue disruption and repair of the ovarian epithelium, predisposes the epithelial cells to cellular DNA damage and neoplastic transformation in susceptible individuals (Schildkraut et al., 1997). This process has been termed “incessant ovulation” and is supported by extensive evidence in animals and human epidemiological studies linking ovulation cycles with ovarian cancer risk (Fleming et al., 2006). At the molecular level, it has been suggested that ovulation can cause mutations in the p53 tumor suppressor and as a result predispose to defective DNA repair. Indeed, in humans and chickens p53 mutations are common in ovarian carcinomas and correlate with the number of ovulation cycles (Hakim et al., 2009). Indeed, women who have been on the contraceptive pill and therefore have switched off their cycles, have a significantly reduced risk of ovarian cancer (Hannaford et al., 2007).

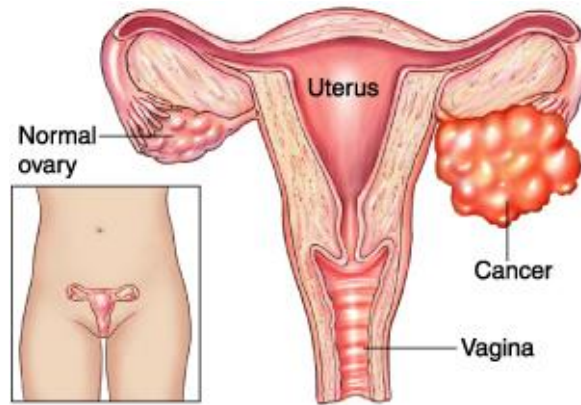


Figure 1. 6 Ovarian cancer.
(<http://www.mdguidelines.com/cancer-ovary>)

Importantly, due to the epithelial pathophysiological basis of the disease, which relies on hormonal patterns and may also have an inflammatory component, as well as the intra-abdominal location of the organ, ovarian cancer is difficult to diagnose at an early stage where most symptoms are mild and non-specific. For instance, pain and distension are often encountered in postmenopausal women and most commonly mistaken for irritable bowel syndrome (Jayson et al., 2014). With regards to the specific pathological classification of most ovarian cancers, high-grade serous (HGS) cancers represent over 80% of cases and are defined by mutations in p53 and low expression of BRCA1, defects in homologous recombination (~50%), CCNE1 amplification and genomic instability (Berns and Bowtell, 2012). By contrast, low-grade serous carcinomas are p53 wild-type and frequently show activating RAS pathway mutations (Landen et al., 2008, Weberpals et al., 2011a).

1.2.3 Current treatment of ovarian cancer.

According to Shelize and Banerjee (2015), for newly diagnosed ovarian cancers, primary surgical debulking, with removal of the uterus, tubes and ovaries, the omentum and any metastatic disease is ideally undertaken. This may not always be possible due to the patient's performance status or site and extent of disease. If it is felt that surgery would carry too high a risk of peri-operative mortality/morbidity or if complete tumor cyto-reduction is not going to be possible then neo-adjuvant chemotherapy (NACT) is undertaken. Following primary surgery, a course of chemotherapy is then undertaken in order to treat any remaining microscopic disease and reduce the risk of recurrence. In the case of NACT the aim is typically to perform interval debulking surgery after 3 cycles of

chemotherapy (Khakoo and Banerjee, 2015). During the past 20 years a large number of trials have established the combination of systemic delivery of carboplatin (alkylating agent) and paclitaxel (microtubule stabilization agent) as the standard of care in advanced hospitals and treatment centers (Ozols et al., 2003). In contrast, paclitaxel has lower side effects on hearing, the nervous system and kidneys, but the addition of cisplatin induces neurotoxicity, weakness and alopecia in most patients, but these are generally acceptable. Most of patients develop resistance to all of these treatments which drive the doctors to give aggressive courses of chemotherapy which made of combinations of all of these in order to save the patient's life.

Recent biological treatment trials that are still under clinical scrutiny are using various modifications of this treatment regime, including intraperitoneal (localised) delivery of chemotherapeutics, high dose paclitaxel regimes, addition of anti-angiogenic substances such as anti-VEGF antibodies (bevacizumab) or inhibition of the tyrosine kinase VEGF receptor (pazopanib)(Du Bois et al., 2014, Sapiezynski et al., 2016) received FDA approval on 2014. Anti-VEGF treatment is mostly considered for maintenance therapy(Monk et al., 2016). Recent therapeutic developments are focusing on the poly-ADP ribose polymerase (PARP) single-strand repair pathway. PARP inhibitors (such as olaparib and Niraparib) can cause significant cell death and reduction in tumor size because cells are unable to repair damaged DNA, especially in women with germline mutations to BRCA1/2 (Fong et al., 2009, Mass, 2017, Mirza et al., 2016) and received FDA approval 2014. This type of treatment is mainly used for patients who developed resistance to first line platinum based chemotherapy and in combination topotecan or pegylated liposomal doxorubicin and paclitaxel. Other recent efforts include drugs that target the PI3K/Akt and mTOR signaling pathways (Behbakht et al., 2011) as well the MAP kinases (Farley et al., 2012).

Typically, responses are expected in over 80% of women who receive standard platinum- and paclitaxel-based treatment (Markman and Bookman, 2000). Nevertheless, the majority of women with advanced ovarian cancer relapse and develop drug-resistant disease (Vasey, 2003). The median progression-free survival of advanced ovarian cancer is about 18 months and unfortunately, most recurrent disease is platinum resistant. Consequently, the long-term 5-year survival for patients with advanced-stage disease does not exceed 30% (Selvakumaran et al., 2003b).

1.2.4 Ovarian cancer cell-lines for in vitro studies

As mentioned above, recent evidence suggests that ovarian cancer could derive from different pelvic tissues with distinct histological and epidemiological features. Therefore, it is important to utilize appropriate cell line-based *in vitro* models to represent the different pathological subtypes and test different treatment options as well as to investigate the likely mechanisms of drug resistance. Currently, there are more than 100 different ovarian-specific cell lines with various characteristics (Barretina et al., 2012). From these there are over 23 ovarian cell lines that can be used to examine the genetic processes underpinning ovarian cancer and to test novel anticancer therapeutic drugs (Lambros et al., 2005). To elucidate mechanisms of cell cycle control in ovarian cancer, the cell line UWB1.289 has been developed, incorporating the breast and ovarian cancer susceptibility gene *BRCA1* within exon 11 of the genome. The cell line also has an acquired somatic mutation in the cell-cycle regulator, p53, which prevents apoptosis in response to DNA damage, allowing the type of unregulated replication observed in ovarian tumours (DelloRusso et al., 2007).

In an effort to uncover the mechanisms of cisplatin resistance in ovarian cancer, the A2780cis cell line has been developed by chronic exposure of the sensitive A2780 ovarian cancer cell line to cisplatin. A2780cis was demonstrated to have a 6.7 fold resistance to cisplatin ($EC_{50}=23.4\mu\text{M}$), compared with the sensitive cell-line. The exact mechanism of this resistance still remains to be elucidated, however it has been shown that A2780cis exhibits a higher cisplatin efflux rate (Kalayda and Jaehde, 2008). An OVCAR4 cell line which represents the high grade serious cell lines will be discussed in more detail below section 2.4.2.

1.2.4.1 A2780 and A2780cis

These cells were not given a histological subtype at origin (Louie et al., 1985). Other than SKOV3 cells, A2780 cells are the most common *in vitro* model of ovarian cancer. They are p53 and RAS wild-type (Vaskivuo et al., 2006) and from gene expression analysis they appear to have little profile similarity to actual ovarian tumors. Together with other commonly used cell types (SKOV3 and IGROV1), A2780 are clearly not representative of the major high-grade serous subtype of ovarian cancers but are more like the endometriosis histological subtype (Beaufort et al., 2014). An increased ability to repair DNA damage after cisplatin treatment has been observed in the original studies that established cisplatin resistance in these cells (Masuda et al., 1988). A more recent study

suggested that alterations in the mitochondrial apoptosis pathways are critical for cisplatin resistance in A2780 cisplatin-resistant cells. The authors showed that p73 and Bax, but not p53, are involved in drug resistance. More specifically, resistance to apoptosis was dependent on reduced Bax and p73 expression after cisplatin treatments, mitochondrial membrane depolarization, cytochrome c release and activation of caspase-3 (Muscolini et al., 2008). Careful analysis of the biological properties of cisplatin-resistant cells, revealed the acquisition of several chromosomal abnormalities generated by exposure to increasing cisplatin concentrations, including monosomy of chromosome 13, DNA copy number changes and cryptic genomic aberrations associated with changes in gene expression. High-throughput gene expression profiling, identified 17 genes as being significantly different between parental A2780 and cisplatin-resistant cell lines (Prasad et al., 2008). In another study, A2780 cisplatin-resistant cells were characterized by reduced proliferation rates and more efficient degradation of basement membrane, indicating a higher invasive potential. Moreover, resistant cells showed up regulation of functional insulin-like growth factor receptor (IGF-IR) and hyper-activation of the receptor, as well as increased phosphorylation of the AKT1 and AKT2 signaling intermediaries (Eckstein et al., 2009).

1.2.4.2 OVCAR-4

These cells were also not given a histological subtype at origin. They have mutations in p53, they show negligible BRCA1 expression (Weberpals et al., 2011c) and low AKT activity (Mabuchi et al., 2007). Although not as frequently used as other cells, their genomic features indicate high-grade serous origin (Barretina et al., 2012). When the line was established the patient was previously treated with cyclophosphamide, cisplatin and doxorubicin and was refractory to treatment, but interestingly the cells have shown varied levels of cisplatin resistance (Henkels and Turchi, 1997). In a study investigating cisplatin resistance and the function of the nucleotide excision repair (NER) pathway, OVCAR-4 cells showed higher ERCC1 protein expression in comparison to cisplatin-sensitive A2780 cells. Expression of ERCC1, a key component of the NER pathway, has been correlated with cisplatin resistance, however, in this study the increased expression of ERCC1 in OVCAR-4 was not associated with enhanced DNA repair capacity (Selvakumaran et al., 2003b). Another study investigating the role of CCNE1 (Cyclin E) as the target of 19q12 gene amplification, which is associated with primary treatment failure and poor outcome in high-grade serous ovarian cancer (Etemadmoghadam et al.,

2009), found that OVCAR-4 had 19q12 amplification and high CCNE1 expression and this was required for survival and clonogenicity after cisplatin treatment (Etemadmoghadam et al., 2009). Interestingly, previous work investigating the role of intracellular thiols such as metallothionein in cisplatin resistance, found that OVCAR-4 cells showed a slight increase in metallothionein expression after exposure to cisplatin and generally exhibited low cisplatin resistance (Schilder et al., 1990). OVCAR-4 cells in culture have been found to express the classic pluripotency stem cell markers CXCR4 and CD133. OVCAR-4 cells that were specifically selected (FACS-sorting) for these markers and were subsequently implanted in nude mice formed higher numbers of tumours in comparison to other cell lines that expressed low levels of CXCR4 and CD133. The authors propose that these cells could represent an ovarian cancer cell population with stem cell-like properties and that they might be useful in studying aggressive tumour development and chemotherapy resistance (Cioffi et al., 2015). IGF-IR is a potential new molecular target in ovarian cancer. A study examining the anti-neoplastic effect of an IGF-IR kinase inhibitor found that OVCAR-4 cells produce IGF-I and IGF-II, and express IGF-IR at the protein level. Activation of the receptor was important for OVCAR-4 survival because treatment of cells with the receptor kinase inhibitor, induced replication inhibition and apoptosis while the cells became more sensitive to cisplatin (Agarwal et al., 2010). Finally, in a study investigating mechanisms of angiogenesis and metastasis, OVCAR-4 cells showed high paracrine angiogenic potential (Agarwal et al., 2010).

1.2.4.3 UWB1.289

These cells were derived from a tumor of papillary serous histology. The cells carry germline BRCA1 mutation within exon 11 with a deletion of the wild-type allele. UWB1.289 cells are estrogen and progesterone receptor negative and have a somatic mutation in p53. The importance of these cells in ovarian cancer research lies in their functional deficiency of BRCA1 (DelloRusso et al., 2007). BRCA genes are necessary for repair of double-stranded DNA damage via homologous recombination. In a recent study comparing different ovarian cancer cell lines, UWB1.289 was not able to form tumors when xenografted in nude mice (Mitra et al., 2015). The cells are sensitive to DNA damage induced by ionizing radiation, with a related lack of S-phase arrest. Restoration of wild-type BRCA1 by transfection improved DNA repair responses and increased survival. Gene expression profiling revealed a clear association between BRCA1 levels

and down-regulation of multiple IFN-inducible genes (IFI16, IFI44, IFI27) while claudin 6 (implicated in cancer invasion and metastasis) was upregulated in cells transfected with functional BRCA1 (DelloRusso et al., 2007).

1.3 DNA damage & repair

DNA damage and repair mechanisms play a dual role in ovarian cancer. Defects in DNA repair via homologous recombination, which is deficient in ~50% of high-grade serous cancers due to BRCA1 gene mutations, epigenetic silencing or other mutations affecting homologous recombination independent of BRCA1, predispose to genetic instability and eventually could drive neoplastic transformation (Liu et al., 2012, Bell, 2011). On the other hand, the most successful therapeutic paradigm for the treatment of ovarian cancer is based on DNA damage induced by platinum chemotherapeutics like cisplatin/carboplatin. As mentioned above, defects in DNA repair as in BRCA1-defective cells (UWB1.289) and ovarian tumours increase sensitivity to treatment. The cytotoxic action of platinum-based drugs is exerted by DNA binding and development of DNA damage manifest as intrastrand and interstrand cross-links, with the latter being the most toxic (Payet et al., 1993). Interstrand cross-link formation and repair processes can lead to the formation of DNA double-strand breaks (DSBs) that represent the most lethal form of DNA damage (Deans and West, 2011).

Oxidative stress via the production of reactive oxygen species (ROS) represents another mechanism of DNA damage in cells and could play an important role in carcinogenesis, including that of the ovarian epithelium. For instance, there is an increase in metabolites associated with oxidative stress in human ovarian cancer specimens (Fong et al., 2011) while markers of oxidative stress-induced DNA damage have been found to correlate with poor outcomes in ovarian cancers (Karihtala et al., 2009). Generally, cancer cells produce higher levels of ROS, which can contribute to cancer formation by altering signalling or causing DNA mutations. On the other hand, excessive ROS could create substantial cytotoxicity and can be harmful even to neoplastic cells, although cancers generally possess potent antioxidant mechanisms. Interestingly, the key drugs used for ovarian cancer management such as taxol and platinum-based agents have been shown to induce avid generation of ROS (Marullo et al., 2013, Kampan et al., 2015) and it has been suggested that drug resistance to these agents might be correlated with increased tumour antioxidant capacity. Interestingly, a recent study of A2780 cells overcomes platinum activity by disrupting the metabolism of the cells leading to the generation of high levels

of ROS (Hearn et al., 2015). Another study showed that OVCAR-3 and A2780 cells were characterised by elevated ROS production through over expression of NOX4 NADPH oxidase (Xia et al., 2007). A recent study showed that UWB1.289 BRCA1-null cells produced large amounts of hydrogen peroxide; this caused oxidative stress and metabolic changes via NF- κ B activation both to cancer cells and other cells present in the tumour stroma. Importantly, oxidative stress could be abolished either by administration of antioxidants or by transfection of wild-type BRCA1 to the UWB1.289 cells. Thus, BRCA1 might suppress tumour growth by functioning as an antioxidant (Martinez-Outschoorn et al., 2012b).

1.4 The Cell Cycle.

The cell cycle is divided into four phases: G1, S, G2, and M. This cycle is normally monitored by safety mechanisms known as cell cycle checkpoints. Their function is to slow down or stop DNA replication (S phase) and progression to mitosis (M phase) if damage in the DNA is detected, so that DNA damage is either repaired prior to progression or dysfunctional cells eliminated by apoptosis. Abnormal control of cell proliferation and lack of appropriate genetic error checkpoints are typical features of neoplasia (Hanahan and Weinberg, 2000). Normal cell division is carefully controlled by a family of serine/threonine kinases, the cyclin-dependent kinases (CDKs) and their inhibitors (CDKIs) that form active heterodimeric complexes with different cyclins, the regulatory subunits. In ovarian cancer there are abnormalities in most cell cycle regulatory genes that control the transition of cancer cells to the different phases of cell division. Alteration of these mechanisms results in uncontrolled cell expansion; cells might accumulate genetic errors eventually leading to carcinogenesis. It is important to note that apart from the well-documented mutations in p53 in most ovarian tumours, most other cell cycle regulators are variably affected. This is presumably related to the inherent heterogeneity of ovarian tumours and the complicated biological mechanisms involved in cell cycle regulation in cancer cells. One comprehensive review highlights the high expression of p16, p53, and p27, contrasted by low expression of p21 and cyclin E in serous ovarian cancers (Nam and Kim, 2008), while a previous and very extensive review thoroughly discusses the involvement of the entire cell cycle regulatory machinery in ovarian tumours (D'andrilli et al., 2004).

Understanding the mechanistic insights of the cell cycle in ovarian cancer is important given that the most commonly used drugs aim to induce DNA damage and cell cycle

arrest, eventually leading to apoptosis. More specifically, platinum-based drugs (cisplatin/carboplatin) cause DNA alterations, which can induce cell cycle arrest at G1-S or G2-M checkpoints while taxol stabilizes microtubule polymerization, arresting the cell cycle at mitosis. To this end, in vitro studies using ovarian cancer cell lines including high grade serous OVCAR-4, cisplatin sensitive and resistance A2780 and BRCA1 mutant UWB1.289 which were used in this study will shed some light into these processes.

1.5 Aims and objectives

Epithelial ovarian cancer (EOC) is the leading cause of death amongst the gynaecological cancers. The vast majority of patients are diagnosed as stage III/IV disease. Despite the currently available evidence-based management, the 5-year survival rates are still dismal with the median survival being 36 months for stage III and 24 months for stage IV disease. The majority of patient's relapse and develop resistance to first line chemotherapy (Moss et al., 2015). Therefore, new strategies are urgently needed to understand mechanisms of resistance and develop novel therapies to eradicate ovarian cancers including drug resistant types. Accumulating evidence on anti-neoplastic properties of frankincense and its putative action through cell signalling pathways, known to be altered in EOC, has recently emerged. However, no such activity has been reported in EOC. Furthermore, there are no reports to suggest that Frankincense extracts might work synergistically, or overcome the resistance to several conventional frontline cytotoxic agents. Thus, we propose to study whether the boswellic acids derived from *B. sacra*, grown in southern Oman, and the cytotoxic effect of AKBA minimize or overcome resistance phenotype. Of the various cell lines implicated in EOC, one of the mostly used serous and the best model of high-grade cancer is the OVCAR-4 cell line, which is known to engage the mTOR pathway via VEGF receptors (Lau M., 2013). Lau and co-authors in 2013 have already demonstrated that an AKBA dose of 50 μ M leads to a loss of cell viability affecting the VEGFR complex by dismantling the epithelial cell structure. As noted in the literature, and evidenced above, various cancer cell lines have been investigated and AKBA has demonstrated a strong cytotoxic effect on these cell lines through a variety of pathways and disruptive actions leading to apoptosis. However, no research has been published related to the effectiveness of AKBA associated with ovarian cancer. Therefore, as AKBA has successfully been demonstrated to disrupt apoptotic pathways (Pang, 2009, Kurman, 2010), one of the objectives of the current research is to investigate the role of AKBA as a successful mediating agent to cause apoptosis in 4 ovarian cancer

cell lines: OVCAR-4, A2780, A2780cis, and UWB1.289. With the expanse of pharmacological chemotherapeutic agents used throughout the world that inherently destroy healthy cells and cause a vast number of negative side effect ranging from hair loss to death due to weakened immune systems and complications, it is important to investigate the role of natural and relatively safe alternative treatments for cancer, and in particular, for ovarian cancer. Yuan et al (2006) highlights, those natural remedies have been successfully used since ancient times for a variety of illnesses ranging from inflammation to cancer. Therefore, another objective of the research is to add to the limited body of research on resistant ovarian cancer cell lines and the effectiveness of AKBA.

1.5.1 Hypothesis

AKBA is a potent anticancer molecule in the ovarian cancer setting (mainly the resistant cancer type), with a mechanism of action via apoptotic pathways as established by different phenotypic assays like cell growth inhibition, DNA damage, cell cycle arrest, apoptosis, protein expression and gene expression.

In this project we propose to examine the cytotoxic effect of AKBA towards various Ovarian Cancer Cell lines, since frankincense had not been investigated in this context. The second aim was to examine if there was a difference in response to AKBA depending on whether the cells were resistant to selected chemotherapeutic drugs commonly used to treat ovarian cancer. In this project we will also study the potential of AKBA to address resistance to cisplatin in A2780cis ovarian cancer cell lines. The other part of the project was to examine the mechanistic role of DNA damage/repair and oxidative stress in the anti-cancer actions of AKBA. Furthermore, to identify mechanisms of action and the genes involved with AKBA treatment in cancer ovarian cell lines. The ultimate goal is to provide evidence to support the use of AKBA in the treatment of ovarian cancer. Research objectives

- To examine the effect of AKBA in different ovarian cancer cell lines, including an investigation of the ability of using AKBA against cisplatin resistant cells in ovarian cancer cell lines, and the effect of ABA in cell cycle and apoptosis.
- To examine the mechanistic role of DNA damage/repair and oxidative stress in the anti-cancer actions of AKBA.
- To conduct a preliminary examination of the mechanisms of action and the genes involved in the actions of AKBA in ovarian cancer cell lines.

Chapter 2

Materials and Methods

2. Materials and Methods:

2.1 Cell-lines for in vitro studies

There are over 23 ovarian cell lines that can be used to examine genetic processes underpinning ovarian cancer and to test novel anticancer therapeutic drugs (Lambros et al., 2005). To elucidate mechanisms of cell cycle control in ovarian cancer, the cell line UWB1.289 has been developed, incorporating the breast and ovarian cancer susceptibility gene *BRCA1* within exon 11 of the genome. The cell line also has an acquired somatic mutation in the cell-cycle regulator, p53, which prevents apoptosis in response to DNA damage, allowing the type of unregulated replication observed in ovarian tumours (DelloRusso et al., 2007).

In an effort to uncover the mechanisms of cisplatin resistance in ovarian cancer, the A2780cis cell line was developed by chronic exposure of the sensitive A2780 ovarian cancer cell line to cisplatin. A2780cis was demonstrated to have a 6.7-fold resistance to cisplatin ($IC_{50}=23.4\mu M$), compared with the sensitive cell-line ($IC_{50} = 3.5 \mu M$). The exact mechanism of this resistance still remains to be elucidated, however it has been shown that A2780cis exhibits a higher cisplatin efflux rate (Kalayda et al., 2008). OVCAR4 cell line is one of the best model of high grade serous cancer available, because it is closely resemble the original ovarian tumour (Domcke et al., 2013).

2.2 Cell lines used in this research

UWB1.289 (BRCA1 mutant) (ATCC® CRL-2945™), were purchased from American type culture collection-(ATCC), LGC standards, USA. Cisplatin-sensitive (A2780) and the cisplatin resistant counterpart (A2780cis) cell lines were obtained from European collection of cell cultures, ECACC, UK. Whilst the high grade serous OVCAR-4 cell line was a kind gift from Professor Iain McNeish, Beatson Institute of Cancer Sciences, University of Glasgow, UK. All cell lines were tested for mycoplasma contaminations every 5-10 passages and all were present as mycoplasma negative. A2780 cisplatin resistant cell line used in this project were tested for cisplatin resistant by Dr Mark Evans at De Montfort University (DMU Leicester) labs and found to be resistances 4-6 folds.

2.3 3 O-acetyl-11-keto-β-boswellic acid (AKBA) Molecular weight 512.72

At the start of the project AKBA was supplied by sigma Aldrich, and after one year of the work this compound was extracted from the Omani frankincense at Nizwa University

by Dr Ahmed Al Harassi, which then compared with sigma product and found to have similar effect, which then was supplied for the project for free.

2.4 Summary of the techniques/approach

Cisplatin sensitive (CSCL) and resistant (CRCL), BRCA1 mutated (BMCL) and OVCAR4 cell line were all treated with different concentrations of AKBA for different periods of times.

Effects on cell viability/proliferation, and cell death by AKBA were investigated in all the cell lines using the Alamarblue assay, and the Coulter cell counter to assess cell number. DNA damage was assessed using comet assay, and cell cycle status and apoptosis examined using flow cytometry (PI staining and Annexin V/PI). Temporal regulation of AKBA-modulated gene expression was undertaken by microarray analysis and subsequent validation using quantitative reverse transcriptase PCR (QPCR) to further examine the effect of AKBA on apoptotic pathways.

2.5 Cell culture medium and supplements

Dulbecco-modified essential Medium (DMEM) (high glucose, pyruvate, no glutamine), RPMI 1640, Geneticin 10131 were Supplied by Fisher Scientific, UK. Mammary Epithelium Basal Medium (MEBM), MEGM medium (50:50 MEBM + RPMI 1640 High Glucose) supplied as a MEGM media plus supplements kit), which contains [Insulin 0.5ml, Bovine Pituitary Extract (BPE) 2ml, Gentamicin Sulfate (GA) Amphotericin-3 0.5ml, Hydrocortisone 0.5ml, Epidermal growth factor (rhEGF) 0.5ml] all were supplied from Lonza, Blackley, UK. RPMI 1640 medium with high glucose was purchased from ATCC; Sodium pyruvate, L-glutamine (GlutaMAX-I) and fetal bovine serum, were all purchased from Fisher Scientific (Loughborough, UK).

2.6 Chemicals and Reagents

3-*O*-acetyl-11-keto- β -boswellic acid (AKBA) was supplied by Prof AL-Harassi, from University of Nizwa, Sultanate of Oman. All other materials were purchased from Sigma Aldrich (Poole, Dorset, UK) or Thermo Fisher Scientific (Loughborough, UK) unless indicated otherwise. Sodium dodecyl sulphate (SDS), tween-20, glycerol, ethanol, methanol, ponceau S. red, acetic acid, glycine, N,N,N,N-tetramethylethylenediamine (TEMED), ammonium per sulphate, 1-butanol, 2-mercaptoethanol, bromophenol blue, dimethyl sulphoxide Hybrid-Max DMSO), phosphate buffer saline (PBS) tablets, normal melting point agarose, ethylenediaminetetraacetic acid disodium salt dehydrate

(Na₂EDTA), sodium chloride (NaCl), sodium hydroxide (NaOH), Trizma-base, propidium iodide solution stock-1mg/mL, ethidium bromide, etoposide, free DNase and RNase free water, hydrogen peroxide (30% v/v) and isopropanol, RNase A, Trypsin EDTA, 0.4% trypan blue stain, low melting point agarose, 2', 7'-dichlorodihydrofluorescein diacetate (H2DCFDA). Proteinase K and Triton X-100, were supplied from Calbiochem. 100 bp DNA ladder, all were purchased from New England Biolabs Ltd, (Hitchin, UK). Gold antifade/DAPI-Slow Fade purchased from Life Technologies (Paisley, UK). Additional Reagents for gene expression technology: [Superscript III Reverse Transcriptase (Life Technologies), RNeasy® MinElute® Clean up Kit (Qiagen) or RNeasy Mini Kit (Qiagen)], were all supplied by Thermo Fisher Scientific, (Loughborough, UK).

2.7 Kits and antibodies

Annexin V-FITC kits for apoptosis detection were purchased from eBioscience, Ltd (Hatfield, UK). Genomic DNA (Blood & Tissue) extraction kits, were purchased from QIAGEN, (Manchester, UK). Anti-phospho-histone H2A.X (ser139) and secondary antibody A21121 Alexa Fluor 488 (Goat Anti-mouse IgG) were purchased from Life Technologies (Paisley, UK). Apoptosis Western Blot Cocktail (pro/p17- caspase 3, cleaved-PARP, muscle actin) Human kit was purchased from Abcam (Cambridge UK). Pierce® ECL Western Blotting Substrate, Qubit® dsDNA HS Assay Kit, plus Qubit® Assay Tubes, and the AlamarBlue® Cell Viability Assay, were all purchased from Thermo Fisher Scientific, (Loughborough, UK). TaqMan® Gene Expression Cells-to-CT™ Kit, TaqMan Array Human Apoptosis Plat (Fast), TaqMan® Gene Expression Master Mix, all was supplied by Life technology. Finally all microarray reagents and kits were supplied through the Department of Genetics, University of Leicester, UK. TargetAmp™- Nano Labelling Kit for Illumina® and Expression Bead Chip® (24 Reactions) were all supplied by illumines, Cambridge, UK.

Table 2. 1 The TargetAmp™- Nano Labeling Kit for Illumina® Expression**BeadChip kit content:**

Kit has been developed for use with Agilent 2100 bioanalyser microarray to provide optimal results with SuperScript® III Reverse Transcriptase (Life Technologies).

Component Name	Tube Label	Volume (24 samples)	Cap Colour
TargetAmp™-Nano T7-Oligo (dT) Primer	T7-Oligo (dT) Primer	30 µL	Red
TargetAmp™-Nano 1st-Strand cDNAPreMix	1st-Strand cDNAPreMix	50 µL	Red
TargetAmp™-Nano 2nd-Strand cDNAPreMix	2nd-Strand cDNAPreMix	125 µL	Red
TargetAmp™-Nano 2nd-Strand DNA Polymerase	2nd-Strand DNA Polymerase	18 µL	Red
TargetAmp™-Nano T7 RNA Polymerase	T7 RNA Polymerase	60 µL	Blue
TargetAmp™-Nano T7 Transcription Buffer	T7 Transcription Buffer	60 µL	Blue
TargetAmp™-Nano NTP PreMix	NTP PreMix	270 µL	Blue
TargetAmp™-Nano UTP / Biotin-UTP	UTP / Biotin-UTP	90 µL	Blue
RNase-Free DNase I	RNase-Free DNase I	60 µL	Clear
100 mM Dithiothreitol (DTT)	DTT	100 µL	Clear
HeLa Total RNA Control (40 ng/µl)	HeLa Total RNA Control	10 µL	Clear
RNase-Free Water	RNase-Free Water	500 µL	Clear

2.8 Preparation of buffers and working reagents

All buffers and working reagents were prepared according to the protocols supplied by the company and lab Standard Operating Procedures. All reagents were stored at the designated temperature. The preparations of the buffers and working reagents required for the methods and techniques used described accordingly.

All protocols used in this project were optimised, cell numbers and sample quantifications were optimised accordingly. All experiments were conducted in triplicates with the cells being cultured in medium only and 0.5% v/v DMSO was used as negative or vehicle control.

2.8.1 The test compound AKBA

5 mg of AKBA as supplied was dissolved in 1mL DMSO to give a 9.74mM stock solution. 100µl aliquots were stored at -20°C. Dilution of working AKBA in medium was prepared to achieve the AKBA final concentrations (5µM, 10µM, 15µM, 25µM, & 50µM) to treat the cells. All AKBA working solutions were freshly prepared immediately prior to use under sterile conditions.

N.B: In this study, calculations of material concentrations and molarities/concentrations of substances and compounds were undertaken using an automatic mathematical formula provided by the GraphPad prism website: <http://www.graphpad.com/quickcalcs/Molarityform.cfm>

2.9 Cell culture

2.9.1 Medium preparation:

2.9.1.1 RPMI 1640 medium:

50 ml of media were removed from a 500 ml bottle and 50ml of foetal calf serum (FCS) was added to the bottle to give 10% v/v FCS final concentration. After that 1% v/v of GlutaMAX™ I was added and mixed, then stored at 4°C until use.

2.9.1.2 MEGM medium (MEBM (Mammary Epithelium Basal Medium) + RPMI 1640 High Glucose 50:50):

All MEGM media supplements were added to the 500ml MEGM medium, then 250ml of MEGM removed and 250ml of RPMI 1640 high glucose was added. After mixing, fetal calf serum (FCS) was added to a final concentration of 3% v/v. The prepared solution was then stored at 4°C until use.

2.9.1.3 DMEM (high glucose, pyruvate, no glutamine):

50 mL of medium was removed from the 500 ml bottle of DMEM media, and 50 mL of FCS added to give 10% final concentration of FCS. After that 1% v/v (5ml) of sodium pyruvate were added and mixed well. Finally the prepared solution was then stored at 4°C until use.

2.10 Cell Culture:

2.10.1 Cell line freezing:

In order to have a backup of the cell lines used cell freezing was undertaken according to the relevant ATCC protocol. Cells were trypsinized and the cells pellet re-suspended in freezing medium, which were contained 10% dimethyl sulfoxide (DMSO) for A2780 & A2780cis and 5% dimethyl sulfoxide for UWB1.289 and OVCAR-4 cell lines. Then 1 mL with total number of 1×10^6 cell of cells suspension was aliquoted into cryogenic vials, which were then placed in a polystyrene box at $-80\text{ }^{\circ}\text{C}$ for overnight. The next day, all vials were stored in liquid nitrogen.

2.10.2 Cell revival:

The vials were removed from liquid nitrogen and immediately defrosted at $37\text{ }^{\circ}\text{C}$ in a water bath for 1-5 minutes. Following this, all the contents of the vial was transferred to a 15ml centrifuge tube which contained pre-warmed cultured medium. Then the suspension was centrifuged at $400 \times g$ for 4 minutes, and the Supernatant discarded. The cell pellet was re-suspended in pre-warmed culture medium and transferred to a T75 culture flask. Finally, cells were incubated at $37\text{ }^{\circ}\text{C}$ with 5% CO_2 . The next day the medium was changed and incubation continued at $37\text{ }^{\circ}\text{C}$ in 5% CO_2 for 3-4 days depending on the cell type. For the cisplatin resistant cell line chronic exposure to $1\mu\text{M}$ cisplatin was undertaken every 4 passages.

2.10.3 Cell line subculture

All cell lines were cultured using different media; OVCAR-4 was cultured in DMEM medium supplemented with 1 mM pyruvate and 10% FCS. The A2780 and A2780cis cell lines were cultured in RPMI1640 supplemented with 1 % Glutamax and 10% FCS and the UWB 1.289 cell line was cultured in MEGEMmedium supplemented with {Insulin 0.5ml, Bovine Pituitary Extract (BPE) 2ml, Gentamicin Sulfate (GA) Amphotericin-3 0.5ml, Hydrocortisone 0.5ml, Epidermal growth factor (rhEGF) 0.5ml}. T25, T75, and T175 culture flasks were used for culturing. Cells were grown at $37\text{ }^{\circ}\text{C}$ in 5% CO_2 incubator for 3-4 days depending on the cell line type and been used after 60% to 70% confluent. For *harvesting* the growth medium was removed and the cells rinsed twice with phosphate buffered saline (PBS). After that, 1X Trypsin/EDTA solution was added and the flask incubated at $37\text{ }^{\circ}\text{C}$ for 10 min to detach the cells. When the cells were detached completely, 4 x the volume of TE, medium was added to stop the trypsin's

action. Then the cell suspension was centrifuged at 400 x g for 4 min. Supernatant was discarded, and then the tube gently tapped to disperse the cell pellet and 1-2 mL of fresh medium added. Finally, the cells were split into new culture flasks by taking 1 mL of harvested cells and adding 10 mL medium in each 75 mL flask. Cells were used when 70-80 confluent for all experiments.

2.10.4 Cell Counting:

To count the cells, the cells were harvested as described above and the cell pellet re-suspend in 1 mL of medium and a 1:10 dilution of cells made using Trypan blue. Then the Trypan blue diluted cells suspension was loaded into a haemocytometer slides. Cell number per 1 ml was calculated using the equation below:

$$\text{Number of viable cells/ mL} = (\text{sum of all viable cells counted/number of counted areas}) \times \text{dilution factor} \times 10^4$$

Equation 2. 1 Cell counting formula

2.11 Methods

2.11.1. Cell morphology examination

In order to examine the effect of AKBA on cell morphology and cell growth images were taken of the cells treated with different concentrations of AKBA at different time points using a Nikon Eclipse light microscope TE 200-4.

2.11.2 Cell growth and proliferation analysis

Cell growth was assessed using different techniques including cell count using Coulter counter and cell viability using AlamarBlue[®] Assay. These techniques were undertaken in triplicate and the results were obtained from at least three independent experiments.

2.11.2.1 AlamarBlue[®] Assay

This is a colorimetric assay for measuring cell viability and proliferation. This is measured quantitatively by cell metabolically reducing the power of the cell and continuously conversion of resazurin (blue) to resorufin (red) in living cells (Fig. 2.1). This leads to an overall increase in the fluorescence and color of the media (Rampersad, 2012). This assay can also be used to measure cytotoxicity (loss of viable cells) in response to external factors.

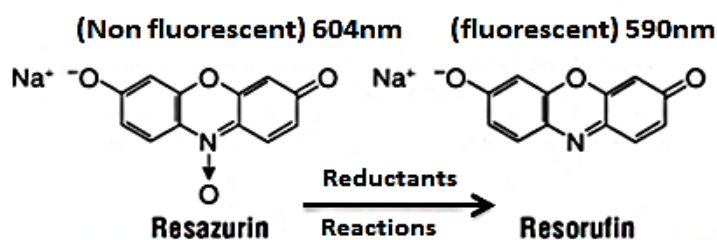


Figure 2. 1 The principle of the AlamarBlue® Assay (Rampersad, 2012).

2.11.2.1.1 Optimizing the cell number for AlamarBlue

Following the protocol supplied by Thermo Fisher Scientific, different cell concentrations (1×10^4 – 1×10^6) in triplicate were suspended 200µl of medium and cultured in 96 well plates for 24 h at 37°C, 5% CO₂ atmosphere. Next day 20 µL of Alamar Blue was added (10 % v/v/ AlamarBlue final concentration) to each well and incubated for 3 h at 37°C. Following incubation the absorbance values were read at 570 nm, using 600 nm as a reference wavelength. Higher absorbance indicates higher number of metabolically active (viable) cells.

2.11.2.1.2 Testing Cell Viability after AKBA treatment

After optimisation $4\text{--}6 \times 10^4$ cells in triplicate were cultured in each well of 96 wells plate for 24 hours, to allow the cells to recover and start growing. Different concentrations of AKBA (5µM, 10µM, 15µM, 25µM & 50µM) were added for different time point (0 min, 6 hrs, 16 hrs, 24 hrs & 48 hrs), plus 2 controls (cells in medium only and cells treated with 0.1% v/v DMSO). Three hours before the end of the treatment incubation time, 20 µL of AlamarBlue were added to each well and incubated for the remaining 3 hours at 37°C. After that, readings were taken using the plate reader at 570 nm.

2.11.2.2 Determination of cell number using the Coulter counter

The cells were cultured in a 6 well plates to 70–80 % confluence (~1 million cells), then cells were treated with different concentrations of AKBA (5µM, 10µM, 15µM, 25µM & 50µM) and incubated at 37 °C for different times in duplicate with vehicle control (DMSO) and growth control. At the end of each time point, the medium was removed and the cells were washed with 2 mL of PBS. After that cell were trypsinised as described in section (2.10.2.3), 2 mL medium was added to each well and the total cell number per mL was counted by suspending 100 µL of control and treated cells in 9.9ml of isoton buffer. The cell counts were under taken and recorded in triplicate using the Coulter counter (Z™ Series Coulter counter® Cell and Particle Counter, Beckman Coulter), and

the results were obtained from three independent experiments. Each cell line has its own sitting in the coulter depends in the size of each cell line type.

2.11.3 Assessment of DNA damage using Alkaline Comet assay (ACA)

In order to examine the DNA damage in each individual cell without extracting the DNA the comet assay was used following a protocol based on that of Singh *et al.* (Singh et al., 1988). This technique is a sensitive method to measure DNA strand breaks by measuring the migration of DNA from individual lysed nuclei (nucleoids) upon alkaline electrophoresis (Collins, 2002b). Then the comet tail length (DNA migration) and relative fluorescence of comet tail intensity of DNA represents the number of strand breaks present in the DNA of each cell (Collins, 2004).

Slide preparation: 30×10^3 cells were cultured in each well of the 12 well plates for 24 hours, to allow cells to attach and recover from manipulation. Then different concentrations of AKBA (5 μ M, 10 μ M, 15 μ M, 25 μ M, 50 μ M) were added for different times (Immediately, 6 hours, 16 hours, 24 hours and 48 hours). Three controls were included (untreated cells, 0.5% v/v/ DMSO treated cells, and 50 μ M H₂O₂-treated cells as a positive control, depending on the cell type) treated in the same manner as the other tested samples. At the end of the treatment all the cells in each well of the plate were harvested (in the dark) for Comet assay. Cells were centrifuged at 11,000 x g for 10 minutes. Then, the cells were re-suspended in 200 μ L of 0.6% w/v low melting agarose (LMP) in PBS, and 80 μ L of the LMP agarose cell suspension was transferred onto a slide pre-coated with 1% w/v normal melting agarose. Immediately, the cover slip was placed on top of the gel, which was left to set on a metal plate on ice for 20 mins and then the coverslip was carefully removed (Fig 2.2).

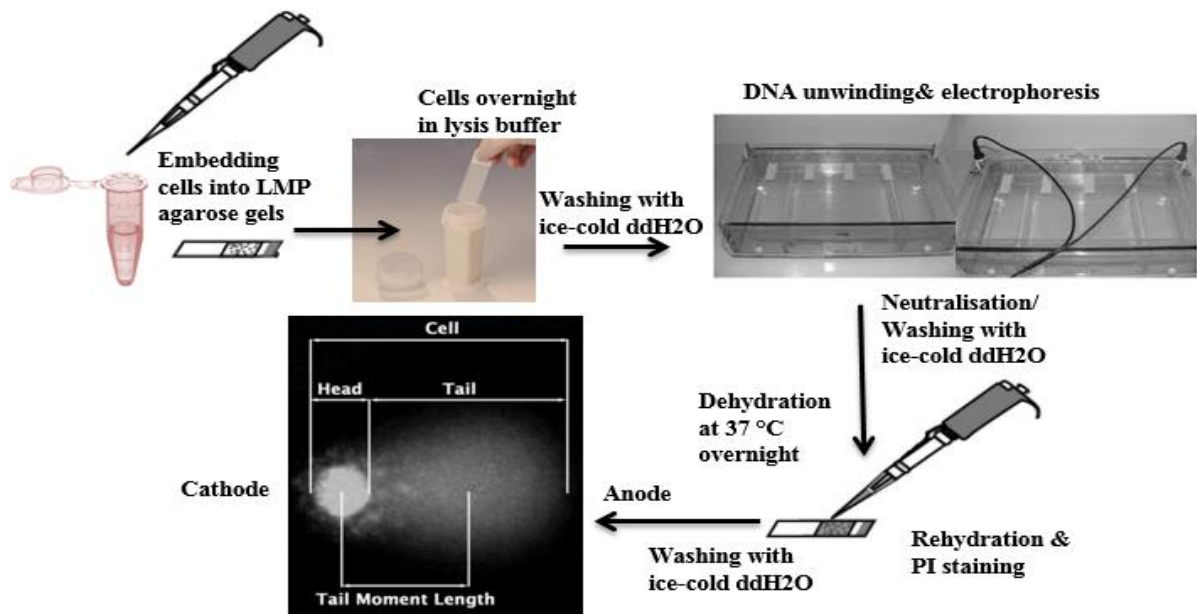


Figure 2. 2 Comet Assay procedure

Finally, the slides were placed in lysis buffer (2.5 M NaCl, 100 mM Na₂EDTA, pH adjusted 10 with 10 M NaOH and 1% v/v Triton X-100) in a coupling jar and incubated at 4 °C overnight.

Electrophoresis: Slides were carefully removed from the lysis buffer and washed with ice-cold ddH₂O (Fig 2.2). Then slides were placed in an ice-cold electrophoresis tank filled with 1 L ice-cold alkaline electrophoresis buffer (10 M NaOH, 200 mM Na₂EDTA, pH 13.0) for 20 min to allow DNA unwinding. Then, the electrophoresis was run at 27 V and 300 mA for 20 min. After the electrophoresis, the slides were removed from the electrophoresis tank and placed on a clean tray (fig 2.2). After that, the slides were covered with 1 mL neutralization buffer (0.4 M Trizma base, pH 7.5) for 20 min. Finally, the slides were washed with ice-cold ddH₂O, moved to a clean tray and left to dry in an incubator at 37°C, overnight.

Staining: The slides were rehydrated with ice-cold ddH₂O for 30 min, then they were moved to a clean tray and each slide was flooded with 1mL of 2.5 µg/mL propidium iodide solution for 20 min (Fig 2.2). Afterwards, the slides were washed with ice-cold double distilled water for 20 min and transferred to a clean tray to dry at 37°C overnight.

Analysis: The slides were scored and comets visualised (Fig 2.2) using fluorescence microscopy at magnification of 20 x, equipped with a green excitation filter. Images were taken by an on-line charge-coupled device (CCD) camera, and then the comets images analysed by Comet Assay IV software 4.2 (Andor Technology). Fifty comets per gel, 2

gels were scored for each individual treatment and time points and each experiment repeated 3 times. Percentage tail DNA (%TD) was selected as the parameter that best reflected DNA damage (Collins, 2002a); %TD is considered to best correlate with the dose of genotoxic agents (Kumaravel. and Jha., 2006, Kumaravel and Jha, 2006). The percentage of tail DNA is calculated using the following equation (Equation 2.2).

$$\text{Tail DNA (\%)} = \frac{\text{Tail DNA intensity}}{\text{Total intensity of whole comet}} \times 100\%$$

Equation 2. 2 The mathematical formula for the calculation of % tail DNA damage using the comet assay scoring software.

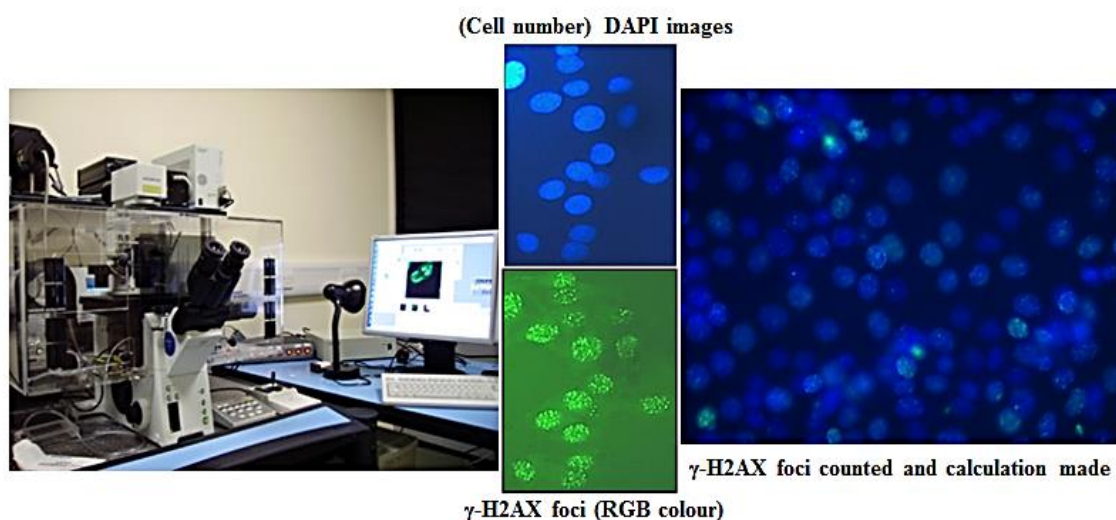
2.11.4 Examination of double strand breaks using γ -H2AX-immunoassay

In order to assess the extent of any double strand breaks (DSB) created by AKBA treatment in ovarian cancer cell lines the γ -H2AX assay was performed. In response to DSB formation Serine-139 residues of the histone variant H2AX in the chromatin undergo rapid phosphorylation to form γ -H2AX (Mah et al., 2010). A γ -H2AX phosphor-specific antibody can be used to detect the foci created by this phosphorylation as a tool to assess the amount of DSB resulting from the effects of genotoxic agents, such as chemicals. Cells were seeded and grown on sterile cover slips attached to the bottom of wells of 6-well plates at approximately 2×10^4 cells per well and left overnight incubated at 37°C with 5% CO₂. Next day, the cells were treated with different concentrations of AKBA (5 μ M, 10 μ M, 15 μ M, 25 μ M, 50 μ M) and incubated for different times (immediately, 6 hours, 16 hours, 24 hours, & 48 hours). Following drug treatment, the cell specific medium was removed from each well and cells were washed with ice cold PBS and fixed in 100% methanol for 24 hours at -20 °C. Next day, the methanol in each well was removed, followed by 15 minutes incubation with fresh 1 x KCM blocking buffer [10ml of 10x KCM buffer {1.2M KCl (8.946g), 200mM NaCl (1.1688g), 100mM Tris-HCl and 10mM EDTA (0.372g) in 60ml of ddH₂O}, 100 μ l Triton X-100 and 89.9ml ddH₂O]. Next day methanol was removed and the fixed cells were washed and rehydrated twice with 1ml of PBS for 20 minutes (10 minutes per each wash). The PBS was then aspirated and the cells were permeabilised with 150 μ l of blocking buffer for 15 minutes. The blocking buffer was then removed, and 150 μ l of primary anti-phosphohistone H2AX (Ser139) antibody (clone JBW301, mouse monoclonal antibody; Upstate, Millipore

Crop) at a dilution of 1:200 with blocking buffer, was added and incubated at room temperature for 2 hours on a shaker. Afterwards, cells were washed four times with KCM washing buffer, and then the secondary antibody (A21121 Alexa Fluor 488 Goat Anti-mouse IgG), (at a dilution of 1:200 blocking buffer) was added to the cells and incubated at room temperature for one hour, on a shaker. Then the cells were washed four more times with KCM washing buffer. After the washing step a drop of SlowFade® Gold antifade reagent with DAPI (10µl) was dispensed on to each labelled slide. Finally, the cells on the cover slip were mounted upside down on the labelled slides; the treated cells being between the cover slip and the slide surface. After the slides had been dried at room temperature, they were stored at 4°C for 24 hours ready for image analysis.

2.11.4.1 γ -H2AX foci visualisation and analysis

The foci number per cell were counted, and images of the treated cells were taken at 40x magnification and captured using velocity software together with Olympus Cytological imaging system which made up of two different types of filters; {(Narrow-band Blue filters (GFP, Alexa 488, FITC and Cy2): exciter filter BP 470-490, beam splitter DM 500, barrier filter BA 515), and the Narrow-band Green filters (Alexa 546, TRITC and Cy3): exciter filter BP 530-550, beam splitter DM 570, barrier filter BA 590, Sky filter set} which all supplied by Applied Spectral Imaging. Automated meta-system was used to assess 6 slides each time and from each sample, 15 fields of view (scoring up to 400 cells) were randomly chosen for analysis by the Fiji software (WCIF Image J version 1.42, available from research services branch NIH) 15 fields captured images from each cover slip and two different filters were used to display γ -H2AX foci and the cell's nucleus. Images of clear γ -H2AX foci were captured using a 485µM filter, whereas the number of DAPI stained nuclei images were captured using a DAPI filter. As a part of the Fiji software's functioning, γ -H2AX foci and nuclei numbers were counted automatically. After exclusion of cells with more than one nucleus, the actual numbers of γ -H2AX foci per cell (DAPI nuclei) were obtained by dividing the total number of γ -H2AX foci by the total number of cells per field. The procedure for foci counting is depicted in (Figure 2.3).



$$\text{Average } \gamma\text{-H2AX foci per cell} = \frac{\text{Number of total foci per field}}{\text{Total number of cells per field}}$$

Figure 2.3 The Olympus meta-system microscope.

Analysis of γ -H2AX foci per field of treated sample using image J software, which was done in triplicate. The lower immune-cytochemistry image shows H2AX phosphorylation (H2AX Foci) (green) which represents DSBs and the upper image the nuclear dye DAPI for measuring cell number per examined field.

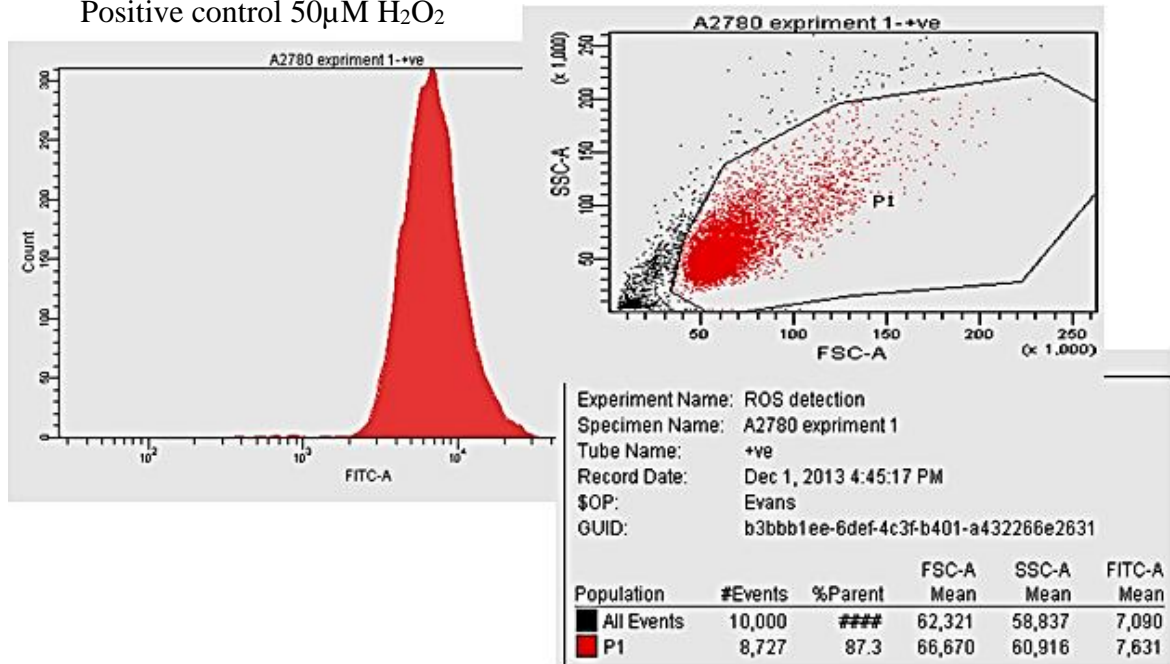
2.11.5 Reactive Oxygen Species (ROS) measurement by flow cytometry

The non-fluorescent probe, H₂DCF is produced intra-cellularly when H₂DCFDA is cleaved by intracellular esterases. The non-fluorescent molecule becomes fluorescent when oxidised by intracellular ROS, This fluorescence at 530nm can be detected and measured by flow cytometry (Eruslanov and Kusmartsev, 2010).

In order to examine the effect of AKBA on ROS production after AKBA treatments, 5 x 10⁵ cells were seeded in each well of the 6-well plate and kept incubated for 24 hours at 37 °C/5% CO₂. Next day, the cells were treated with different concentrations of AKBA (5 μ M, 10 μ M, 15 μ M, 25 μ M and 50 μ M) for different times (immediately, 6 hours, 16 hours, 24 hours, & 48 hours). Cells were then harvested normally using 1X trypsin EDTA. After that cells were transferred to FACS tubes, protected from light and washed with 1mL PBS. After removing all the PBS, fresh 500 μ LPBS with DCFA staining solution (0.5 μ L of diluted H₂DCFDA per 1ml of PBS) was added and incubated at 37°C for 30 minutes. 50 μ M H₂O₂ (oxidant) was used as positive control and added 20 minutes prior analysis (Fig 2.4). The fluorescence was measured immediately using a BD FACSCanto™ II Flow Cytometer and the decrease or increases fluorescence evident

from the shift in the in mean fluorescence intensity (MFI) quantified (%) = $[(MFI_{treated} - MFI_{untreated}) / MFI_{untreated}] \times 100$ calculated according to (Kaminski et al., 2007).

Positive control 50 μ M H₂O₂



5 μ M of AKBA treatment tested immediately for ROS production

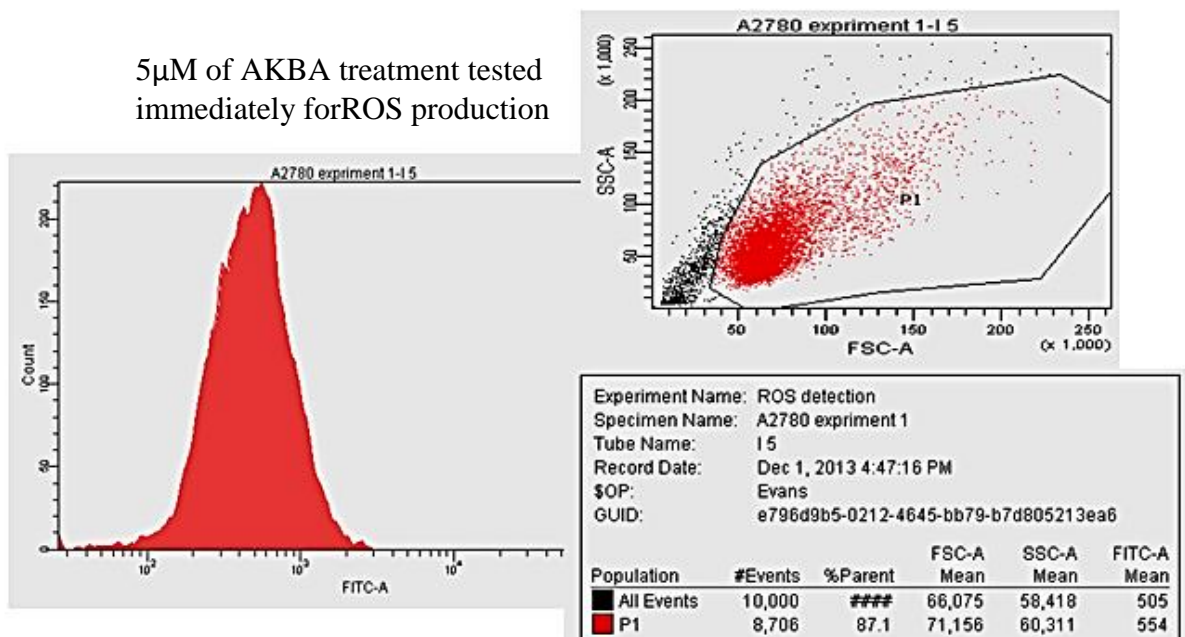


Figure 2. 4 ROS production measured by BD FACSCanto™ II Flow Cytometer shows the shift in FITC gating in the + positive control.

Decreases or increase in the ROS levels is indicated as a shift in the histograms showing frequency distribution of values of DCF fluorescence versus number of events or cells.

2.11.6 Assessment of AKBA effect on cell cycle phase distribution

The effect of AKBA on cell cycle phase distribution was assessed by measuring the DNA content (PI staining) of each cell passing through a fluidic stream (flow), which contains a stationary set of fluorescent detectors. Four distinct phases could be recognized in a proliferating cell population: the G1, S (DNA synthesis phase), G2 and M (mitosis) phase (Fig 2.5). Normally the cell DNA is protected by the cell membrane and it cannot be stained with PI stain without permeabilisation of the cell membrane by fixation in order to enable the dye enter the cell to stain the DNA. PI usually stains both DNA and RNA. 8×10^5 to 1×10^6 Cells were counted and cultured in 25 ml flask for 24h for cell recovery using serum free medium. The next day medium was removed and growth medium containing the AKBA at the required concentrations for treatment was added to each flask. After each time point all the medium from each flask was removed and transferred to a specific tube labelled with the specific treatment and time point. The cells were rinsed with PBS and the PBS washes transferred to the same tube containing the medium. The cells were harvested normally as described in section 2.9.2.3. Then the cell suspension with the medium and trypsin were transferred to the same tube containing the old medium and PBS washes. All tubes were centrifuged at $600 \times g$ for 6 minutes. After that the supernatant was discarded, each tube was then gently tapped. Cells were then washed twice with PBS and centrifuged at $600 \times g$ for 6 mins. Then the cells were fixed gently with 70% v/v ice cold ethanol and stored at -20°C until staining for analysis. On the day of staining, the cells were washed twice with PBS and after the last wash, $500 \mu\text{L}$ of PBS was added to the cells and the tube gently tapped. Then cells were treated with ribonuclease A (RNase A) ($2.5 \mu\text{L}$ of 10 mg/mL). This ensures that only DNA, not RNA, is stained. Then $25 \mu\text{L}$ of 1 mg/mL propidium iodide was added to each tube and mixed gently. Tubes were incubated at 37°C for 30 mins in the dark. Finally, all the contents of the sample tube were transferred to FACS tubes and placed on ice immediately, then taken for flow cytometry. The relative DNA content of these cells and its distribution across the cell cycle was analysed within an hour using FACSDiva software on a FACSCalibur flow cytometer (Becton Dickinson Coulter) based on red PI fluorescence. A total of 10,000 of cells were acquired for each sample. Results were obtained in duplicate from three independent experiments.

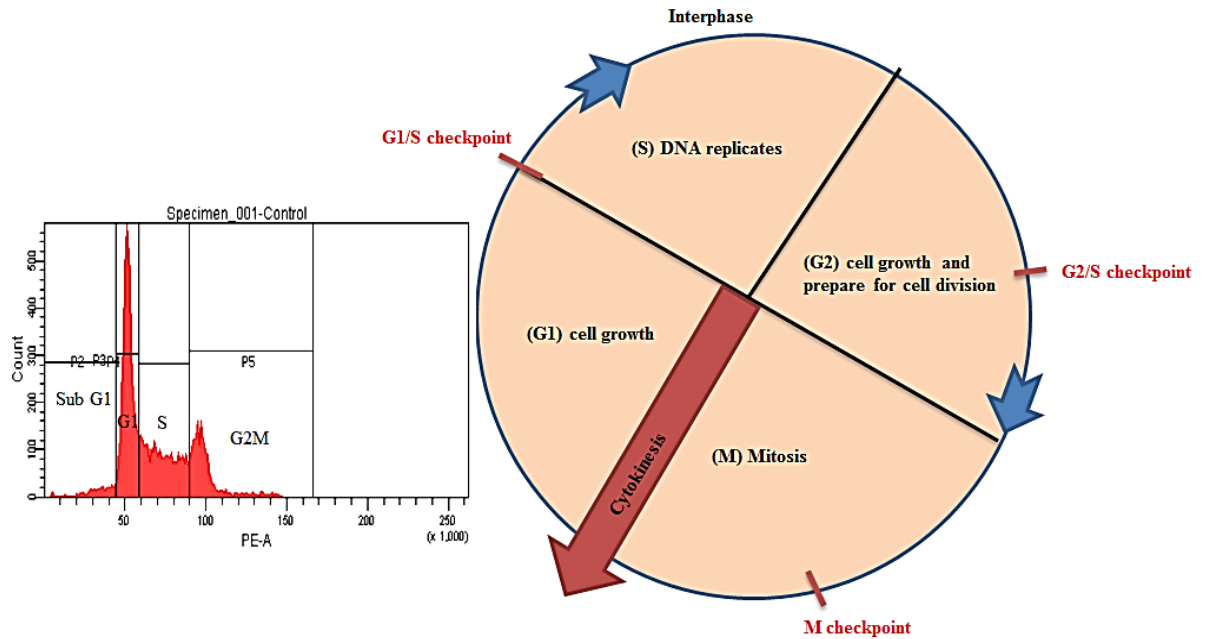


Figure 2.5 An illustration of the gating of each phase of the cell cycle.

There are 4 phases of the cell cycle and three checkpoints which the cell has to pass then to continue the process of the cell cycle: two gap phases (G1 and G2); an S phase for DNA synthesis and genetics materials are duplicated, and an M phase, mitosis phase where the genetics materials divided to two individual cells. This was observed using PI staining analysis by flow cytometry.

2.11.7 Examination of apoptosis using the Annexin V/PI assay

The Annexin V/PI assay was used to assess the extent of early and late apoptosis, including necrotic cells induced by AKBA in a population of cells exposed to AKBA. This method has been used to detect early apoptotic cells using a flow cytometer. Normally the cell membrane contains phosphatidylserine (PS) solely located in the inner side of the cell membrane lipid bilayer. During apoptosis PS is translocated to the outer surface of the membrane. Annexin V, a 35-36kDa protein, is a very sensitive Ca^{2+} -dependent probe with a high affinity for PS and its binding to PS can monitored by fluorescence. In response to apoptosis cells shrink and their membrane loses integrity, so first Annexin V staining becomes detectable (early apoptosis) and then during late apoptosis cells become permeable to a DNA-binding stain such as PI (Fig 2.6). PI is nucleic acid-specific and intercalates into the DNA (Rieger et al., 2011).

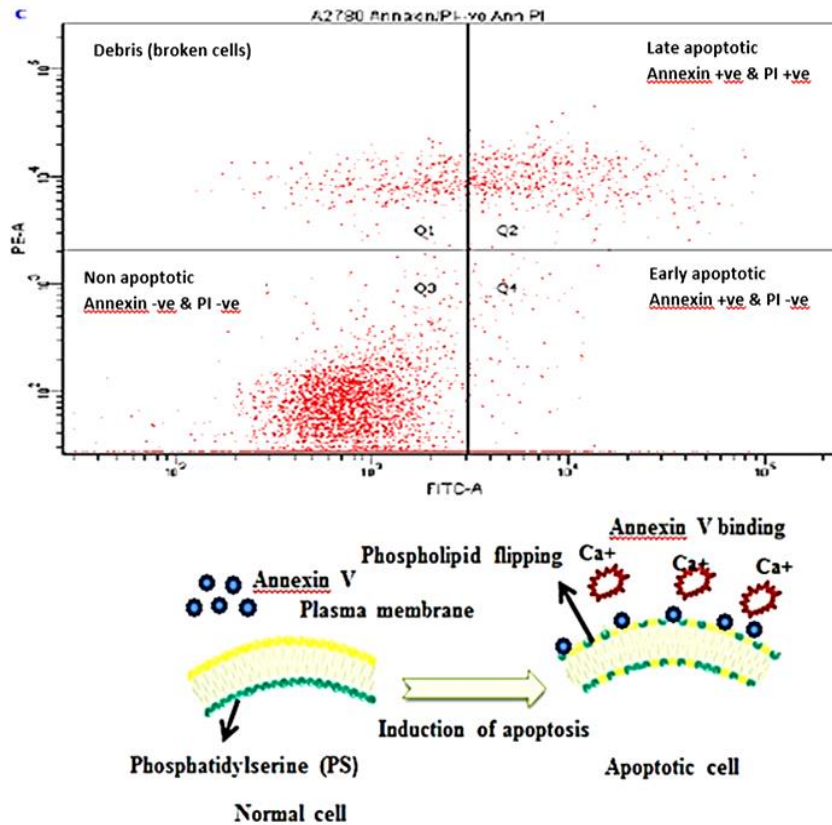


Figure 2.6 The plotted 4-quadrant gate.

The plotted 4-quadrant gate presents the four populations (non-apoptotic, early apoptotic, late apoptotic and debris) (from this thesis's results data).

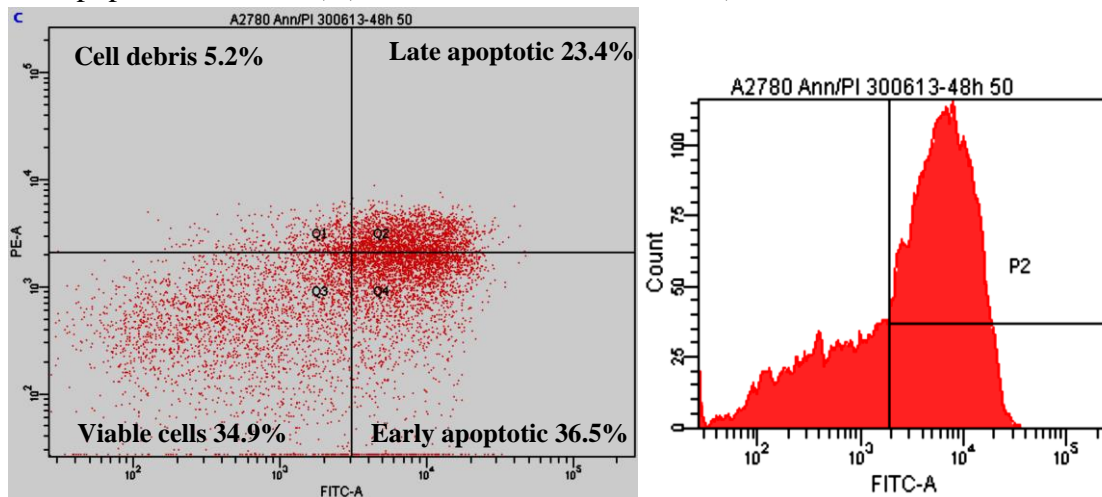


Figure 2.7 Annexin V/PI apoptosis assay.

Example cytogram (left), gates are shown on left hand image to quantify viable cells (unstained); early apoptotic cells [Annexin V labelled (FITC fluorescence)], late apoptotic cells (Annexin V and PI stained) and 'cellular debris' (PI stained only). Histogram of cell counts on right shows gate above which cells are considered positively stained and counted by the instrument (from the thesis results data).

The work was done following the kit manufacturer's instructions and each experiment

had up of 5 controls as follows: The negative control (NO stain, PI stained, Annexin V stained cells and Annexin V/PI stained) and a positive control for Annexin V/PI staining only. These controls are very important to gate each specific cell population in order to be able to run an accurate apoptosis assay.

$2-5 \times 10^5$ cells were counted and cultured in a T25 flask, and incubated at 37 °C in 5% CO₂ for 24 h for cell recovery. Next, the old media was removed and new media with different concentrations of AKBA (5µM, 10µM, 15µM, 25µM & 50µM) was added. All flasks were incubated for different times (Immediately, 6 hours, 16 hours, 24 hours, & 48 hours). After each time point all the medium from each flask was removed and transferred to a specific tube labelled with the specific treatment and time point. Then all flasks containing the treated cells were harvested as described in section 2.9.2.3 and added to the above tubes containing the washing step products. In the last step of harvesting the supernatant was discarded, then each tube was gently tapped to disburse the cells and 5 mL of medium was added. All tubes containing the cell suspension were incubated at 37 °C in 5% CO₂ incubator for 30 minutes for cell recovery. All tubes were centrifuged and cells washed with 1x PBS once, then the cells washed with 500 µL of 1x Annexin V binding buffer (50 mM HEPES, 700 mM NaCl, 12.5 mM CaCl₂, PH 7.4). Supernatant was removed completely, with the excess liquid being drained off onto a tissue. The cells were re-suspend in 195 µL 1x Annexin V binding buffer, and then 5µL of Annexin V Stain was added to the cells, mixed gently and incubated at room temperature for 10 mints. Cells were then washed with 1x Annexin V binding buffer and re-suspended in 190 µL of 1x Annexin V binding buffer. Finally 10 µL of PI (20 µg/mL) was added to each tube and the cells were diluted in 300 µL of binding buffer and analysed immediately using the BD FACS Canto™ II flow cytometer. A total of 10,000 of cells were acquired for each time. Results were obtained from at least three independent experiments (Fig 2.7). Next, the data were analysed using FACS software and plotted in graphs using prism software. The fraction of the cell population in different quadrants was analysed using quadrant statistics.

2.11.8 Western Blotting

Western blotting was used to assess a mixture of proteins modulated by AKBA treatment, by separating these proteins using SDS-polyacrylamide gel electrophoresis (SDS-PAGE). This allows the proteins to migrate according to their molecular weight. After this

the separated proteins are transferred from the gel to a nitrocellulose membrane by the application of electric current, then incubated with a blocking solution like milk to block the nonspecific binding sites. Next the membrane is incubated with a specific primary antibody for the protein of interest. Finally secondary conjugated antibodies (Conjugated with horseradish peroxidase (HRP) are applied and immediately ECL is used to visualize the protein of interest (Mahmood T. and P-C., 2012).

2.11.8.1 Protein extraction and quantification

The cells were seeded at approximately 5×10^5 cells per mL in a T75 flask and incubated overnight. Next day old media removed and new media with different concentrations of AKBA (5 μ M, 10 μ M, 15 μ M, 25 μ M, 50 μ M) was added. All flasks were incubated for different times (immediately, 6 hours, 16 hours, 24 hours, & 48 hours). Laemmli buffer (2 % w/v SDS, 10 % v/v Glycerol and 50 mM Tris-HCl, pH6.8) was heated to 95°C on a hot shaker (Grant-Bio Thermo-Shaker). At the specific time point after treatment cells were washed twice with PBS at room temperature. Proteins were extracted by suspending the cells in 500 μ l of hot Laemmli buffer followed by incubation at 95°C for 5 minutes on a hot shaker. After that the cell lysates were cooled to room temperature, samples were sheared using MSE Soniprep 150 Ultrasonic Disintegrator for 15 seconds at amplitude 14 KHZ and centrifuged briefly for a minute at 16,000 x g. The resulting supernatant (protein lysate) was collected into pre-labelled 1.5 mL Eppendorf tubes and stored at -20°C until used for protein quantification.

2.11.8.2 Quantification of extracted protein by bicinchoninic acid assay (BCA assay)

Protein concentration was determined by using a Pierce™ BCA Protein Assay kit. Bovine serum albumin (BSA, 2 mg/mL) was used as a stock solution for preparing a series of protein standard solutions by diluting in PBS (Table 2.2). A 15 μ L aliquot of protein lysate was diluted in 135 μ L of PBS (1:10). 25 μ l of each protein lysate and standard solution were transferred into 96-well plate, followed by 200 μ L of Working Reagent (provided in kit) into each loaded well. The volume of the working reagent was calculated and prepared according to the following formula: (# standards + # unknowns) \times (# replicates) \times (volume of working reagent per sample). After the well contents were mixed thoroughly on shaker for 30 seconds, the 96 well plates was incubated at 37 °C for 30 minutes and allowed to cool at room temperature. The absorbance of protein standard and samples were measured using a FLUOstar OPTIMA Multi-detection microplate reader (BMG

Labtech) at a single wavelength of 562nm. Thus, the concentrations of the protein lysates (mg/mL) were determined by plotting standard curves and corrected for the dilution factor using GraphPad Prism 6 software.

Table 2. 2 Standard dilution scheme:

Vial	Volume of BSA (μ L)	Volume of Diluents (μ L)	Final BSA Concentration (μ g/mL)
A	100 of stock	0	2,000
B	150 of stock	150	1,000
C	200 of vial B dilution	200	500
D	200 of vial C dilution	200	250
E	200 of vial D dilution	200	125
F	200 of vial E dilution	300	50
G	200 of vial F dilution	200	25
H	100 of vial G dilution	400	5
I	0	100	(Blank)

2.11.8.3 Preparation of protein lysates

The frozen protein lysates were thawed to room temperature. The volumes of each protein lysate were calculated to achieve a concentration of 20 μ g in a loading buffer containing bromophenol blue (0.005% w/V), Laemmli buffer (2% w/v SDS, 10% v/v glycerol and 50mM Tris-HCL pH 6.8) and 2-mercaptoethanol (1% v/v) to a final volume of 200 μ L. The protein samples were denatured at 99°C in a hot block for 5 minutes, followed by a brief centrifugation and stored on ice before electrophoresis.

2.11.8.4 Western Blotting technique

For further confirmation of AKBA's effects on ovarian cancer cell lines (A2780, A2780cis, UWB1.289 & OVCAR4 cells), proteins involved in apoptosis were analysed by the western blotting technique using a BioRad mini-Protean gel electrophoresis system. To prepare the gels, a 1.50 mm gel-casting apparatus was used and a SDS (resolving) gel was prepared according to the molecular weight of the protein of interest (12 % SDS gel is suitable to separate proteins in the range 20–100 kDa and 5% stacking

gels) (see Table 2.3 for composition of gels), and allowed to set for 5 to 10 minutes. A 10-well comb was inserted immediately into the stacking gel before the gel solidified. A 20 μ L aliquot of prepared protein (20 μ g protein) and 4 μ L of pre-stained protein molecular weight standard marker was loaded into the wells. The gel was then electrophoresed in running buffer (0.3% w/v Tris-HCl, 1.4% w/v glycine and 0.1% w/v SDS) and proteins were separated at 160V for 1 hour. After electrophoresis, the SDS-PAGE gel was soaked in a cold transfer buffer (0.3% w/v Tris-HCl, 1.4% w/v glycine and 20% v/v methanol) and proteins were electro transferred onto a PVDF membrane at 25 V overnight or 100 V for 1 hour.

To determine the successful transfer of protein, the membrane was stained with Ponceau S red dye to visualize the protein bands that had been separated and then washed with ultrapure water twice to remove excess dye. After washing with TBST (50 mM Tris-base pH 7.65, 150 mM sodium chloride and 0.1% v/v Tween-20) once, membrane was blocked with TBST-milk (1g of dried, skimmed milk in 20 mL TBST) for 1 hour at room temperature with shaking (20 rpm) and this was followed by washing again for 5 minutes in TBST twice.

Table 2. 3 Summary of the composition of 12% SDS-PAGE gels:

Compositions: Volume of compositions per gel (ml).

	Resolving	5 % Stacking
Ultrapure water	3.3	1.4
30% acrylamide	4.0	0.33
Tris-Cl (1.5M, pH 8.8)	2.5	0.25
10% SDS	0.1	0.02
10% ammonium persulphate	0.1	0.02
TEMED	0.004	0.002

The membrane was then incubated in a cocktail of primary antibodies (pro- and cleaved caspase 3, cleaved-PARP and muscle actin) at a dilution of 1:8000 (according to the kit manufacturer's instruction) in TBST-5% w/v BSA for 1 hour at room temperature on a rotator at 6 rpm or overnight at 4°C on shaker. p16 and p21 antibodies were tested individually as they had been ordered separately. Next, the membrane was washed 5 times

in TBST with agitation. Then the membrane was incubated with secondary antibody horseradish peroxidase (HRP)-conjugated goat anti-rabbit antibody (dilute of 1:5 in TBST-milk) for 1 hour with shaking at room temperature. Any unbound antibodies were removed by applying a further 5 washes with TBST, allowing 5 minutes for each wash. The immune reactivity of antibodies that bound to proteins on the membrane was detected by using HRP chemiluminescent (ECL) substrate reagent for 1 min at room temperature. Subsequently the membrane was wrapped in Saran Wrap, placed in a cassette, exposed to X-ray film and the latter developed using an X-ray film processor (Agfa Curix-60). All western blotting materials were cleaned with 70% v/v IMS before use to prevent unnecessary background signal. Protein band intensities were calculated as absorbance units/mm² by densitometry using SyngeneGeneSnap software (Syngene, UK). The protein band intensities were normalized to actin. Each protein was assessed from at least three independent experiments.

2.11.9 Gene expression

2.11.9.1 Analysis using Micro-Array

Firstly, the cells were seeded at approximately 5×10^5 cells/mL in a T25 flask and incubated overnight. The next day the old medium was removed and new medium with different concentrations of AKBA (10 μ M, 15 μ M, 25 μ M & 50 μ M) added. All flasks were incubated for different times (6 hours, 16 hours and 24 hours). After each treatment time cells were washed with PBS and trypsinised using 1X trypsin EDTA. Cells were then washed with cold medium and the cell pellet stored at -80°C.

Whole-transcriptome profiling was performed using the Illumina HumanHT-12 v4 Expression BeadChip which allows parallel quantification of 48,000 transcripts. Total RNA was extracted using on a Promega Maxwell® 16 System using the Maxwell® 16 LEV simplyRNA Purification Kit according to manufacturer's protocol. RNA quality was assessed on an Agilent Bioanalyzer and the samples with an RNA integrity Number (RIN) < 7 were excluded (Fig 2.10).

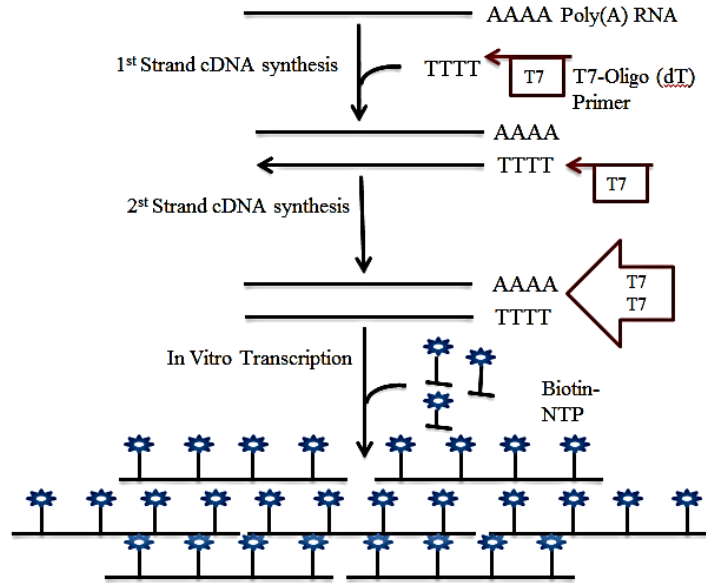


Figure 2. 8 The cDNA synthesis using TargetAmp™-Nano Labeling Kit for Illumina® Expression BeadChip steps.

Secondly, cRNA was then prepared using the TargetAmp™- Nano Labeling Kit for Illumina® Expression BeadChip (Epicentre) according to manufacturer instructions. Briefly, first-strand cDNA was synthesized from total RNA using oligo(dT)-primers containing a phage T7 RNA Polymerase promoter sequence at its 5' end. The reaction was performed at 50°C for 30 minutes using the SuperScript III reverse transcriptase (Invitrogen). Second strand cDNA was then synthesized from the obtained cDNA at 65°C for 10 minutes using a 2nd strand DNA polymerase. Lastly, anti-sense RNA was synthesized and Biotin-labelled in a single reaction that utilizes the 2nd strand cDNA as a template. The reaction was catalysed by a T7 RNA polymerase and the biotin-labelling was enabled by the use of biotin-UTP in the reaction (Fig 2.8). The size and concentration of each library was quantified using the Agilent Bioanalyzer (Fig 2.10).

Assay Class: Eukaryote Total RNA Nano
 Data Path: C:\...Eukaryote Total RNA Nano_DE729C
Electrophoresis File Run Summary

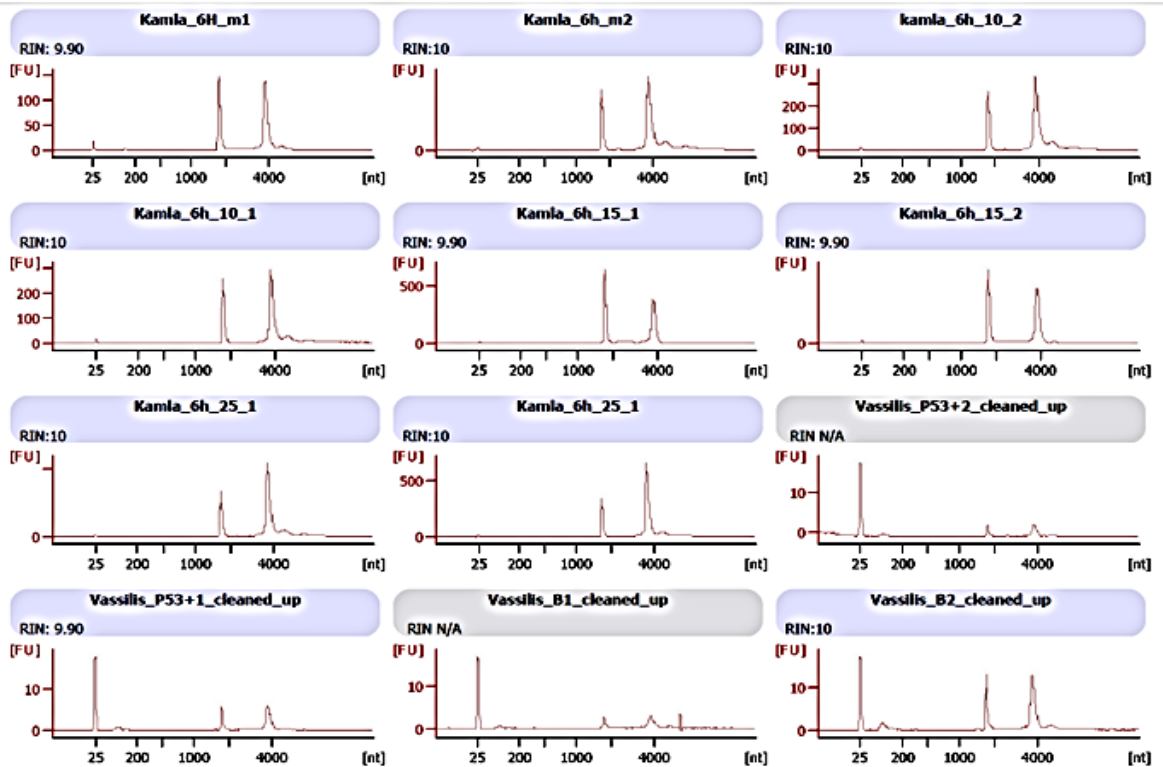
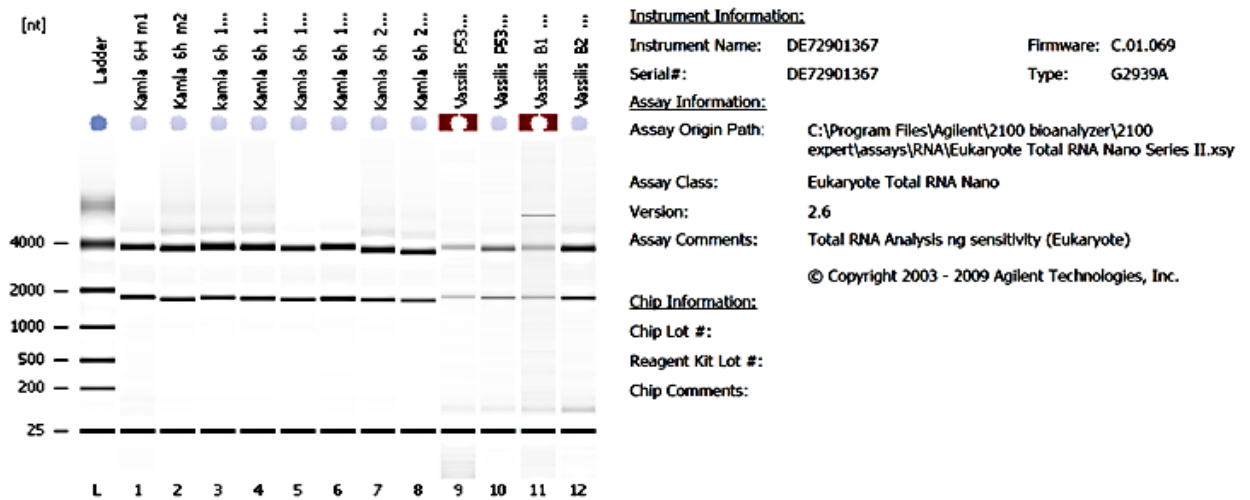


Figure 2. 9 The total RNA analysis in ng using Agilent 2100 bioanalyser. Nanoseries II.

Thirdly, each library was then hybridized on the Illumina Beadchips. Hybridization was conducted at 58°C overnight. The Beadchips were then subjected to a series of washing steps (10 minutes at 55°C in Illumina High temperature wash buffer, 10 minutes at room temperature in 100% ethanol, 2 minutes at room temperature in Illumina wash buffer) before being scanned using an Illumina Scan (Fig 2.11). The raw microarray data were

normalized by quantile normalization using the Illumina Genome Studio V2011.1. No background correction was applied. The probes with a signal intensity below the background level were considered as not confidently detected and were excluded from the downstream analysis. This profiling was performed in the Genomic Core Facility of the University of Leicester which is run by Dr. Nicolas Sylvius.

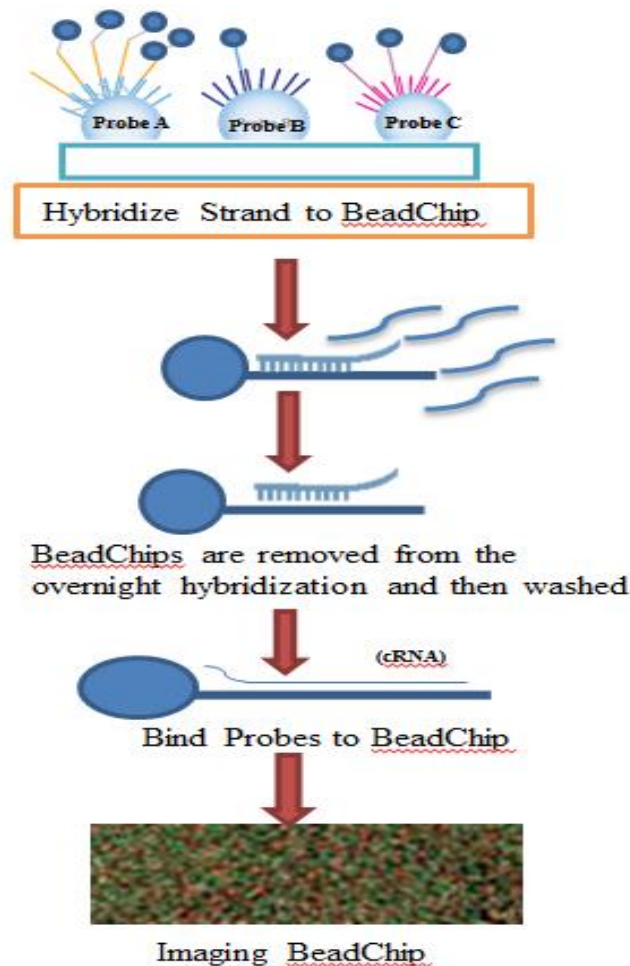


Figure 2. 10 Direct Hybridization Assay Workflow from ILLUMINA Whole-Genome Gene Expression Direct Hybridization Assay Guide.

The above sections describe the overall Direct Hybridization Assay workflow for Twelve-sample BeadChips. Detailed descriptions of each step are described in the Illumina Whole-Genome Gene Expression Direct Hybridization Assay workflow.

The BeadChip™ platform offers twelve-sample whole-genome formats:

Each array in the matrix holds tens of thousands of different oligonucleotide probe sequences. These are attached to 3-micron beads that are assembled into the micro-wells of the BeadChip substrate. Because the micro-wells outnumber probe sequences, multiple

copies of each bead type are present in the array. This built-in redundancy improves robustness and measurement precision. The BeadChip manufacturing process includes hybridization-based quality control of each array feature, allowing consistent production of high-quality, reproducible arrays (cRNA).

2.11.9.2 Microarray data analysis:

Results were analysed using Array-Track Microarray Data Analysis software from <http://www.fda.gov/ScienceResearch/BioinformaticsTools/Arraytrack/>

The filtered data (normalised by taking \log_{10} of the results) was provided by Nicolas Sylvius in Excel spreadsheet. Data were subsequently analysed using the Array Track programme using t-test and filtered by p value <0.001 and fold change of 1.8 or greater. More details will be described in the results chapter (5).

2.11.10 Quantitative-PCR (Q-PCR)

2.11.10.1 Sample preparations for Q-PCR

2.11.9.1.1 RNA extraction: TaqMan® Gene Expression Cells-to-CT™ Kit:

Cell number was optimised following the TaqMan® Gene Expression Cells-to-CT™ Kit protocol with slight variation depending in the cell type.

The cells were seeded at approximately 20×10^5 cells/mL in a T25 flask and incubated overnight. Next day old medium was removed and new medium with different concentrations of AKBA (5 μ M, 10 μ M, 15 μ M, 25 μ M, 50 μ M) was added. All flasks were incubated for 6 hours and 16 hours. After each time point cells were washed with PBS and trypsinised using 1X trypsin EDTA. Cells were then washed with cold medium and centrifuged, and then the supernatant discarded. After that cell were again washed, and after centrifugation re-suspend again with 2 ml of ice cold PBS and transferred to 2 pre-labelled Eppendorf tubes (each tube contains around 10×10^5 cells). This experiment was done in parallel with the micro-array sample preparations. Then cells were centrifuged and kept on ice ready for extraction. Immediately RNA extraction was started using cells in the CT kit as described in figure 2.12 and stored at -20°C .

2.11.9.1.2 DNA quantification

The cDNA was quantified using a Qubit™ Fluorometer according to the manufacturer's protocol. The Qubit™ working solution was prepared by diluting the Qubit™ dsDNA

HS reagent 1:200 in Qubit™ dsDNA HS buffer, and the standards (0 ng and 10 ng dsDNA) were prepared by adding 190 µL of Qubit™ working solution and 10 µL of each Qubit™ standard to a Qubit® Assay Tube and mixed using vortex for 2–3 seconds. After that, the cDNA sample was prepared by adding 195 µL of Qubit™ working solution and 5 µL of the sample to a tube and vortexed for 2–3 seconds. All tubes were incubated at room temperature for two minutes. Following the incubation, the standards were run using a Qubit® Fluorometer for instrument calibration, next the sample was measured. Then, the cDNA concentration was calculated using the following equation 2.3:

$$\text{Concentration of sample} = \text{QF value} \times (200 / X)$$

Where: QF value = the value given by the Qubit X 2.0 Fluorometer

X = the number of microliters of samples added to the assay tube

Equation 2.3 Formula for calculating DNA concentration.

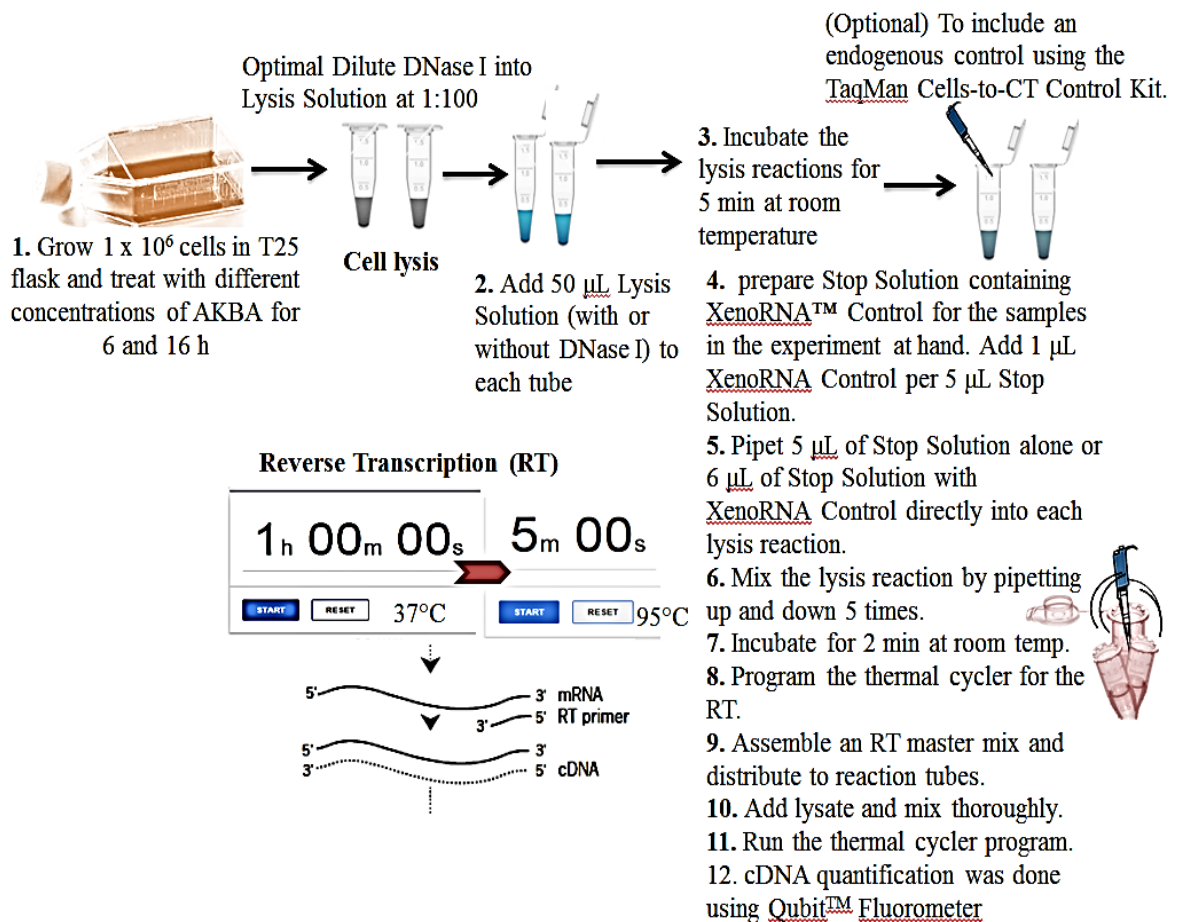


Figure 2.11 TaqMan® Gene Expression Cells-to-CT™ Procedure Overview

2.11.10.2 Quantitative RT-PCR analysis

Quantitative RT-PCR analysis was undertaken in order to confirm the apoptotic genes affected by AKBA as assessed by Microarray analysis. A QPCR Applied Biosystems®

TaqMan® Array Human Apoptosis, which made up of a 96-well Plate contains 92 assays for apoptosis associated genes (along with 4 assays as a candidate endogenous control genes) was used. These TaqMan® Array 96 well Plates are made up of a single TaqMan® Assay for each well (single primer for each gene). This plate is specific and pre-configured for the most appropriate TaqMan® Gene Expression Assays involved in apoptosis. The plate contains most genes involved in apoptosis pathway, and four endogenous controls. Each gene primer is dried-down in separate wells, ready for accurate assessment of an entire gene signature in one experiment. The apoptosis pathway panel targets genes from the death receptor regulated pathway and the BCL-2 family pathway. In this study, apoptosis pathway assessment was considered a confirmation of the apoptosis genes expressed by microarray.

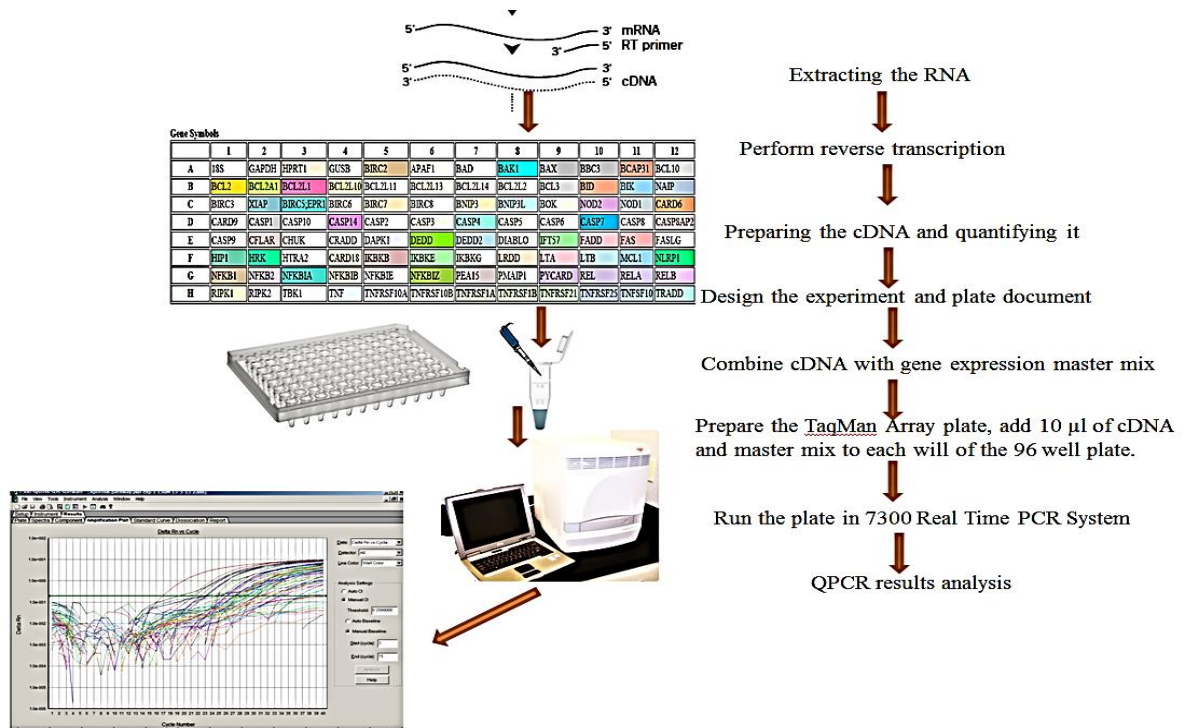


Figure 2.12 TaqMan® Gene Expression Array plate work flow.

After preparing the cDNA sample using the cells to CT kit, samples were processed for QPCR using the QPCR TaqMan Array Human Apoptosis Plate for confirmation of the microarray results focusing on apoptosis pathways. Analysis allowed quantification of the extent of gene expression up- or down-regulation in the apoptosis pathway (Fig 2.12). Samples stored at -20 °C and allowed to thaw on ice; at the same time QPCR 7300 machine was switched on and allowed to warm up, and the gene expression Master Mix X2 was kept on ice as well. While samples were thawing the QPCR TaqMan Array

Human Apoptosis Plate was centrifuged at 2000 rpm for 5 minutes to make sure that all the lyophilised primers were on the bottom of the 96 well plates to avoid cross contaminations. 10 ng of cDNA was prepared and diluted with a volume of 1.5 ml from each treatment. The plastic cover on the top of the plate was removed carefully and precisely. In a separate 1.5 mL eppendorf tube 550 μ of TaqMan® Gene Expression Master Mix (2 \times) (ready to use) was added to 550 μ L of cDNA sample in the same tube, which then mixed together. Immediately 10 μ L of the cDNA and the master mix suspension were added carefully to each well of the 96 QPCR TaqMan Array Human Apoptosis Plate. After that, the plate was carefully covered and sealed using the MicroAmp® Optical Adhesive Film. The plate was then centrifuged at 2000 rpm for 2 minutes. Finally, the plate was loaded in the QPCR 7300 according to specific thermal cycling conditions profile supplied by the plate manufacturer. The PCR parameters included firstly a 2 min denaturation step at 50 °C, and then 95 °C for 10 min, followed by 40 cycles of 15 s at 95 °C, and 10 min at 60 °C (Fig 2.12).

In this experiment: all preparations were done on ice and TaqMan® Array Fast Plates were run using standard run thermal cycling parameters and TaqMan® Fast Universal PCR Master Mix (2 \times). Each treatment was done twice and run in duplicate.

Table 2. 4 QPCR conditions for TaqMan® Array Plates run on QPCR 7300:

	Hold†	Hold‡	PCR (40 cycles)	
			Melt	Anneal/Extend
Temp	50 °C	95 °C	95 °C	60 °C
Time	2:00	10:00	0:15	1:00

The data were then analysed by observing the amplification plots for the entire plate. After setting the baseline and threshold values the comparative CT method was used to analyse the data.

2.11.11 Statistical Analysis

All statistical analyses were performed using GraphPad Prism. The statistical differences between control and treated cells were determined using a two-way ANOVA test. Data were presented as mean \pm standard error of the mean (SEM). A p value less than 0.05 was considered statistically significant.

Chapter 3

Investigations for the ability of AKBA to address cisplatin resistance in ovarian cancer cell lines

3.1 Introduction

3.1.1 Ovarian Cancer:

The vast majority (around 90%) of ovarian cancers originate in the epithelial layer of the ovaries and symptoms include frequent urination, difficulty in eating due to an abdominal mass, tiredness and pelvic pain (Coleman et al., 2011b). At the cellular level, there are two distinct subtypes of ovarian epithelial cell tumour, Type I and Type II. Whereas Type I tumours are localised to the ovary, Type II tumours are aggressive and consist of undifferentiated cells that have the capability to spread or to metastasise and so disseminate cancer cells around the body (Kurman and Shih Ie, 2010).

Advances have been made in chemotherapeutic treatments; for example administering chemotherapeutic drugs intraperitoneally has been shown to increase survival in patients with stage IIIc epithelial ovarian adenocarcinomas (Armstrong et al., 2006), even though the majority of these patients relapse, and ultimately develop resistance to first line chemotherapy. Therefore, there is an urgent need to understand mechanisms of chemo-resistance in ovarian cancer and to design strategies to overcome this resistance.

Combination chemotherapy represents a standard treatment for patients with ovarian cancer. The drugs are generally platinum-based. However, treatments result in resistance in approximately one-third of cases (Stewart et al., 2006). Cisplatin resistance significantly reduces the effectiveness of the treatments and the cellular mechanisms that determine resistance are not well understood (Zhu et al., 2005). Researchers performed a proteomic analysis to elucidate the proteins expressed in cisplatin-resistant ovarian cancer cells but not in sensitive cell lines (Stewart et al., 2006). The authors reported 58 proteins with a five-fold or higher expression compared with sensitive cells. These proteins included the recognition molecule CASPR3, S100 protein family members, junction adhesion molecule Claudin 4 and CDC42-binding protein kinase β (Stewart et al., 2006). In an effort to uncover the mechanisms of cisplatin resistance in ovarian cancer, the A2780cis cell line was developed by chronic exposure of the sensitive A2780 ovarian cancer cell line to cisplatin. A2780cis was demonstrated to have a 6.7-fold resistance to cisplatin ($IC_{50} = 23.4\mu M$), compared with the sensitive cell-line ($IC_{50} = 3.5\mu M$) (Pan B. et al., 2002). The exact mechanism of this resistance is as yet to be identified, however it has been shown that A2780cis exhibits a higher cisplatin efflux rate (Kalayda et al., 2008).

3.1.2 AKBA therapeutic effect in cisplatin resistant cell line

Recently, many research studies have focused on the use of AKBA as anticancer therapeutic agent in different types of cancers. AKBA has been known to reduce inflammation and boswellic acids are known to cause cell death by promoting apoptosis in various tissues (Glaser et al., 1999, Liu et al., 2002b, Syrovets et al., 2005), accompanied by increased caspase activity (Liu et al., 2002b, Riedl and Shi, 2004). Therefore, the possibility exists that boswellic acids could form the basis for novel anticancer therapies. Apoptosis induction has been observed in human promyelocytic leukemia (HL-60) cells, where boswellic acid led to decreased cell proliferation and increased cell differentiation (Jing et al., 1992). Jing et al. (1992) reported that HL-60 cells underwent morphological changes and DNA damage occurred and these cytotoxic effects were replicated separately in HL-60 cells treated with AKBA (Hoernlein et al., 1999b). Boswellic acids also inhibit DNA and RNA replication and protein-synthesis (Shao et al., 1998) in a mechanism of that is not associated with free radical scavenging (Upaganlawar and Ghule, 2009). Additionally, *in vitro* cell culture studies have determined a mechanism for AKBA-induced apoptosis by causing interruption to the cell cycle at G1, leading to a marked decrease in concentrations of cyclin D1, cyclin- E, CDK-2, CDK-4 and pRb and an associated increase in p21 levels which is marker of cell cycle arrest and cell senescence (Liu et al., 2006).

The availability of a range of cell lines has allowed the cytotoxic effect of boswellic acids to be elucidated in many cancer cell culture systems. Several studies have identified boswellic acid-induced apoptosis in a range of cancer types including: glioblastoma, leukaemia (Hostanska et al., 2002), human leukemic lymphoblast (Hoernlein et al., 1999b), human myeloid leukaemia (Xia et al., 2005), liver cancer (Liu et al., 2002a), brain tumours (Hostanska et al., 2002), colon cancer (Liu et al., 2006, Liu et al., 2002b), prostate cancer (Syrovets et al., 2005) and fibro-sarcoma (Zhao et al., 2003). However, no such activity has been reported to date in ovarian cancer.

Aim

The aim of this Section of the thesis is to investigate the ability of AKBA to be an effective agent in addressing cisplatin resistance ovarian cancer cell lines.

Summary of the techniques/approach

Cisplatin sensitive and resistant ovarian cells were treated with AKBA at different concentrations and for different times.

Modulation of cell viability/proliferation and cell death by AKBA was investigated in all ovarian cell lines using a light microscope at 40X magnification to analyse the changes in cell growth and identify any morphological changes in the cells. In addition, cell viability was examined by the Almar Blue assay, a Beckman Coulter Counter was used to assess cell number. Damage to DNA was assessed using the comet assay, whilst cell cycle status and apoptosis were tested using flow cytometry (PI staining and Annexin V/PI staining). The temporal association and regulation of AKBA modulated protein expression was identified by western blotting. All the materials and methods used for this chapter have been described in Chapter 2.

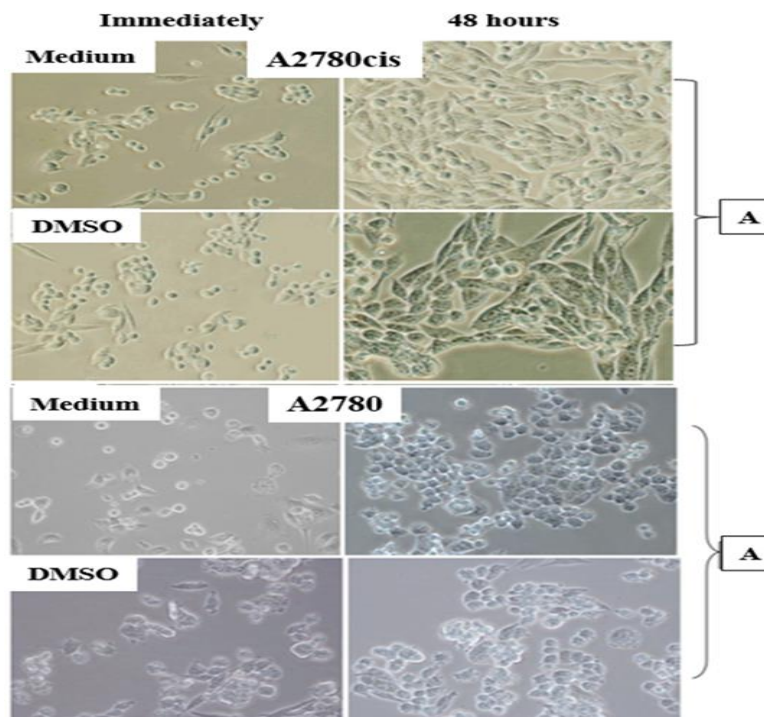
3.2 Results

3.2.1 The effect of AKBA on cell growth and proliferation

3.2.1.1 Effect of AKBA on cell structure and morphology using light microscopy

In order to examine the effect of AKBA on the morphology of exposed cells, images were taken of the cultured cell lines after treatment at different times and different concentrations of AKBA, using an Nikon Eclipse microscope TE 200-4 with 40X magnifications (Figure 3.1.1).

After 48 hours exposure to AKBA, cells of the cisplatin-sensitive human ovarian carcinoma cell line, A2780 were morphologically distinct from cells cultured in medium (+/- DMSO) (Fig 3.1.1). The most considerable effect was observed at AKBA concentrations starting at 15 μM and becoming more apparent as the concentration of AKBA increased at 16 h of exposure (Fig 3.1.1 & Fig 3.1.2). At the highest AKBA concentration (50 μM), microscopic visualisation revealed considerably smaller, floating and more fragmented cells than at lower concentrations or in the control samples. The cisplatin-resistant form of A2780 (A2780cis) had a distinctive elongated morphology when grown in culture medium (Fig 3.1.1), which became smaller and more rounded as after the addition of AKBA at higher concentrations (25 μM -50 μM). These changes in morphology were accompanied by growth inhibition in A2780cis cells at the same concentrations after 6 -16 hours.



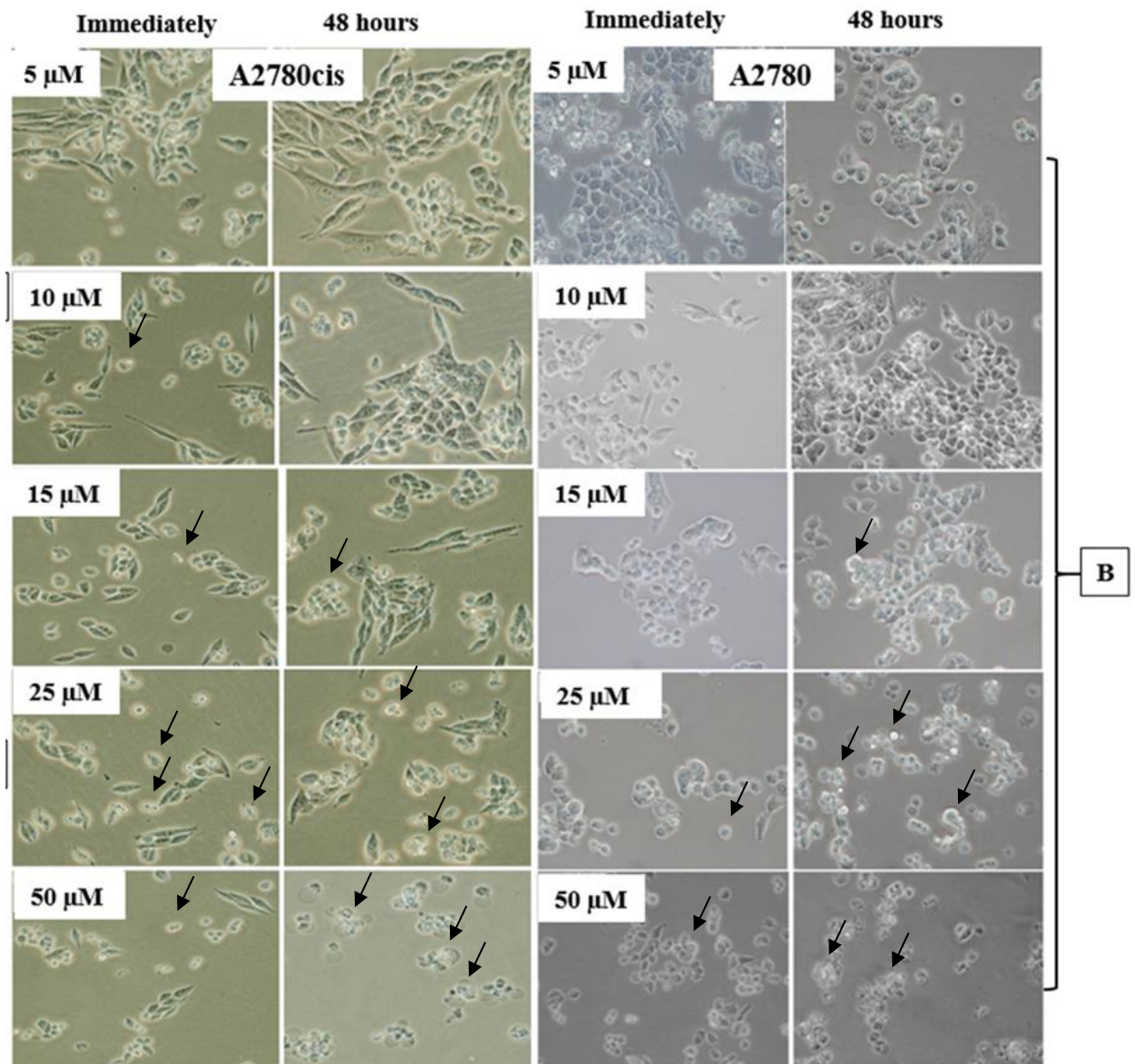


Figure 3.1. 1 Microscopic images of A2780 cell line cells exposed to AKBA.

Negative control samples (A) consist of cell culture medium, and 0.5% (v/v) DMSO. Cells challenged with AKBA (B) were grown for 24 hours in cell culture medium to recover before AKBA was added at various concentrations (μM) and examined immediately, 6 h, 16 h, 24 h and 48 h (dead cells shown using the black arrows).

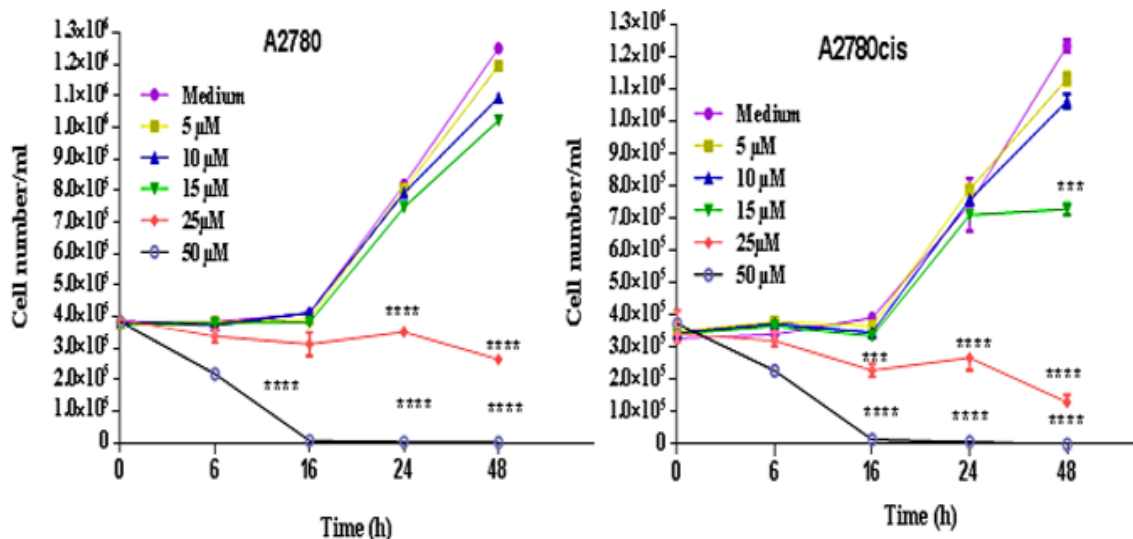


Figure 3.1. 2 AKBA-induced cell growth inhibition in A2780 & A2780cis

Cells were treated with a range of concentrations and cell growth (cell number) compared with negative controls: culture medium (media), 0.5%DMSO. The number of cells was analysed using a cell counter. Results were expressed as mean \pm SEM and are the mean of three separate experiments. * $P < 0.05$, ** $P < 0.01$, *** $P < 0.001$ and **** $P < 0.0001$ compared to control.

3.1.2.1.2 Effect of AKBA on the inhibition of cell growth

In order to test the hypothesis that AKBA causes cell growth inhibition in ovarian cancer cell lines, A2780 cells were exposed to a range of concentrations of AKBA (5 μ M-50 μ M). Cell growth inhibition was tested and recorded using different techniques; cell counting and proliferation using a cell counter and cell viability assessed by the Almar Blue assay at various time points over 48 hours (Fig. 3.1.2- 3.1.3). In each experiment, the effects of AKBA were compared with negative control cells grown in media only and using 0.5% v/v DMSO as vehicle control.

The effect of high concentrations of AKBA was even more pronounced in A2780cis cells, which decreased cell numbers to below detectable limits after 24 hours. After 24 hours, exposure to the 25 μ M concentration there was a significant decrease in cell growth ($P < 0.0001$) a trend that continued after 48 hours exposure. In contrast, by 48 hours an effective dose of 15 μ M AKBA was sufficient to cause a significant inhibition of growth of A2780cis cells (Fig 3.1.1- Fig 3.1.3) ($P < 0.0001$).

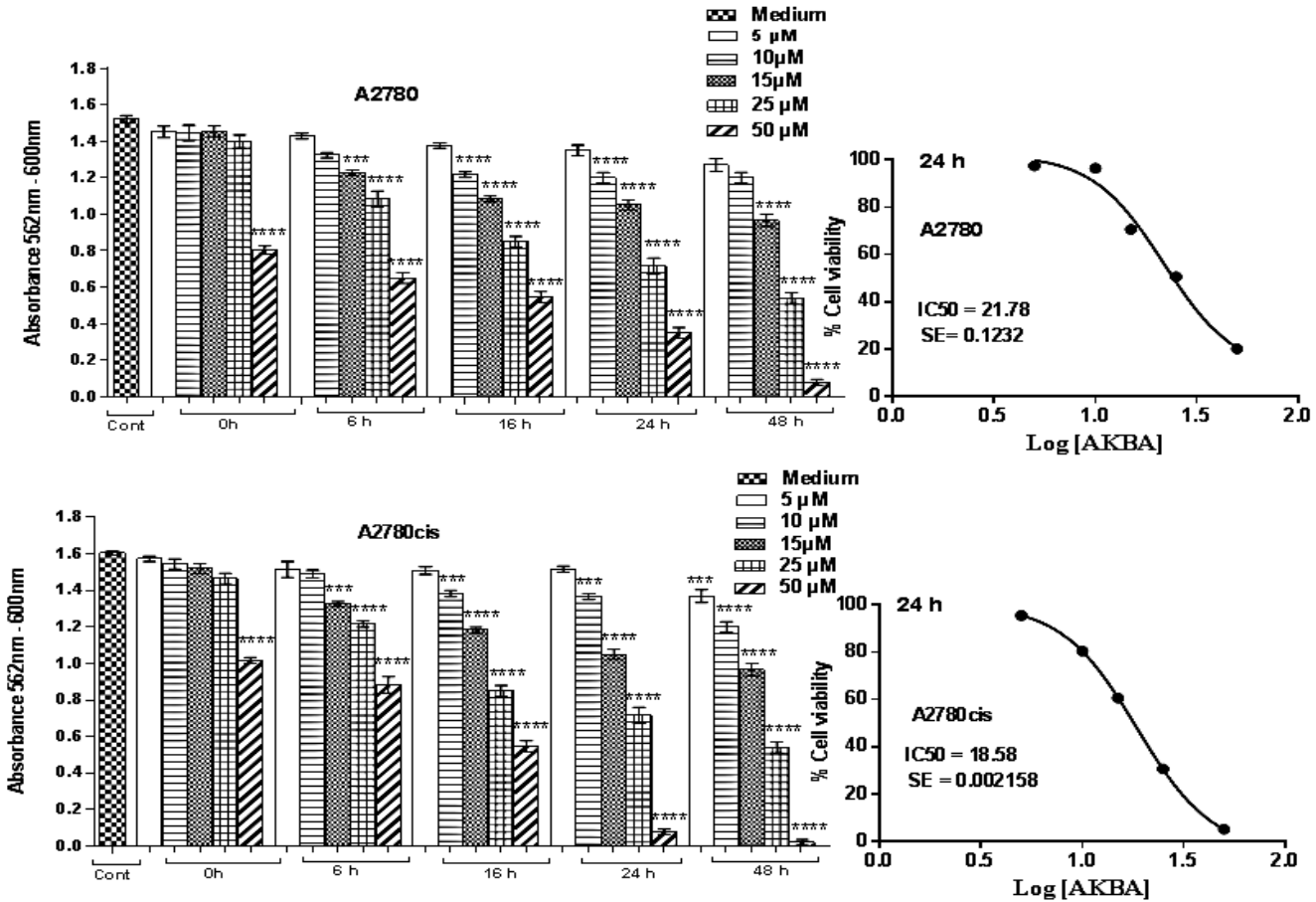


Figure 3.1. 3 AKBA induced cell growth inhibition in A2780 & A2780cis cells.

A2780 with IC50 of 21.78 μM and A2780cis with IC50 of 18.58 μM at a range of concentrations, compared with negative controls: culture medium (media), 0.5% DMSO. The inhibition of cells growth was analysed using Almar blue with the plate reader at wavelength of 562-600 nm. Results are expressed as mean ± SEM and are representative of 3 independent experiments, (*P<0.05, **P<0.01, ***P<0.001 and ****P<0.0001).

In both cell lines, lower concentrations of AKBA, (<10 μ M) did not have a significant impact on cell growth and there was a less dramatic overall morphological effect on the cells although small populations of cells did show distinctive apoptotic-like morphology upon exposure to AKBA at concentrations of 10 μ M. Overall, the effect on cell morphology appeared less pronounced in A2780cis than its cisplatin-sensitive counterpart. However, the effective lethal dose was lower in A2780cis cells than in A2780 (IC₅₀ A2780cis = 18.6 μ M; IC₅₀ A2780 = 21.8 μ M) using Almar Blue assay (P<0.01), indicating that A2780cis cells were less able to survive exposure to AKBA (Fig 3.1.3).

3.2.2 The effect of AKBA on the cell cycle

It was found that the highest AKBA concentration triggered an immediate cell cycle arrest of A2780 and A2780cis cells, causing a significantly increased population of cells to be held at the sub-G1 stage of cell death, and a significant decrease of cells in the G1 phase. Over a longer exposure time (48 hours), sub-G1/G1 in A2780cis cell was evident at concentrations as low as 10 μ M AKBA (Fig 3.2.3). More than 80 % of cells exposed to the highest concentration of AKBA for 48 hours remained in the sub-G1 stage, which represent the dead cells or the cells in the apoptotic process, with approximately 5 % of both cell line populations presented in other stages of the cell cycle (Fig 3.2.1 & Fig 3.2.2).

The effect of AKBA on the cisplatin-sensitive A2780 cell line was broadly similar to the cisplatin-resistant version. Addition of 50 μ M AKBA immediately increased the number of cells in the sub-G1 phase (Fig 3.2.1) in A2780cis, resulting in approximately 7-fold increase in the proportion of cells in this dormant state of the cell cycle, compared with the control samples. After 48 hours, addition of AKBA at concentrations as low as 10 μ M were sufficient to cause a significant increase in the number of cells in sub-G1. However the most dramatic effect was seen after 48 hours, when exposure to 50 μ M AKBA resulted in nearly three-quarters of the population being in the G1 phase (Fig 3.2.1 & Fig 3.2.2). The subG1/G1 effect of AKBA was almost twice as potent as the topoisomerase inhibitor chemical, etoposide (used at 50 μ M) included in the experiment as a positive control. Based on the results of the experiments studying apoptosis, it is clear that the G1 and other phases of the cell cycle arrest stages were followed by programmed cell death in both A2780 and A2780cis. Which means that the cells in G1, G2/M and S phase have already entered cell cycle arrest and did not pass the check points, so they are well

progressed in terms of programmed cells death and that were evident by the increases in cell shifted to subG1 cell populations with all the different concentrations and with the progress in the AKBA exposure time. Both early and late apoptotic cells were observed at highest AKBA concentrations in A2780 cells after 48 hours (Fig 3.3.2), with exposure to a minimum concentration of 15 μM resulting in a significant increase in apoptotic cells, and a decrease in viable cells compared with control samples. This effect was more significantly seen with the cisplatin resistance cell line (A2780cis) mainly with 15 μM to 50 μM AKBA even with lower time of exposure 16 h, 24 h and 48 h (Fig 3.2.1).

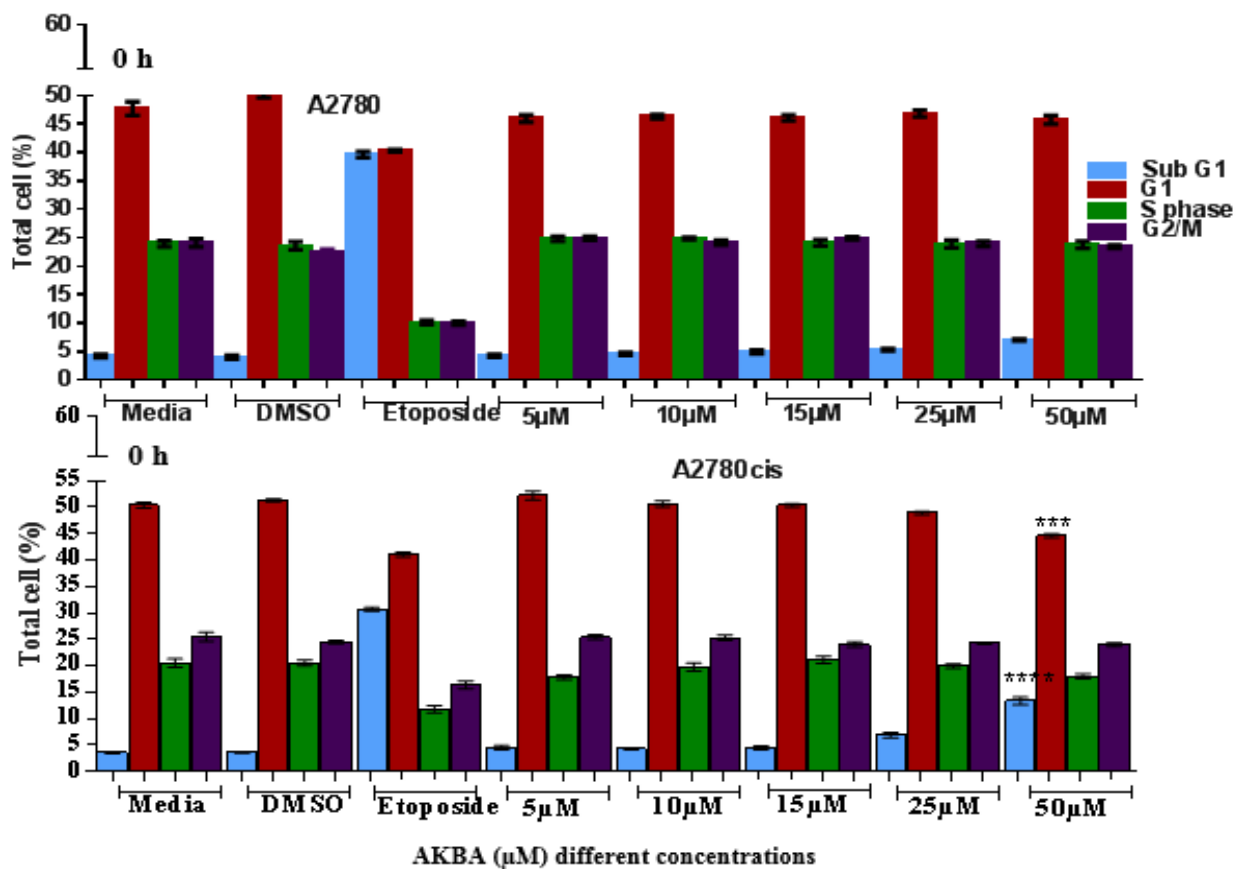


Figure 3.2. 1 Immediate exposure with AKBA to assess cell cycle arrest in A2780 and A2780cis cells.

Cells were exposed to arrange of concentrations and compared with negative controls: culture medium (media), 0.5%DMSO. Results were expressed as Mean \pm SEM and are representative of three independent experiments. * $P < 0.05$, ** $P < 0.01$, *** $P < 0.001$ and **** $P < 0.0001$ compared to control.

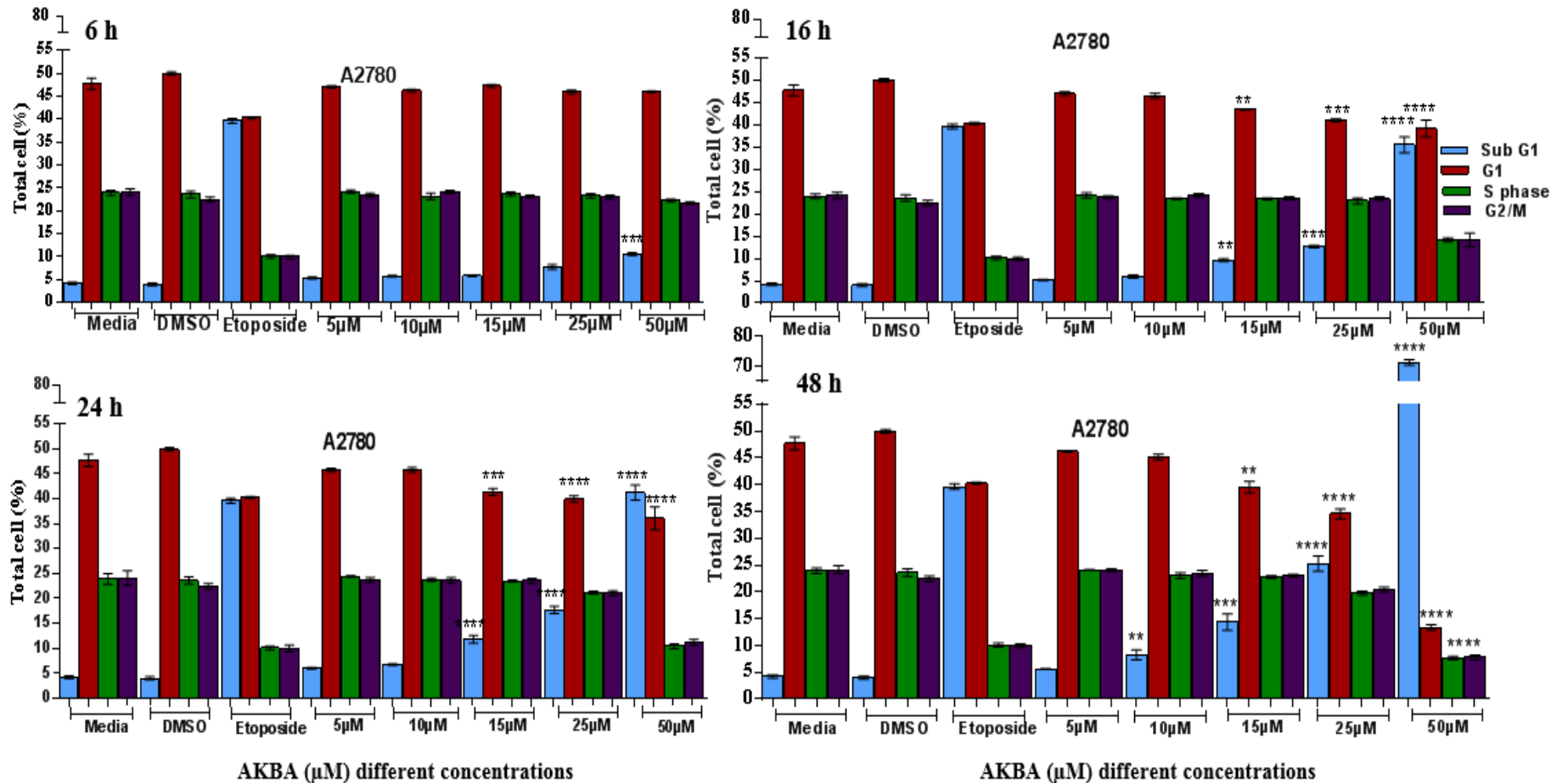


Figure 3.2. 2 AKBA exposure for different time points, to assess cell cycle arrest in A2780 cells at a range of concentrations.

Cells were exposed to a range of concentrations and compared with negative controls: culture medium (media), 0.5%DMSO. Results are expressed as Mean \pm SEM and representative of three independent experiments. * $P < 0.05$, ** $P < 0.01$, *** $P < 0.001$ and **** $P < 0.0001$ compared to control.

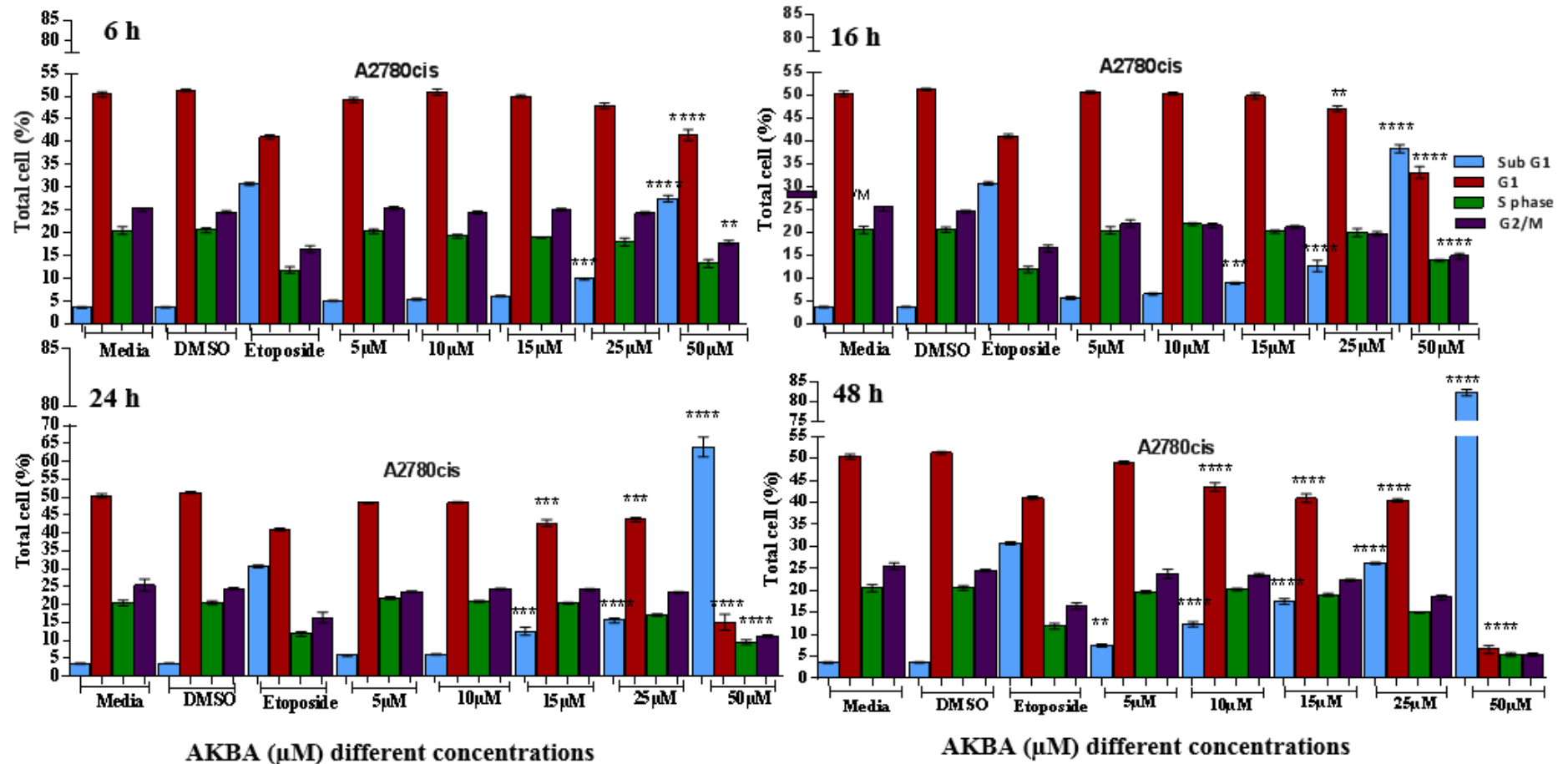


Figure 3.2. 3 AKBA exposure for different time points, to assess cell cycle arrest in A2780cis cells at a range of concentrations.

Cells were exposed to a range of concentrations and compared with negative controls: culture medium (media), 0.5% DMSO. Results are expressed as Mean \pm SEM and are representative of three independent experiments. *P<0.05, **P<0.01, ***P<0.001 and ****P<0.0001 compared to control.

3.2.3 AKBA induces apoptosis

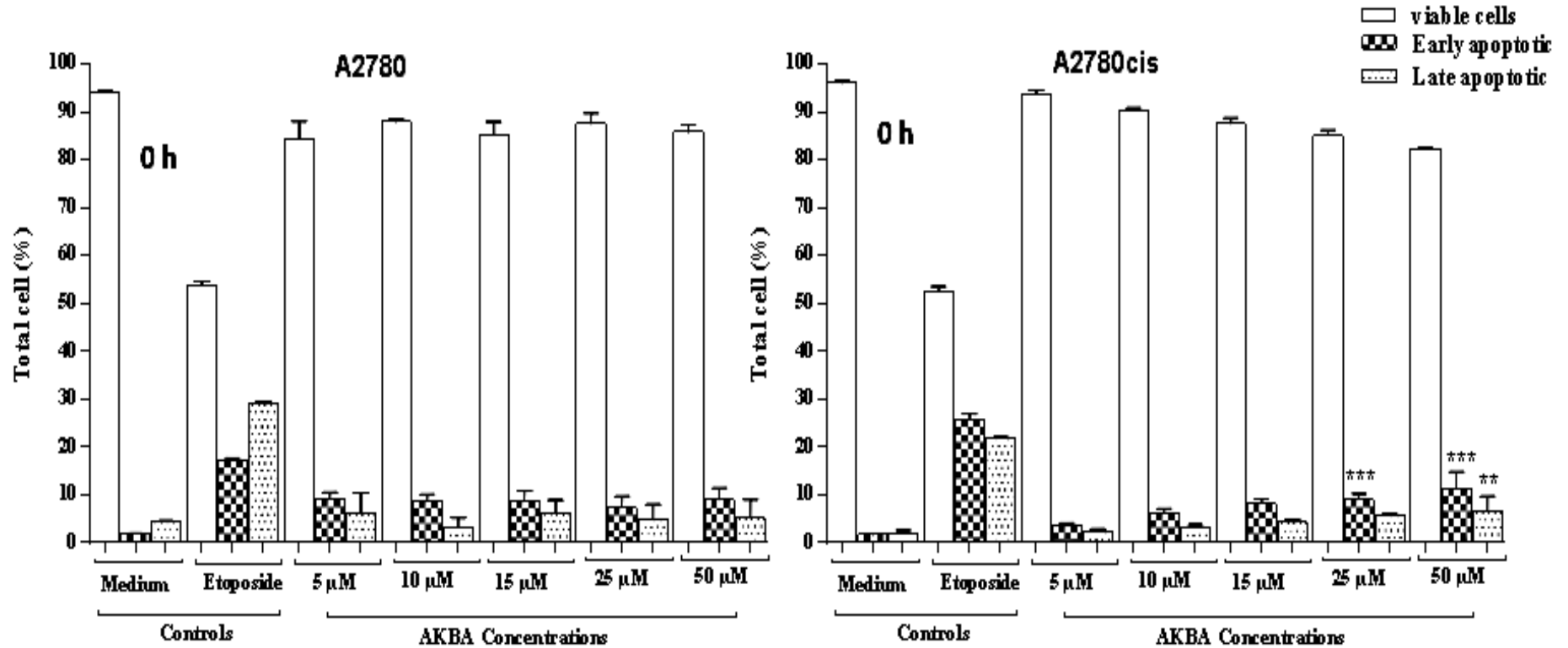


Figure 3.3. 1 Immediate exposure with AKBA to assess cell death in A2780 and A2780cis cells.

Cells were exposed to a range of concentrations and compared with negative controls: culture medium (media), 0.5% DMSO. Results were expressed as Mean \pm SEM and are representative of three independent experiments. *P<0.05, **P<0.01, ***P<0.001 and ****P<0.0001 compared to control.

Based on the cell cycle arrest data it appears that AKBA has the potential to cause an early effect on cell cycle, as cells were noted to immediately (within 30 mins) enter SubG1 after 50 μ M treatment ($P < 0.001$). After exposure to high levels of AKBA there were a high proportion of cells did not progress to G1 (cell growth), remain instead either in a non-active state (G0), or undergoing cell death by presenting at the Sub G1 stage. This immediate effect was particularly evident in the cisplatin resistant A2780cis line (fig 3.2.3), which showed a cell death, resulting in a significantly decreased population of cells in the G1 stage of growth, even at relatively low AKBA concentrations (15 μ M) ($P < 0.001$) within 16 h of incubation with AKBA. After prolonged exposure (48 hours) to the highest concentration of AKBA, both cell lines exhibited significant decreases in cells at all later stages of the cell cycle (G1, S and G2/M) (fig 3.2.1 & 3.2.2) ($P < 0.0001$). For A2780cis it was clear that AKBA effect was significant even with 5 μ M compare to cisplatin sensitive cell line (A2780). This was evident with results in early and late apoptotic (Fig 3.3.1- Fig 3.3.3) where A2780cis shows significant increase in apoptotic cells immediately with 25 μ M and 50 μ M, followed with continues significant increases in dose and time dependent manner.

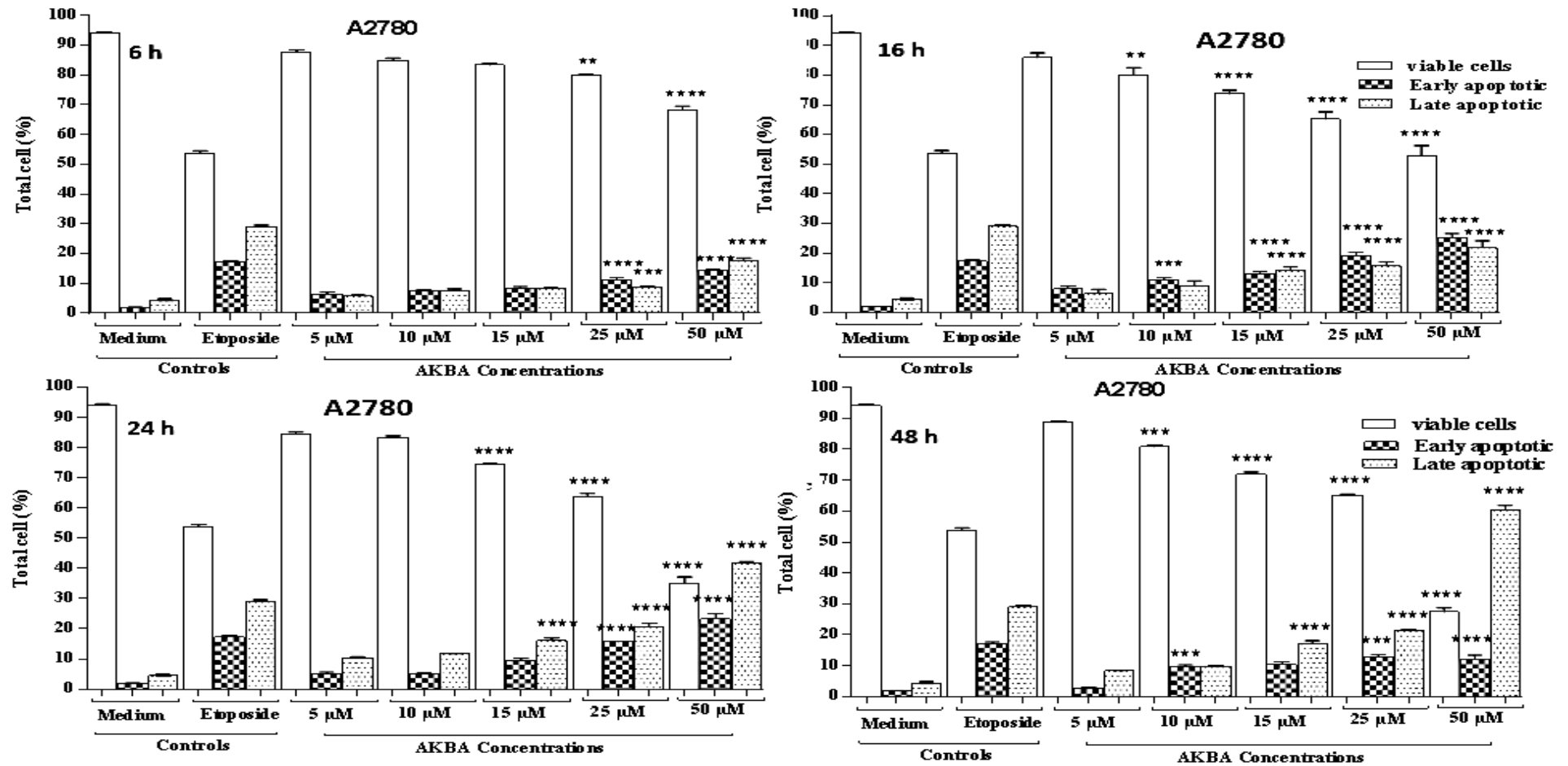


Figure 3.3. 2 AKBA exposure for different time points (6 h, 16 h, 24 h & 48 h) to assess cell death in A2780 cells at a range of concentrations.

Cells were exposed to a range of concentrations and compared with negative controls: culture medium (media), 0.5% DMSO Results were expressed as Mean \pm SEM and are representative of three independent experiments. *P<0.05, **P<0.01, ***P<0.001 and ****P<0.0001 compared to control.

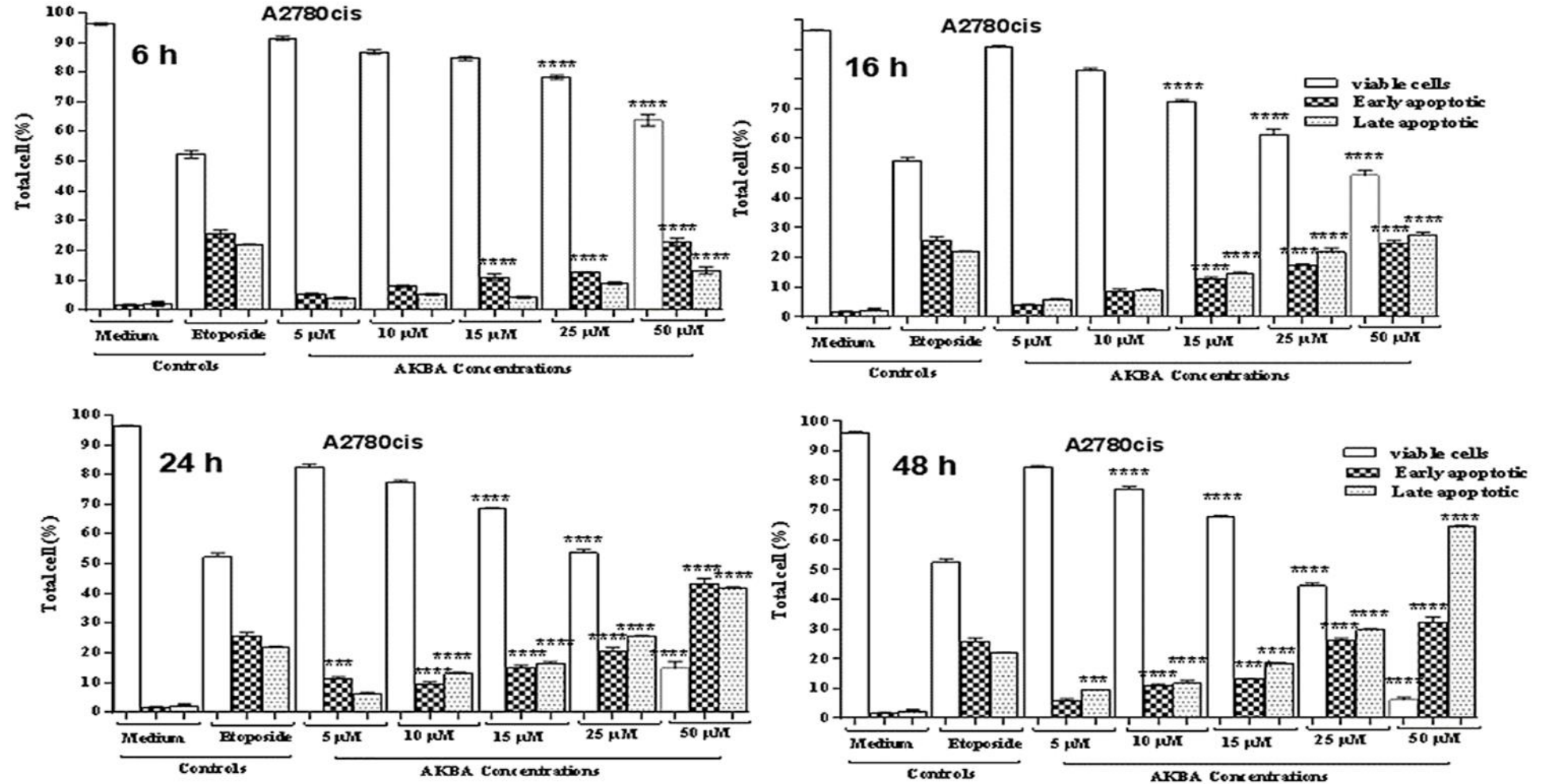


Figure 3.3. 3 AKBA exposure for different time points (6 h, 16 h, 24 h & 48 h) to assess cell death in A2780cis cells at a range of concentrations.

Cells were exposed to arrange of concentrations compared with negative controls: culture medium (media), 0.5% DMSO. Results were expressed as Mean \pm SEM and are representative of three independent experiments, (*P<0.05, **P<0.01, ***P<0.001 and ****P<0.0001).

3.2.4 AKBA induces DNA damage and ROS generation

The ovarian cancer cell line, A2780cis exhibited signs of significant DNA damage, as determined by the comet assay, at AKBA concentrations above 15 μM and at exposure times from 6 hours up to 24 hours. In A2780 and A2780cis cells, the 50 μM concentration of AKBA resulted in immediate significantly detectable DNA damage ($P < 0.001$). In the cisplatin-sensitive variant, 6 hours exposure resulted in DNA damage at concentrations $\geq 25 \mu\text{M}$ 6% ($P < 0.001$) and after 48 hours exposure, the lowest effective dose was 10 μM which results in 7% tail DNA and there was no cells detected with 50 μM as all cells were dead. A2780cis cells were slightly more sensitive to AKBA-induced DNA damage over prolonged periods; after 48 hours exposure, even the lowest concentration (5 μM) showed a significant amount 6% of tail DNA damage in these cells. Once again the DNA was shown to consist largely of SSB and DSB (fig 3.4.1& 3.4.2), and the degree of this molecular damage positively correlated with the concentration of AKBA and the exposure time. In A2780cis cells, the damage caused by 50 μM AKBA was severe enough to decrease the number of cells by 24 hours and, by the end of the experiment (48 hours) the cell number was below detectable levels (Fig 3.4.1). The increase in the number of foci per cells present the level of DSB which was evident that A2780cis shows more sensitivity to the higher concentration of AKBA after 24 h and 48 h in parallel with the SSB presented by comet assay.

The impact of DNA damage by AKBA and the generation of apoptotic proteins such as cleaved caspase-3 coincided with a decrease in the production of reactive oxygen species (ROS) across the cell lines, which might be due to the reduction in the metabolic activity of the cells as the cells were dead/dying in both cell lines. A2780cis cells showed a significant decrease ($P < 0.001$) in the production of ROS compared with control samples immediately after exposure to 50 μM , the highest concentration of AKBA. By the end of the experiment a minimum concentration of 15 μM AKBA resulted in a significant ($P < 0.001$) reduction in ROS production in A2780cis. Whereas A2780 cells required a higher concentration of AKBA (25 μM) AKBA over the same period to cause a significant effect (Fig 3.4.1).

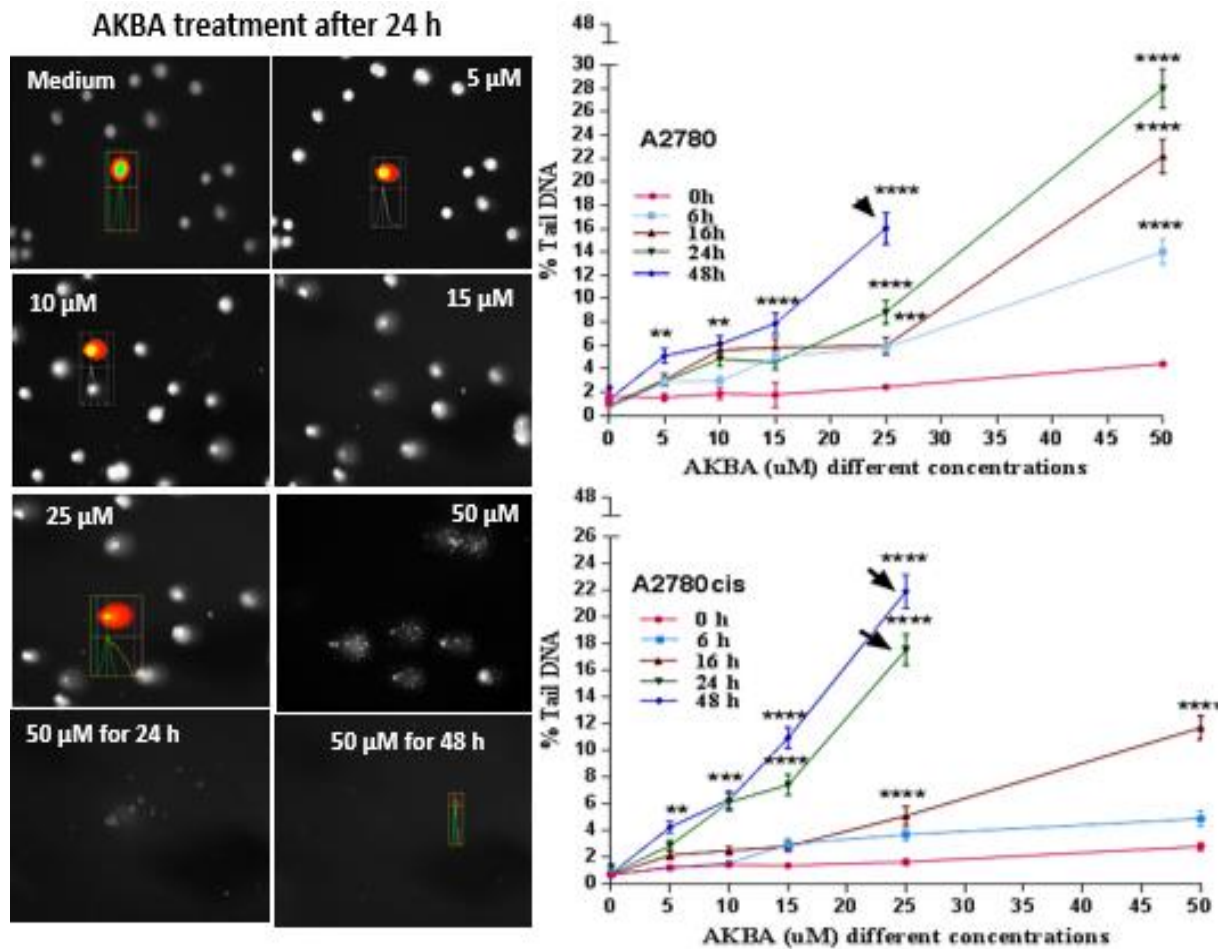


Figure 3.4. 1 AKBA-induced DNA damage in A2780 and A2780cis cells for different time and at a range of concentrations.

Cells were exposed to different concentrations and compared with negative controls: culture medium (media), 0.5% DMSO, and 50μM H₂O₂ as positive control. Error bars show the mean ± SEM of 3 independent experiments (300 comets scored per treatment). Note the level of DNA damage with 50 μM was highly affected with the tail being disconnected from the head to the tail (hedgehogs) which gives us false negative results as the comet software was not able to give us the proper level of the damage in fact it delivers a no damage.

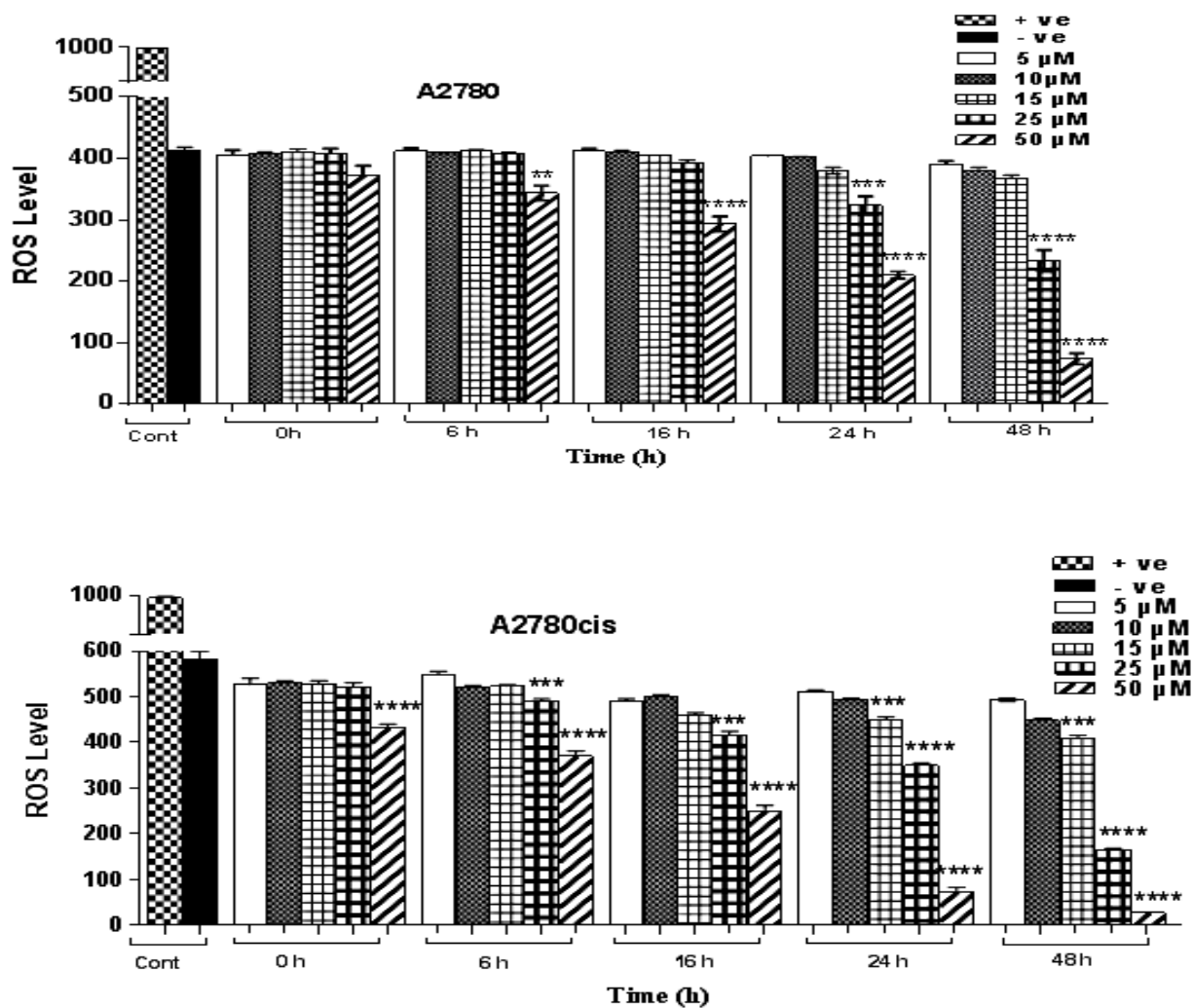


Figure 3.4. 2 AKBA-induced ROS generation in A2780 and A2780cis cells for different time and at a range of concentrations.

Cells were exposed to different concentrations and compared with negative controls: culture medium (media), 0.5%DMSO, and 50μM H₂O₂ as positive control. Error bars show the mean ± SEM of 3 independent experiments. Note the level of ROS with 50 μM was highly affected where the cells mostly lost their viability (cells are dying) and level of ROS dramatically decreases.

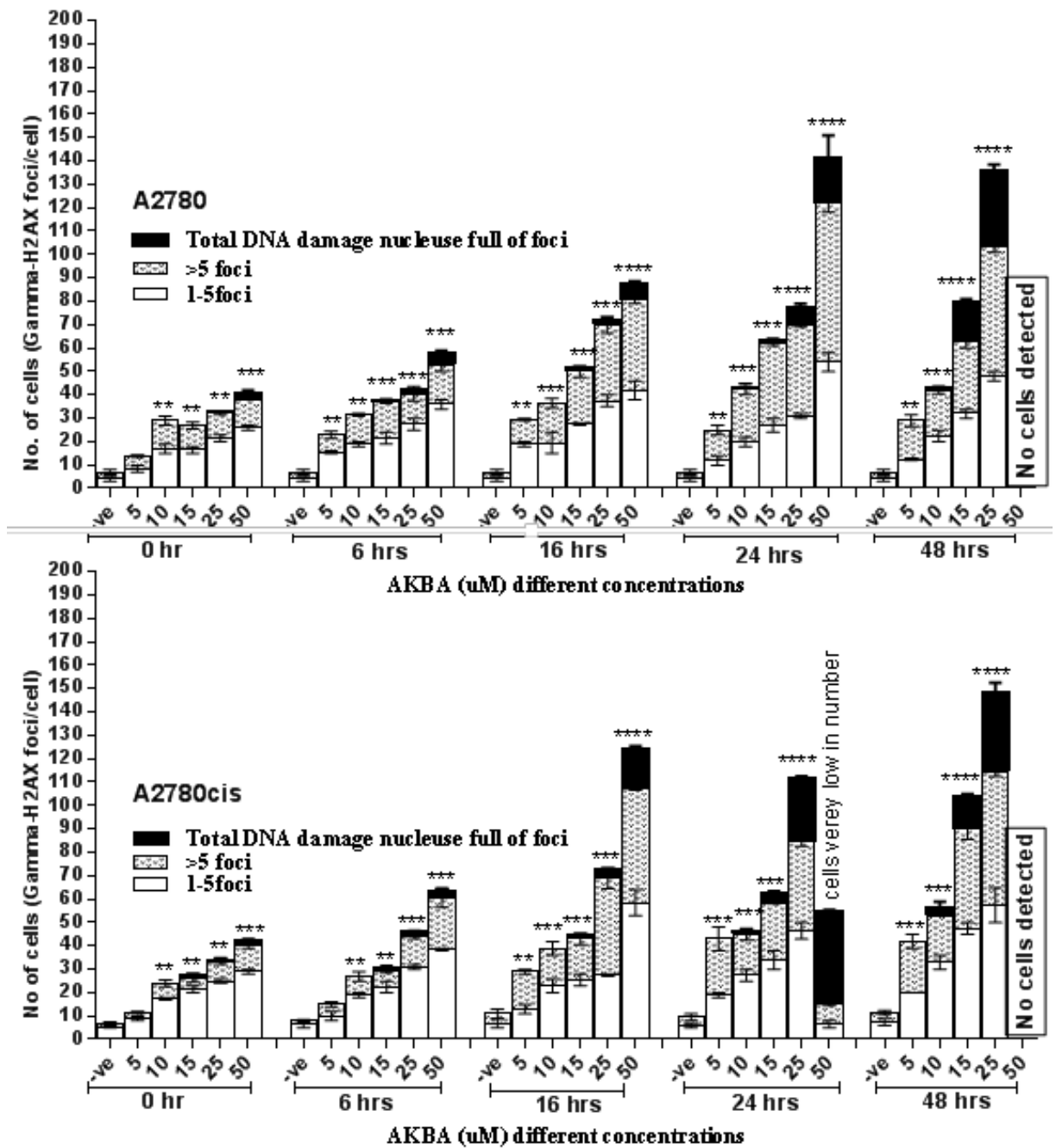


Figure 3.4.2 AKBA-induced Double strand DNA damage using Gamma-H2AX Assay in A2780 and A2780cis cells.

Cells were exposed to a range of concentrations and compared with negative controls: culture medium (media), 0.5% v/v DMSO. Results were expressed as Mean \pm SEM and are representative of three independent experiments (45 image fields scored per treatment). *P<0.05, **P<0.01, ***P<0.001 and ****P<0.0001 compared to control.

3.2.5 Proteins expression analysis by western blotting

At the same time points, western blot visualisation of cellular protein production revealed an increased concentration of cleaved caspase-3 in response to AKBA exposure across the both cell lines investigated in the study. Production of this apoptotic marker was observed maximally at the highest concentrations of AKBA, suggesting that upstream caspase signalling occurred as a consequence of AKBA affecting cellular processes and triggered programmed cell death (Fig 3.5.1- Fig 3.5.4).

The production of cell cycle regulating proteins p16 and p21 signalled the arrest of the cell cycle at the G1/S checkpoint, highlighting that normal cell growth had been perturbed which was not clear by flow cytometry (PI staining), which might be the case that the cells were dying at the same time. After 48 hours exposure to the highest AKBA dose, both cell lines showed at least the same proportion of dead cells in the sub-G1 phase compared to negative control samples (45-55%) ($P < 0.0001$). For both cell lines (A2780 and A2780cis), the sub-G1 proportion was up to 50% significantly ($P < 0.0001$) higher than that of the cells in G1-phase for the negative controls. A mechanistic outcome/confirmation of cell cycle arrest and the production of apoptotic proteins at the same time was provided by the presence of early and late apoptotic cells (Fig 3.3.1), which occurred immediately across the cell lines at the highest AKBA concentrations ($P < 0.001$) and after prolonged exposure at lower concentrations. For example, after 48 hours the cell line A2780cis (Fig 3.3.3) demonstrated a significant increase in early and late apoptotic cells at AKBA concentrations as low as 10 μM , which correlated with an accumulation of DNA damage and restriction of cell cycle progression to the sub-G1. In both cell lines, the production of pro-apoptotic cleaved caspase-3 was higher than production of p16, p21 and PARP (Fig 3.5.1 – Fig 3.5.4), all of which were induced to modest, but significant, with levels in an AKBA concentration-dependent manner. There was a considerable increase in cleaved caspase-3 levels in the cisplatin resistance ovarian cancer line, A2780cis exposed to an AKBA concentration of 5 μM to 25 μM , which was accompanied by a marked increase in the concentration of p21, but a less obvious increase in p16 and cleaved PARP (Fig 3.5.3 & Fig 3.5.4). There were significant increases in cleaved PARP which was significant for the level of DNA damage observed earlier in both cell lines in dose and time dependent manner.

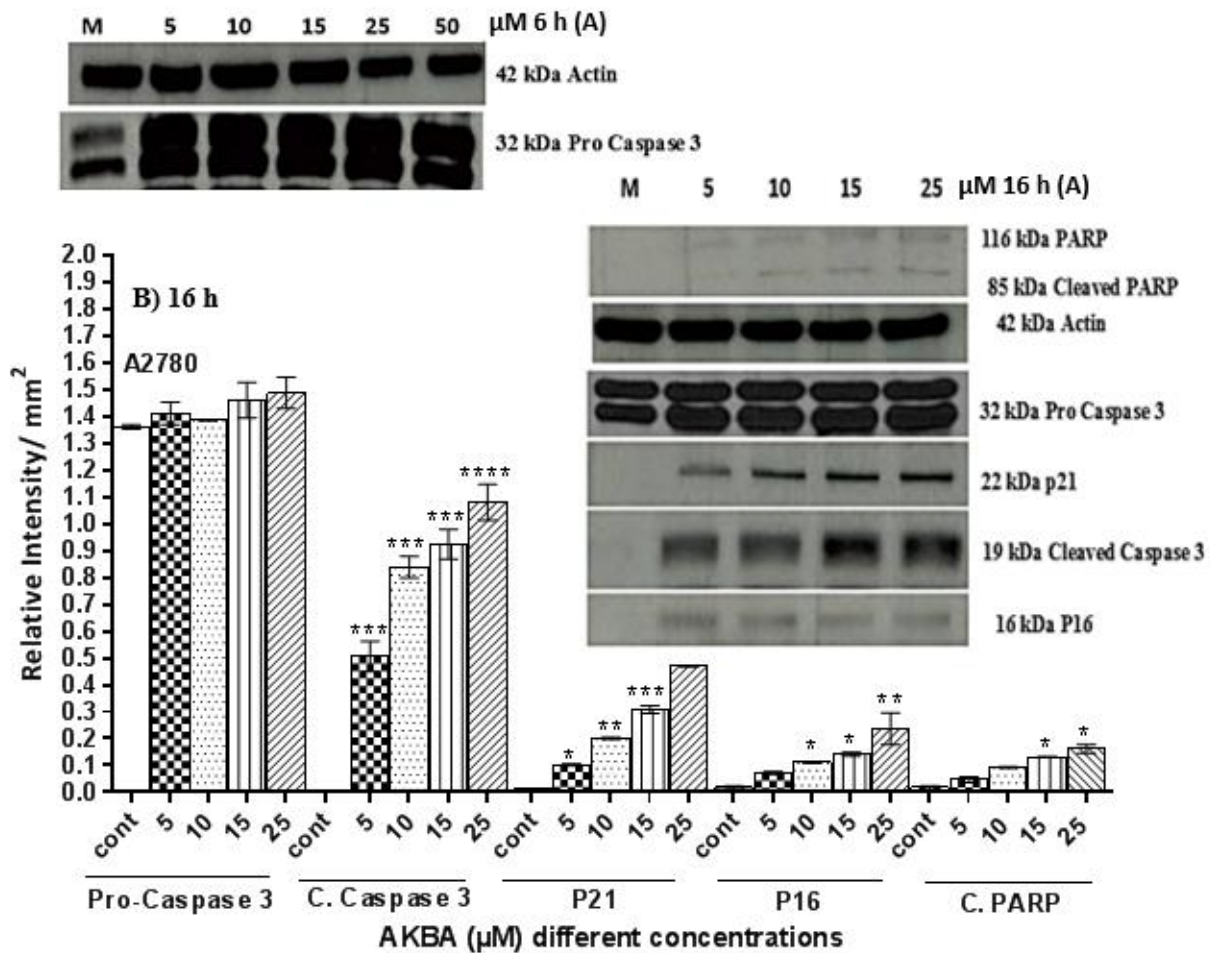
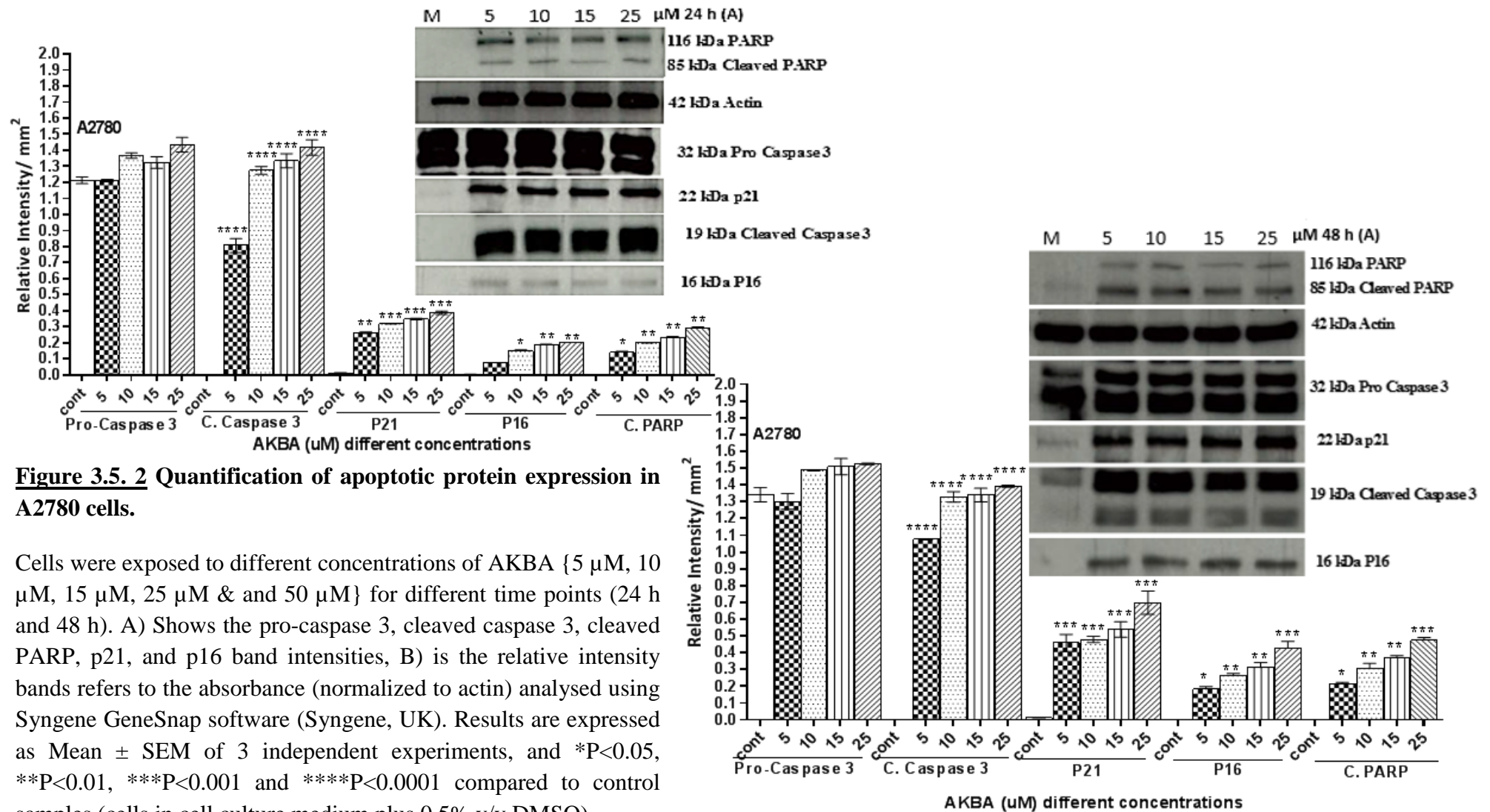


Figure 3.5. 1 Quantification of apoptotic protein expression in A2780 cells.

Cells were exposed to different concentrations of AKBA {5 μM - 25 μM & and 50 μM (6 h only)} for different time points (6 h, 16 h). A) Shows the pro-caspase 3, cleaved caspase 3, cleaved PARP, p21, and p16 band intensities, B) is the relative intensity bands refers to the absorbance (normalized to actin) analysed using SyngeneGeneSnap software (Syngene, UK). Results are expressed as Mean ± SEM of 3 independent experiments, and *P<0.05, **P<0.01, ***P<0.001 and ****P<0.0001 compared to control samples (cells in cell culture medium plus 0.5% v/v DMSO).



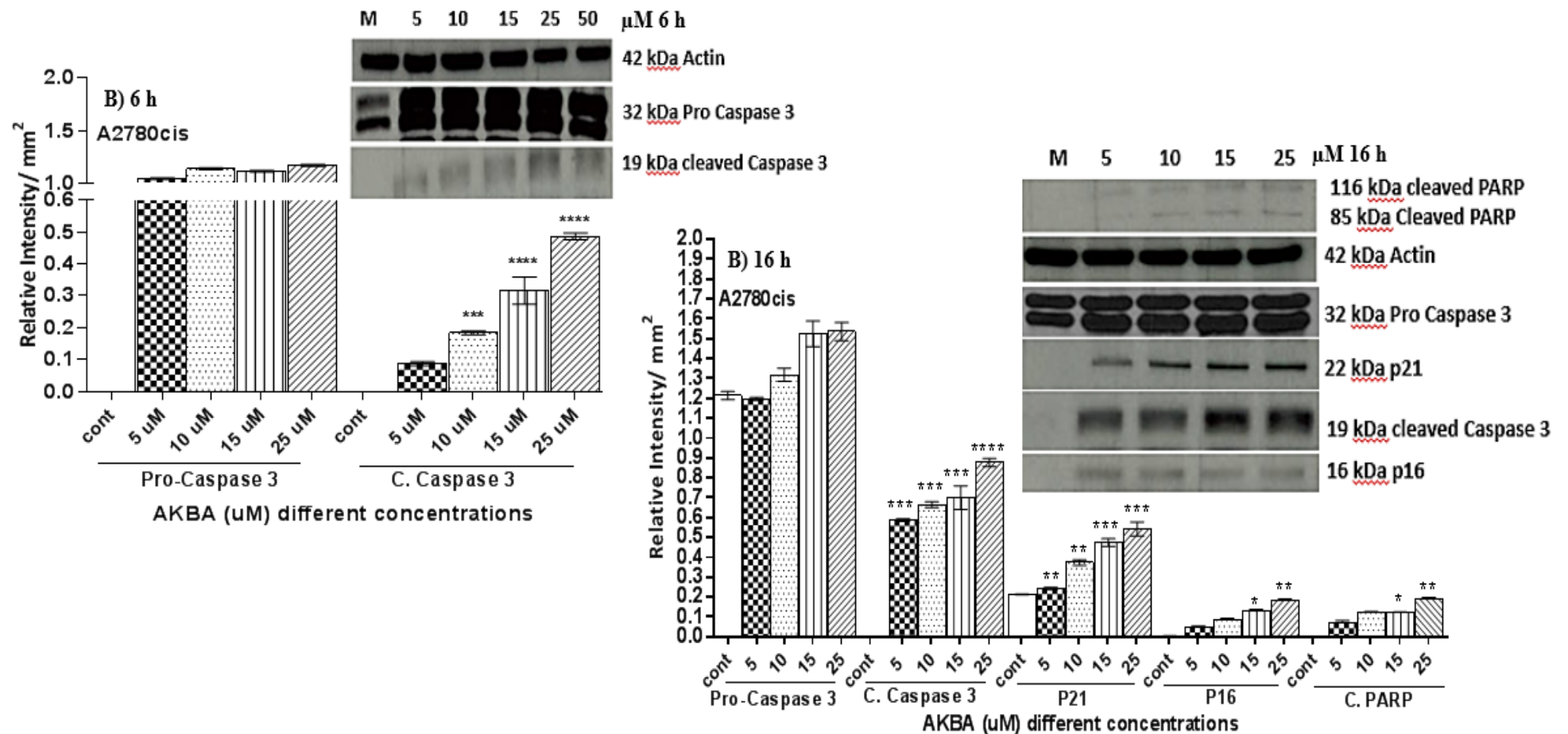


Figure 3.5.3 Quantification of apoptotic protein expression in A2780cis.

Cells were exposed to different concentrations of AKBA {5 μM, 10 μM, 15 μM, 25 μM & and 50 μM (6 h only)} for different time points (6 h and 16 h). A) Shows the pro-caspase 3, cleaved caspase 3, cleaved PARP, p21, and p16 band intensities, B) is the relative intensity bands refers to the absorbance (normalized to actin) analysed using Syngene GeneSnap software (Syngene, UK). Results are expressed as Mean ± SEM of 3 independent experiments, and *P<0.05, **P<0.01, ***P<0.001 and ****P<0.0001 compared to control samples (cells in cell culture medium plus 0.5% v/v DMSO).

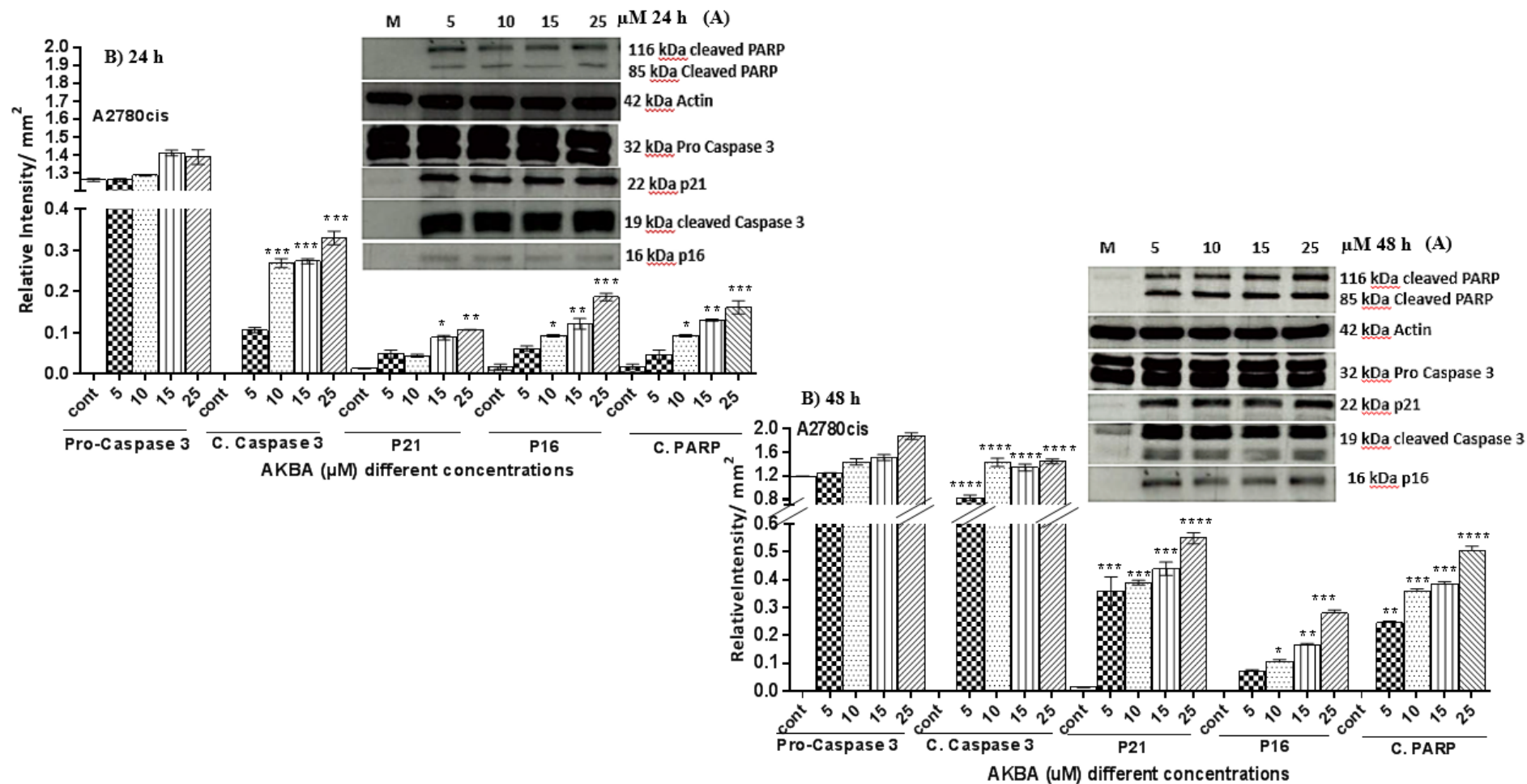


Figure 3.5. 4 Quantification of apoptotic protein expression in A2780cis.

Cells were exposed to different concentrations of AKBA (5 μM, 10 μM, 15 μM, 25 μM) for different time points (24 h and 48 h). A) Shows the pro-caspase 3, cleaved caspase 3, cleaved PARP, p21, and p16 band intensities, B) is the relative intensity bands refers to the absorbance (normalized to actin) analysed using Syngene GeneSnap software (Syngene, UK). Results are expressed as Mean ± SEM of 3 independent experiments, and *P<0.05, **P<0.01, ***P<0.001 and ****P<0.0001 compared to control samples (cells in cell culture medium plus 0.5% v/v DMSO).

3.3 Discussion

3.3.1 The effect of AKBA in A2780 and A2780cis

The cisplatin-resistant cell line A2780cis was developed by chronic exposure of A2780 to cisplatin; A2780cis has a 6.7-fold resistance to cisplatin ($IC_{50} = 23.4 \mu M$), compared with A2780 cells ($IC_{50} = 3.7 \mu M$) (Pan B. et al., 2002). It has been suggested that the mechanism underpinning this resistance is an increased activity of general efflux mechanisms, which decrease the intracellular impact of the chemotherapeutic drug (Kalayda et al., 2008). In particular, the intracellular copper ion transporters ATP7A and ATP7B have been implicated in cisplatin removal (Samimi G. et al., 2004), and a different distribution of these transporters has been noted between A2780 and A2780cis cells, with a mechanism suggested whereby A2780cis is able to sequester and traffic bound cisplatin to cellular lysosomes, away from genomic DNA (Kalayda et al., 2008). Protein profiling comparisons between cisplatin-sensitive parent strains and their resistant counterparts found similar proteomes between A2780 and A2780cis, (Zhu et al., 2005), suggesting the mechanism for cisplatin resistance occurs as part of post-translational modifications.

In the present study, the cisplatin-resistant line demonstrated less susceptibility to morphological changes than A2780 after exposure to moderate concentrations of AKBA. However, it should be noted that the microscopy images of cell morphology showed only a broad overview of the physical impact of AKBA, and the calculation of the IC_{50} concentrations in both lines indicated that the effect of AKBA was more pronounced in the cisplatin-resistant line. In both cell lines, the efficacy of AKBA in halting cell death progression was clearly demonstrated by the approximate seven-fold increase in the proportion of cells that were in the sub-G1 phase compared with control samples. These data, coupled with the presence of early and late apoptotic cells at higher AKBA exposure concentrations, demonstrated the impact of this compound in triggering cancer cell death. There was a significant increase in the number of early and late apoptotic cells in both of these lines, but it was interesting to note that the cisplatin resistance strain underwent apoptosis after 6 h of exposure to AKBA compared to the cisplatin sensitive which was evident only after 16 h ($P < 0.0001$). The cell viability data also indicated that A2780cis cells were marginally more sensitive to AKBA at concentrations of $25 \mu M$, requiring just 6 hours exposure to lose viability and 24 hours at $15 \mu M$, compared with 24 hours for A2780 cells.

The impact of AKBA on non-cancer cells was not investigated in the present study, nor was any toxicology data presented; however, it is promising that the effective doses of AKBA noted for both these cell lines were relatively low (10-25 μ M) ($P < 0.001$). Previous research, revealed that extracts of *Boswellia serrata* had little effect on chemically-induced colitis in mouse models, therefore the impact on normal epithelial cells may be low (Kiela et al., 2005). Based on the data presented in the current study in the effect of AKBA on A2780cis cells, it is tempting to speculate that AKBA could be used as a novel therapeutic for chemotherapy-resistant cancers, especially as the cisplatin-resistant cell line was generally more susceptible/sensitive to AKBA than the sensitive A2780 cell line.

It should be noted that the impact of AKBA on the viability of both versions of A2780 was significant, therefore the possibility remains that AKBA could be used as an anticancer treatment, if applied in conjunction with existing chemotherapeutic approaches. The mechanism of cisplatin-induced cell death is similar, but distinct to the cytotoxic effect of AKBA; cisplatin binds to DNA causing inter and intra-strand crosslinks to cause cell division cessation and apoptosis whereas AKBA is thought to induce DNA damage through a separate mechanism, possibly involving inhibition of topoisomerases (Chashoo et al., 2011b). These different mechanisms could be crucial to explain A2780cis resistance to cisplatin but sensitivity to AKBA, and may decrease the chance of cross-resistance, as reported between other chemicals in ovarian cancer lines (Gore et al., 1989).

A2780cis cells were more susceptible to DNA damage after prolonged AKBA exposure (24 hrs to 48 hrs) ($P < 0.0001$) than A2780 cells. The lowest (10 μ M) concentration of AKBA was sufficient to cause significant SSB and DSB DNA damage in A2780cis (Fig. 3.4.1 & Fig. 3.4.2), resulting in the PARP cleavage, production of apoptosis-inducing proteins and caspase 3 cleavage (Fig. 3.5.3 & Fig. 3.5.4). The exact cause of AKBA higher sensitivity with A2780cis was not deeply investigated further by the current research.

3.3.2 Protein expression in the ovarian cancer cell lines following AKBA treatment

Boswellic acids in general have been shown to trigger cell death by promoting apoptosis in several cancer cell types (Liu et al., 2002b, Syrovets et al., 2005). In each of these cases apoptosis was accompanied by an increase in caspases (Liu et al., 2002b, Liu et al., 2002a,

Riedl et al., 2004), providing evidence that caspase production is a key marker for AKBA-induced cell death. Disruption of the cell cycle, in response to DNA damage, caused progression from G1 phase to S phase to be blocked by the production of the cell regulator proteins, p16 and p21 (Yasmeen et al., 2011). In the present study, production of these cell cycle regulating proteins should result in an accumulation of cells in the G1 phase. However, it is clear from the cell cycle data that the vast majority of these cells were in fact present in the sub-G1 phase, suggesting that cells were dying and entering sub-G1 without cell cycle arrest seen using PI staining with the evident of cell cycle proteins were expressed using western blotting. It might be other regulating proteins were having an effect in this mechanism which is not clear for us at this level. The results outlined here confirmed in a recent study, which looked at the effect of the terpanoid compound torreyol (δ -cadinene) on the viability of a well-established ovarian cancer cell line (OVCAR-3). The authors identified that δ -cadinene was able to arrest the growth of these cells in sub-G1 phase after 48 hours exposure and induced caspase-mediated apoptosis (Hui LM. et al., 2015). In the present study, the induction of active caspase-3, cleaved from the inactive pro-enzyme indicated that apoptotic pathways had been initiated. Caspase-3, the executor enzyme for apoptosis and the production of cleaved form is highly indicative of apoptosis occurring in the cell. Caspase-3 is a known inhibitor of p21 (Riedl et al., 2004), therefore it is curious that increased production of cleaved capase-3 did not result in decreased cellular concentrations of p21 which can be referred that even though some of the cells were promoted to apoptotic at the same time there might be some other cells gown through cell cycle arrest. Indeed, in A2780cis cells, addition of 25 μ M induced a substantial increase in p21 levels. It has been shown previously that as part of its role in negative regulating the G1-S cell cycle progression, p21 binds to and inhibits cyclin-dependent kinases (CDK-) 4 and 6 from binding and forming a complex with cyclin D. The AKBA-induced interruption of the cell cycle at G1 is known to lead to a marked decrease in concentrations of cyclin D1, cyclin- E, CDK-2, CDK-4, and pRb and an increase in p21 levels (Liu et al., 2006), in line with the data presented here. Cyclin-CDKs form part of the phosphorylation cascade that ultimately releases transcription factors to promote G1-S cell cycle progression. The concentration of p16 is important in regulating the level of p21 in the cell, explaining why there is apparent co-production of these two cell cycle proteins. Increased cellular levels of p16 are known to inhibit the formation of cyclin D-CDK4/6 complexes, which in turn frees up bound p21, enabling this protein to take part in further pro-apoptosis pathways, including the binding and inhibition of

CDK1/2 complexes (Piccolo and Crispi, 2012). It has been reported that the role of p21 in apoptosis is highly complex, with the protein playing a dual activating and inhibiting role in the regulation of cell death (Piccolo et al., 2012). Nonetheless, from the present study, it was apparent that levels of p16, p21 and cleaved caspase-3 all correlate with increased AKBA concentrations and with apoptosis in the both cell lines studied here. The concentration of PARP remained relatively low in the present study across the both cancer cell lines; activation of PARP is known to be triggered in response to DNA damage (Los et al., 2002). PARP helps to mediate the SSB repair pathways. Its cleavage by caspase-3 is a major signal for the cell to cease DNA repair and to activate programmed cell death pathways. The cell lines which have increased in sensitivity to DNA damaging agents have increased level in PARP expression and inhibition in the strand break re-joining mechanism in the damaged DNA (Herceg, 2001). This might be the case with A2780 and A2780cis cell lines where it leads to apoptosis.

3.3.3 The anti-ovarian cancer potential of AKBA

Extracts from the gum of *Boswellia* spp. have been reported for thousands of years as exhibiting medical properties, mostly reported as anti-inflammatory and analgesic effects (Hamidpour et al., 2013). However, more recently the putative medicinal effect of certain boswellic acids in treating a broad range of cancers has been investigated. In one, study a broad range of boswellic acids were investigated and found to have anti-tumour properties, involving DNA, RNA and protein synthesis inhibition, which occurred in a dose-dependent manner. AKBA was identified as the compound with the most potent anti-tumour activity, preventing cellular growth of human promyelocytic leukaemia (HL-60) cells, but not impacting cell viability *in vitro* (Alam et al., 2012). AKBA has been studied, to prevent the spread of tumours by suppressing the production of vascular endothelial growth factor receptor 2, thereby inhibiting angiogenesis and cancer metastasis (Pang et al., 2009) In addition to HL-60 cells, the anticancer properties of boswellic acids, such as AKBA, have been demonstrated in other leukaemia cell lines (NB4, HL-60, SKNO-1, ML-1, U937, and K562) (Xia et al., 2005) , liver cancer cells (HepG2) (Liu et al., 2002a), colon cancer cells (HT-29) (Liu et al., 2002b), brain cancer lines (LN-18, LN-229)(Hostanska et al., 2002)and prostate cancer (PC-3).The range of cell lines in which AKBA and other boswellic acids have been tested *in vitro*, provides growing evidence that these compounds can exhibit a broad and non-tissue-specific anti-cancer effect in future clinical trial.

However, despite a large number of studies having evaluated the specific use of AKBA, the exact mechanism whereby the compound causes DNA damage and induces apoptosis as still not been elucidated. Although the function of AKBA as a topoisomerase inhibitor has been demonstrated (Hoernlein et al., 1999b, Syrovets et al., 2000), other studies have pointed to the function of AKBA as a potent inhibitor of 5-lipoxygenase (5-LO) (Safayhi et al., 1992, Safayhi et al., 1996, Sailer et al., 1996). Under normal conditions, 5-LO is required to convert essential fatty acids into leukotriene signalling molecules (Funk et al., 1989) and inhibition by AKBA would result in a build-up of hydroxyl free radicals with the potential to cause DNA damage and induce apoptosis which was not the case in our study. The level of ROS in cancer cells is permanently high due to the cellular activities inside, the concentration of AKBA achieved *in vivo* is not sufficient to inhibit 5-LO, so anti-inflammatory properties are probably due to some other effect. Researchers demonstrated that a class of boswellic acid was able to induce the accumulation of ROS instead (Wang and Yi, 2014), as reported in the present study there was a reduction in metabolic activity of the cell, which result reduction in ROS level, which might be due to cell death (Altmann et al., 2004). However, the present study did not further examine the AKBA mechanism for DNA damage in detail and it is clear that further confirmatory experiments are required to elucidate whether a single or combined mechanism is employed by AKBA in killing cells. Like the current investigation, another study found that treatment of human multiple myeloma cells with AKBA negatively affected cell proliferation, through inhibition of cyclin D1 and arrested cell cycle progression (at sub-G1 and G2/M points) (Kunnumakkara et al., 2009). In addition, the authors found that inhibition of the signal transducer and activators of transcription (STAT)-3 family of transcription factors by AKBA resulted in decreased chemo-resistance and angiogenesis in tumours, suggesting that AKBA may have a therapeutic role to play in decreasing the size and metastatic capabilities of existing tumours and functioning alongside conventional chemotherapeutic treatments (Kunnumakkara et al., 2009).

There is a lot of research going on to prove the metabolic activity of AKBA *in vivo*, and 0.2- 0.4 μM of AKBA was found in plasma after oral administration of 240 mg/kg of *B. serrata* extract, and 0.3 μM was found in the brain (Kruger et al., 2008). The present study was among the first to investigate the use of AKBA at pharmacologically relevant concentrations to determine its impact on ovarian cancer lines. AKBA was shown to effect the cell replication and viability potential of the ovarian cancer cell lines studied at concentrations between 10 μM and 25 μM . At these levels, AKBA caused significant

DNA damage, resulting in early cell cycle arrest and apoptosis 24-48 hours after initial treatment. Prolonged exposure to AKBA concentrations at around 15 μM caused cell death in the ovarian cancer cells included in the present study. These concentrations were relatively high compared with AKBA concentration used to treat other cancer types; meningioma cells from a brain tumour had an IC_{50} concentration of 2-8 μM (Park et al., 2002a). Nonetheless, boswellic acids in general and AKBA in particular have been reported as non- or low-toxicity compounds and so are suitable for use as therapeutic agents. For example, food supplementation with more than 5g per kg (0.5 % w/w) was required before a lethal dose was reached in Sprague-Dawley rats (Lalithakumari et al., 2006). Boswellic acid does not have a toxic effect on either mice or rats ($\text{LD}_{50} > 2 \text{ g/kg}$) and did not cause the formation of ulcers (Singh et al., 1986). Clinical experiments have shown that extracts of *B. serrata* do not have any severe side effects when administered to patients suffering from grade 2 ulcerative colitis at a dose of 350 mg, taken orally three times daily, over a period of 6 weeks (Gupta et al., 1997). AKBA in particular has received approval as a safe substance to be administered to patients (Gupta et al., 1997) and oral preparations of the compound have shown no toxicity (Raja et al., 2011).

This study has demonstrated the potential of AKBA as a putative novel anticancer therapeutic in two clinically relevant cell lines, revealing similar cytotoxic responses in each of them. However, it should be noted that there are more than 23 cell lines that have been developed to investigate the effect therapeutic of chemotherapeutic drugs on ovarian cancer alone (Lambros et al., 2005). At this stage, it is unclear whether the cytotoxic effect at low doses of AKBA, has been maintained in the both cell lines. Further work should focus on the exact mechanism for AKBA-induced cell death, by testing lower concentrations. As has been proposed previously, this may be due to inhibition of topoisomerases, leading to elevated rates of DNA supercoiling and DNA strand breaks, or AKBA may induce DNA damage and inhibit the DNA repair mechanisms. In particular, differences in the cell killing mechanism between A2780 and A2780cis observed in this study may help to overcome chemotherapy resistance induced by repeated exposures during treatment. Nonetheless the fact that AKBA showed a greater effect on cell viability and cell cycle arrest in the cisplatin-resistant cell line A2780cis compared with the A2780, suggests that AKBA may be a promising anticancer therapeutic to tackle chemo-resistance.

3.3.4 Concluding remarks

The results outlined in this study clearly demonstrate that AKBA has the ability to prevent the growth of ovarian cancer cells through a mechanism that involves the formation of DNA damage in the form of single strand and double strand breaks. Together, this DNA damage triggers cell apoptosis by presenting the cell populations at the sub-G1 stage, in a process mediated by p16 and p21, likely through regulation by the p53 independent pathway. The level of DNA damage in each of the cancer cell lines was considerable, resulting in apoptosis with the evidence from cell cycle, cell apoptosis and western blotting results. Importantly, the study has demonstrated that AKBA has a significant impact on both cisplatin-sensitive and cisplatin-resistant cell lines *in vitro*, with no indication of relative AKBA-resistance apparent in these experiments. The findings of this research add to the existing scientific literature regarding the anticancer properties of boswellic acids, and provide compelling evidence that AKBA may be used in anticancer strategies, to supplement existing chemotherapeutic approaches mainly in instances of resistance to treatment, notably cisplatin. At this stage, further pre-clinical studies (animal and human) are required to confirm the results presented here and to evaluate the compatibility of this compound with conventional Platinum-based treatment.

By gathering both cell line results we thought to examine the cell lines which present with the most common mutations like BRCA1 and TP53 in the next chapter.

Chapter 4

**Effect of AKBA on a known BRCA1
mutated ovarian cancer cell line and a
high grade serous ovarian cancer cell line**

4.1 Introduction

Ovarian cancer is a highly lethal cancer (Fong et al., 2010), with an average of only 30% of patients achieving five-year survival. It is believed that BRCA mutations in ovarian cancer cells, as highlighted by some researchers (Petrillo et al., 2016, Al-Salmani et al., 2013), present with the “germline mutation-associated cancers”, due to the defect in DNA repair mechanisms, which present with PARP inhibition (Fong et al., 2010). Genetic variations are particularly important in ovarian cancer, with researchers reporting that there are 54 genes implicated in the expression of ovarian cancer (Cheung et al., 2011); although the Cancer Genome Atlas (TCGA) identified upwards of 500 high grade serous ovarian cancer genomes. Cheung reported that unique feature of ovarian cancers are the frequent recurrent genomic events manifest in most cases (Cheung et al., 2011). Therefore, the role of agents that disrupt the various deduced pathways, inhibit cell growth or lead to apoptosis are particularly important, as the majority of ovarian cancer cases are diagnosed when ovarian cancer is well advanced (Cheung et al., 2011). Whilst AKBA has previously been shown to reduce proliferation in a number of different cancer cell lines (Pang et al., 2009, Park et al., 2011a, Lu et al., 2008, Liu et al., 2006, Suhail et al., 2011, Zhao et al., 2003, Yadav et al., 2012, Ni et al., 2012, Burlando et al., 2008 , Frank et al., 2009) and this study by our group investigated the role of AKBA on ovarian cancer cell lines for the first time. Whilst each of these studies used various cancer cell lines, AKBA treatment was an effective cytotoxic/growth inhibitory agent and various pathways were implicated. Therefore, given the varied pathways associated with ovarian cancer, only the main pathways will be briefly detailed.

Ovarian cancer cell lines are derived from patients with ovarian cancer. Of the various cell lines implicated in EOC, one of the most important of the high-grade cancer cell lines is OVCAR-4, which is known to engage the mTOR pathway via VEGF receptors (Lau et al., 2013). The OVCAR-4 cell line was established from a patient with ovarian cancer and subsequently found to have a ‘genetic profile’ that was representative of high grade serous ovarian cancer, thus making it a reasonable *in vitro* model of such cancers (Domcke et al., 2013). As has been reported in the literature, various cancer cell lines have been investigated and have demonstrated that AKBA has a strong cytotoxic effect, mediated by a variety of pathways and through a variety of disruptive actions, ultimately leading to apoptosis. To date there is no research published related to the effectiveness of

AKBA on ovarian cancer cells except in preliminary form by our group at University of Leicester (Al-Salmi et al., 2013). Therefore, as AKBA has successfully demonstrated the ability to disrupt VEGF receptors along the mTOR pathway (Pang et al., 2009, Kurman et al., 2010), one of the objectives of the current research is to investigate the role of AKBA as a successful mediating agent to cause apoptosis in the high grade serous ovarian cancer cell line OVCAR4.

UWB1.289 cells carry germline BRCA1 mutation within exon 11 (2594delC) with a deletion of the wild-type allele. UWB1.289 is estrogen and progesterone receptor negative and have a somatic mutation in p53. The importance of these cells in ovarian cancer research lies in their functional deficiency of BRCA1 (DelloRusso et al., 2007). BRCA genes are necessary for repair of double-strand break DNA damage via homologous recombination. In a recent study comparing different ovarian cancer cell lines, UWB1.289 were not able to form tumours when xenografted in nude mice (Mitra et al., 2015). The cells are sensitive to DNA damage induced by ionizing radiation, with a related lack of S-phase arrest. Restoration of wild-type BRCA1 by transfection improved DNA repair responses and increased survival. Gene expression profiling revealed a clear association between BRCA1 levels and down-regulation of multiple IFN-inducible genes (IFI16, IFI44, IFI27) while claudin 6 (implicated in cancer invasion and metastasis) was upregulated in cells transfected with functional BRCA1 (DelloRusso et al., 2007). Recent findings have indicated that UWB1.289 cells show increased expression of Ubc9 (SUMO-conjugating enzyme), which is essential for nuclear architecture and chromosome segregation. In a proposed molecular mechanism, BRCA1 deficiency may increase Ubc9 expression and in turn promote ovarian carcinogenesis (Qin et al., 2012). Many chemotherapeutic agents inherently destroy healthy cells and cause a vast number of negative side effects ranging from hair loss to death, due to weakened immune systems and complications. It is important to investigate the role of natural and safe alternative treatments for cancers, and in particular for the low survival rate cancers to improve their survival rate e.g. ovarian cancer. Yuan and co-workers highlighted natural remedies that have been successfully used since ancient times for a variety of illnesses ranging from inflammation to cancer (Yuan et al., 2006). Another objective of this research is to add to the limited body of research on high-grade serious ovarian cancer cell lines and the effectiveness of AKBA.

Aim: Examine the mechanistic role of DNA damage/repair and oxidative stress in the anti-cancer actions of AKBA in a known BRCA1 mutated ovarian cancer cell lines.

Summary of the techniques/approach

BRC1 and high grade serous ovarian cancer cells were treated with AKBA at different concentrations and for different times.

Modulation of cell viability/proliferation and cell death by AKBA was investigated in all ovarian cell lines using a light microscope at 40X magnification to analyse the changes in cell growth and identify any morphological changes in the cells. In addition, cell viability was examined by the AlmarBlue assay, a Beckman CoulterCounter was used to assess cell number. Damage to DNA was assessed using the comet assay, whilst cell cycle status and apoptosis were tested using flow cytometry (PI staining and Annexin V/PI staining). The temporal association and regulation of AKBA-modulated protein expression was identified by western blotting. All the materials and methods used for this chapter have been described in Chapter 2.

4.2 Results

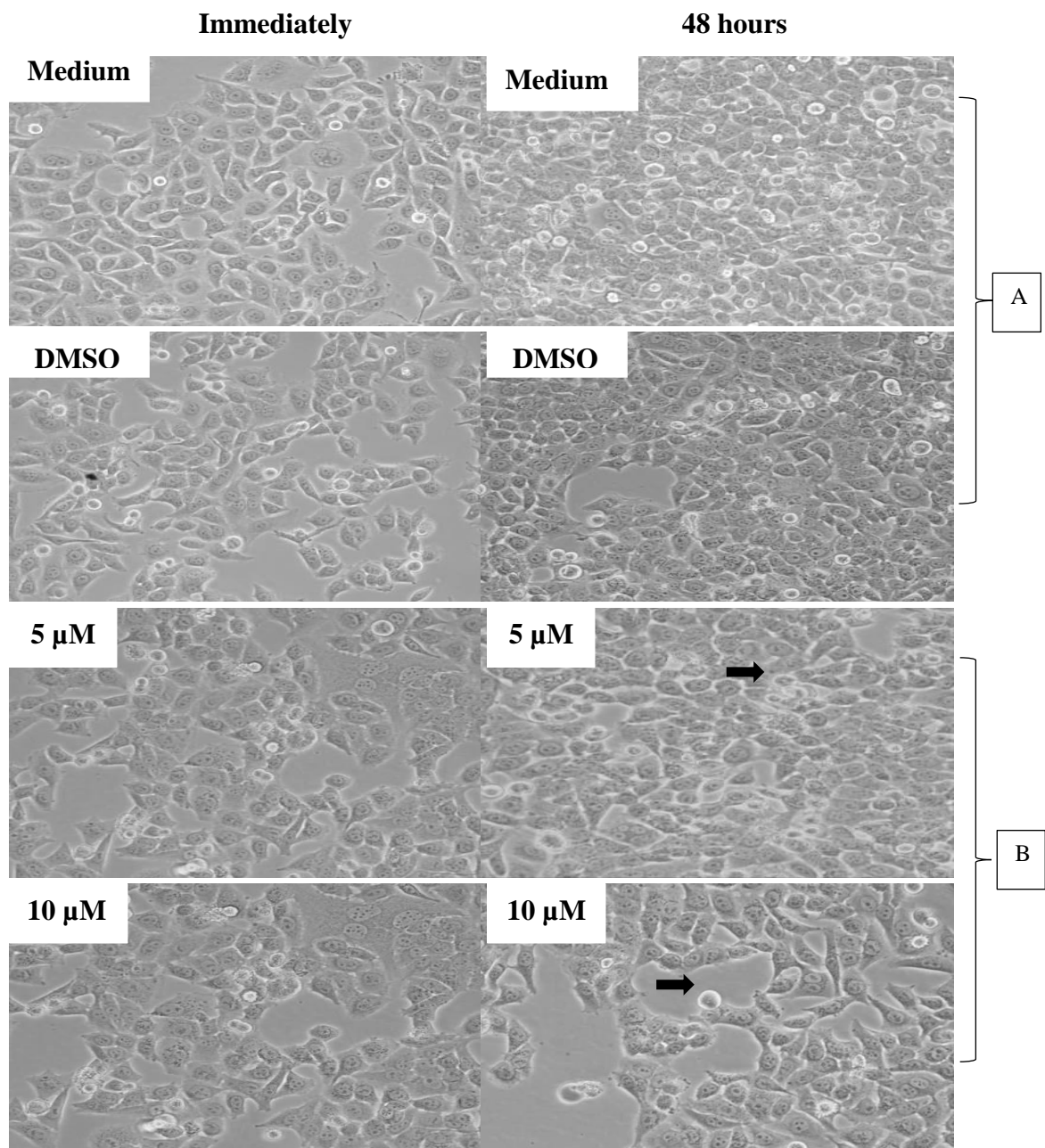
4.2.1 AKBA effect in BRCA1 mutant ovarian cancer cells and OVCAR4 cells.

4.2.2 The effect of AKBA on cell growth and proliferations

4.2.2.1 Examination of cell morphology using light microscopy

In order to examine the effect of AKBA on the morphology of exposed cells, microscopy images were taken of the cultured cell lines after treatment with different concentrations of AKBA for different times.

Cell morphology of UWB 1.289 cells



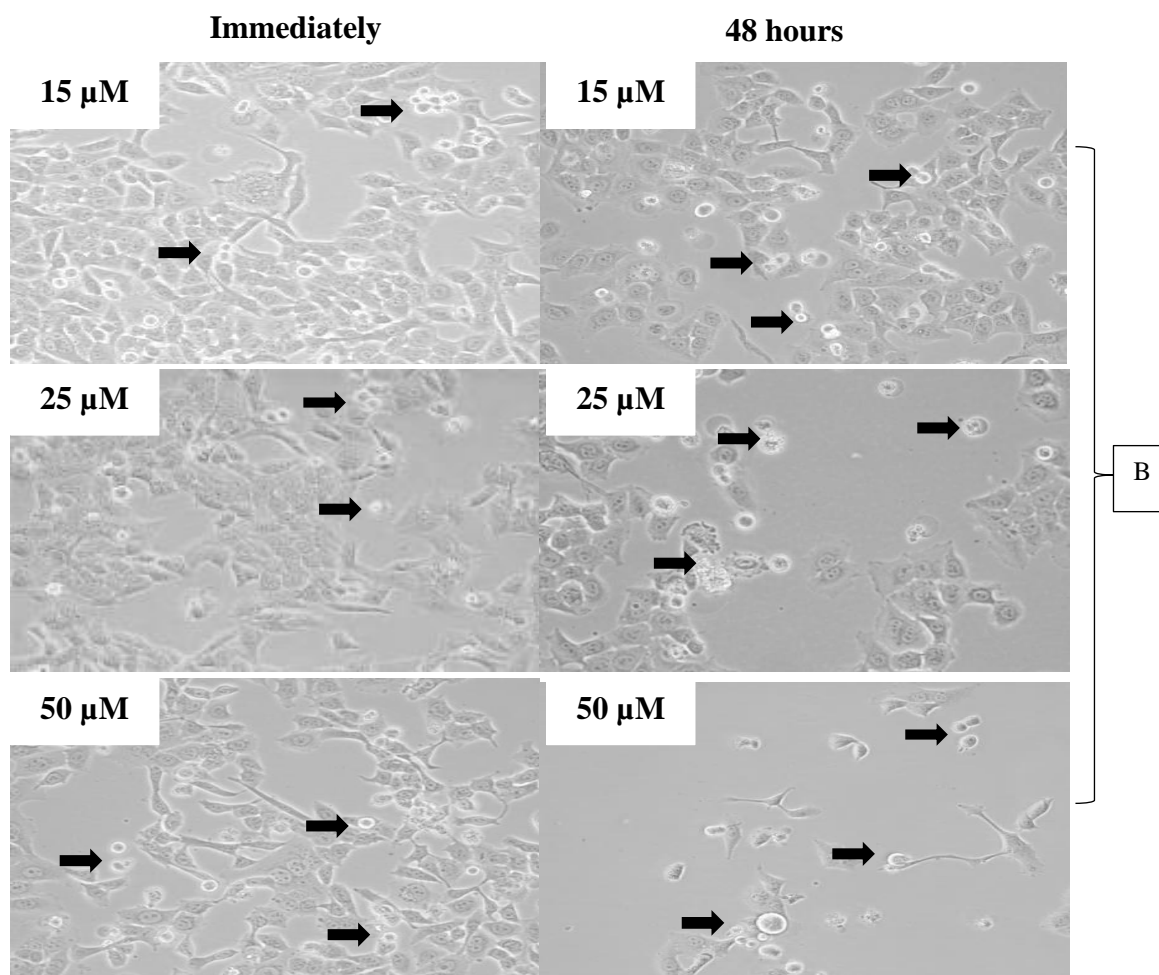


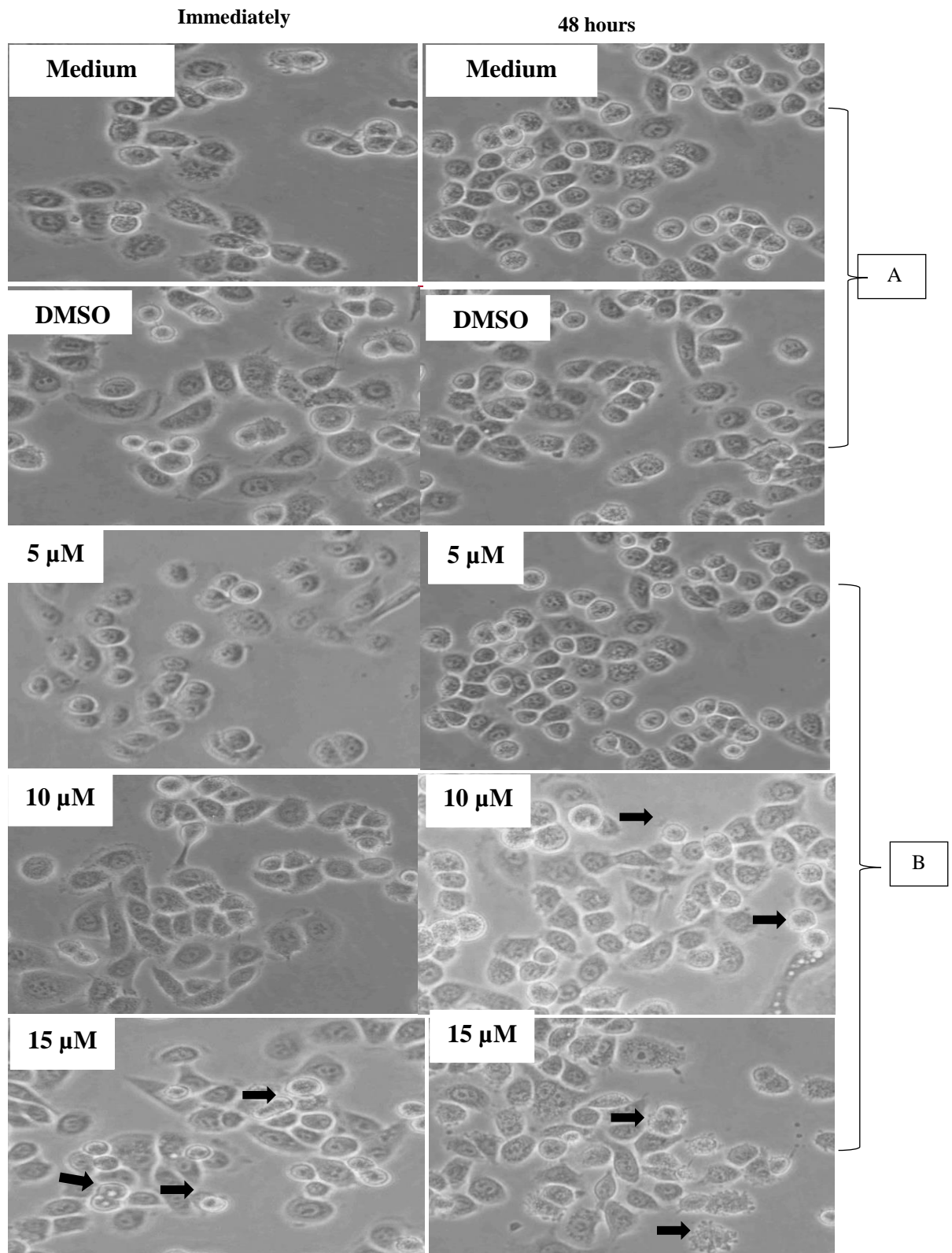
Figure 4.2.1 Microscopic images of UWB1.289 cells exposed to AKBA.

Negative control samples (A) consist of cell culture medium and 0.5% (v/v) DMSO. Cells challenged with AKBA (B) were grown for 24 hours in cell culture medium to attach and recover before AKBA was added at various concentrations (μM) and left for 6 or 48 hours. Morphological changes of treated cells were observed with apoptotic features such as small and large blebs pinching off the cells and residual apoptotic bodies (black arrow).

In the cell line, UWB1.289, AKBA has a discernible effect on cell morphology mostly at the highest concentration. It appeared that there were fewer cells surviving after 48 hours' exposure to $\geq 15 \mu\text{M}$ AKBA than in either the lower AKBA concentrations or the control samples. The significant decrease in visible intact cells was most evident at the highest AKBA concentrations (25 μM and 50 μM) (Fig. 4.2.1). Use of 15-50 μM AKBA gave rise to increased cell death compared with control samples. 5 μM of AKBA exposure shows that the majority of the cell lines remained healthy and proliferated (about 70%), where is 10 μM of AKBA is slightly decreased UWB1.289 cell number after being treated for 48 hours, no cell proliferation indicated. However, 50 μM induced an acute lethal effect whereby many cells died after treatment, as indicated by the black arrows in fig.

4.2.1. From the microscopy observations, evidence of cells rounding up and detaching and also cell debris evident dead cells.

Cell morphology of OVCAR4 cells



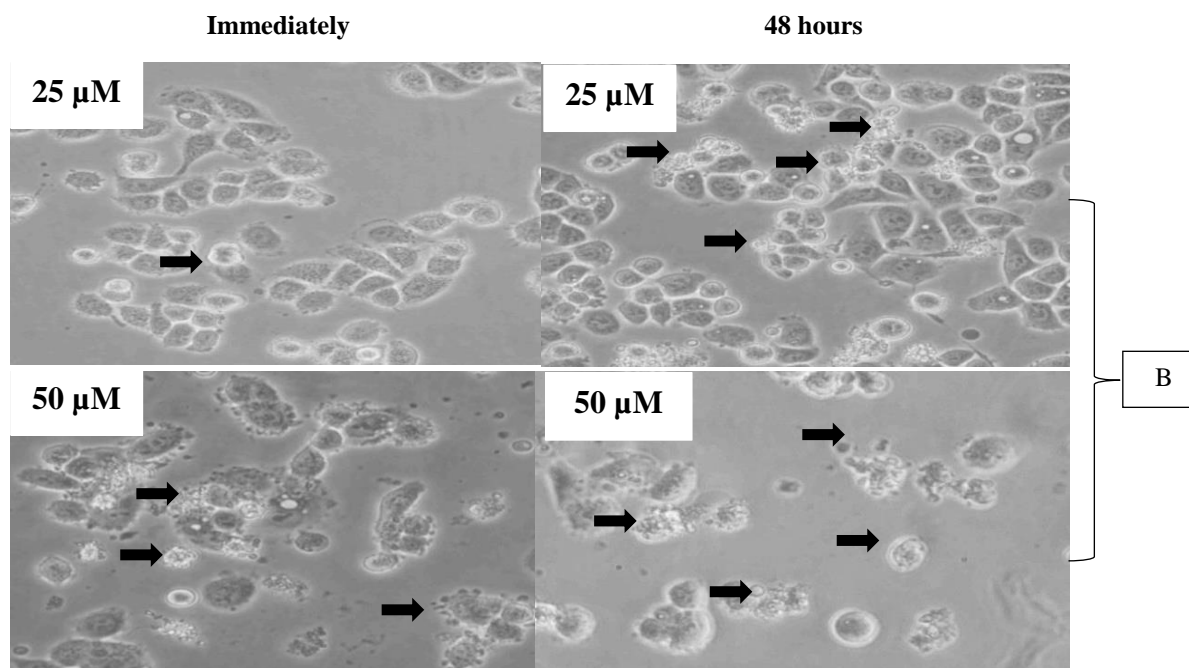


Figure 4.2. 2 Microscopic images of OVCAR-4 cells exposed to AKBA.

Negative control samples (A) consist of cell culture medium and 0.5% (v/v) DMSO. Cells challenged with AKBA (B) were grown for 24 hours in cell culture medium to attach and recover before AKBA was added at various concentrations (μM) and left for 6 or 48 hours. Morphological changes of treated cells were observed with apoptotic features such as small and large blebs pinching off the cells and residual apoptotic bodies (black arrow).

Similarly, OVCAR4 cells grown in either standard cell culture medium or medium supplemented with 0.5% (v/v) DMSO exhibited a mixture of circular, oval and slightly elongated morphologies that that continue in proliferations and did not change between the 6 hour and 48 hour time points. Cell morphology was largely maintained in the cells treated with AKBA at relatively low concentrations (5-10 μM). However, at AKBA concentrations of 15 μM or higher there were some discernible effects on the overall cell shape and structural integrity as highlighted by black arrows in the figure. After 6 hours exposure to 15, 25 and 50 μM AKBA, microscopy images showed the presence of small round-shaped cells with condensed chromatin, in contrast to the control samples (culture medium and the medium with DMSO) with evidence of cellular debris. After 48 hours, the OVCAR4 cell morphology change was even more marked, with indications of cell lysis occurring in the samples exposed to concentrations of 15 μM AKBA or higher, with a lot of fragments which might be due to cell lysis (Fig 4.2.2).

4.2.2.2 Effect of AKBA on the inhibition of cell growth:

In order to confirm the hypothesis of AKBA causing cell growth inhibition in ovarian cancer cell lines, UWB1.289 and OVCAR4 cells were exposed to a range of concentrations of AKBA (5 μ M-50 μ M) for different time points (0 h, 6 h, 16 h, 24 h, 48 h) and cell growth inhibition was tested and recorded using both cell counting and the Almar Blue assay at various time points over 48 hours (Fig. 4.2.3&Fig. 4.2.5) In each experiment the effect of AKBA was compared with the negative control containing 0.5% (v/v) DMSO as the vehicle control.

The apparent decrease in UWB1.289 and OVCAR 4 cells was confirmed quantifiably by measuring the cell number over time, which showed that concentrations of at least 15 μ M AKBA were sufficient to cause a statistically significant decrease ($P<0.001$) in cell number after 48 hours in UWB1.289 (Fig 4.2.3). The loss of cells occurred more extensively when exposed to higher concentrations of AKBA; at 25 μ M exposure, the number of cells was significantly less than the control samples after 24 hours, and at the highest AKBA concentration (50 μ M)($P< 0.0001$) cell growth was inhibited from as early as 6 hours. This experiment showed the growth inhibition effect of AKBA on UWB1.289 and similarly in OVCAR4 cell lines; however, to determine the metabolic activity of the surviving cells, an additional experiment was performed using the Alamar Blue assay (Fig. 4.2.4). This experiment, revealed a correlation between AKBA concentration and time-dependent inhibition of metabolic function that mirrored the results of cell counting. Together these experiments highlighted the potency of AKBA at concentrations of 15 μ M or higher in inhibiting metabolic activity, with the addition of 50 μ M causing a statistically significant decrease ($P<0.001$) in the metabolic activity of both UWB1.289 and OVCAR4 cell lines within minutes. The assay demonstrated that a minimum concentration of 15 μ M AKBA was required to significantly impact the metabolic activity of UWB1.289 cells within 48 hours. At the concentrations of AKBA tested, the chemical caused a halving of growth (IC₅₀) at a concentration of approximately 20 μ M, with the rate of inhibition of viability increasing at concentrations greater than 10 μ M (Fig.4.2.5). Interestingly the high grad serous OVCAR4 cell lines shows cell growth inhibition (IC₅₀) at a concentration of approximately 17.8 μ M, which is lower than UWB1.289 (Fig.4.2.5).

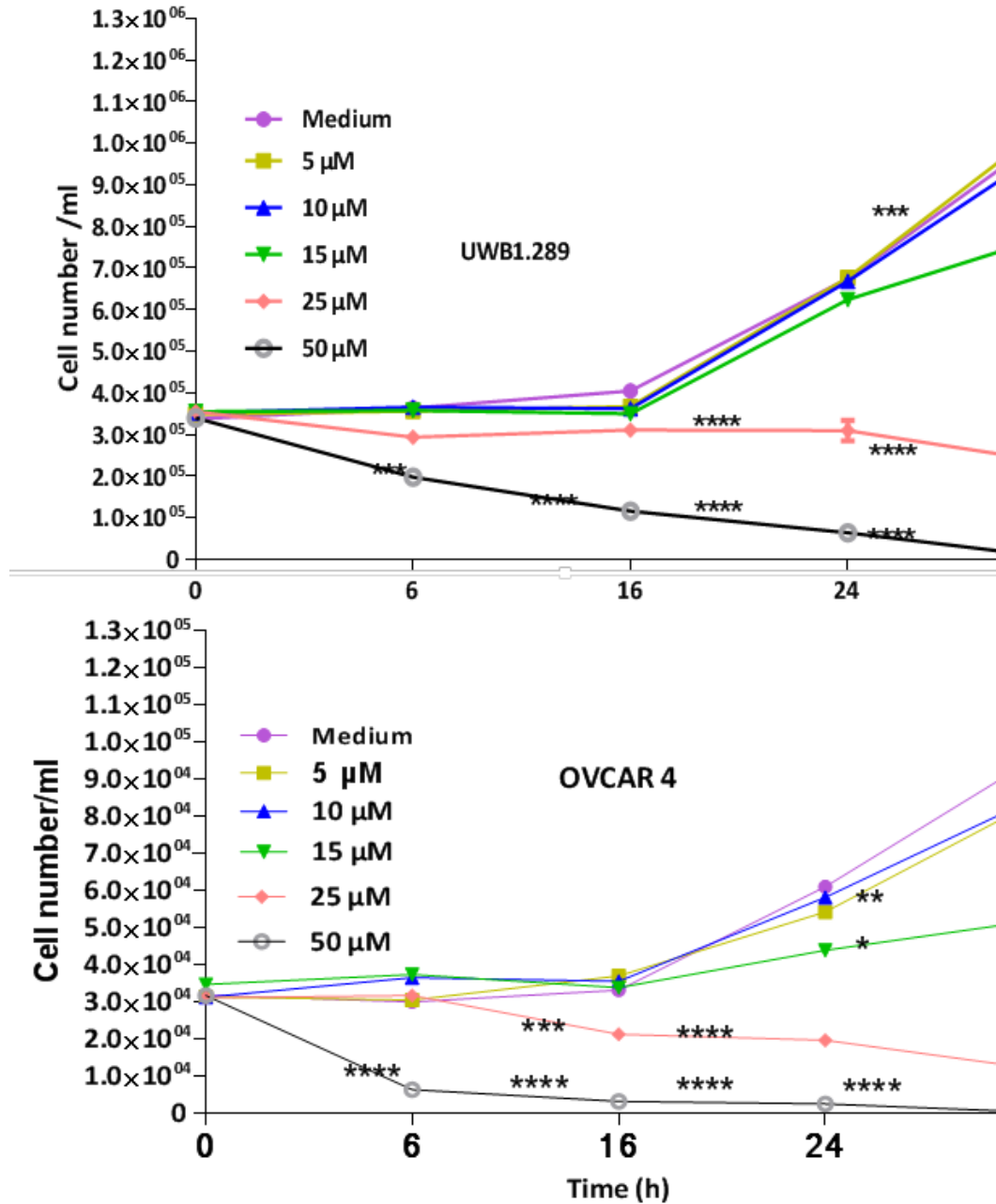


Figure 4.2. 3 AKBA-induced cell growth inhibition in UWB 1.289 and OVCAR 4 cells at different concentrations over time.

Negative controls consist of culture medium (media) plus 0.5%DMSO.Cell number was analysed using a cell counter. Results are expressed as Mean \pm SEM and are representative of three separate experiments. *P<0.05, **P<0.01, ***P<0.001 and ****P<0.0001 compared to control.

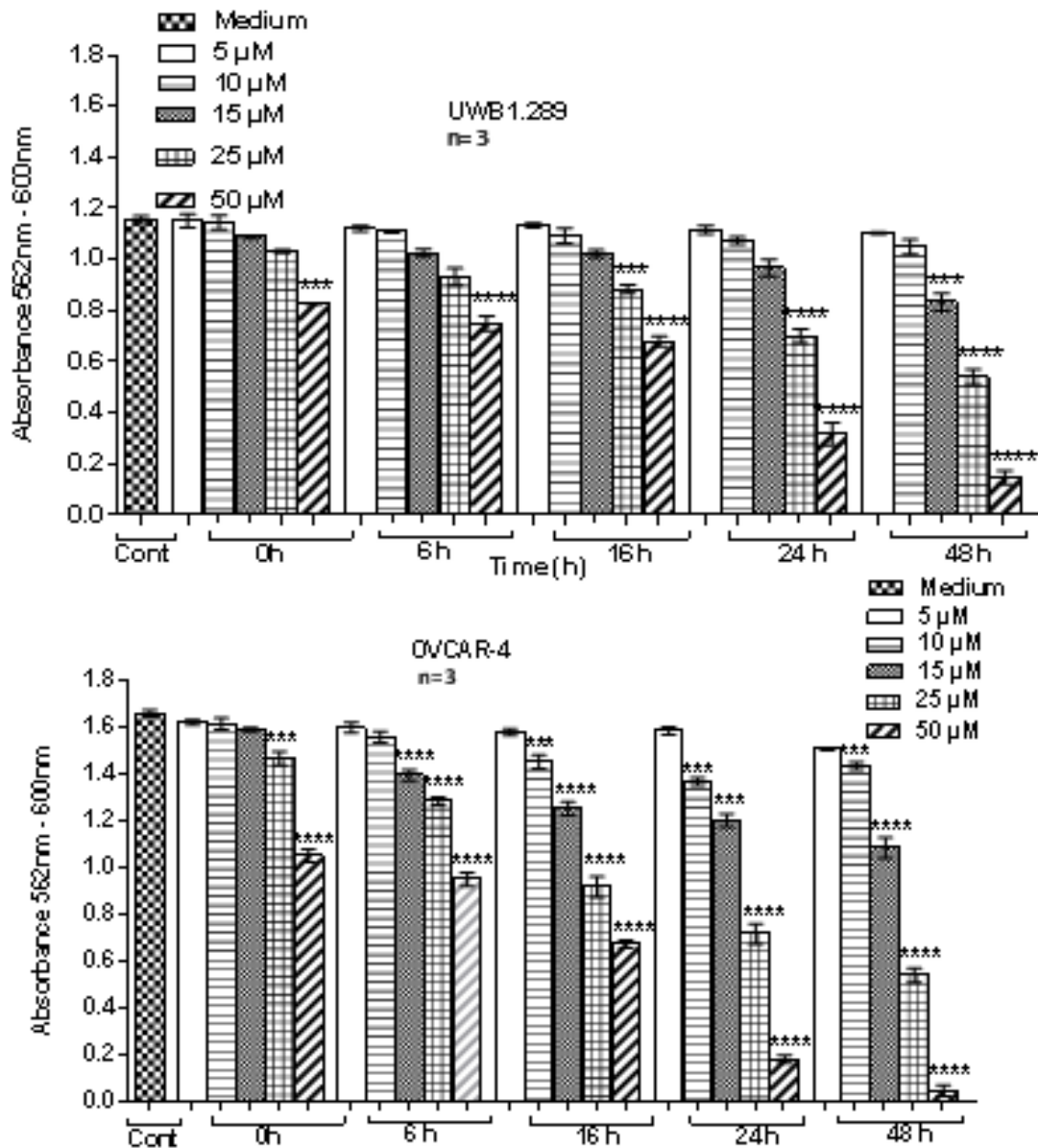


Figure 4.2. 4 AKBA-induced cell growth inhibition in UWB 1.289 and OVCAR4 cells using different concentrations over time.

Negative controls consist of culture medium (media) plus 0.5%DMSO. The inhibition of cells growth was analysed using the Almar Blue assay. Results are expressed as Mean \pm SEM and are representative of 3 independent experiments. *P<0.05, **P<0.01, ***P<0.001 and ****P<0.0001 compared to control.

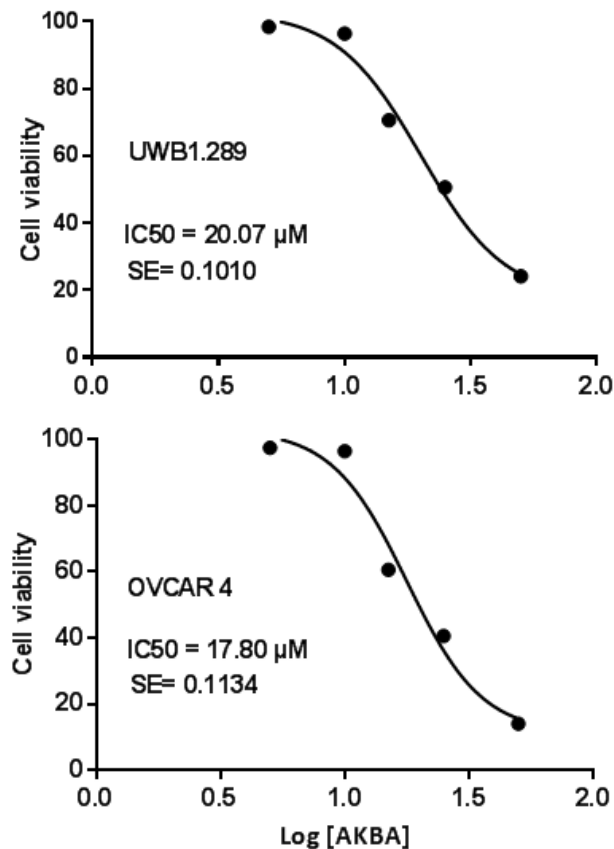


Figure 4.2. 5 AKBA-induced cell growth inhibition after 24 hours in UWB 1.289 (IC50 = 20.07) and OVCAR4 (IC50 = 17.80).

Using different concentrations (5 μM, 10 μM, 15 μM, 25 μM & 50 μM) for 24 h. the inhibition of cells growth was analysed using Almar Blue assay. Results are representative of 3 independent experiments.

From chapter 3 and chapter 4 IC50 results for all 4 cell lines were almost similar (Table 4.1) (Fig 4.2.6) which shows that AKBA has a similar effect in all the type of ovarian cancer cell lines whatever mutations the have and cisplatin treatment response they have.

Table 4. 1 cell growth inhibition IC50 after 24 hours of treatment.

Ovarian cancer Cell line	A2780	A2780cis	UWB1.289	OVCAR4
IC50	21.78	18.58	20.07	17.80

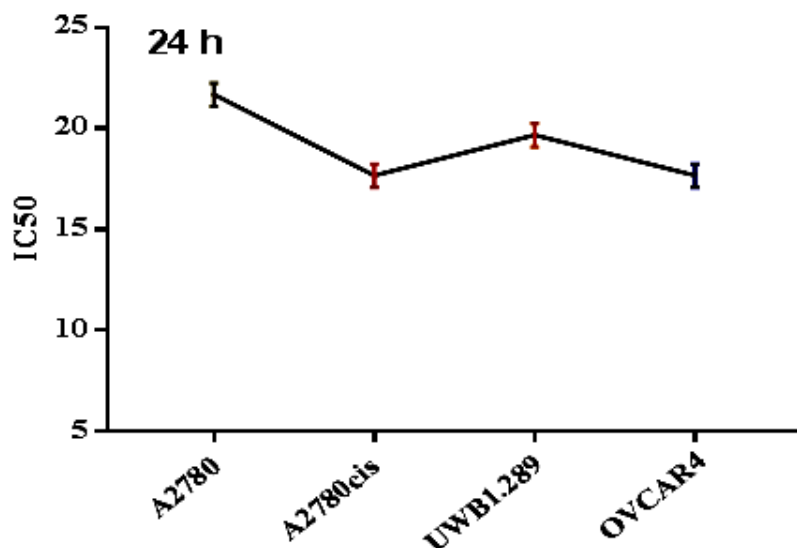


Figure 4.2.6 AKBA-induced cell growth inhibition after 24 hours in A2780 (IC₅₀= 21.78), A2780cis (IC₅₀= 18.58), UWB 1.289 (IC₅₀ = 20.07) and OVCAR4 (IC₅₀ = 17.80).

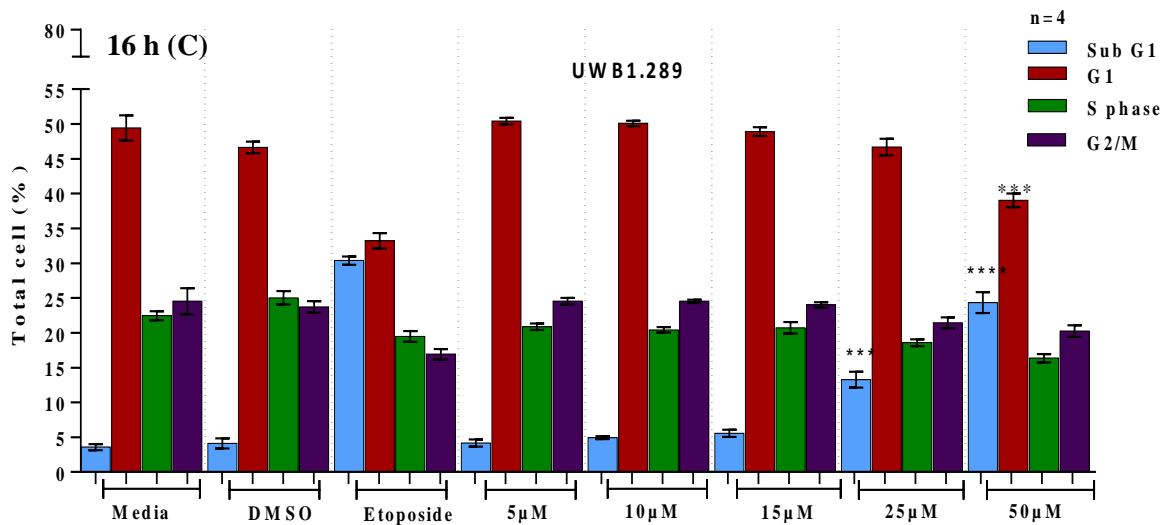
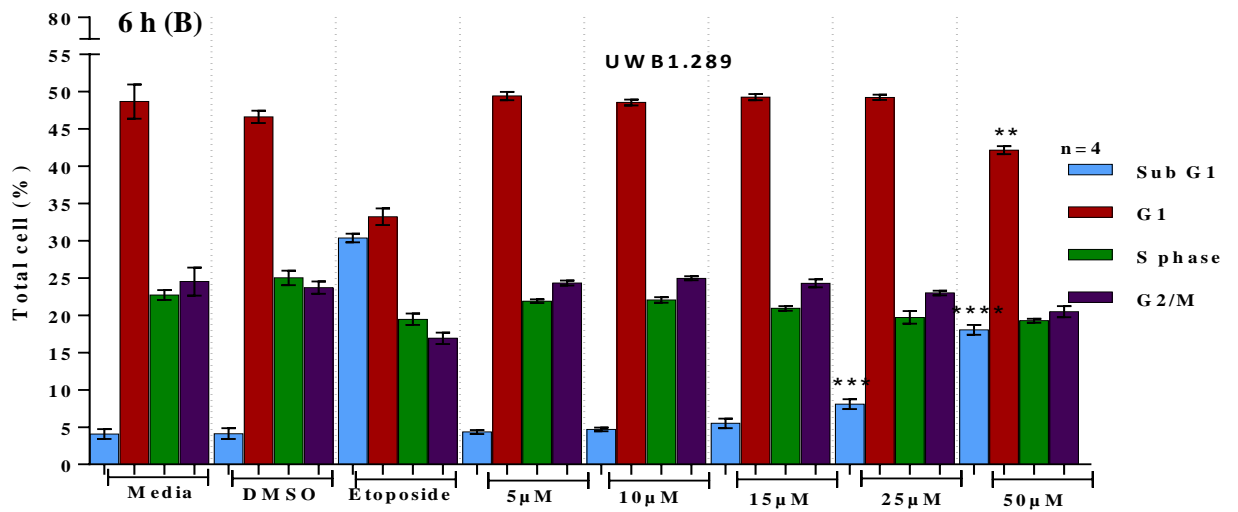
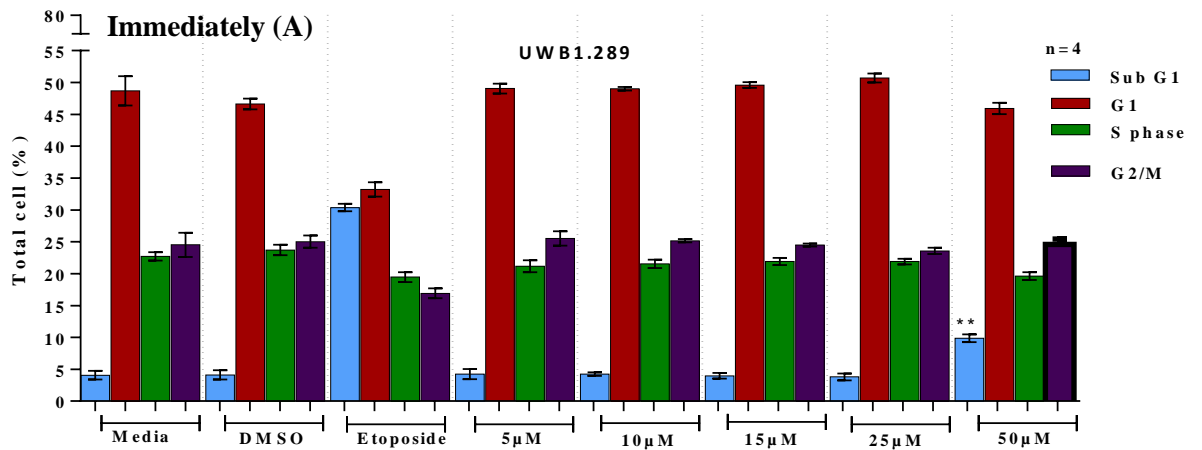
Using different concentrations (5 μ M, 10 μ M, 15 μ M, 25 μ M & 50 μ M) for 24 h. the inhibition of cells growth was analysed using Almar Blue assay. Results are representative of 3 independent experiments.

4.2.3 AKBA effect on cell cycle and apoptosis in UWB1.289 and OVCAR4 cell lines

4.2.3.1 AKBA-induced cell cycle arrest and apoptosis in UWB1.289 cells

4.2.3.1.1 Cell cycle arrest

Cell cycle arrest is one of the mechanisms which were examined following treatment with AKBA for both cell lines, using PI staining and assessed by flow cytometry. Consistent with the AKBA effect on cell growth suppression, high levels of cell death (increased percentage of cells in sub-G₁ phase) were observed after exposing cells to increasing concentrations of AKBA (Fig. 4.3.1.1 & Fig. 4.3.2.1). The DNA histogram showed cells were shifted towards and accumulated significantly at sub-G₁ with increasing concentrations of AKBA treatment compared to control cells.



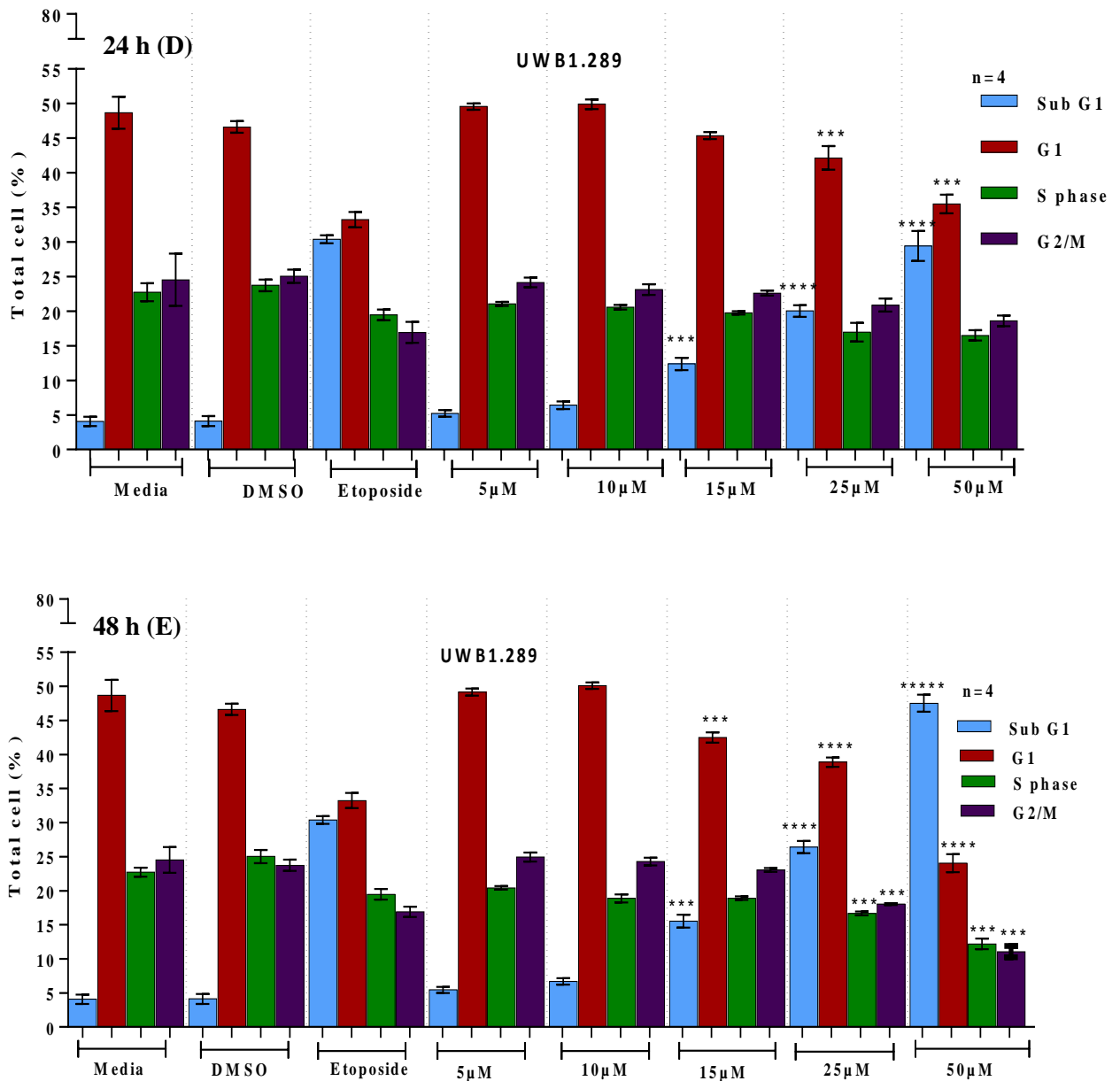


Figure 4.3. 1 Effect of AKBA on cell cycle of UWB1.289 cells.

Effect of AKBA on cell cycle of UWB1.289 cells using different concentrations over time (A) Immediately (< 30 mins), (B) 6 h, (C) 16 h, (D) 24 h and (E) 48 h after exposure to AKBA. Controls consisted of culture medium (media) plus either 0.5% v/v DMSO (negative control) or Etoposide (positive control) after 24 h of exposure. The results are representative of at least 4 independent experiments. Cells were seeded using serum free medium; then after 18 hrs the medium was changed for culture medium containing 5% serum and the AKBA treatment. Results are expressed as Mean \pm SEM. *P<0.05, **P<0.01, ***P<0.001 and ****P<0.0001.

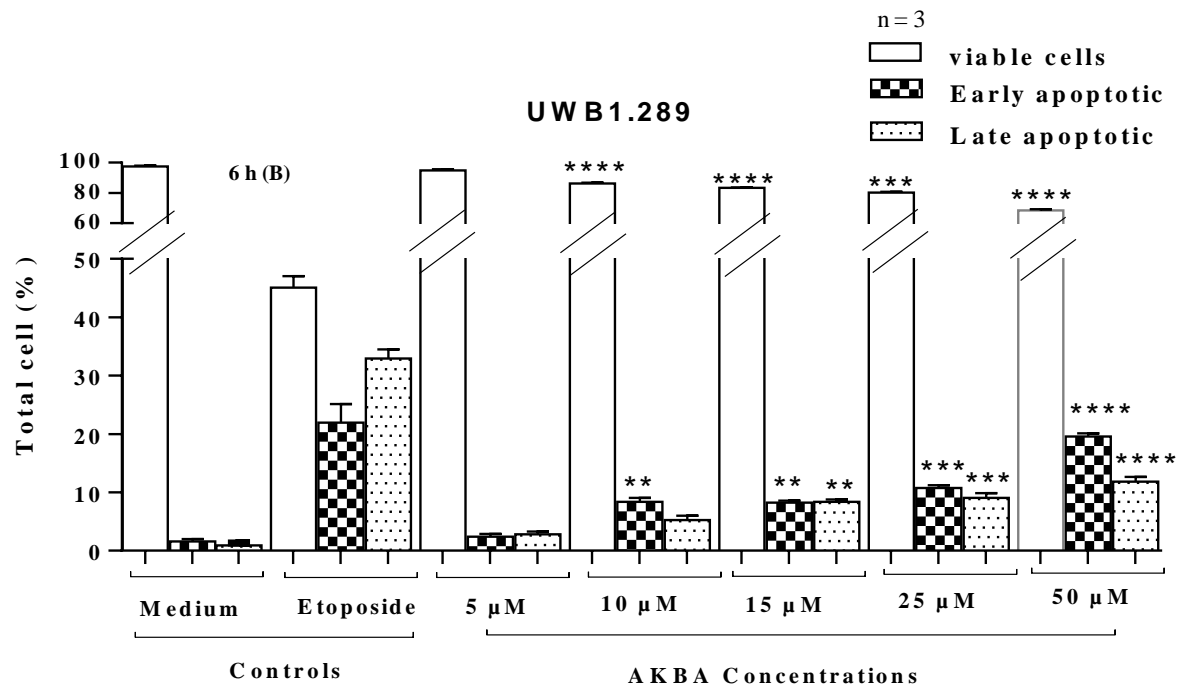
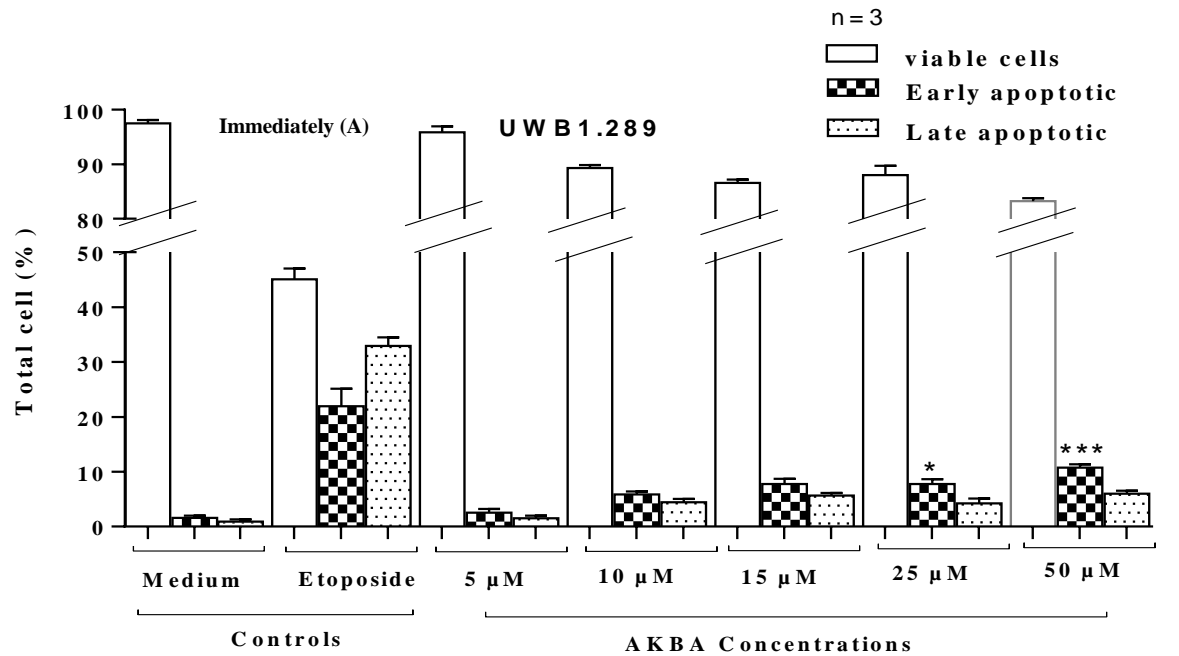
Cell cycle analysis shows that at the highest concentration investigated, AKBA induced

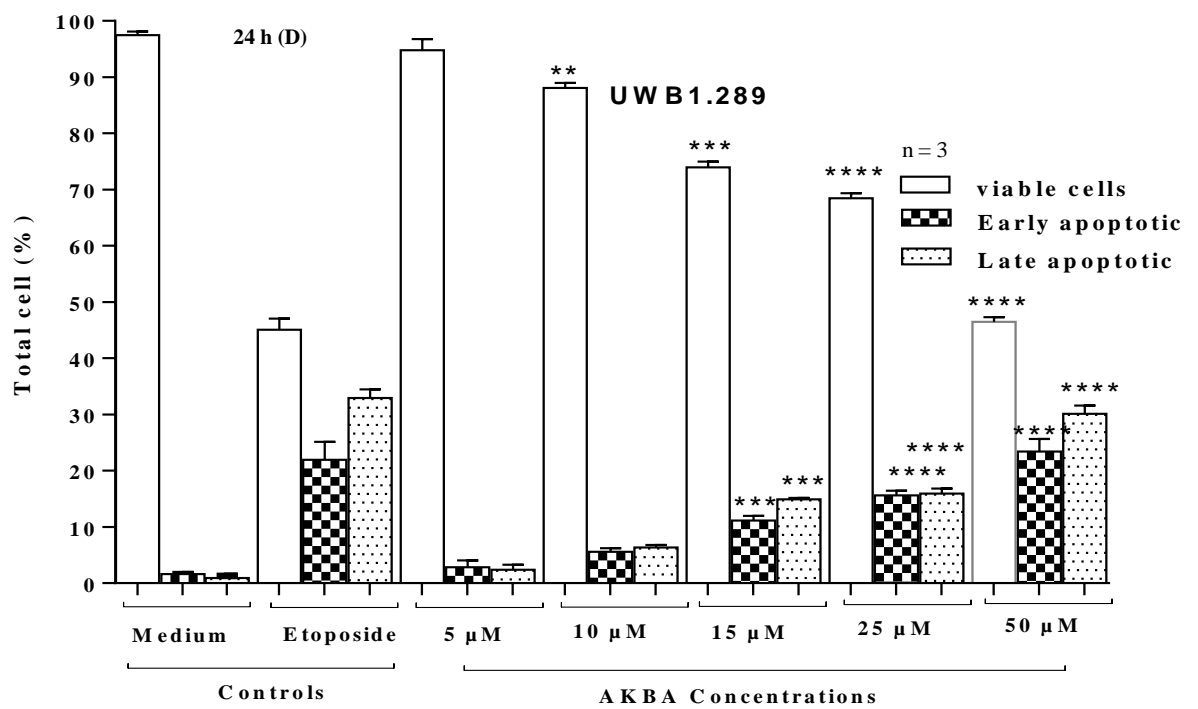
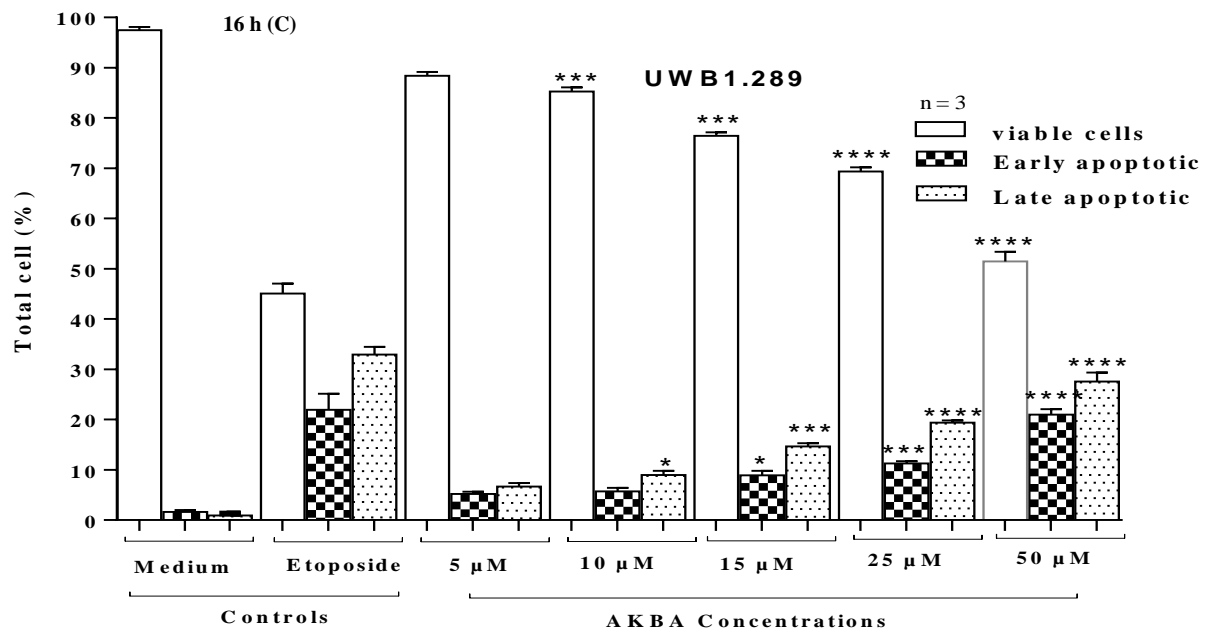
immediate cell death in UWB1.289 cells, resulting in approximately a 10 % response for cells in the sub-G₁ stage (dead cells) ($P < 0.01$), compared with less than 5 % for the medium-only control sample. As exposure time increased, lower AKBA concentrations had the same effect as the initial high dose treatment, causing the cell to go into sub G₁ phase of the cell cycle; resulting in a high proportion of the cells remaining in SubG₁ phase. As exposure times increased, the proportion of replicating cells decreased dramatically in all the cell cycle phases which might be possibly due to all the cells being blocked in all the different phases of the cycle till death; so that by the end of the experiment (48 hours) 50 μ M AKBA treatment resulted in approximately 50 % of cells in UWB1.289 (Fig 4.3.1.1) and 80 % of OVCAR4 cells (Fig. 4.3.1.3) in sub-G₁ (dead) ($P < 0.0001$), and one quarter completing G₁ phase (compared with almost half the cell population of the control samples) 11 % in S phase and G₂/M phases (compared to 23 % and 24 %, respectively, in the control samples). OVCAR4 shows slightly lower population at G₁ phase which is around 20 % and around 10 % with S phase and G₂/M. It is also possible that UWB1.289 and OVCAR4 cells entered a quiescence phase and then move to the sub-G₁ stage and died. Interestingly OVCAR4 cell lines were notably more sensitive to AKBA than UWB1.289. The proportion of cells in each phase of the cell cycle is the same at all doses and times of exposure to AKBA, the only difference is that AKBA kills the cells with more cells being in the subG₁ phase. Treatment with 50 μ M had an immediate effect, 25 μ M takes 6h to affect cells ($P < 0.001$) whilst 15 μ M had a significant effect at 24 h ($P < 0.001$).

4.3.1.2 AKBA induces apoptosis in UWB1.289

To confirm the sub G₁ results and the likely apoptotic effects reported in section (4.3.1.1) Annexin V/PI staining was used to more directly assess apoptosis. Based on this data, it was clear that the arrest in the cell cycle was coupled with programmed cell death, with a decrease in viable cells demonstrated at AKBA concentrations of 10 μ M, coupled with increase in the proportion (5-25% in early apoptotic and 10- 65% late apoptotic, depending on AKBA concentration) of apoptotic cells by the end of the experiment. Interestingly, exposure to the two highest concentrations of AKBA resulted in an immediate formation of early apoptotic cells, correlating with the initial increase in cells in sub-G₁. With 50 μ M of AKBA there were 15 % of early and late apoptotic cells immediately after exposure, which increased with time to 24% early and 30% late after 24h and 25% early and 65% late apoptotic cells after 48 h of treatment. Similar scenario was with lower concentrations $> 10 \mu$ M and the level of early and late apoptotic depends

on AKBA concentrations and time of exposure. 25 μ M gives 18% early and 25 late apoptotic cells after 48 h of exposure which all are significantly higher than controls ($P < 0.0001$).





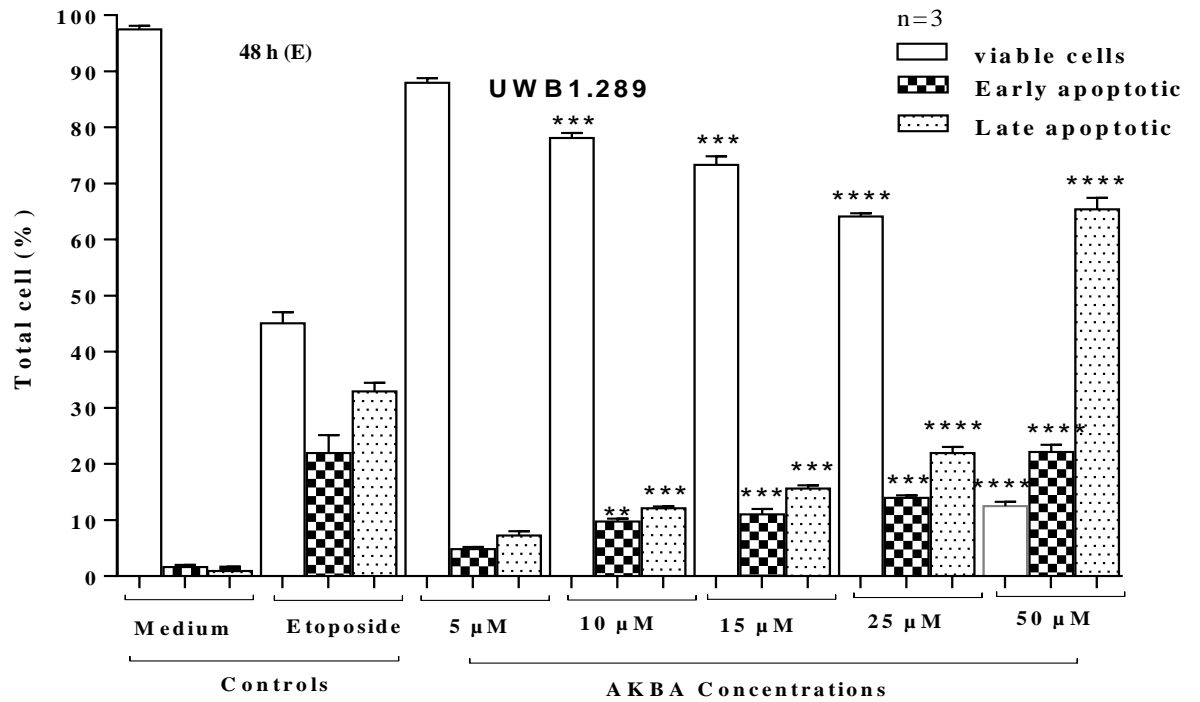
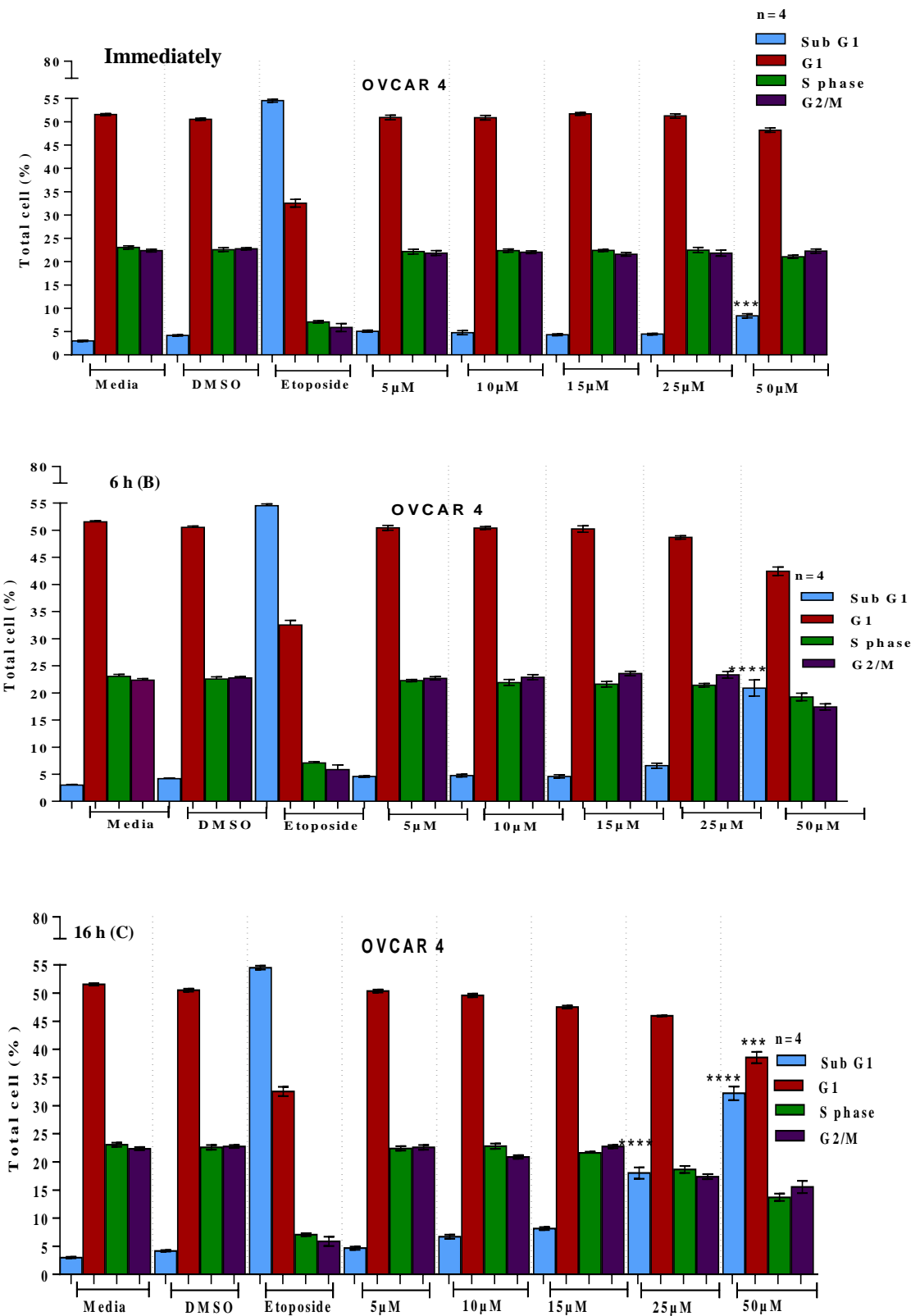


Figure 4.3. 2 Effect of AKBA on cell death of UWB1.289 cells using Annexin V/PI.
Effect of AKBA

Effect of AKBA on cell death of UWB1.289 cells using Annexin V/PI(A) immediately (< 30 mins), (B) 6 h, (C) 16 h, (D) 24 h and (E) 48 h after exposure to AKBA. UWB1.289 cells were treated at a range of concentrations, compared with negative controls consisting of 0.5% v/v DMSO, and positive control (Etoposide) after 24 h of exposure. The results are representative of at three independent experiments and expressed as mean \pm SEM. *P<0.05, **P<0.01, ***P<0.001 and ****P<0.000.

4.2.3.2 AKBA induce cell cycle arrest and apoptosis in OVCAR4

4.2.3.2.1 Cell cycle arrest



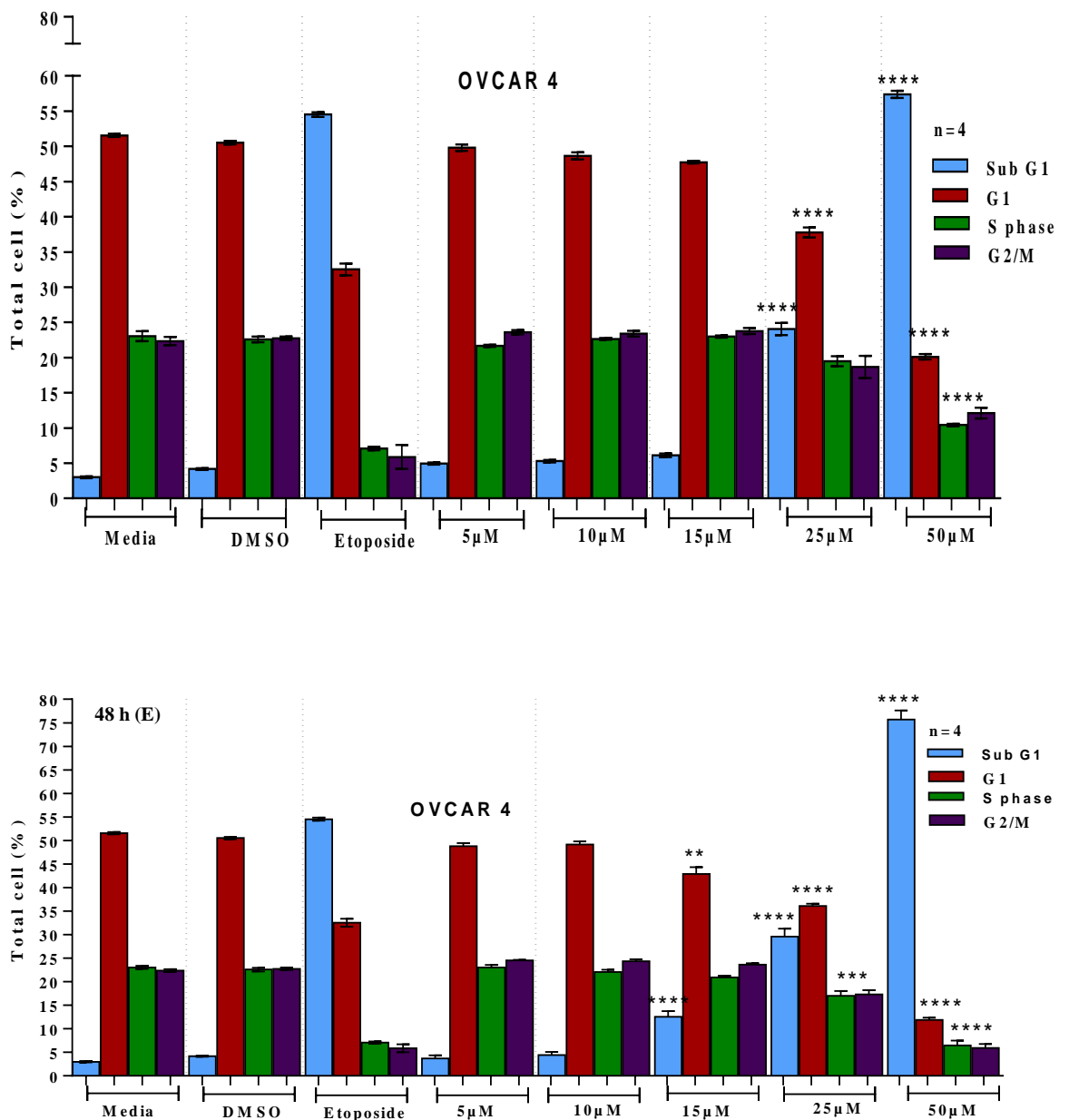


Figure 4.3. Effect of AKBA on cell cycle of OVCAR4 cells.

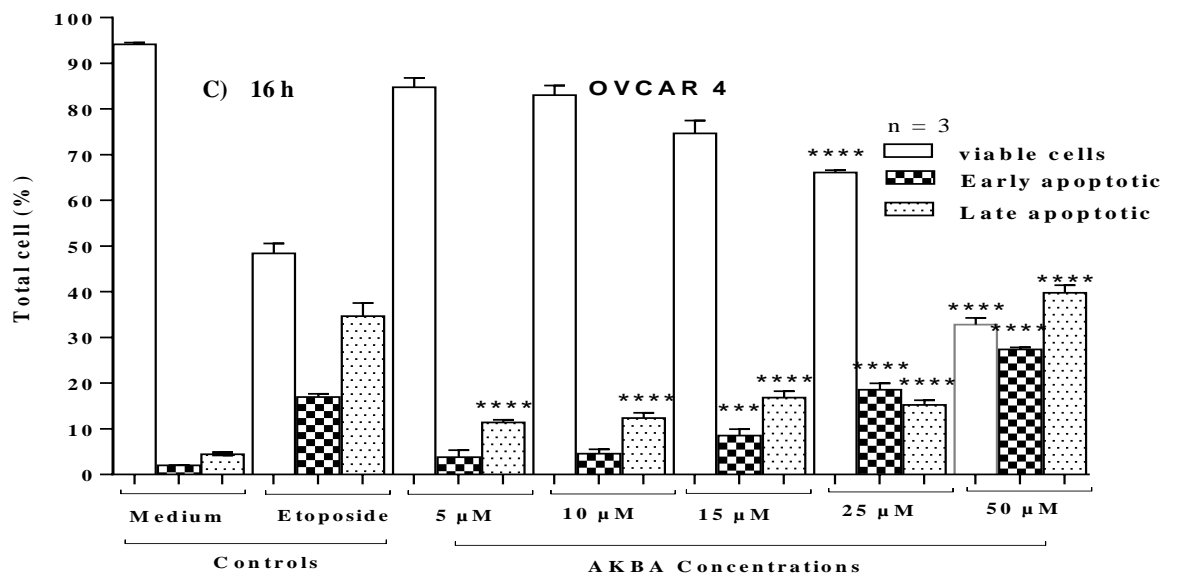
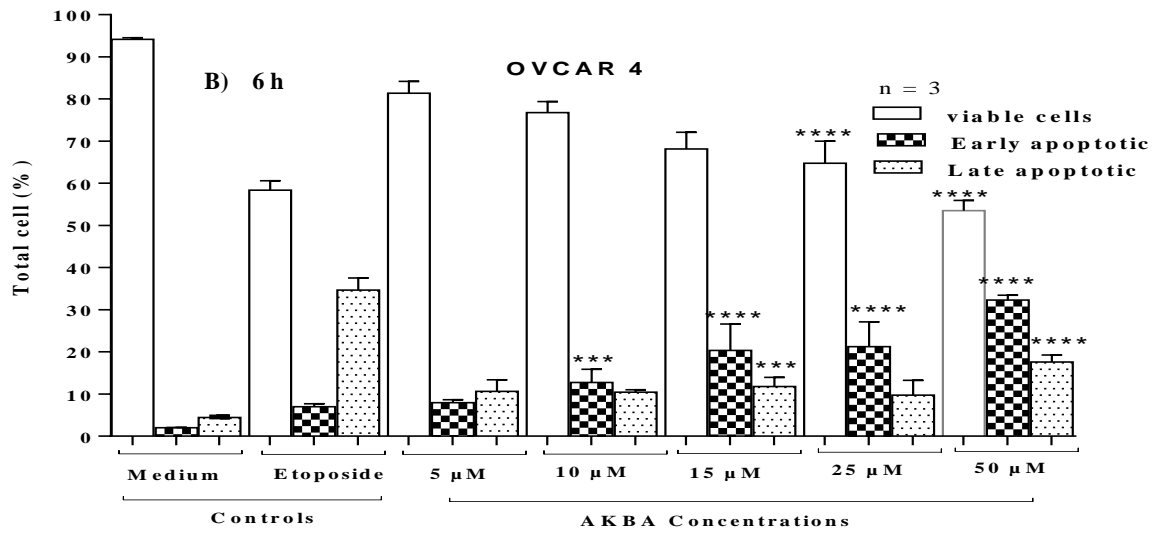
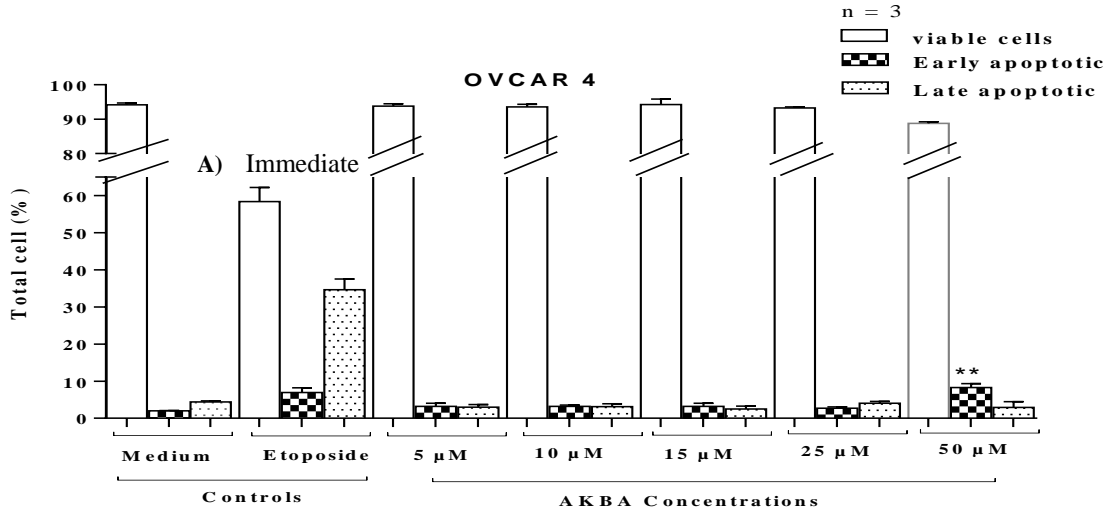
Effect of AKBA on cell death of UWB1.289 cells using Annexin V/PI (A) immediately (< 30 mins), (B) 6 h, (C) 16 h, (D) 24 h and (E) 48 h of exposure to AKBA. OVCAR4 cells were treated at a range of concentrations and compared with controls consisting of culture medium (media), 0.5% v/v DMSO (negative) and Etoposide (positive) control (Etoposide) after 24 h of exposure. The results are representative of 4 independent experiments, and expressed as Mean \pm SEM. * $P < 0.05$, ** $P < 0.01$, *** $P < 0.001$ and **** $P < 0.0001$ compared to control samples. Cells were seeded using serum free medium then after 18 hrs medium changed with culture medium containing 5% serum and the AKBA treatment.

OVCAR4 is a cell line derived from an ovarian adenocarcinoma and represents a useful

cell line to assess the anticancer potential of AKBA, since OVCAR4 cells have a gene expression profile closely resembling that of cancer cells found in high grade serous ovarian cancer tumours. From the results of experiments performed in this study it is clear that AKBA is able to inhibit cell growth, initiate apoptosis-causing DNA fragmentations in OVCAR4 cells and induce DNA damage that then induces apoptosis. Cell growth inhibition was dose-dependent with low concentrations of AKBA (15 μ M) ($P < 0.001$) having an effect after prolonged exposure (48 hours) (fig 4.2.1.3.1 – 4.2.1.3.2). Similar to the UWB1.289 cell lines included in this study, higher AKBA doses showed cytotoxicity and DNA damaging effects with shorter exposure times. For example, treatment with 25 μ M AKBA showed a growth inhibition effect within 16 hours, whereas 50 μ M gave the same effect within just 6 hours. OVCAR4 growth inhibition was coupled with evidence of loss of viability immediately after exposure to AKBA when treated with the highest concentrations of AKBA, while prolonged exposure over 48 hours caused a loss in cell viability at concentrations as low as 10 μ M. The IC₅₀ concentration for AKBA was calculated at 17.8 μ M, however, at a concentration lower than the IC₅₀ (15 μ M) the morphology of OVCAR4 cells became discernibly altered after 6 hours exposure.

4.2.3.2.2 AKBA induces apoptosis in OVCAR4

In order to confirm the sub G₁ results obtained from the cell cycle analysis and the apoptosis evaluations caused by AKBA, after treatment, the apoptotic response was examined by flow cytometric analysis using Annexin V-FITC and PI staining (Fig. 4.3.2.2) Viable OVCAR4 cells were significantly decreased upon AKBA treatment at 15 μ M ($P < 0.001$), 25 μ M and 50 μ M ($P < 0.0001$) after 6 hours incubation respectively compared to control cells. In parallel, the percentage of early and late apoptosis increased significantly with the increase in AKBA concentrations and with increasing time of exposure. A gradual increase was observed in the apoptotic population with higher concentration of AKBA 15 μ M – 50 μ M (Fig. 4.3.2.2). After 48 hours incubation, the percentage of early apoptotic was 15% and late apoptotic cells increased dramatically to 75% after treatment with 50 μ M. The level of late apoptotic was significantly increased at the concentrations of 10 – 25 μ M while late apoptotic cells only were seen with 5 μ M AKBA exposure when compared with control cells. In OVCAR4 cells with 25 μ M around 55% of cells were in early and late apoptotic after 48 h of exposure compared to 40% in UWB1.289. The number of apoptotic cells increased with 50 μ M where in BOTH cell lines to 90% with respect to early and late apoptotic deference's.



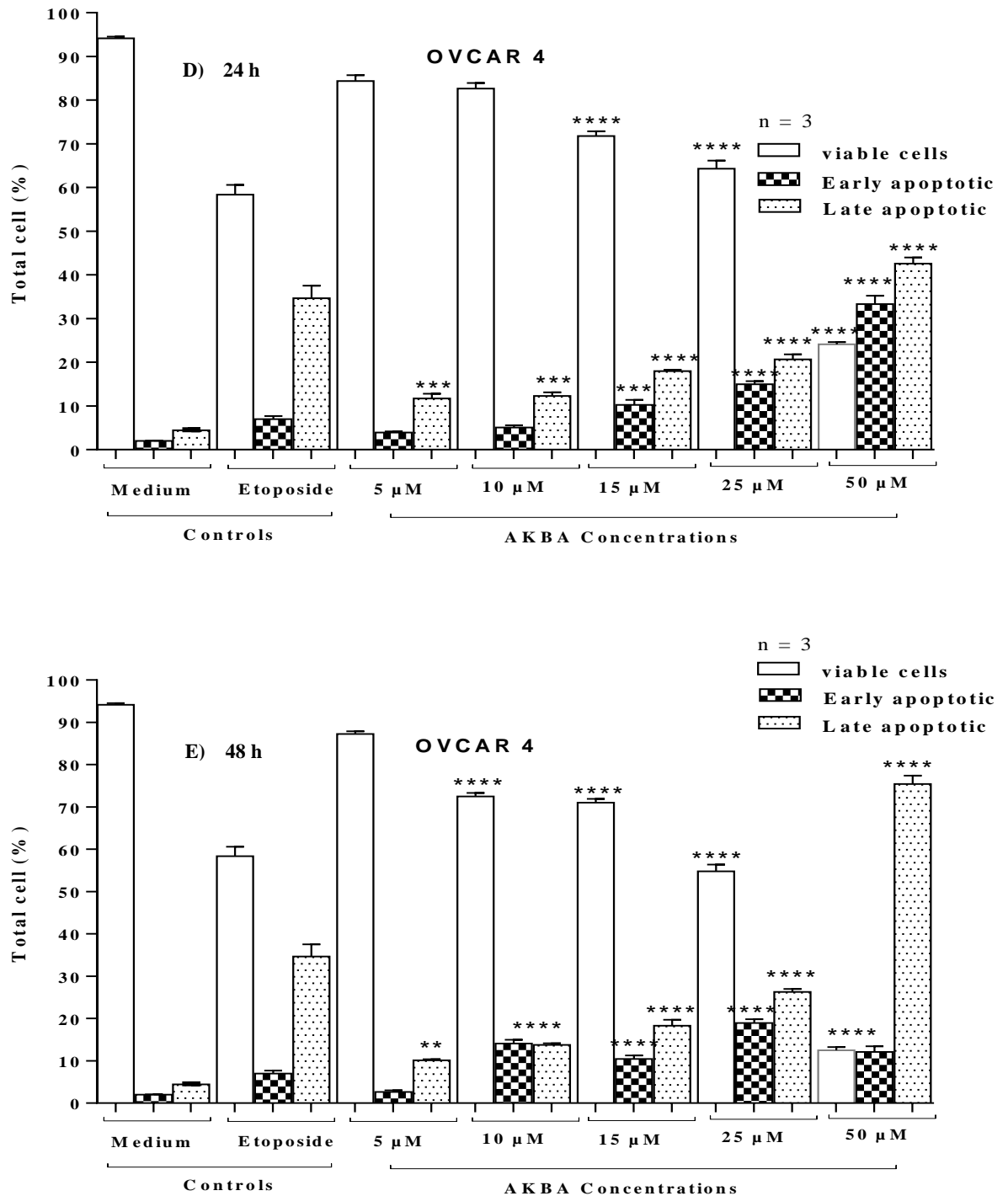


Figure 4.3. 4 Effect of AKBA on cell death of OVCAR4 using Annexin V/PI.

Effect of AKBA on cell cycle of OVCAR4. (A) Immediately (< 30 mins), (B) 6 h, (C) 16 h, (D) 24 h and (E) 48 h exposure to AKBA. OVCAR4 cells were treated at a range of concentrations, compared with negative controls consisting of 0.5% v/v DMSO, and positive control (Etoposide) after 24 h of exposure. The results representative of at 3 independent experiments. Results are expressed as Mean \pm SEM. *P<0.05, **P<0.01, ***P<0.001 and ****P<0.0001.

4.2.4 AKBA induces DNA damage and reduces ROS generation in UWB1.289 and OVCAR4 cell lines

4.2.4.1 AKBA induces DNA damage in both cell lines

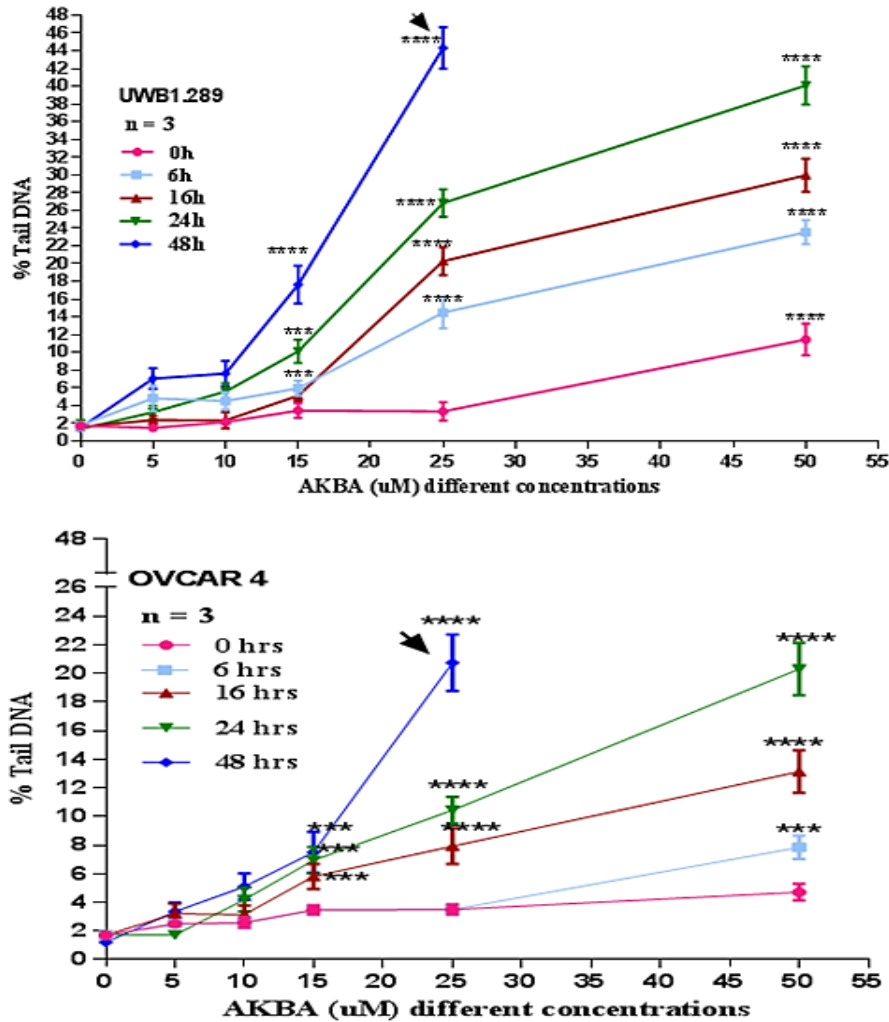


Figure 4.4. 1 AKBA-induced DNA damage in UWB1.289 and OVCAR4.

AKBA induced DNA damage in UWB1.289 and OVCAR4 cells by Comet assay. Cells were treated with different concentrations of AKBA for different time. Negative controls consisted of culture medium (media), 0.5% DMSO, with 50 μ M H₂O₂ as positive a control. Results are expressed as Mean \pm SEM of 3 independent experiments (50 comets scored per treatment). *P<0.05, **P<0.01, ***P<0.001 and ****P<0.0001.

Comet assay measured damage arising from AKBA. The DNA damage is significantly greater in UWB1.289 compare to OVCAR4 cells for all the time points assessed at the 50 μ M concentration. Whilst 15 μ M and 25 μ M with OVCAR4 show a significant increase at 6 h and greater, the amount of apoptotic cells is about the same (30% early + late apoptotic) (P<0.001).

4.2.4.2 AKBA induced double strand DNA break damage as assessed using the γ -H2AX Assay in UWB1.289 cells and OVCAR 4

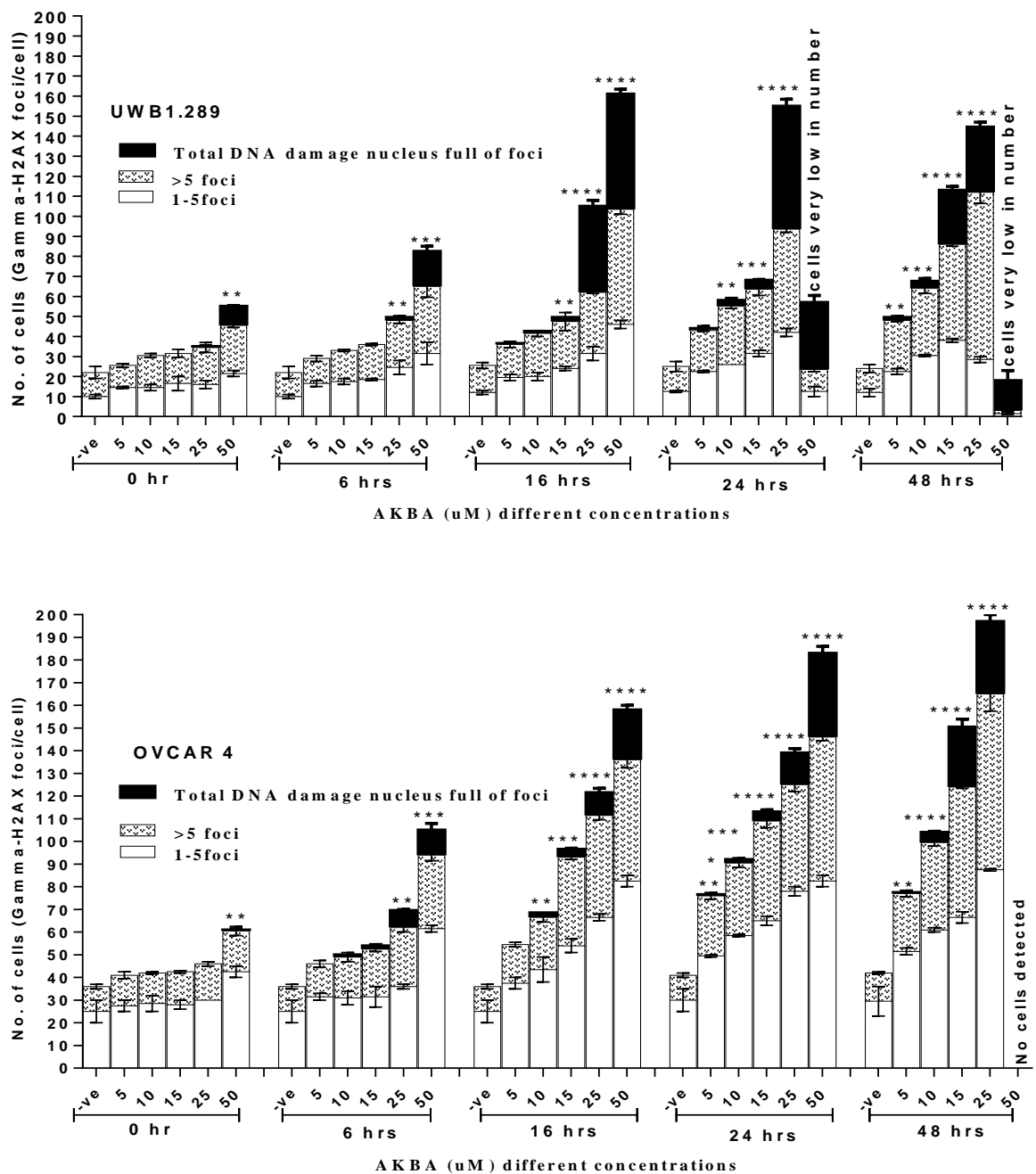


Figure 4.4. 2 AKBA-induced DNA double strand breaks presented by the number of foci per cell in Both UWB1.289 and OVCAR4 cells.

DNA double strand breaks were analysed using γ H2AX assay at different time points and concentrations of AKBA. Results are expressed as Mean \pm SEM of 3 independent experiments (45 image fields scored per treatment). *P<0.05, **P<0.01, ***P<0.001 and ****P<0.0001 compared to control samples.

4.2.4.3 AKBA diminishes ROS generations in both cell lines

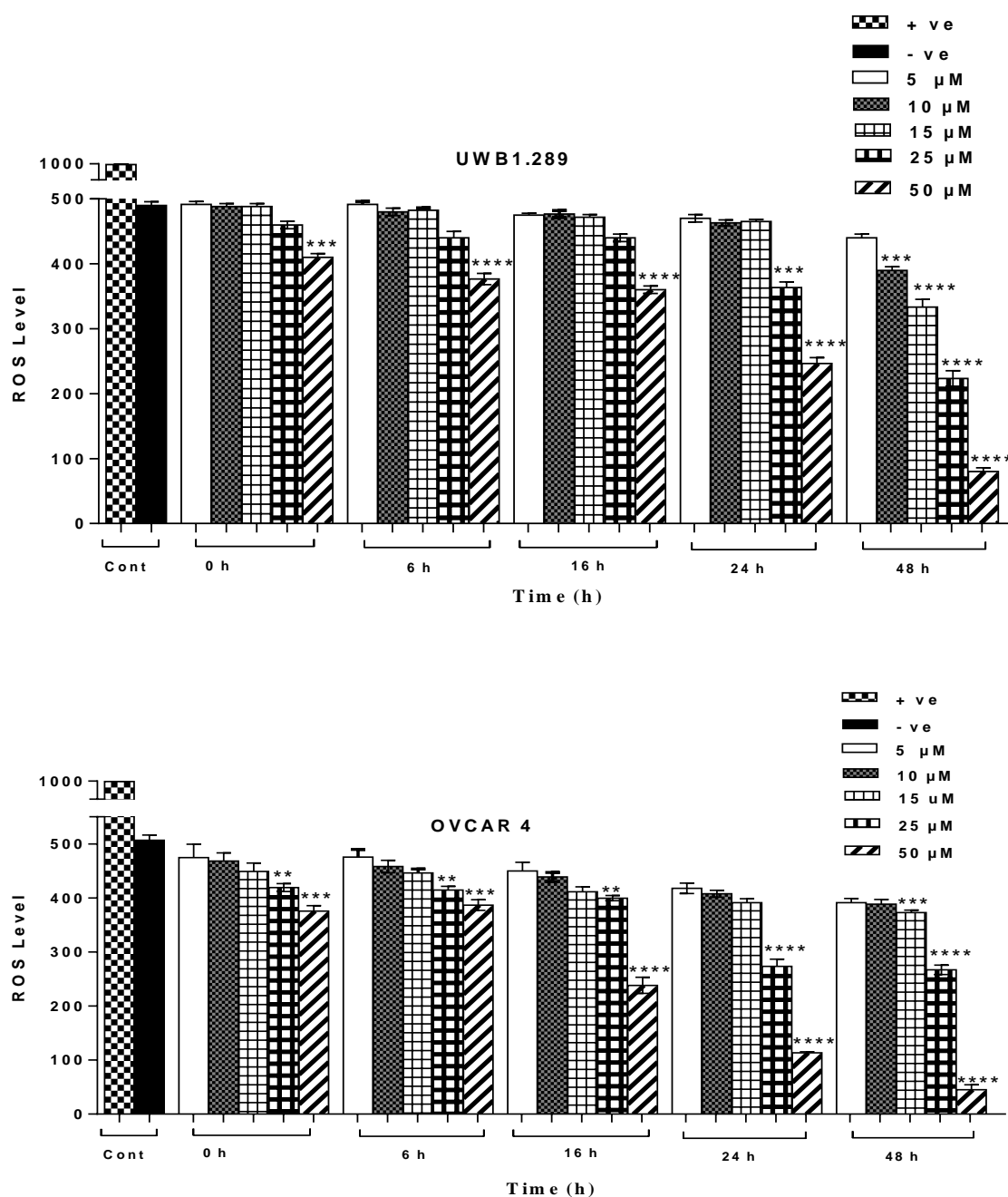


Figure 4.4. 3 ROS generation in UWB1.289 and OVCAR4 cell lines after treatment with AKBA.

ROS generation in UWB1.289 and OVCAR4 after treatment with different concentrations of AKBA for different periods. Negative controls consisting of culture medium, 0.5% v/v DMSO, and 50μM H₂O₂ as the positive control. Results are expressed as Mean ± SEM of 3 independent experiments (45 image fields scored per treatment). *P<0.05, **P<0.01, ***P<0.001 and ****P<0.0001 compared to control samples.

The morphological and cell viability data correlated with a build-up of DNA damage, which occurred immediately at the highest dose of AKBA (Fig. 4.4.1). AKBA treatment after 48 hours exposure, showed an effect at concentrations as low as 15 μ M. This damage to the DNA was evident by the number of foci present using γ H2AX assay, indicating histone phosphorylation caused by DSB (Fig. 4.4.2). For both cell lines DNA damage resulted in increased proportion of cells in sub-G₀/G₁ phase which was matched by increased early and late apoptotic populations. This was observed immediately upon exposure to 50 μ M AKBA, causing a significant increase in the relative abundance of sub-G₁ cells compared to negative control $P < 0.001$, along with a decrease in the proportion of cells at other cell cycle stages (Fig.4.3.2.1). After prolonged exposure at the highest concentration, approximately 75 % of the cell population was non-viable (sub-G₁). Conversely, concentrations of AKBA below 10 μ M did not significantly affect cell cycle progression in OVCAR4 cells, even after 48 hours exposure, with only a fraction of the cell population in the sub-G₁ stage (~5%). Cell cycle arrest after 48 hours exposure correlated with a significant increase in apoptotic cells. In OVCAR4 cell lines, apoptosis was induced by relatively low concentrations of AKBA; a significant increase in late apoptotic cells was evident from concentration as low as 5 μ M which were not easily detected in cell cycle using PI staining. Exposure to concentrations of AKBA greater than 10 μ M resulted in the presence of both early and late apoptotic cells (Fig.4.3.2.2), accompanied by significantly decreased cell viability as determined by the Almar blue and cell counting assays. Apoptosis was confirmed by western blot analysis, which revealed increases in the cellular production of cleaved caspase-3, cleaved poly ADP ribose polymerase (PARP), as well as cell cycle-regulating proteins p21 and p16 (Fig.4.4.4.1 & Fig.4.4.4.2). With the possibility that the arrested cells have disappeared by proceeding to the apoptotic process directly, and in that case it was missed by cell cycle, but this was evident by protein expression of P16 and P21. Taken together, these data provide evidence of AKBA-induced DNA damage, resulting in cell cycle arrest and programme cell death in this clinically relevant cell line.

4.2.4.4 Protein expression to confirm the apoptotic effects of AKBA

Further validation of the effect of AKBA treatment on induction of apoptosis was investigated by analysis of relevant proteins by western blotting at different time points (0 h, 6 h, 16 h, 24 h and 48 h) and for different AKBA concentrations (5 μ M, 10 μ M, 15 μ M, and 25 μ M).

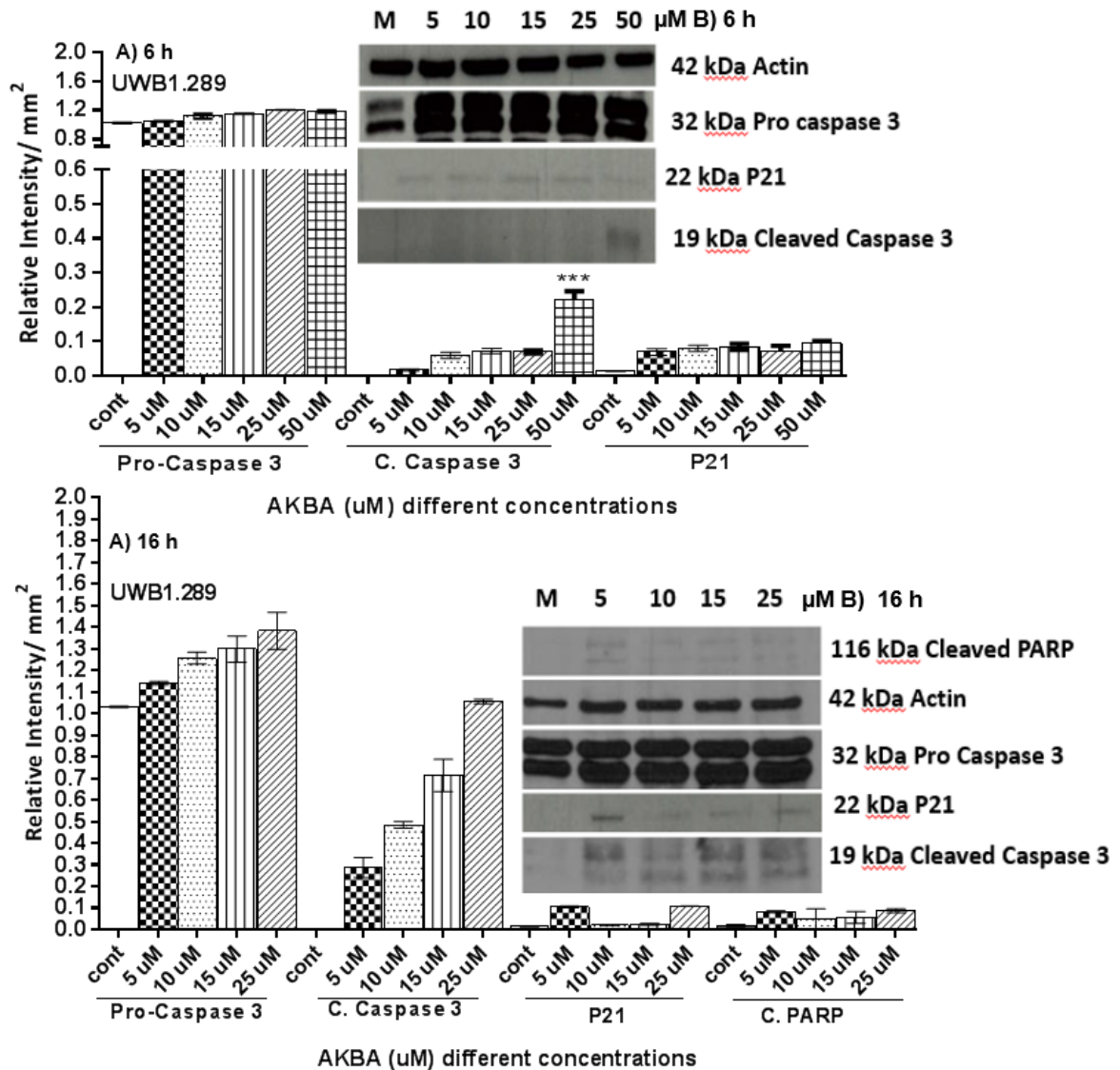


Figure 4.4. 4 Quantification of apoptotic protein expression in UWB 1.289 cells.

Cells were exposed to different concentrations of AKBA {5 μM, 10 μM, 15 μM, 25 μM & (50 μM for 6 h only)} for different time points (6 h & 16 h). A) Shows the pro-caspase 3, cleaved caspase 3, p21, p16 and cleaved PARP band intensities, B) is the relative intensity bands refers to the absorbance (normalized to actin) analysed using SyngeneGeneSnap software (Syngene, UK). Results are expressed as Mean ± SEM of 3 independent experiments, and *P<0.05, **P<0.01, ***P<0.001 and ****P<0.0001 compared to control samples (cells in cell culture medium plus 0.5% v/v DMSO).

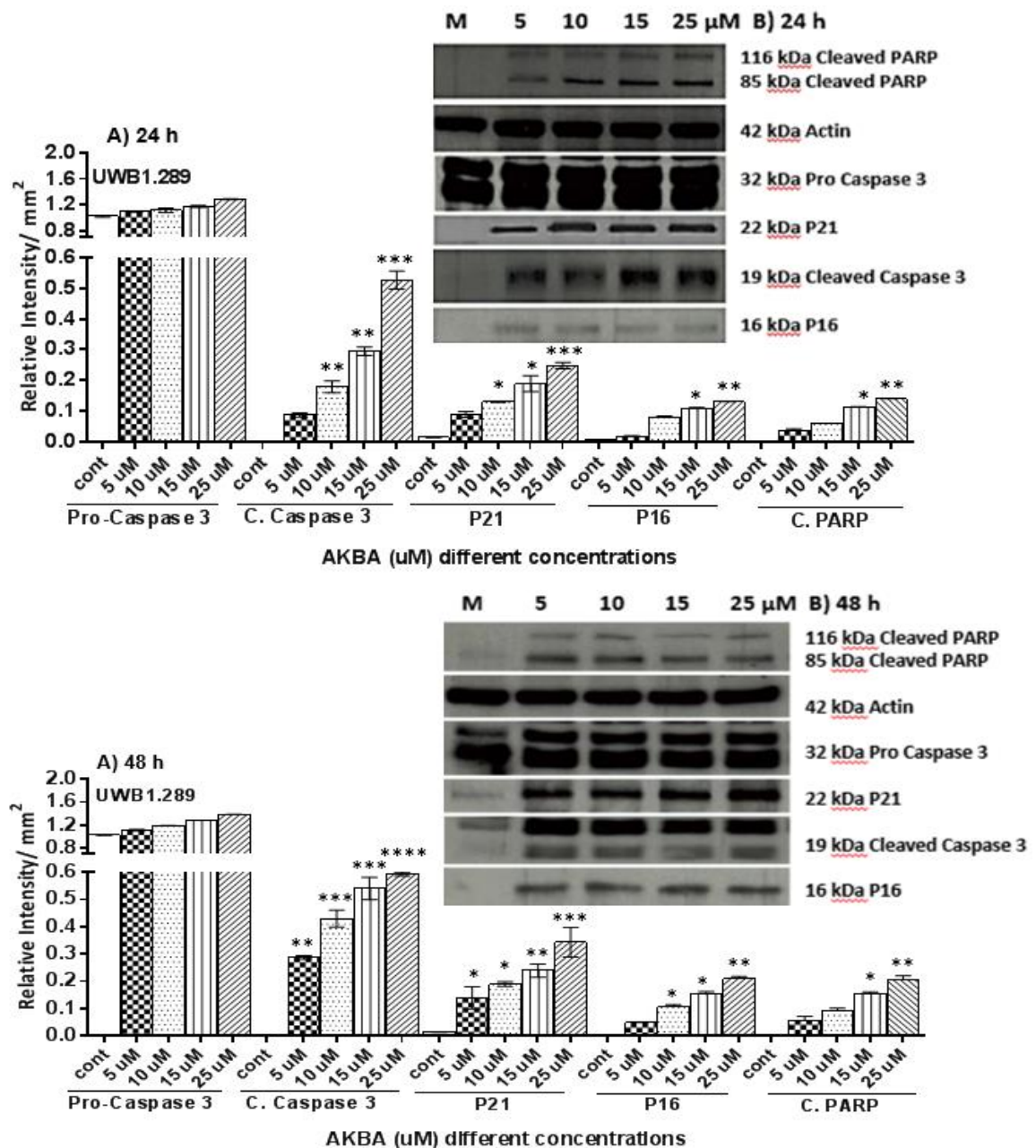


Figure 4.4.5 Quantification of apoptotic protein expression in UWB 1.289 cells.

Cells exposed to different concentrations of AKBA (5 μM, 10 μM, 15 μM & 25 μM) for different time points (24 h and 48 h). A) Shows the pro-caspase 3, cleaved caspase 3, cleaved PARP, p21, and p16 band intensities, B) is the relative intensity bands refers to the absorbance (normalized to actin) analysed using SyngeneGeneSnap software (Syngene, UK). Results are expressed as Mean ± SEM of 3 independent experiments, and *P<0.05, **P<0.01, ***P<0.001 and ****P<0.0001 compared to control samples (cells in cell culture medium plus 0.5% v/v DMSO).

The expression of procaspase-3 and cleaved caspase-3, involved in apoptotic mechanisms, with higher concentrations of AKBA, started significantly within 16 h. The precursor procaspase-3 was highly expressed and was relatively similar in control and

treated cells for all time points for both cell lines. Meanwhile, the active cleavage fragment of caspase-3 was increased with increasing doses for all AKBA treatment concentrations. However, cleaved PARP was significantly increased within 24 h ($P<0.01$) gradually with the increase in concentrations. Western blot analysis of P16 and p21, which were taken as a marker for cell cycle arrest and apoptosis and related to intrinsic pathway activation, was increased with the increase in time points and concentrations of AKBA. With UWB1.289 cells the activation of P21 started earlier than OVCAR4 cells at 6 h of treatment, whereas OVCAR4 cell lines started expressing P21 and P16 at 16 h with higher significance ($P<0.01$) compare to UWB1.289 mainly with 50 μM , which might be the case of OVCAR4 being more sensitive to AKBA than UWB1.289 upon longer exposure.

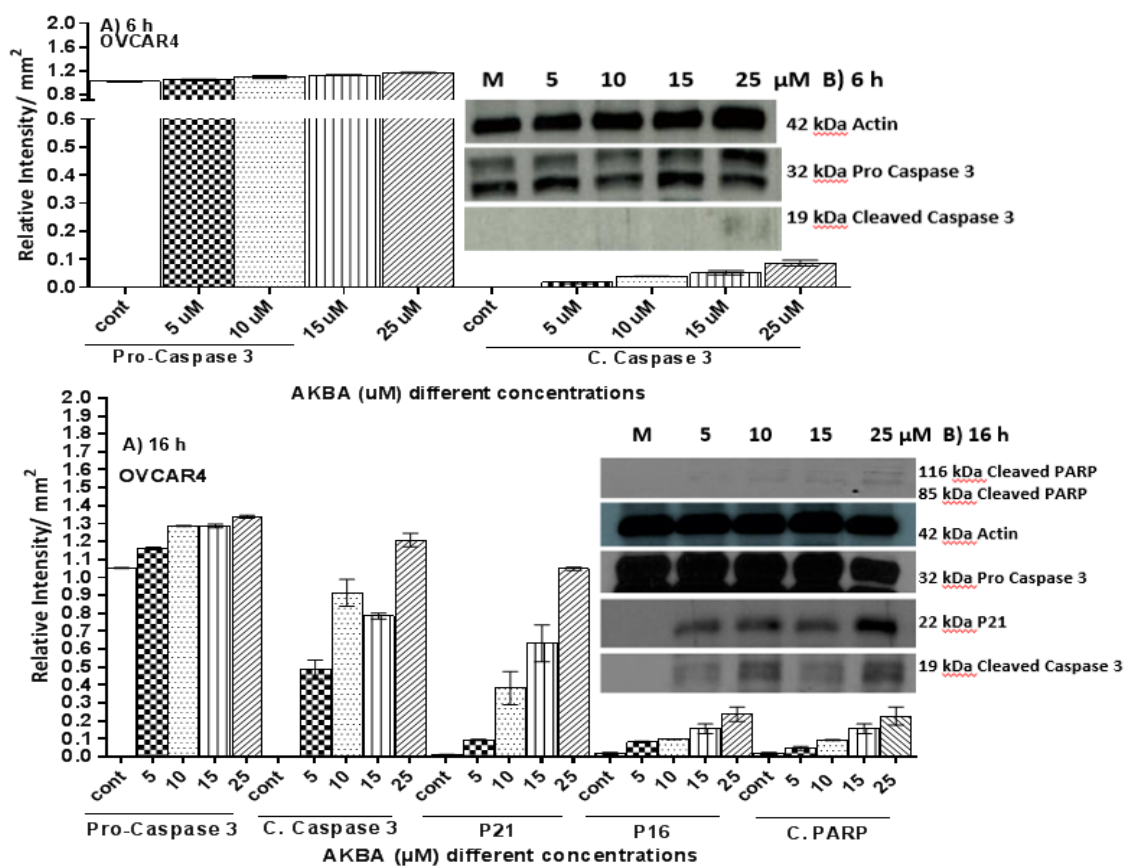


Figure 4.4.6 Quantification of apoptotic protein expression in OVCAR4 cells.

Cells were exposed to different concentrations of AKBA (5 μM , 10 μM , 15 μM , & 25 μM) for different time points (6 h & 16 h). A) Shows the pro-caspase 3, cleaved caspase 3, cleaved PARP, p21, and p16 band intensities, B) is the relative intensity bands refers to the absorbance (normalized to actin) analysed using SyngeneGeneSnap software (Syngene, UK). Results are expressed as Mean \pm SEM of 3 independent experiments, and * $P<0.05$, ** $P<0.01$, *** $P<0.001$ and **** $P<0.0001$ compared to control samples (cells in cell culture medium plus 0.5% v/v DMSO).

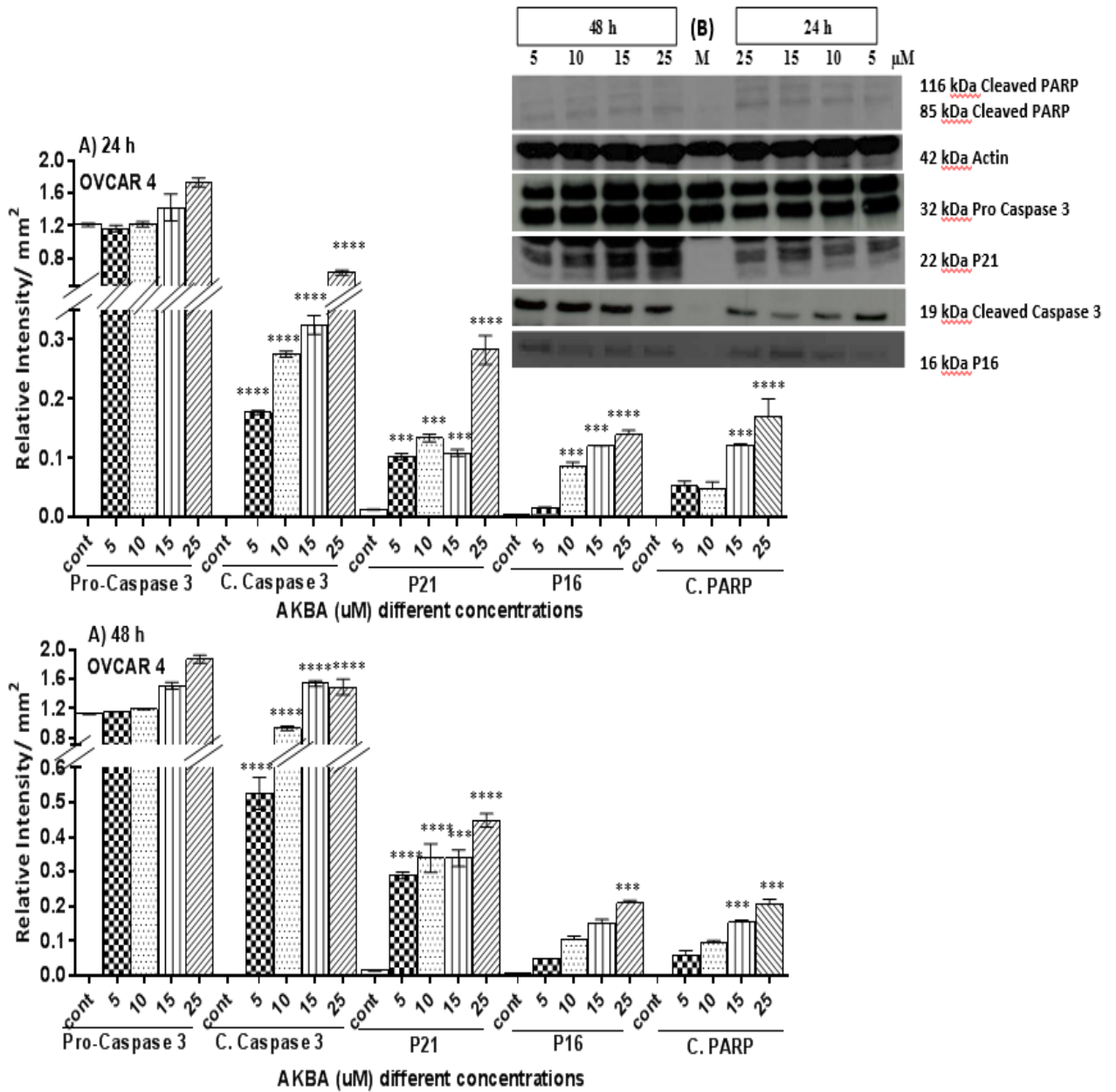


Figure 4.4.7 Quantification of apoptotic protein expression in OVCAR4 cells.

Cells exposed to different concentrations of AKBA (5 μM, 10 μM, 15 μM & 25 μM), for different time points (24 h and 48 h). A) Shows the pro-caspase 3, cleaved caspase 3, cleaved PARP, p21, and p16 band intensities, B) is the relative intensity bands refers to the absorbance (normalized to actin) analysed using SyngeneGeneSnap software (Syngene, UK). Results are expressed as Mean ± SEM of 3 independent experiments, and *P<0.05, **P<0.01, ***P<0.001 and ****P<0.0001 compared to control samples (cells in cell culture medium plus 0.5% v/v DMSO).

4.3 Discussion

4.3.1 AKBA induces DNA damage in UWB1.289 cells

Mutations in the BRCA1 tumour suppressor gene are associated with cases of hereditary breast cancer (Buchholz et al., 1999). As part of the present study, the UWB1.289 cell line was investigated; these cells contain a mutation in BRCA1 within exon 11 of the gene, leading to loss of functional BRCA1, as well as a crucial somatic mutation in the cell-cycle regulator, p53. Together, these mutations make the UWB1.289 cell line highly susceptible to uncontrolled cell division and decreased apoptosis in response to DNA damage (DelloRusso et al., 2007). The impact of various concentrations of AKBA on UWB1.289 cells was investigated in this study, which found that there was a negative effect by AKBA on cell proliferation, cell cycle progression and viability, which might be through a p53 independent pathway. AKBA also induced a significant amount of DNA damage, as determined by comet assay, which is likely to have contributed to the observed decrease in cell viability. As part of the response to DNA damage, cells can initiate DNA repair pathways, lesion bypass mechanisms or, in the case of severe damage, cell cycle arrest and apoptosis (Nur et al., 2003, Huang et al., 1996, Elmore, 2007). Although each of these types of DNA aberration has the potential to induce the cytotoxic effects described in the present study, one of the most potent forms of damage are single strand and double strand breaks (SSB and DSB, respectively). DSB were inferred by the presence of foci, appearing as the accumulation of DNA damage-responsive proteins, which aggregate at sites of damage and can be visualised via microscopic imaging after histo-chemical staining or protein-specific tagging (Rothkamm et al., 2015). In the present study, the protein used to infer DSB was γ H₂AX, the C-terminal phosphorylated form of the histone variant H₂AX (Stiff et al., 2004). It was significantly clear that UWB1.289 cell line has a higher level of DSB, which was evident by the level of foci presents compared to the control.

One mechanism of AKBA has been suggested that may explain the high level of DSB after treatment with this compound. Boswellic acids have been shown to inhibit topoisomerases responsible for controlling DNA topology and regulating DNA replication. This might be due to γ -H₂AX activated by DSB induction. For example, 3-O-acetyl- β -boswellic acid (ABA) has been shown to inhibit topoisomerase 1 and 2- α at a higher potency than the respective inhibitors camptothecin and etoposide (Syrovets et al., 2000). Etoposide, which itself has been used previously as an anti-cancer

therapeutic (Hande, 1998), was used in the present study as a control inhibitor for cell cycle progression, resulting in a marked increase in the proportion of cell to exhibit G₀ (the quiescent phase of the cell cycle) and sub-G₁/G₁ phase. By inhibiting the function of topoisomerase enzymes, excess supercoiling occurs during DNA replication (S phase) resulting in DSB and apoptosis (Chashoo et al., 2011b). UWB1.289 cell lines carry the defect in DNA repair mechanism which increases the ability for apoptosis to take place more predominantly (Yi et al., 2014).

The current study examined total DNA damage (as assessed by comet assay) and DSB formation (as assessed by γ -H2AX foci formation). The addition of AKBA causes DNA damage, resulting in SSB and DSB that arrest the cell cycle and cause fatal DNA damage without ROS generation (Driessens et al., 2009). Alkali-labile sites can be detected by the comet assay after DNA unwinding occurs and, under alkaline conditions, will degrade further to form strand breaks (Garaj-Vrhovac and Kopjar, 2003). This suggests that part of the mechanism of action for boswellic acids, including AKBA, does not involve the formation of free radicals that may account for the damage to DNA, identified in the current study (Altmann et al., 2004). *In vitro* studies of epithelial breast cancer cells and stromal fibroblasts highlighted that loss of BRCA1 function results in the build-up of intracellular hydrogen peroxide and associated oxidative stress (Martinez-Outschoorn et al., 2012a, Martinez-Outschoorn et al., 2012b). Previous research has implicated the BRCA1 gene in conferring antioxidant activity through control of a series of antioxidant response elements that regulate redox flux and repair mechanism of oxidative damage within the cell (Bae et al., 2004, Marks, 2013). Interestingly, despite the number of *in vitro* studies implicating BRCA1 in oxidative stress resistance, a study by the Kotsopoulos et al (Kotsopoulos et al., 2008) concluded that heterozygous BRCA1 mutations in non-affected breast cancer carrier patients did not lead to increased oxidative stress, as measured by three clinical biomarkers. In the present study, exposure to increasing concentrations of AKBA does not correlate with increased ROS production in both cell lines, even with the addition of the highest concentration (50 μ M); in fact it led to a significant decrease in ROS level which might be due to the reduction in cell metabolism which leads to cell death. The lack of a pro-oxidative effect by AKBA was confirmed in both cell lines; pro-oxidative effect have been the mechanism of several therapeutics to induce apoptosis in a range cancer cells (Gorrini et al., 2013). The expected mechanism which AKBA might work through it is function as inhibitor of

lipoxygenase and topoisomerase I and II which was been reported earlier. AKBA induces DNA damage by the inhibition of lipoxygenase and topoisomerase which leads to inhibition of DNA unwinding, and might have leads to apoptosis (Syrovets et al., 2000). This was the same scenario for irinotecan which is also a topoisomerase I inhibitor, causing DNA damage single strand breaks (SSBs), which then leads to the formation of double strand breaks (DSBs) and leads to apoptosis (Wood et al., 2015).

4.3.2 The effect of AKBA in OVCAR 4 cells

OVCAR4 is a cell line derived from an ovarian adenocarcinoma previously isolated from a 42-year-old female patient (Hamilton et al., 1984), which was used in the current study as a cell line model of high grade serous ovarian cancer (Mitra et al., 2015) for the assessment of AKBA, along with the UWB1.289 ovarian cancer cell line. In a study comparing the genomes of forty-seven ovarian cancer cell lines, another researcher demonstrated that OVCAR4 cells contain 4.63 mutations per million bases with 70% of the genome showing some degree of alteration (Domcke et al., 2013). Although OVCAR is not classified as a hyper-mutated cell line, it is more mutated than the A2780 line (4.59 mutations per million bases; 7% genomic alterations) which is one of the most common cell lines used in cancer research. Previous studies have shown that OVCAR4 exhibits high cisplatin resistance, compared with the A2780 line (Selvakumaran et al., 2003a, Godwin et al., 1992), and so was an interesting model with which to study the putative anti-cancer effect of AKBA. This section will discuss the results of AKBA exposure on OVCAR4 cells and therefore highlights the potential for AKBA to be used in the treatment of cancers that have demonstrated resistance to conventional chemotherapies. Based on the data from the present study, it is apparent that AKBA has the potential to effect the cell growth in OVCAR4 cells by killing cells as it is seen in the sub-G1 stage. The data from the Comet assay indicated that cell cycle arrest was triggered by significant levels of DNA damage, which occurred after 24 hours at low AKBA concentrations (10 μ M). Higher AKBA concentrations induced DNA damage after shorter exposure times, and triggered both a decrease in cell growth and loss of viability. The presence of early and late apoptotic cells, along with western blot visualisation of apoptotic proteins provided evidence that OVCAR4 cells initiated programmed cell death through the production of the effector enzyme, caspase-3. OVCAR4 cells exhibited dose-dependent growth inhibition at AKBA concentrations as low as 15 μ M after an exposure time of 48hours.

OVCAR4 showed more susceptibility to AKBA (IC₅₀ = 17.8 μM) than UWB1.289 (IC₅₀ = 20.07 μM), suggesting that BRCA1 mutation did not confer cross-protection to AKBA in the case of the low ability for DNA repair. BRCA1 mutation results in the accumulations of DNA damage which leads to cell apoptosis (Deng, 2003). Relatively low AKBA concentrations (15 μM) effective in causing significant DNA damage after 16 hours exposure and western blot analysis showed this DNA damage, as well as the associated cell cycle arrest had induced the production of cleaved caspase-3, p16 and cleaved PARP proteins. Interestingly, low concentrations of AKBA (<15 μM) did not induce cell death even after 48 hours exposure. This was likely to be due to a deletion of the TP53 gene in the OVCAR4, which encodes the cell cycle regulator p53 (Domcke et al., 2013). The absence of p53 prevented the early cell cycle arrest, although the proportion of late apoptotic cells after ≥15 μM AKBA exposure increased and the decreased cell viability indicates that programmed cell death continued in the absence of p53.

OVCAR4 (and the related OVCAR3) cell lines have been used previously to evaluate the effect of the anti-diabetes drug, metformin on ovarian cancer cells. These studies had implicated metformin as having a direct effect on a wide range of cancer cell types including ovarian cancer (Malek et al., 2013, Ben Sahra et al., 2010). Similar to the effect of AKBA on OVCAR4, the metformin study demonstrated that OVCAR4 cells underwent apoptosis, triggered by an increase in caspase-3 and caspase-7 (Yasmeen et al., 2011).

4.3.3 Anti-ovarian cancer potential of AKBA

Impetus to utilise the anti-tumorigenic properties of the *Boswellia Serrata* Extract (BSE) derived compound AKBA is driven by an increasing weight of literature showing it to be an effective inducer of apoptosis in an increasingly large range of cancer cells. This is supported by numerous animal studies showing an effective reduction in tumours upon AKBA treatment and a low toxicity even at high doses (Pang et al., 2009, Liu et al., 2002b).

Here we employed UWB1.289 and OVCAR4 cell lines to investigate the effect of AKBA for the first time, on ovarian cancer cells. Both cell lines presented as a good examples of ovarian cancer cells for pharmacological research and both cell lines has the BRCA1 mutations (Stordal et al., 2013, Weberpals et al., 2011b). Our initial results using a simple visual growth assay, suggested that AKBA was efficacious in inhibiting the growth of

both cell lines in a dose dependent manner. Indeed, at the highest concentration of 50 μM , AKBA treatment effectively prevented any proliferation from taking place over the 48 h period whereupon the cells appeared non-viable in all techniques performed. There have been numerous studies suggesting that AKBA can induce G_1 phase arrest. Our data however, suggested, there were no cell cycle arrest in fact there was cell death at different stages of the cell cycle that's why there was reduction in the cells in all the cell cycle phases by the end of the 48 h of incubation. However, at 50 μM cells began to undergo apoptosis immediately ($P < 0.001$), and a high proportion of sub- G_1 cells were observed, this was seen in both cell types.

A clear dose-dependent and time dependent increase in DNA strand break damage was seen following treatment with AKBA as assessed by Comet assay. This was again observed for both cell lines tested and suggests that AKBA is a consistent and potent inducer of DNA fragmentation, a phenotype associated with the induction of apoptosis. Taken together with the cell cycle studies, this strongly suggested that AKBA treatment was causing UWB1.289 and OVCAR4 cells to undergo cell death. Given the dramatically increased fragmentation of DNA observed using PI staining and comet assay techniques upon treatment of cells with 15-50 μM AKBA, Annexin V\PI was performed in parallel to directly observe apoptosis.

It was known that AKBA is a topoisomerase I/II inhibitor (Syrovets et al., 2000) this increase its cytotoxic effect by inducing DNA damage. AKBA induces SSBs DNA damage with the defect in topoisomerase I increases the effect in forming the DSBs, with cell growth inhibition and ultimately leads to apoptosis.

Following staining for Annexin V, it was again observed a high level of apoptosis in OVCAR4 cells that had been treated with 10-50 μM AKBA, an effect which increased over time. Similarly with UWB1.289 cells, when flow cytometric analysis was used to differentiate between early and late apoptosis, it was clear that 10-50 μM AKBA treatment induced the cells to progress through the process of apoptosis. Confusingly however, very little induction of early or late apoptosis was observed in cells treated with any dose less than 10 μM , despite earlier observations which suggest an AKBA dose dependent decrease in proliferation in both cell lines (Fig 4.2.3 - Fig 4.2.4) and an AKBA dose dependent increase in cell apoptosis in both cell lines (Fig 4.3.1.1 - Fig 4.3.2.2). We observed in both the apoptosis and the cell cycle assays that with the low concentration of AKBA there appeared to be very low response.

As noted, the effects of AKBA on apoptosis were observed only at the highest concentration of $>10\mu\text{M}$. This concentration range is in contrast to previous studies where potent growth inhibitory effects have been observed at concentrations 1-log lower than this (Park et al., 2002a, Park, 2002b), between 2 and $8\mu\text{M}$. Another study supported this data, showing that topoisomerase I from calf thymus was inhibited by AKBA at a concentration of $10\mu\text{M}$. Which might be due to the different apoptosis mechanisms for each type of cell line?

By Going back to chapter 3 and 4 results of IC₅₀, it was evident that all the four cell lines (A2780, A2780cis, UWB1.289 and OVCAR4 has similar IC₅₀ with slightly increase (not significant) in sensitivity with cisplatin resistance cell line and high grade serous. Importantly AKBA shows evident of sensitivity to those cell line with cisplatin resistance and the most aggressive cancer cell lines like OVCAR 4, which may give an efficacious and important addition to the management and treatment of cisplatin resistant ovarian cancers.

4.3.4 Conclusion

Herein, we have shown for the first time using standard *in-vitro* assays to assess cellular proliferation and apoptosis, that AKBA is an agent capable of potently inducing apoptosis in all the four ovarian cancer cell types which make AKBA an interested agent to be studied clinically for future anticancer drug developments and the treatment of HGSC and cisplatin resistant patients. AKBA works by unknown mechanism and effect different cellular process including DNA damage and repair mechanisms, cell growth inhibition, cell cycle, and activating apoptosis pathways. These all together are the major important hallmarks, which are required in cancer treatments. Putting all the results we had from chapter 3 and 4 together we precede with chapter 5 to study the mechanism of action for AKBA on OVCAR4 cell lines as it represent all the other 3 cell lines (A2780, A2780cis, and UWB1.289). OVCAR4 cell lines carry the mutation on p53, has low expression of BRCA genes and it represent the HGSC cell lines with cisplatin resistance.

Chapter 5

**A preliminary examination for
mechanisms of action and the genes
involved in the actions of AKBA in
ovarian cancer cell lines**

5.1 Introduction:

One of the most severe forms of ovarian cancer are those with of EOC, and one of the most typical of the cancer cell lines is OVCAR-4, which is known to engage the mTOR pathway via VEGF receptors (Lau et al. 2013). Due to the ambiguous symptoms of ovarian cancer, which often leads to late diagnosis, most of the cases with ovarian cancer appear with late stage, and most of them developed resistance to the first line chemotherapy, e.g. platinum drugs such as carboplatin. The OVCAR4 cell line was one of the cell lines which was considered as a good model for example for research into ovarian cancer treatment (Moss et al., 2015). High grade serous ovarian cancer account for the majority of metastatic ovarian cancer and relapse cases, and requires more attention in researching anticancer therapy (Moss et al., 2015). From preliminary results with AKBA treatment, which were described in chapter three and four, the decision was made to pursue gene expression work using the OVCAR4 cell line.

There have been several studies into the anti-tumour effects of boswellic acids, which is reportedly due to interference with intrinsic cancer cell growth processes including modulation of Ca^{2+} influx (Poeckel et al., 2006), actions of mitogen-activated protein kinases (MAPK) and Akt (Takada et al., 2006). The precise effect depends on the structure of the specific boswellic acid and cancer type. For example, growth of colon cancers is known to be interrupted by boswellic acid through a p21-dependent pathway (Liu et al., 2006) and keto-boswellic acids are thought to target different molecules compared with their non-keto counterparts.

Considering all these studies together, we conclude that AKBA is one of the primary bioactive ingredients of the boswellic acids in frankincense, which has very promising results in treating inflammatory disease and has emerged as a potential treatment for different type of cancers (Ammon P., 2006). Clinical trials using AKBA are very rare due to the lack of any supporting evidence of the direct and indirect toxicity of this compound (Moussaieff A. and Mechoulam R., 2009). Therefore, more studies are urgently needed to understand mechanisms of action of AKBA in cancer cell lines to be able to develop novel therapies to treat cancers including high-grade serous ovarian cancers.

Aim:

The mechanism of action for AKBA effect in all the different cell types which have been studied before is unknown; therefore this study was undertaken with the aim of assessing the mechanism of action for AKBA which leads to cell growth inhibition and apoptosis of the cancer cell lines.

5.2 Gene expression results

The microarray samples were prepared and taken to the Genomic Core Facility of the University of Leicester, which then were undertaken and run by Dr Nicolas Sylvius, who ultimately provided us with the results data. These results were filtered and analysed using the <http://www.fda.gov/ScienceResearch/BioinformaticsTools/Arraytrack/> website.

First, we compared shared gene expression patterns between control cells (non-treated) with the cells treated with different AKBA concentrations (10 μ M, 15 μ M, 25 μ M and 50 μ M (for 6 h only)) for different times (6 h, 16 h & 24 h), to find the most common markers and/or molecular mechanisms involved in AKBA action and treatment response. A total of 47,000 genes transcripts were interrogate on the microarray chips and the microarray data analysed, and a subset of 215 genes, was found significantly changed based on the filtering criteria used. These genes were selected by initial filtering at a confidence of p -value ≤ 0.05 , followed by filtering using an expression level change of ≥ 1.8 -fold. Using these selection criteria, 110 genes were found to commonly have gene expression changes up-regulated and 105 genes to be down regulated for all the different time points and different concentrations (Tables 5.2.3, 5.2.4 & 5.2.5). Table 5.2.1 shows a list of selected functionally related groups of genes that were differentially expressed (≥ 1.8 -fold) in all selected concentrations and time points. As seen from Table 5.1, comparable numbers of genes with suggested functions in apoptosis, cell adhesion, cell cycle control and stress (defence) response were both up- and down-regulated; this was similar to the finding of another researcher (Hongmei, 2012). Genes, functionally associated with DNA repair, DNA replication and cell cycle arrest were exclusively over expressed (Table 5.2.6(a)). Genes implicated in cell growth and maintenance, transcription regulation, signal transduction and transport were predominantly down regulated, while genes linked to immune and inflammatory response, metabolism (especially lipid metabolism), protein biosynthesis, protein modification and RNA processing, were uniquely suppressed following all treatments (Table 5.2.6(b)). The genes involved in apoptosis pathways and DNA degradations have been up regulated.

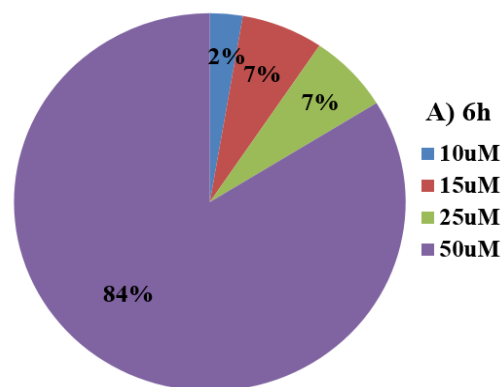
5.2.1 Gene functions and pathways:

Gene functions were determined and analysed using the Genecards website *e.g.* (<http://www.genecards.org>) by selecting each gene individually and the genecards summaries were used to assess the function of each gene.

A total number of 215 genes in different pathways were analysed by genecards after filtering (table 5.2.1). Around 57 genes were apoptosis related genes, 63 were genes related to cell cycle, 41 were genes related to DNA damage and repair, 2 gene was related to DNA synthesis, 19 genes were related to cell metabolism, 4 were genes related to stress response, 15 were genes related intracellular signalling, 2 genes were related to cellular transport mechanism and finally 5 genes were related to cell adhesion & metastasis (table 5.2.5).

5.2.2 Gene percentage of OVCAR 4 gene affected after AKBA treatments

A number of genes expressed were increased with the increase in AKBA treatment concentrations and time periods. It was evident that the number of genes significantly and differentially expressed at 25 μM . This was notably increased from 7 % to 88% after 16 h of treatment, whereas 15 μM took a longer time, 24 h to express 23 % of genes. After 6 h of treatment with AKBA, the total number of significant gene expression changes out of all the transcripts interrogated on the chips. 84 % of the genes show significant change in expression at 50 μM AKBA, 7 % at 25 μM , 7 % 15 μM and 2% at 10 μM .



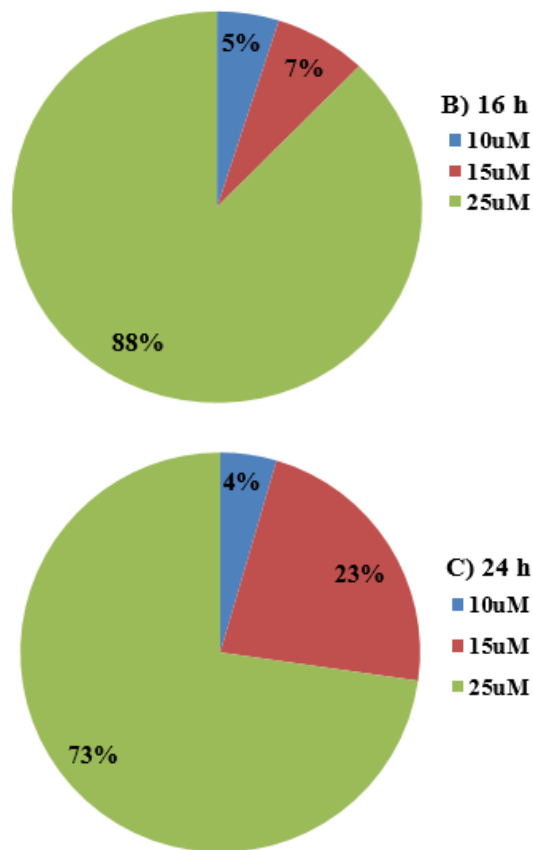


Figure 5.2. 1 Affected genes percentage of OVCAR4 cell lines gene expression (described in table 5.2.3).

Following AKBA treatment at various concentrations, Gene expression was assessed using microarray gene expression technology following exposure to different concentration of AKBA (10 μ M, 15 μ M, 25 μ M and 50 μ M for 6 h only) for different time points (a- 6 h, b-16h & c-24h). The normalised data was analysed using Array Track data analysis software using $P \leq 0.05$ and ≥ 1.8 fold-change cut-offs (five independent experiments were pooled together and run on microarray chips in duplicate).

From figure 5.2.1a, it can be seen that the number of genes expressed following 50 μ M treatment was high within 6 h of exposure (84 %) and it was not possible to detect any living cells after this time point using 50 μ M concentrations. In figure 5.2.1 b, the number of genes expressed with 25 μ M increased after 16 h to 88 %, whereas 15 μ M shows 7 % gene expression at this time point. After 24 h the 15 μ M treatments showed an increase in the number of genes expressed to 23 % in parallel with 25 μ M which shows 73 % (fig 5.2.1 c) indicating that AKBA effects at lower concentrations increases with the increasing in time.

5.2.3 The Molecular function and the biological mechanism of the genes expression changes affected by AKBA exposure of OVCAR 4 cells

Table 5.2. 1Number of genes affected by 50 μ M of AKBA in different molecular functions and biological process of OVCAR 4 cells after 6 h of exposure.

	Molecular function	Gene no	%
1	transporter activity (GO:0005215)	1	0.80%
2	translation regulator activity (GO:0045182)	2	1.60%
3	protein binding transcription factor activity (GO:0000988)	1	0.80%
4	enzyme regulator activity (GO:0030234)	10	7.90%
5	catalytic activity (GO:0003824)	47	37.00%
6	receptor activity (GO:0004872)	3	2.40%
7	nucleic acid binding transcription factor activity (GO:0001071)	11	8.70%
8	structural molecule activity (GO:0005198)	8	6.30%
9	binding (GO:0005488)	44	34.60%
	Biological process	Gene no	%
1	cellular component organization or biogenesis (GO:0071840)	16	12.60%
2	cellular process (GO:0009987)	45	35.40%
3	localization (GO:0051179)	10	7.90%
4	apoptotic process (GO:0006915)	6	4.70%
5	reproduction (GO:0000003)	1	0.80%
6	biological regulation (GO:0065007)	24	18.90%
7	response to stimulus (GO:0050896)	21	16.50%
8	developmental process (GO:0032502)	14	11.00%
9	multicellular organismal process (GO:0032501)	1	0.80%
10	biological adhesion (GO:0022610)	2	1.60%
11	metabolic process (GO:0008152)	76	59.80%
12	immune system process (GO:0002376)	13	10.20%

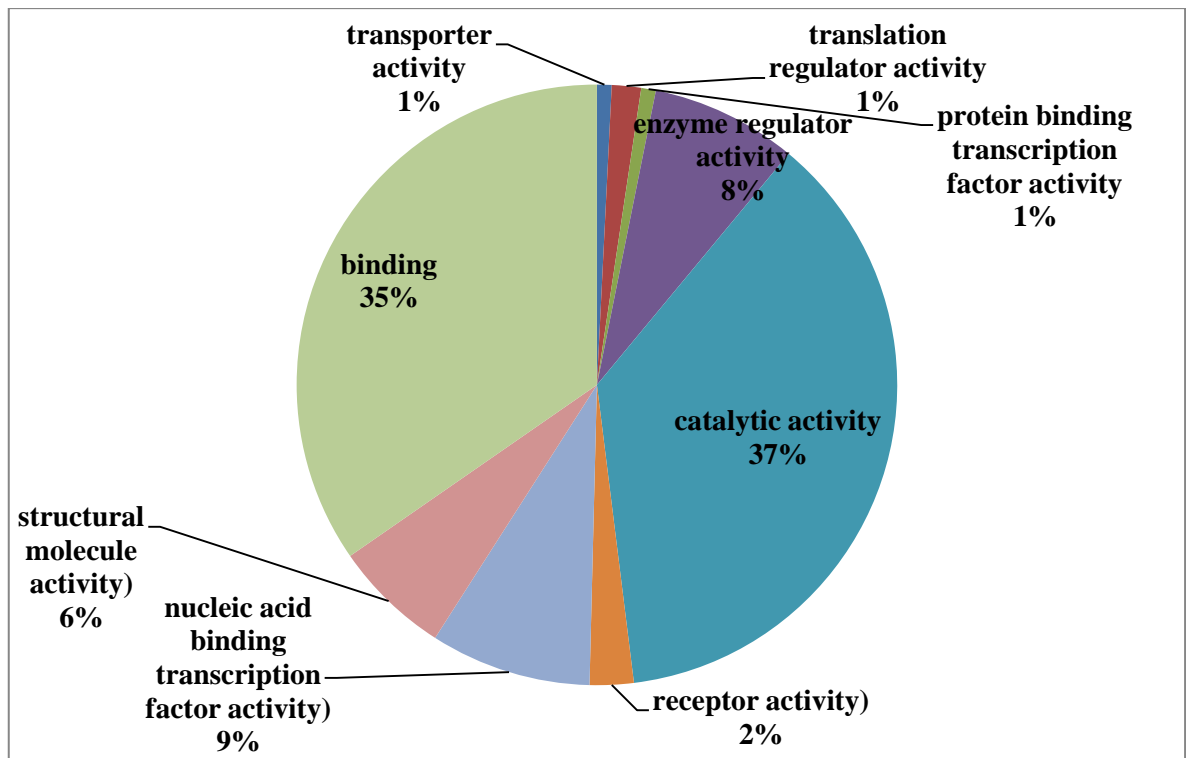


Figure 5.2.2 Molecular function classifications determined by gene ontology analysis.

The percentage gene expression changes of molecular function of the genes affected and expressed in OVCAR4 cell lines after exposure to different concentrations of AKBA for different times using microarray gene expression technology. The normalised data were analysed using Array Track data analysis software with $P \leq 0.05$ and a fold change of ≥ 1.8 ; graphs were plotted using PANTHER GO Geneontology. (Five independent experiments were pooled together and run in microarray chips in duplicate, to minimise variation).

In total there were 215 genes determined to be significantly affected by AKBA, after using ≥ 1.8 fold change and P value ≤ 0.05 cut-offs. These genes were responsible for different functions in the cells, which have direct or indirect effect in cell survival or apoptosis (fig. 5.2.2 & fig. 5.2.3). Thirty three percent of genes were related to metabolic process, 20 % were related to cellular processes and 11 % related to apoptotic processes. The vast majority of these genes were expressed with the higher concentrations 25 μ M and 50 μ M, and the most significant effect in number of gene expression for AKBA in OVCAR4 cells was after 6 h treatment with 50 μ M.

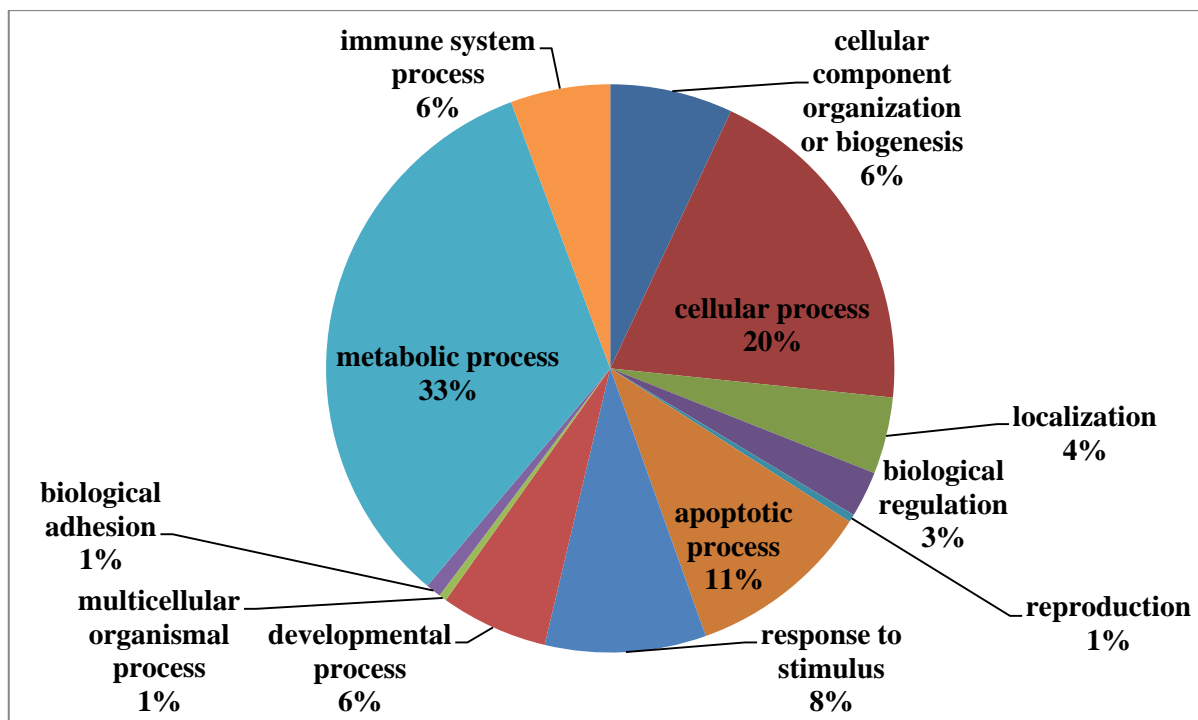


Figure 5.2. 3 Biological processes classification as determined by gene ontology analysis.

The pie charts sectors represent the percentage for the number of genes associated with each biological processes expressed in OVCAR4 cell lines after exposure to different concentrations of AKBA for different times using microarray gene expression technology. The normalised data was analysed using array track data analysis software using $P \leq 0.05$ and a fold change of ≥ 1.8 ; graphs were plotted using PANTHER GO Geneontology. (Five independent experiments were pooled together and run on microarray chips in duplicate, to minimise variation).

List of genes expressed using microarray gene expression:

Table 5.2. 2 Total number of Genes up regulated and down regulated as determined using array track.

Time point	6 h				16 h			24 h		
	10 μ M	15 μ M	25 μ M	50 μ M	10 μ M	15 μ M	25 μ M	10 μ M	15 μ M	25 μ M
Total genes	2	5	5	89	3	3	44	2	11	51
Total	100				50			64		
Up	50				19			41		
Down	51				31			23		
Total	214 genes (up 109 & down 105)									

Table 5.2. 3 6h treatments with AKBA using a cut off p value of <0.05 and fold change of >1.8

Apoptosis Metabolism DNA damage & repair Cell Cycle and DNA Synthesis Signal Transduction

<i>Medium vs 10 μM</i>			<i>Medium vs 50 μM</i>		
gene	P value	Fold change	gene	P value	Fold change
FKBP1A	0.0005	(+) 1.8447	C7orf40	0.0045	(-) 1.8292
FAM100A	0.0013	(+)1.8779	STARD13	0.0046	(+) 1.9273
<i>Medium vs 15 μM</i>			C12orf47	0.0046	(-) 1.809
GGH	0.0002	(-) 1.8059	DGCR2	0.0047	(+) 1.8303
LOC729978	0.0012	(+) 1.9187	CEBPG	0.0048	(-) 2.1668
APPL2	0.0064	(+) 1.8041	TUBE1	0.0049	(-) 2.5398
NFKB2	0.0065	(+) 2.428	HSPA13	0.0052	(-) 1.8182
LOC100132394	0.0083	(+) 2.3881	ASNS	0.0053	(-) 2.6821
<i>Medium vs 25 μM</i>			UBA1	0.0012	(+) 1.7588
PLS1	0.0073	(-) 1.8073	BRI3BP	0.0053	(+) 1.8259
DHRS2	0.0274	(-) 2.3911	SLC3A2	0.0056	(-) 2.4422
HAS3	0.0296	(-) 1.8733	EIF4G1	0.0057	(+) 1.8446
IER3	0.049	(+)1.8351	UFM1	0.0057	(-) 1.8984
SLC3A2	0.0497	(+) 1.8324	SPIRE1	0.0058	(-) 1.84
MTHFD2	0.005	(-) 2.0194	NFKB2	0.0059	(+) 3.8234
GADD45A	0.0084	(+) 3.6049	PRKAB1	0.0064	(-) 1.8453
<i>Medium vs 50 μM</i>			ANP32C	0.0064	(+) 1.8363
C9orf6	0.0001	(-) 1.8923	RIOK2	0.0064	(-) 1.9102
DDIT3	0.0002	(+) 8.0892	BOK	0.007	(+) 1.8174
TMEM39A	0.0003	(-) 1.885	TNFAIP3	0.007	(-) 3.3005
C17orf48	0.0004	(-) 1.9269	SNHG5	0.0071	(-) 1.8697
CCNE1	0.0004	(+) 2.4431	TERF2IP	0.0074	(-) 1.8695
UHRF1BP1	0.0006	(-) 1.8646	HAS3	0.0074	(+) 1.8888
NFIL3	0.0007	(-) 3.9388	HSPA5	0.0075	(-) 1.8007
STARD13	0.0007	(+) 1.966	ZNF165	0.0078	(-) 2.0248
TARS	0.0011	(-) 1.8163	XPOT	0.0083	(-) 1.8378
SYVN1	0.0013	(+) 1.8257	DNASE2	0.0087	(+) 1.8097
MTMR9	0.0014	(-) 1.8372	BCL2	0.0091	(+) 1.8226
LOC643668	0.0014	(+) 1.8482	TRAPPC6B	0.0091	(-) 1.886
GADD45A	0.0017	(+) 4.2202	CDK6	0.0024	(+) 1.5139
TXNL4B	0.002	(-) 1.8624	SYVN1	0.0094	(-) 2.3176
EAF1	0.0022	(-) 1.8352	MOCOS	0.0095	(-) 1.8357
XYLT2	0.0022	(+) 1.819	RAB33B	0.0097	(-) 1.8789
SCG2	0.0023	(-)1.8071	CBX6	0.0099	(+) 1.8908
CERK	0.0023	(+) 1.8768	MAPK12	0.01	(+) 1.8897
MAP1LC3B	0.0029	(-) 2.331	NACCI	0.003	(-) 2.1935
NFE2L2	0.0033	(-) 1.8804	RERE	0.0145	(+) 2.2762
RAB9A	0.0035	(-) 1.8929	XRCC3	0.005	(+) 2.4016
FNBP1L	0.0037	(-) 1.815	BAX	0.0042	(+) 2.225
CEBPB	0.0039	(-) 2.1696	TP53	0.0012	(+)1.9327
MTHFD2	0.0044	(-) 2.1641	ZNF616	0.0044	(-) 1.9166
BCL2A1	0.0124	(-)2.114	BAK	0.0082	(+) 1.934

MAFF	0.0044	(-) 1.8563	Casp9	0.0022	(+) 1.978
BOK	0.0014	(+) 2.1.25	Casp10	0.012	(+)1.94
PKN1	0.0213	(+) 1.8123	Casp8	0.0089	(+) 1.847
PAK4	0.032	(-) 1.847	IER3	0.004	(+) 1.882
CTTN	0.0013	(-) 1.879	TRIB3	0.012	(-) 1.801
CERK	0.0321	(+) 1.921	BIRC3	0.048	(-) 1.812
ATG4D	0.0432	(+) 1.884	BAD	0.001	(+) 1.849
FAS	0.0497	(+) 1.969	FASLG	0.0022	(+) 2.94
FADD	0.002	(+) 1.997	Casp7	0.0014	(+) 2.147
Casp3	0.0071	(+) 1.879			

Total = 100, 49 up & 51 down

Table 5.2. 4 16h treatments with AKBA using cut off p value of < 0.05 and fold change of 1.8

Apoptosis metabolism DNA damage and repair Cell Cycle and DNA synthesis Signal transduction

<i>Medium vs 10 μM</i>			<i>Medium vs 25 μM</i>		
gene	P value	Fold change	gene	P value	Fold change
FOSL1	0.0024	(+) 1.8273	CDKN1A	0.0171	(+) 1.9154
PKMYT1	0.0032	(+) 1.8768	TUBE1	0.0184	(-) 1.8318
MCM10	0.0067	(-) 1.81	ARHGAP23	0.0202	(+) 1.905
DHRS2	0.0456	(-) 1.8898	LOC650215	0.0217	(-) 1.8399
<i>Medium vs 15 μM</i>			BBS2	0.022	(-) 1.903
LOC729779	0.0007	(-) 1.8626	LAMP2	0.022	(-) 1.8157
LEMD1	0.0075	(-) 1.8176	C4orf34	0.0223	(-) 1.8172
PCK2	0.0497	(-) 1.8917	MYEOV	0.024	(-) 1.8733
DHRS2	0.0293	(-) 2.0629	HAS3	0.0269	(+) 1.8238
<i>Medium vs 25 μM</i>			HINT3	0.0307	(+) 2.2238
PI3	0.0014	(+) 1.8533	ASNS	0.0325	(-) 2.7757
MCM10	0.0026	(-) 1.848	ZNF323	0.0359	(-) 1.8562
PSAT1	0.008	(-) 1.8097	PCK2	0.0376	(-) 1.9204
CITED4	0.0086	(+) 1.8752	PHLDA2	0.0387	(+) 1.8647
TM4SF4	0.0102	(+) 1.8225	UBA52	0.0404	(+) 1.9076
ATP7B	0.0104	(+) 1.8922	HMOX1	0.0406	(-) 2.7078
MTHFD2	0.0105	(-) 1.8342	TGM2	0.0421	(+) 2.1037
DNASE2	0.0113	(+) 1.8525	UGT1A6	0.0433	(-) 1.8726
ST6GALNAC3	0.0113	(-) 1.9258	GARS	0.0462	(-) 1.9504
MTHFD2	0.0114	(-) 1.8891	ATF4	0.0467	(-) 1.8687
SERPINI1	0.0123	(-) 1.9325	HSPA9	0.0142	(+) 1.809
VNN1	0.0128	(+) 1.9155	Casp9	0.0035	(+) 1.812
RRP15	0.0137	(+) 1.9073	BCL2A1	0.0024	(-) 1.945
TMEM173	0.0166	(-) 1.8474	BRCA2	0.042	(-) 1.893
TXNL4B	0.006	(+) 1.934	PCTK3	0.042	(-) 1.80
DHRS2	0.0045	(-) 2.2805	BRCA1	0.050	(-) 1.92

Total = 50, 19 up & 31 down

Table 5.2. 5 24h treatments with AKBA using cut off p value of <0.05 and fold change of 1.8

Apoptosis metabolism DNA damage and repair Cell Cycle and DNA synthesis Signal transduction

<i>Medium vs 10 μM</i>			<i>Medium vs 25 μM</i>		
gene	P value	Fold change	gene	gene	gene
CTNNB1	0.0197	(-) 1.818	PPFIBP1	0.019	(-) 1.8379
NCKAP1	0.0417	(-) 1.8557	DNMT3B	0.0192	(-) 1.8223
<i>Medium vs 15 μM</i>			IARS	0.0193	(-) 1.9249
MTHFD2	0.0004	(-) 1.8075	SHPK	0.0208	(+) 1.8006
TMEM137	0.0008	(+) 1.8017	CLIC4	0.0212	(-) 1.9371
XPOT	0.0069	(-) 1.8942	IL13RA2	0.0219	(+) 1.8054
NAMPT	0.0078	(-) 1.9321	SORBS1	0.0228	(+) 1.8036
BHLHB2	0.0108	(-) 1.9439	ZNF207	0.0236	(+) 1.863
UBE2E1	0.0113	(+) 1.8166	IDH1	0.0248	(-) 1.8553
YWHAZ	0.0196	(-) 1.9873	MARS	0.0252	(-) 1.8022
CTNNB1	0.0294	(-) 1.9178	UBXN2B	0.0258	(-) 1.8075
SDCBP	0.0308	(-) 1.8643	RRP7A	0.0268	(+) 1.8503
MYC	0.0414	(-) 1.9378	SNRNP70	0.0271	(+) 1.8775
ASNS	0.0414	(-) 1.8193	SARS	0.0289	(-) 1.9912
MTHFD2	0.0449	(-) 2.0077	CEP152	0.0297	(+) 1.9124
<i>Medium vs 25 μM</i>			CLDN1	0.031	(-) 1.9864
TGFR3	0.0017	(+) 1.8628	NCKAP1	0.0314	(-) 1.8788
OSBPL9	0.0019	(-) 1.8116	HSPA1B	0.0331	(+) 1.9369
MCM10	0.002	(+) 1.8925	TUBE1	0.0362	(-) 1.9478
CCNE1	0.0039	(+) 1.9212	SLC3A1	0.0368	(-) 1.8138
DNASE2	0.0043	(-) 1.8754	GRB10	0.0374	(+) 1.9394
YARS	0.0044	(-) 1.9408	SDCBP	0.0387	(-) 1.8258
UPP1	0.0065	(-) 1.9272	LAMP2	0.0407	(-) 1.8923
LONP1	0.007	(-) 1.8136	EFHD2	0.0432	(+) 1.8831
TUBA4A	0.0093	(+) 1.8757	KLF2	0.0437	(-) 1.8726
IFRD1	0.0109	(-) 1.8145	HIST1H2BK	0.0437	(-) 1.9945
ABCC5	0.0129	(-) 1.8192	CYP4V2	0.0485	(-) 1.9298
MTHFD2	0.0158	(-) 2.8238	WARS	0.0494	(-) 2.0435
ASNS	0.0163	(-) 3.4201	Casp7	0.0327	(+) 2.014
STARD13	0.0176	(+) 1.8747	BAX	0.0057	(+) 2.211
Casp3	0.0026	(+) 1.984	BAK	0.0082	(+) 2.114
BOK	0.0014	(+) 1.958	RASSF7	0.0461	(-) 1.957
BCL2A1	0.0412	(-) 1.946	BAD	0.0048	(+) 2.001

Total =64, 23 up &41 down

Table 5.2. 6 The most common genes affected after filtering.

Selected from table (5.2.2 – 5.2.4) According A)up and B) down regulation effect in different mechanisms.

A) All up regulated genes:

Apoptosis	UBA52, TGM2, NFKB2, ANP32C, EFHD2, DNASE2, TP53, RERE, MAPK12, GADD45A, BAX, Casp3, Casp7, CERK, ATG4D, FAS, PKN1, FADD, Casp3,RERE, UBA1, Casp8, IER3, BAD, FASLG, Casp7, Casp9, BOK, BAK,PKN1, STARD13
Cell cycle	CCNE1, STARD13, CBX6, FOSL1, PKMYT1, MCM10, TM4SF4, RRP15, CDKN1A, UBA52, UBE2E1, SHPK, ZNF207, SNRNP70, CEP152, GRB10,CDK6, TXNL4B, HSPA9, GADD45A
DNA damage and Repair	HINT3, RRP7A, BRI3BP, UBA1,GADD45A, MAPK12,DDIT3
DNA synthesis	Non
Metabolism	XYLT2, CERK, SORBS1
Response to stress	MAPK12, GADD45A, ATG4D
Intracellular signalling (signal transduction)	MAPK12, APPL2, IER3, ARHGAP23, IL13RA2, CITED4, ATP7B, FKBP1A
Transport	CERK
Cell adhesion & metastasis	PKN1,STARD13,HAS3

B) All down regulated genes:

Apoptosis	PCK2, DNASE2, DHRS2, MYEOV, LAMP2, HMOX1, TMEM39A, C9orf6, MAP1LC3B, WARS, MYC, TNFAIP3, SYVN1, NACC1, PKN1, RASSF7, BCL2A1, DHRS2, PCTK3, ATF4,MAFF, PAK4, CTTN, NACC1, TRIB3, BIRC3
Cell cycle	MTMR9, TXNL4B, FNBP1L, CEBPB, ZNF616, TUBE1, HSPA13, ASNS, EIF4G1, SPIRE1, RIOK2, TERF2IP, HSPA5, ZNF165, XPOT, SERPINI1, TUBE1, BBS2, LAMP2, ASNS, ZNF323, PCK2, ATF4F, BHLHB2, YWHAZ, CTNNB1, SDCBP, MYC, ASNS, OSBPL9, IFRD1, PPFIBP1, MARS, UBXN2B, SARS, CLDN1, NCKAP1, TUBE1, SDCBP, LAMP2, HIST1H2BK, UHRF1BP1, PAK4,
DNA damage and Repair	LEMD1, ST6GALNAC3, C4orf34, GARS, NAMPT, LONP1, SLC3A2, NFIL3, TARS, EAF1, SCG2, NFE2L2, MAFF, C7orf40, C12orf47, CEBPG, SNHG5, MOCOS, BRCA1, BRCA2,XRCC3
DNA synthesis	MCM10,YARS
Metabolism	GGH, MTHFD2, SLC3A2, RAB33B, PCK2, PSAT1, DNMT3B, IARS, CLIC4, IDH1, CYP4V2, ABCC5, UPP1, NAMPT,RAB9A,NAMPT
Response to stress	RASSF7
Intracellular signalling (signal transduction)	PLS1, PRKAB1, TRAPPC6B, HMOX1, UGT1A6, XPOT, KLF2.
Transport	PCTK3
Cell adhesion & metastasis	PAK4, CTTN

After the analysis of each of these genes functions, using the gene card website, genes were divided into 9 mechanisms, including apoptosis, cell cycle, DNA damage and repair, DNA synthesis, metabolism, response to stress, intracellular signalling, transport and cell adhesion and metastasis. These genes were either up or down regulated, and majority of these pathways are directly or indirectly linked to apoptosis pathways.

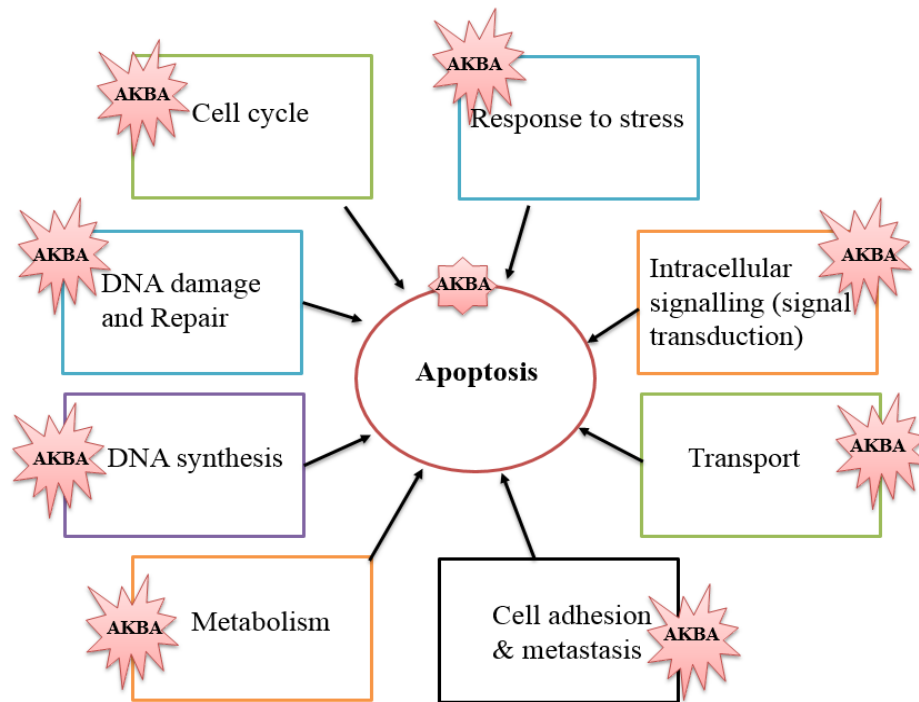


Figure 5.2. 4 Effect of AKBA on pathways impacting on apoptosis.

Either by directly effecting apoptotic pathway genes (either the extrinsic or the intrinsic pathway) or indirectly by effecting other mechanism genes in cancer cells, AKBA ultimately leads to apoptosis.

The cellular process of apoptosis is a pathway that has attracted much research due to its pivotal role in the pathogenesis of many diseases like cancer, neurodegenerative and acute injury (i.e. stroke) (Wong, 2011, Gerl and Vaux, 2005, Favaloro et al., 2012). From this aspect, the apoptosis pathway was a major topic of study in this project, particularly after the microarray results as it was evident that this pathway plays a major role of AKBA effect in OVCAR4 cell lines. Simply, with cancer cells blocking cell death mechanisms, it was found that AKBA can activate apoptosis by affecting different related pathways such as aspects of cell metabolism, DNA damage and repair mechanisms (Low and Lin, 2000).

The global transcriptomic data provided by microarrays indicated that the global gene expression of OVCAR-4 cells are impacted by AKBA in a concentration and time

dependent manner, with eighty-four percent of the global transcriptome differentially-expressed within six hours of exposure to 50 μ M AKBA compared to just two percent of the total gene expression after treatment with 10 μ M AKBA (Figure 5.2.1). The data also indicate that cellular metabolic processes and catalytic activities of OVCAR-4 cells are most impacted by AKBA treatment (Figures 5.2.2 and 5.2.3). A large number of genes characterised as being involved with cellular processes were either significantly up- or down-regulated after treatment with 50 μ M AKBA. Interestingly, just eleven percent of the genes that were differentially-expressed in the microarray experiments were annotated as being involved in apoptosis, despite the pro-apoptotic and cytotoxic effects of AKBA that have been described in previous chapters and reported elsewhere (Suhail et al., 2011, Noaman and Kandil, 2009, Takada et al., 2006, Xia et al., 2005). There were also 21 genes down regulated and 7 genes up regulated responsible for DNA damage and repair and two of them were significantly highly expressed. GADD45A was up regulated with fold change of 4.2 and DDIT3 with fold change of 8.1. GADD45A is known to have increased expression in situations of stressful growth arrest and with treatment with DNA damaging agents (Zhan, 2005) whereas DDIT3 is activated by endoplasmic reticulum stress and promotes apoptosis and arrest cell growth (Oyadomari and Mori, 2004). Nonetheless, the apoptotic genes affected by AKBA represent key components of the cell signalling and the apoptotic pathways. According to the gene expression data from the microarray experiments, programmed cell death progresses through both the intrinsic and extrinsic apoptotic pathways culminating with the increased expression of the genes encoding the executioner caspases-3 and -7 (McIlwain et al., 2013). After six hours post treatment with the highest concentration of AKBA (50 μ M), the gene encoding the type-II trans-membrane protein, FAS and its receptor were both up regulated. These proteins bind to the so-called Fas-Associated protein with Death Domain (FADD), which is involved in the binding and cleaving of procaspase-8 to its activated form as part of the extrinsic apoptotic pathway (Ashkenazi, 2008). The microarray data indicated that this pathway was activated by 50 μ M AKBA addition after 6 hours, with an up-regulation of FAS (+1.97-fold), FASLG (+2.94-fold), FADD (+2.00-fold) and the activator caspase-encoding gene CASP8 (+1.85-fold). As part of the apoptotic response, caspase-8 is known to interact with and activate the executor of apoptosis, caspases-3 and 7 (Cullen and Martin, 2009, Lakhani et al., 2006). The microarray data presented in this study demonstrated up-regulation of critical executor caspase-encoding genes CASP3 (+1.88-fold) and CASP7 (+2.15-fold).

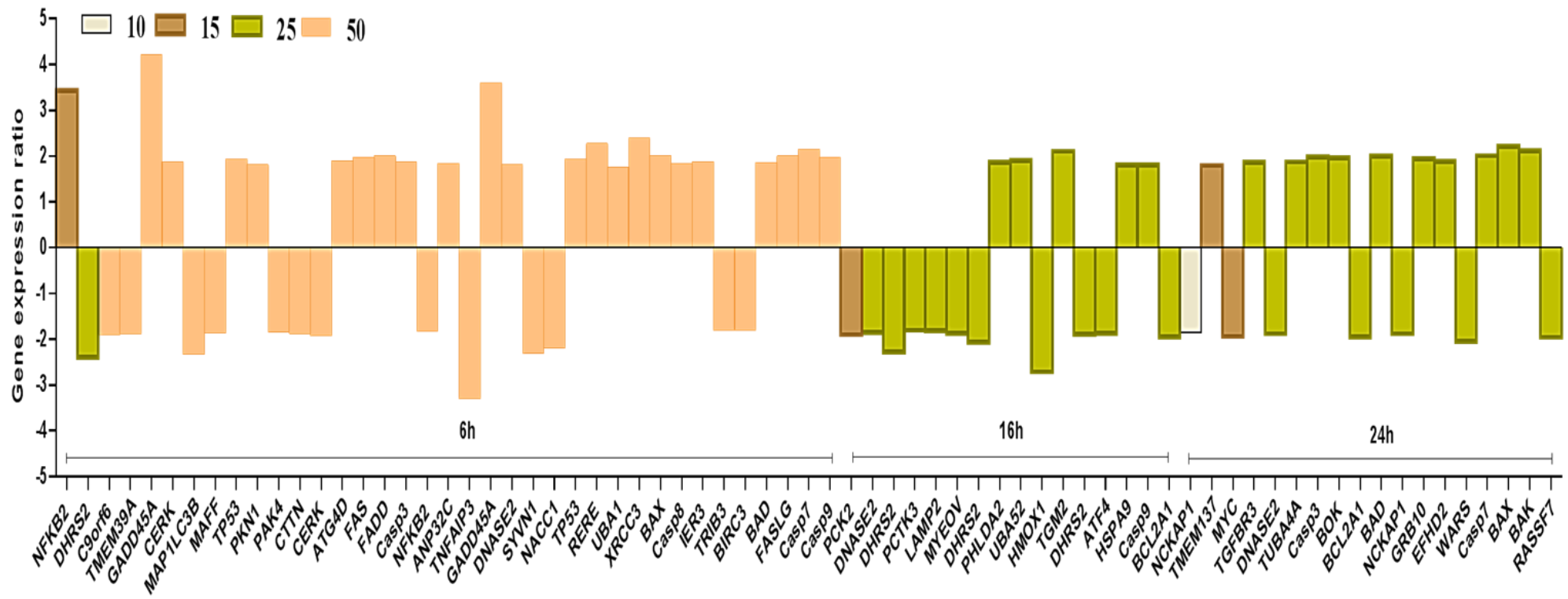


Figure 5.2. 5 Apoptotic genes affected by AKBA treatments from the microarray analysis.

Apoptotic genes affected by AKBA treatments using different concentrations (10 μM, 15 μM, 25 μM and 50 μM (only 6 h) and different time points (6 h, 16 h and 24 h).

5.2.4 Apoptosis Pathway confirmation:

Although the global analysis provided by microarrays allows a lot of data to be generated, the quality of the data is known to vary considerably according to the methods and technology employed (Morey et al., 2006). Therefore, the microarray data were validated using quantitative PCR (qPCR) of specific genes. There was a general agreement between the qPCR and the microarray data for AKBA-dependent gene expression, with increases in the level of transcripts identified after six hours exposure to AKBA for the genes involved in apoptosis, such as caspases- 3, 7, 8 and 9. The effect was found to be AKBA concentration-dependent with the highest expression of these genes observed at the maximum dose (50 μ M). The qPCR provided additional information on the expression of other critical parts of the apoptotic pathway including the up-regulation of CASP2 and the apoptotic protease activating factor 1 (APAF1), which had been shown previously to bind to the initiator caspase-9 (Bratton and Salvesen, 2010).

Based on the transcriptomic data gathered in the present study, a mechanism of AKBA induction of apoptosis can be postulated, wherein AKBA is recognised extracellularly by the FAS ligand as part of the extrinsic apoptosis pathway activation, resulting in the internalisation of FAS and subsequent binding by FADD. This results in an intracellular signalling cascade involving the cleavage of pro-caspase-8 and the activation by caspase-8 of the intrinsic apoptotic pathway through caspase-9. The activated extrinsic pathway is also activated by caspases 7 and 3 resulting in programmed cell death.

Apoptotic gene expression was examined using a QPCR plate panel provided by TaqMan life technologies. The plate was constructed of a manufacturing control (MC), 18S rRNA, with other Candidate Endogenous Control Genes (EC) [GAPDH (EC1), HPRT1 (EC2), GUSB (EC3)] and 92 inventoried genes related to apoptosis. This assay was run using different concentrations of AKBA (10 μ M, 15 μ M, 25 μ M & 50 μ M) but only one time point (6 h) was selected because of the assay cost.

5.3 QPCR analysis

Table 5.3. 1 QPCR Assay plate.

	1	2	3	4	5	6	7	8	9	10	11	12
A	18S	GAP DH	HPRT1	GUSB	BIRC2	APAF1	BAD	BAK1	BAX	BBC3	BCAP 31	BCL10
B	BCL2 2	BCL2 A1	BCL2L1	BCL2 L10	BCL2L1 1	BCL2L1 3	BCL2L 14	BCL2L 2	BCL3	BID	BIK	NAIP
C	BIR C3	XIAP	BIRC5,E PR1	BIRC 6	BIRC7	BIRC8	BNIP3	BNIP3 L	BOK	NOD2	NOD1	CARD 6
D	CAR D9	CASP 1	CASP10	CASP 14	CASP2	CASP3	CASP4	CASP5	CASP6	CASP7	CASP 8	CASP8 AP2
E	CAS P9	CFL AR	CHUK	CRA DD	DAPK1	DEDD	DEDD2	DIABL O	IFT57	FADD	FAS	FASLG
F	HIP1	HRK	HTRA2	CAR D18	IKBKB	IKBKE	IKBKG	LRDD	LTA	LTB	MCL1	NLRP1
G	NFK B1	NFK B2	NFKBIA	NFKB IB	NFKBIE	NFKBIZ	PEA15	PMAIP 1	PYCA RD	REL	RELA	RELB
H	RIP K1	RIPK 2	TBK1	TNF	TNFRSF 10A	TNFRS F10B	TNFRS F1A	TNFRS F1B	TNFRS F21	TNFRS F25	TNFRS F10	TRAD D

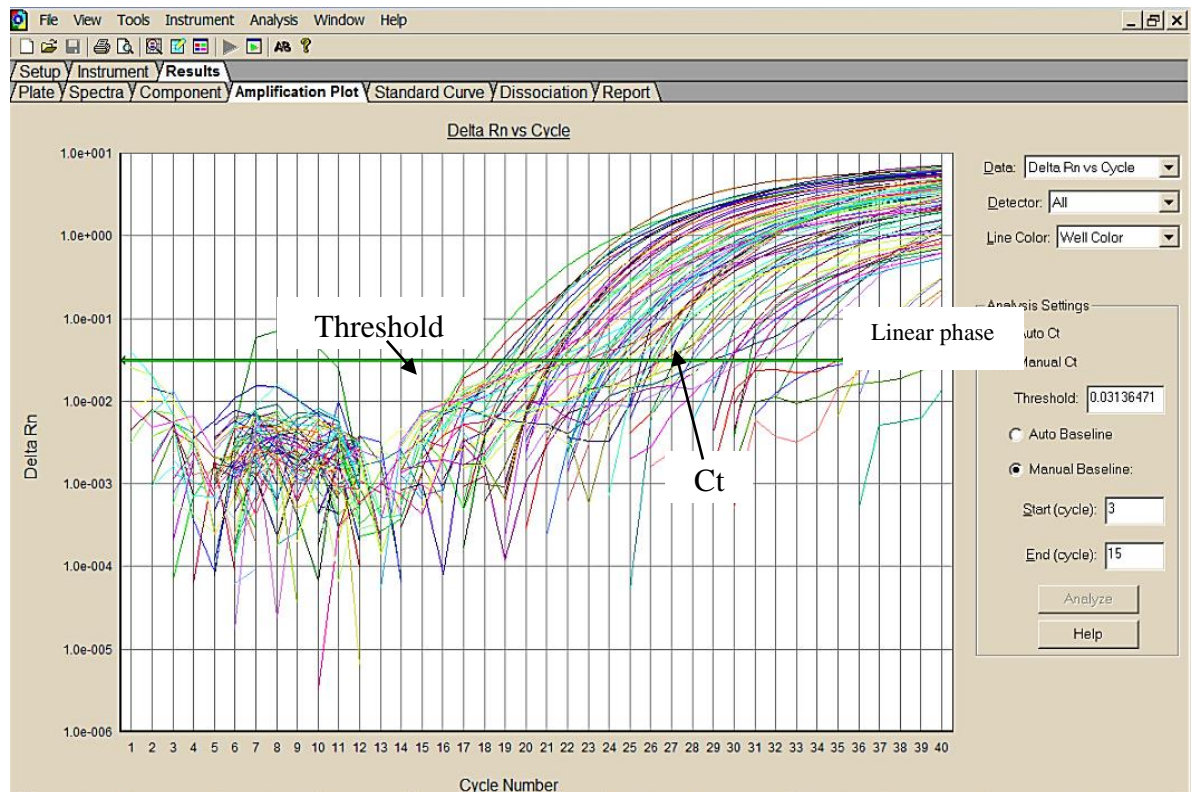
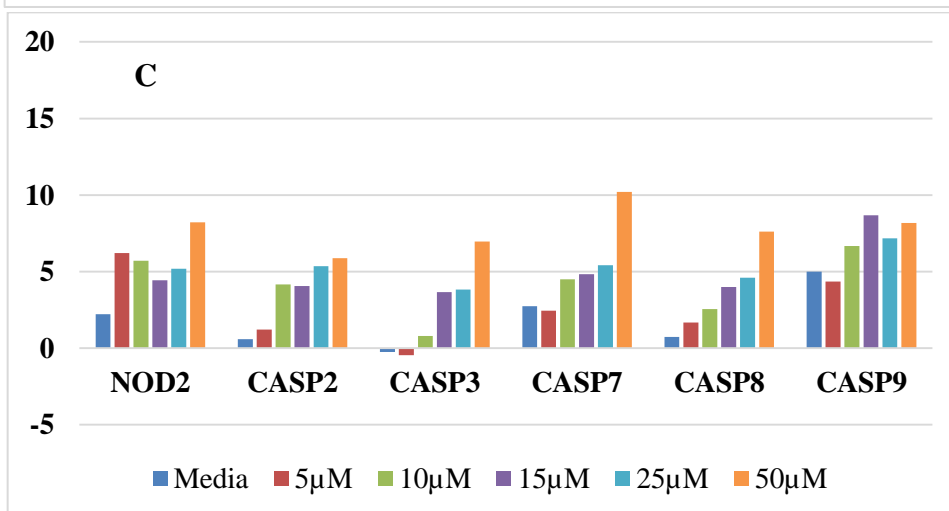
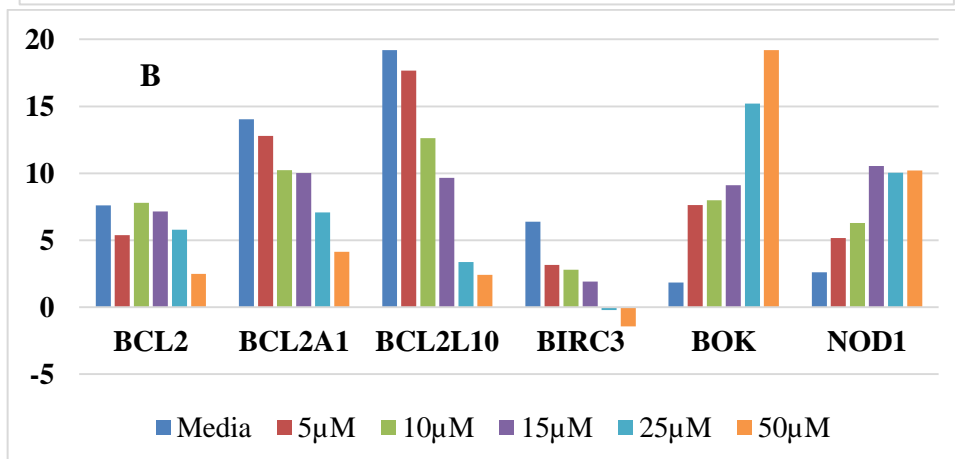
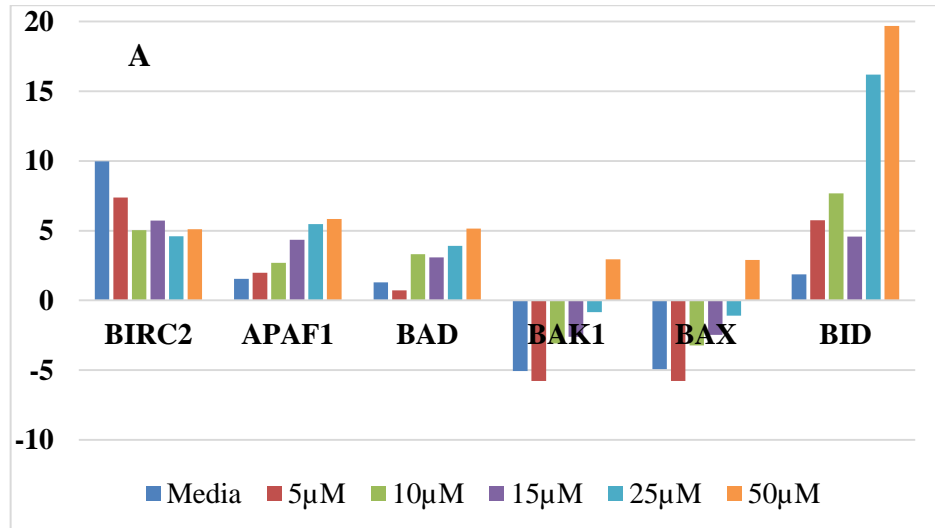


Figure 5.3.1 Quantitative real time PCR Amplification Plot results using the Applied Biosystems 7300 Q PCR System.

A plot of PCR cycle number against PCR amplified product after qPCR for all the apoptotic genes on the plate.

5.3.1 QPCR results analysis

Analysis was undertaken by first deriving the average of the 4 controls, then the Delta Ct was calculated by subtracting the Ct results of each gene from the controls average. Then the delta Ct. was subtracted and finally the results were plotted using Microsoft Excel. This experiment was conducted in triplicate then the mean was calculated and plotted.



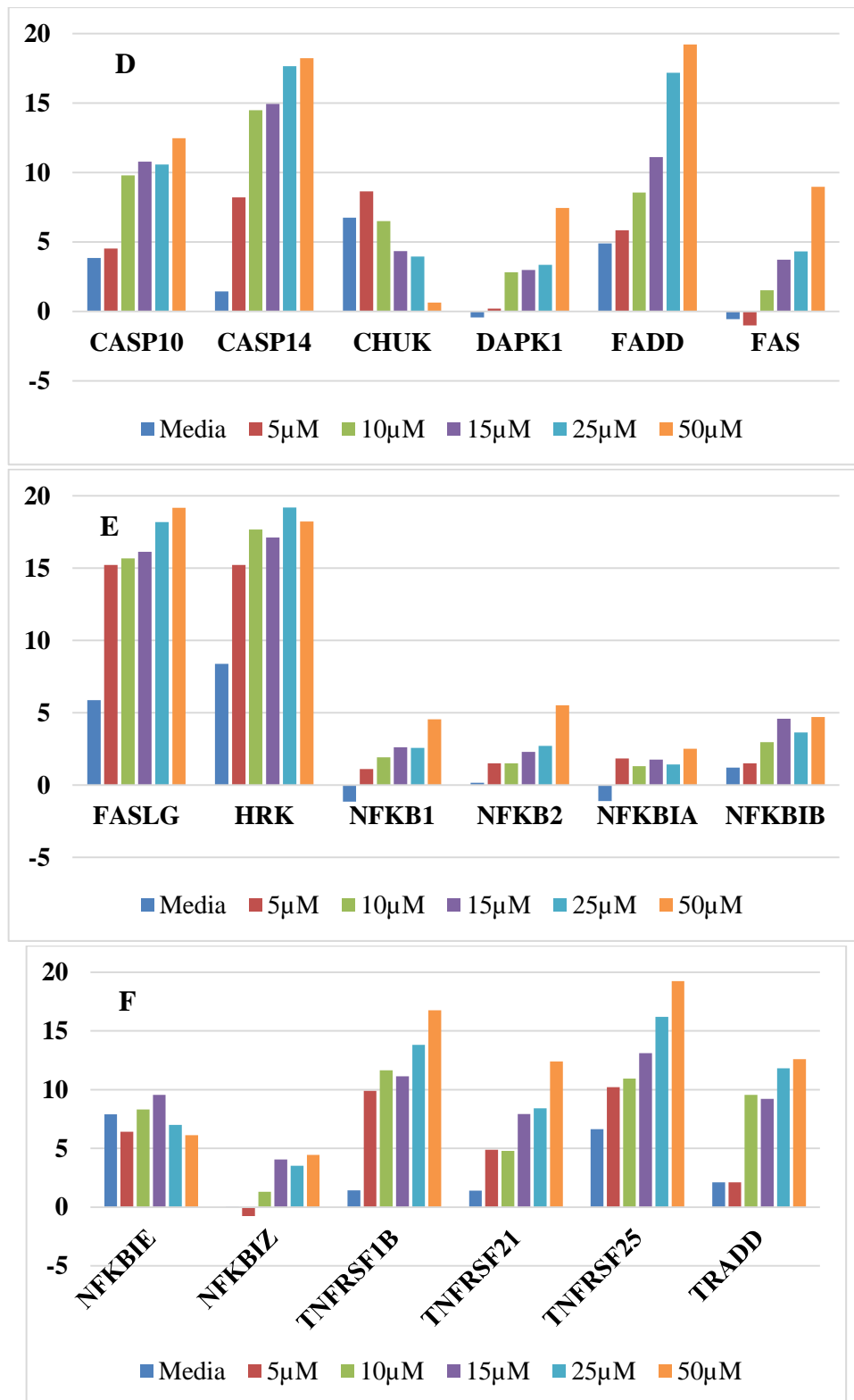


Figure 5.3. 2(A-F) Apoptotic genes expression in OVCAR4 cell lines.

Apoptosis was assessed using the TaqMan® Array Fast Plates for the apoptosis gene panel following exposure to different concentration of AKBA (10 μM, 15 μM, 25 μM & 50 μM) for 6 hours. The data was analysed from three independent experiments then the mean was plotted after calculating and subtracting the Delta Ct.

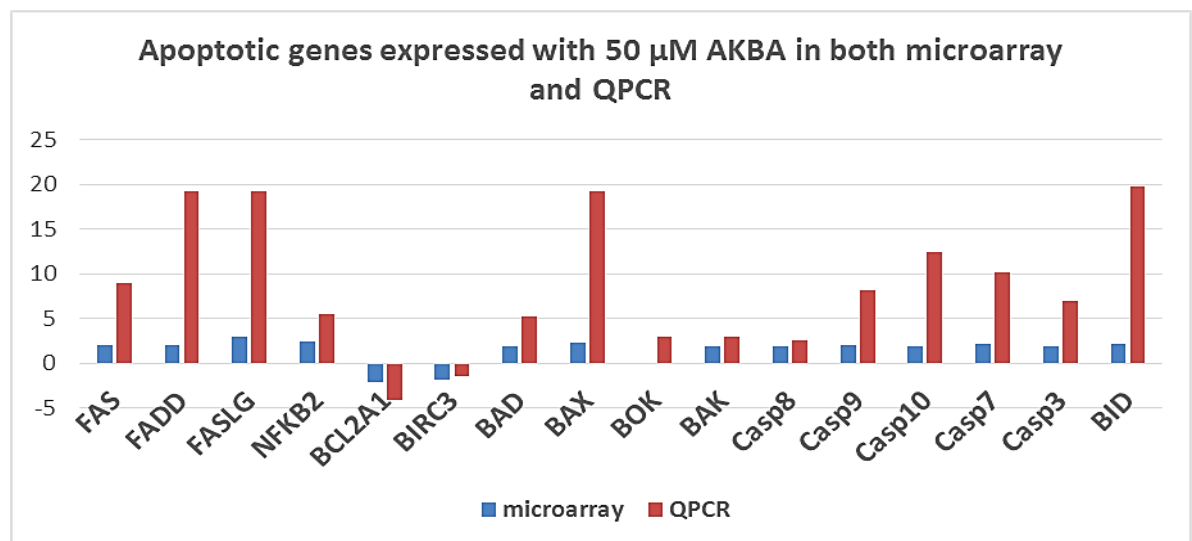
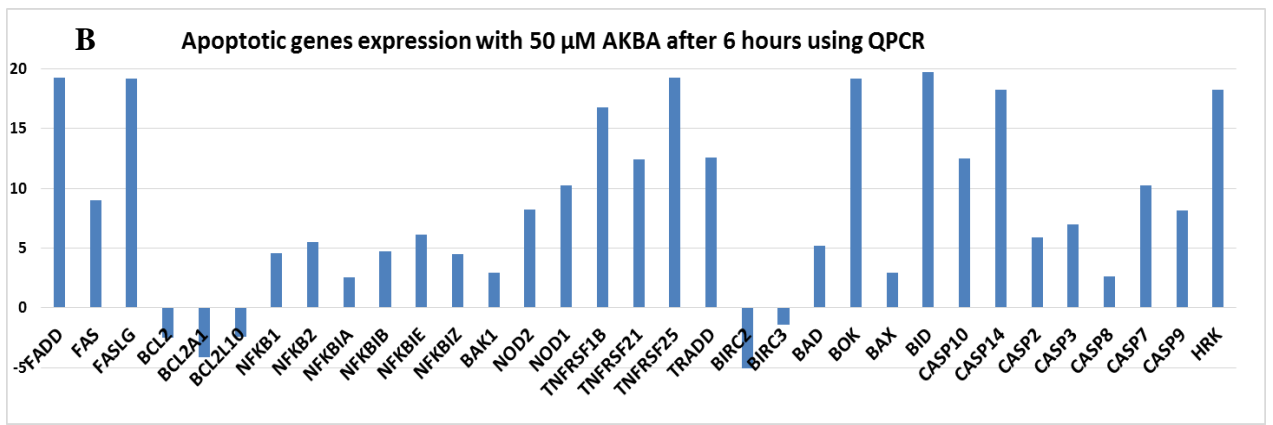
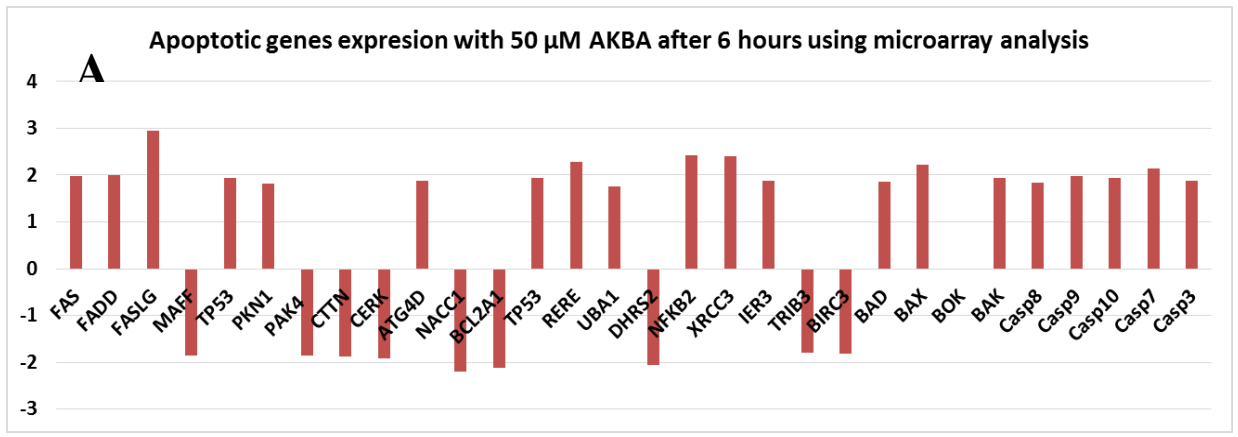


Figure 5.3.3 The most common apoptotic genes affected in OVCAR4 cells.

The most common apoptotic genes affected in OVCAR4 cells treated with 50 μ M AKBA for 6 hours and analysed using microarray gene expression technology and QPCR TaqMan® Array Fast Plates. The data was analysed from 3 independent experiments then the mean was plotted after calculating and subtracting the Delta Ct. These results used to compare the expression of apoptotic genes between the two technologies.

From the QPCR results it was found that most of the apoptotic genes expressed by AKBA

upon microarray analysis, were similarly expressed in the QPCR analysis (Fig 5.3.2 (A-F)) plus or minus and with similar fold change to that seen by microarray. Specific genes were selected to construct the expected apoptosis pathway that AKBA has significant effect on; notably to activate intrinsic and extrinsic pathway of the OVCAR4 cell lines within 6 h of exposure with 50 μ M.

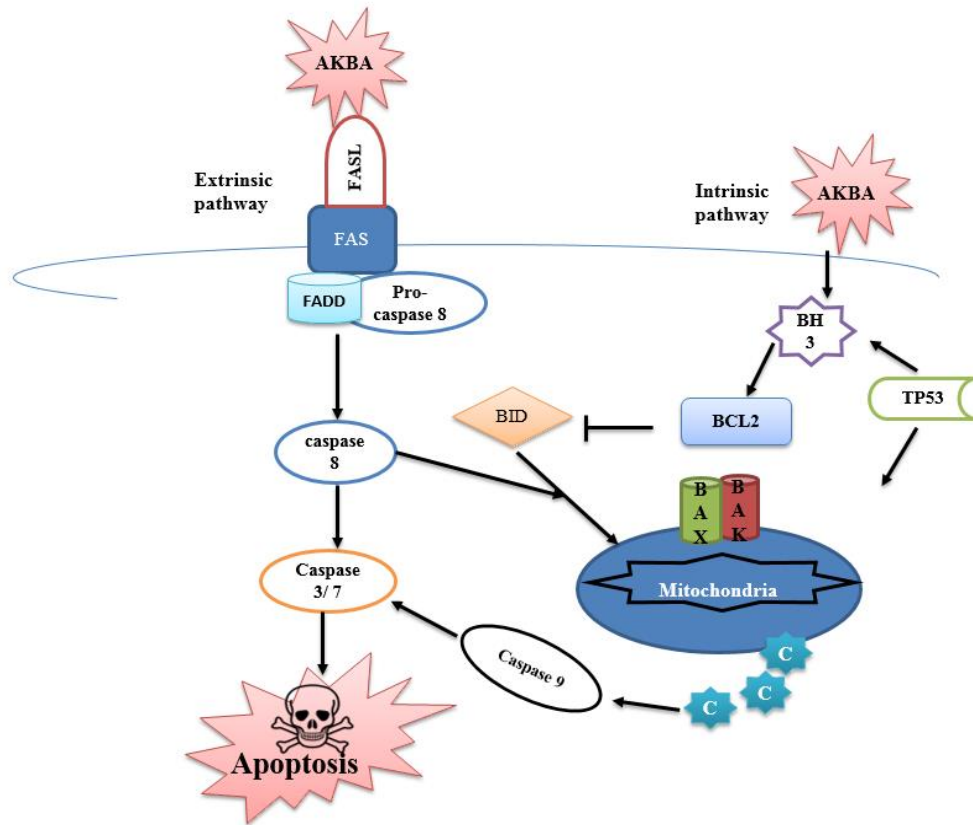


Figure 5.3.4 Apoptotic pathways in OVCAR4 cell lines affected by AKBA.

50 μ M of AKBA causes extrinsic pathway activation by increase in expression of Fas which binds and interact to FAS ligands (FASLG), which results in the formation of the death-inducing signalling complex (DISC), which contains FADD. This then activates pro-caspase 8 and leads cleavage of caspase 8. This leads to cleavage of caspase 3 and 7 which leads to apoptosis. The intrinsic pathway was activated as well at the same time through TP53 pathway, where BCL2 gene has been blocked. Then BAD and BAX genes were activated and cause the release of cytochrome c from the mitochondria which leads to the activation of caspase 9, which then activates the downstream caspases 3 and 7, which end up with a cell death.

5.4 Discussion

The gene expression results gathered from the microarray and qPCR experiments allowed a potential mechanism for AKBA-induced apoptosis to be elucidated. The number of apoptotic genes differentially expressed in the microarray experiments ($P \leq 0.05$, fold change ≥ 1.8), in response to treatment by AKBA was dependent on both the concentration of AKBA and the exposure time. At the highest concentration (50 μM), 84% of the OVCAR-4 genes were significantly differentially expressed within 6 hours, whereas at a lower AKBA concentration (25 μM) an exposure of 16 hours was required to significantly alter the expression profile of the transcriptome to the same extent. The microarray technique enabled the global effect of AKBA on OVCAR-4 cells to be identified, allowing the impact on the overall cellular functions to be revealed as well as the specific impact on individual pathways, such as apoptosis. Apoptosis in human cells is a complicated process involving several distinct, but partially interconnected pathways. Programmed cell death may involve the detection of DNA damage from within the cell and the subsequent triggering of the intrinsic apoptotic pathway, or the extracellular detection of signalling molecules to initiate the extrinsic apoptotic pathway.

The gene expression data indicated that both of these pathways were activated by exposure to AKBA. Up-regulation of genes in the extrinsic apoptotic pathway provided evidence that AKBA is detected by OVCAR-4 cells extra cellular, through the increase expression and activation of FAS ligand, which is internalised and triggers an intracellular signalling cascade, resulting in the activation of caspase-8. This caspase activated the effector caspases 3 and 7 resulting in the completion of apoptosis via the extrinsic pathway. However, the gene expression data gathered also provided evidence for the activation of the intrinsic apoptosis pathway, with its potential activation by caspase-8. The transcriptional suppression of several genes encoding inhibitors of apoptosis revealed by the qPCR data highlighted a likely scenario for this second apoptosis route. The proteins BCL2, BCL2A1, and BCL2L10 are involved in the release of the apoptosis activator APAF1 from the mitochondria (Youle and Strasser, 2008) and BIRC2 and BIRC3 are involved in the inhibition of caspase activators, thereby preventing apoptosis (Wang et al., 2012). In the model organism, *Caenorhabditis elegans*, the BCL family of proteins directly inhibit the APAF1 homolog, ced-4 thereby enabling apoptosis to proceed (Yan et al., 2005). The results obtained in the present study reveal a marked down-regulation of the BCL2 and BIRC2/3 genes as well as an up-regulation of BAX and BAK

that encode proteins involved in the release of cytochrome c from the mitochondria and the subsequent activation of APAF1 (Shankar and Srivastava, 2007). The release of cytochrome c also results in the activation of caspase 9, one of the critical initiator caspases for apoptosis, which carried out by caspases 3 and 7. The microarray data for the highest dose of AKBA showed a significant up-regulation in CASP3, CASP7 and CASP9, strongly indicating that this apoptotic pathway was utilised by the OVCAR-4 cells.

As well as identifying specific activated pathways, the data gathered from the transcriptomic experiments provided evidence of broader transcriptional control of apoptosis through control of DNA binding proteins. Data from the qPCR approach revealed that the inhibitor of nuclear factor kappa-B kinase subunit alpha-encoding gene, CHUK, was down-regulated by AKBA in a concentration-dependent manner. The inhibitory function of CHUK on the transcription factor, NF- κ B (encoded by NFKB genes) is critical to apoptosis, as NF- κ B functions in the cell nucleus to regulate anti-apoptotic genes such as TRAF1 and TRAF2 (Oeckinghaus et al., 2011). This mechanism is different to the one previously proposed by Syrovets et al. (2005) in prostate cancer cells; the authors observed that acetyl-boswellic acids promoted apoptosis through inhibition of NF- κ B.

Finally, the up-regulation of TP53, encoding the critical cell cycle regulator p53 is intriguing. Under normal conditions in response to DNA damage, p53 induces cell cycle arrest and apoptosis via the release of mitochondrial cytochrome c and the subsequent activation of effector caspases (Vakifahmetoglu et al., 2006). It has also been reported previously that boswellic acid induces apoptosis and cell cycle arrest in the hepatocellular carcinoma cell line, HEP-G2 and this is mediated through accumulation of p53 (Noaman et al., 2009). However, the study by Cui et al. (2007) determined that p53 was induced along with the subsequent apoptotic signal cascade in the MCF-7 human breast cancer cell line in response to treatment with oridonin, a diterpenoid from *Rabdosiarubescens*, or Chinese sage. The similar structure between oridonin and AKBA indicates a possible similar anticancer mechanism and it is interesting that Cui et al. (2007) concluded that apoptosis occurred via a mechanism that was independent of caspase-3 but that was dependent on caspase-9. Further research is required to determine whether AKBA-induced apoptosis occurs in a caspase-3-dependent or independent manner.

5.4.1 Potential clinical applications from this research

Previous studies have shown a link between boswellic acids, such as AKBA, with programmed cell death, suggesting a potential anticancer treatment (Takahashi et al., 2012). The results presented here confirmed much of the existing scientific literature and supported the hypothesis that AKBA may form the basis of a novel anticancer therapeutic agent. The results of the present study have also demonstrated a possible mechanism whereby AKBA is detected extracellularly by cancer cells and triggers an apoptotic response within the cells. Although it has been suggested from the data presented in this study that AKBA is recognised by the FAS ligand as the first step in the extrinsic pathway, the exact mechanism for apoptosis initiation through FAS has been explained in through fig 5.3.4. Nonetheless, the impact of AKBA on the induction of programmed cell death appears to be well supported by the gene expression data outlined in this study. There are a number of reports of activation of apoptosis through FASL when bound to the membrane of one cell. Which could then interact with FAS on another cell, it is in contact with (without the FASL being released) and engage FADD, and so lead to apoptosis (LA et al., 2009, Bush et al., 2001, Delmas et al., 2003, Shao et al., 2001, Wajant, 2002). Another researcher reported that the Fas pathway during apoptosis can be activated independently of FasL, via topoisomerase I-mediated DNA damage-induced apoptosis which involves activation of the Fas pathway. without Fas-ligand activation in CPT-treated cells (Shao et al., 2001).

One area for concern with all conventional and novel anticancer therapeutics is the potential for drug resistance. AKBA treatment may overcome this issue through its mechanism of triggering cancer cell apoptosis. It is also promising that after exposure to AKBA, the OVCAR-4 cells exhibited two apoptotic pathways: extrinsic and intrinsic. The two forms of apoptosis help to decrease the likelihood of cancer cell resistance to AKBA, however it is possible that the apoptotic cascade may be blocked through the inhibition of caspase-8, which has an important role in both the intrinsic and extrinsic signalling pathway. However, the transcriptomic data presented here raises the possibility of an alternative apoptotic control mechanism through inhibition of CHUK and the release of NF- κ B to prevent inhibition of apoptosis. Despite the promising results gathered from this transcriptomic study, it is important to note that much of the caspase signalling cascade is dependent on post-translational control by regulator proteins, highlighting that further investigation is required to elucidate the exact mechanism of AKBA-induced apoptosis before any anticancer properties can be exploited in vivo.

One additional concern of this approach as the basis of a novel therapeutic is the potential for the induction of apoptosis in healthy cells, primarily through the extrinsic signalling cascade. As AKBA does not target a cancer specific molecule or receptor, the apoptotic effect is likely to impact neighbouring cells in affected tissues. To mitigate this potentially adverse effect, the cancer cell targeting treatment dose and exposure time will have to be carefully considered. A first step towards this has been made in this study with a range of AKBA concentrations having been investigated (10-50 μ M), and a dose- and treatment duration-dependent mechanism having been established.

5.4.2 Conclusion

From the gene expression results we concluded that AKBA affected different major pathways in ovarian cancer cells (DNA damage and repair, cell metabolism, cell adhesion and metastasis, cell cycle and cell proliferation) which leads to cell growth inhibition and apoptosis. Both extrinsic and intrinsic pathways (fig 5.3.4) were activated as confirmed by QPCR.

Chapter 6

General Discussion and Thesis Summary

6.1 Discussion

The Impetus to utilise the anti-tumorigenic properties of the BSE derived compound AKBA is driven by an increasing weight of literature showing it to be an effective inducer of apoptosis in an increasingly large range of cancer cells (Abdel-Tawab et al., 2011, Abou-Nassar and Brown, 2010, Ali and Mansour, 2011, Andotra et al., 2012, Bone, 2006). This is supported by a number of animal studies showing an effective reduction in tumours upon AKBA treatment and a low toxicity even at high doses (Singh et al., 2007, Park et al., 2011a, Yadav et al., 2012, Zhang et al., 2013).

Here we employed OVCAR-4, UWB1.289, A2780 and A2780cis cell lines to investigate the effect of AKBA for the first time, on ovarian cancer cells. Our initial results using a simple visual growth assay, suggested that AKBA was effective in inhibiting the growth of all the four cell lines in a dose dependent manner. Indeed, at the highest concentration of 50 μ M, AKBA treatment effectively prevented any proliferation from taking place over the 48h periods where upon the cells appeared unviable. Cell cycle analysis was then performed to assess the effect of AKBA treatment on the cell cycle. There have been numerous studies suggesting that AKBA can induce G1 phase arrest. Our data however, suggested, contrary to this, that very little G1 arrest had taken place. Indeed, between 0-25 μ M AKBA there was minimal difference between cell cycle phasing and different time-points. However, at 50 μ M cells quickly began to undergo apoptosis within 30 mins, and a high proportion of sub-G1 cells were observed. This was seen in all cell types.

Given the dramatically increased fragmentation of DNA observed using PI staining techniques upon treatment of cells with 50 μ M AKBA, comet assays was performed in parallel and directly observe DNA fragmentation. Despite the failure of AKBA to observe the DNA fragmentary phenotype observed in the cell-cycle analysis experiments using lower concentrations, a clear dose and time dependent increase in DNA fragmentation was seen following treatment with AKBA. This was again observed for all cell lines tested and suggests that AKBA is a consistent and potent inducer of DNA damage which was detected by comet assay, DNA fragmentation which was evident in SubG1, a phenotype associated with the induction of apoptosis. Taken together with the cell cycle studies, this strongly suggested that AKBA treatment was causing OVCAR-4, UWB1.289, A2780 and A2780cis cells to undergo cell death.

Following staining for Annexin V, again it was observed high levels of apoptosis in OVCAR-4 and A2780cis cells that had been treated with 15-50 μ M AKBA, an effect which increased over time compare to the other two cell lines. Similarly, when FACS analysis was used to differentiate between early and late apoptosis, it was clear that 50 μ M AKBA treatment induced the cells to progress through the process of apoptosis immediately. Confusingly however, very little induction of early or late apoptosis was observed in cells treated with any dose equal to or less than 15 μ M at the same time point(fig 3.3.1, fig 3.3.2, fig 4.3.1.2 and fig 4.3.2.2) and the AKBA dose and time dependent increase in cell toxicity and leads to cell death(fig 3.4.1, fig 4.4.1). It was observed in both the apoptosis and the cell cycle assays that with the low concentration of AKBA there appeared to be responded more clearly after 24 h at this level of analysis.

As noted, the effects of AKBA on apoptosis were observed only at the highest concentration of 25 - 50 μ M or in some instances at 15 μ M. This concentration range is in contrast to previous studies where potent growth inhibitory effects have been observed at concentrations 1-log lower than this(Park et al., 2002a, Park, 2002b), between 2 and 8 μ M. Another study supported this data, showing that topoisomerase I from calf thymus was inhibited by AKBA at a concentration of 10 μ M. The discrepancy between the AKBA concentrations required for functional induction of apoptosis in our study, and the lower concentrations identified in previous studies may be due to numerous reasons; i) the mechanism of apoptosis induction may differ between cell types, therefore requiring different concentrations of AKBA to initiate or inhibit the relevant cell machinery; ii) differing levels of expression of downstream cellular effector molecules, such as signalling pathway proteins.

The DNA damage results obtained by comet assay and the Gamma-H2AX Assay reflects a similar hypothesis as a significant level of DNA damage has been obtained at this concentration with all the four cell lines. AKBA is DNA damage inducer, causing PARP cleavage, topoisomerases inhibition and from the gene expression results it inhibits the DNA repair mechanisms by inhibiting genes such as BRCA1, BRCA2 and NFIL3; on the other hand up regulation of genes like GADD45A, DDIT3, MAPK12 and XRCC3. The majority of genes affected related to cell cycle arrest, check points and apoptosis even though the flow cytometry PI staining did not indicate any cell cycle arrest; but from the gene level examination a number of genes have been affected including the up regulation of CCNE1, STARD13, MCM10, CDK6, STARD13 and FOSL1, with down regulation

of MYC and MTMR9, in parallel with the protein expression of P21 and P16. These results can be linked to the apoptosis pathway over expression which leads to the death of the majority of cells and the correct time and concentration might have been missed to detect the cell cycle arrest.

6.1.1 AKBA as anticancer Therapy

Various forms of boswellic acid are known to cause extensive cellular and DNA damage, resulting in cell-cycle arrest and apoptosis (Suhail et al., 2011). This study investigated whether the cytotoxic, apoptosis-inducing effect of one of these forms of boswellic acid (BA) is 3-O-acetyl-11-keto- β -boswellic acid (AKBA), could have therapeutic potential in the treatment of ovarian cancer. Four ovarian cancer cell lines were utilised for these *in vitro* experiments, (OVCAR4, UWB1.289, A2780 and A2780cis) to determine the concentration of AKBA and the duration of exposure to generate a significant cytotoxic effect. As a result of these experiments, a dose-dependent effect was identified across the cell lines, with changes in cell morphology, associated with an overall decreased cell viability. Further investigations involving γ -H2AX and comet assays revealed considerable DNA damage in the form of single and double-strand breaks, seemingly without the accumulation of reactive oxygen species in all the four cell line. Further analysis revealed that the DNA damage did not appear to result in cell cycle arrest in all the four cell lines with a large proportion of cells dead and shifted to sub-G1 stage of the cell cycle after treatment with AKBA. Western blotting revealed the production of the cell cycle regulating proteins p16 and p21 (Roy et al., 2016), signalling cell cycle arrest at the G1/S checkpoint; similar *in vitro* finding have been published by another researcher (Liu et al., 2006), that showed that an AKBA-mediated G1/S arrest resulting from a decrease in the concentration of the cell cycle biomarkers, cyclin D1, cyclin- E, CDK-2, CDK-4 and pRb in colon cancer cells (Roy et al., 2016, Khan et al., 2016). From the flow cytometry data there was no cell cycle arrest even though with the protein expression in all cell lines there were significant increases in expression for P21 and P16 proteins, which are Cyclin-dependent kinase inhibitors, the regulators of the cell cycle. These genes were also noted to be expressed by microarray (El-Deiry, 2016). The gene expression changes suggest that arrest might be occurring at G1 phase or according to previous literature at G1/S (Liu et al., 2006), but for some reason it is not visible by flow cytometry.

In the present study, apoptosis analysis followed the cell cycle analysis using annexin

V/Pi staining (Rieger et al., 2011), along with the accumulation of the apoptotic marker caspase-3 (Lakhani et al., 2006), as well as cleaved poly ADP ribose polymerase (PARP) (Qurishi et al., 2013, Bhushan et al., 2013), which has a role in inducing programmed cell death (Chaitanya et al., 2010). At the highest AKBA concentration tested (50 μ M) immediate cell death was observed across all cell lines in concordance with a previously published study showing similar effects in a hepatocellular carcinoma cell line subjected to various boswellic acids (Noaman et al., 2009). 50 μ M concentrations gives cell death in just less than 30 minutes in A2780cis, UWB1.289 and OVCAR 4 cells. This supported by other researchers who pointed that apoptosis can occurs within 10 mins (Green, 2005). The findings presented here describe a mechanism in which cellular damage, cellular arrest and programmed cell death follow from treatment with AKBA at concentrations (≥ 15 μ M). These results support previously published scientific studies that have described perturbations to the physiology of cancer cells by boswellic acid (Park et al., 2011b) and implicated AKBA as a particularly favourable candidate as an anticancer therapeutic agent (Pang et al., 2009, Mullard, 2016). Microscopy assessment revealed that low concentrations of AKBA (10 μ M) resulted in the generation of structures that resembled apoptotic bodies – a clear physical marker of programmed cell death (Elmore, 2007, Tewary et al., 2016). These same structures were described in one of the studies (Chashoo et al., 2011b), which identified the formation of apoptotic bodies upon exposure to a closely related compound of AKBA, propionyloxy derivative of 11-keto-beta-boswellic acid. The presence of the active form caspase-3, known to be an apoptosis executor (Lakhani *et al.*, 2006), confirms that the mechanism of controlled cell death rather than necrosis was responsible for the decrease in cell viability (Elmore, 2007).

Although the cytotoxic response was generally replicated across the ovarian cancer cell lines tested in this study, it was interesting to note that some lines were particularly sensitive to the effects of AKBA. For example, the cisplatin-resistance cell line A2780cis was more susceptible to AKBA at lower concentrations (≤ 15 μ M) compared to other cell lines. This finding highlights the possibility of a shared cytotoxic mechanism of action between cisplatin and AKBA, likely through the formation of DNA damage (Wang et al., 2010).

UWB1.289 cells contain a *BRCA1* deletion mutation (2594delC) within exon 11 and also

have a mutation in p53 (625delAG) which makes them more chemo-sensitive and patients have better outcomes. These mutations result in decreased apoptosis and Sub-G1 populations in response to DNA damage (DelloRusso et al., 2007), allowing this cancer cell line to divide rapidly, making UWB1.289 cells more resistant to therapeutics that target cell cycle arrest through p53 and BRCA1. In the present study, UWB1.289 cells showed a high reduction in the reactive oxygen species after treatment with AKBA. Despite extensive DNA damage caused by this process, UWB1.289 DNA synthesis have been shown previously to continue without the cells entering into apoptosis (DelloRusso et al., 2007). Therefore, it was interesting to observe that the addition of AKBA to the cell culture medium resulted in a significant increase in the sub-G1 population, with twice as many cells present in sub-G1 than for the control sample. This result suggested that AKBA might be able to induce cell death through different pathways including p53 independent, caspase dependent pathways or DNA damage and repair (BRCA1-independent mechanism), which may represent a promising novel approach to treat cancerous cells that are resistant to compounds that target these mechanisms (Wang et al., 2010).

6.1.2 Gene expression data

The gene expression data gathered from microarray and qPCR experiments allowed the physiological effects of AKBA on OVCAR4 cells to be elucidated at the transcriptomic level. The differential expression of genes in response to the addition of AKBA was concentration and time dependent, with 85 genes significantly affected after 6 h of exposure with 50 μ M. This includes genes from apoptosis pathways being up regulated (UBA52, TGM2, NFKB2, ANP32C, EFHD2, DNASE2, TP53, RERE, MAPK12, GADD45A, BAX, Casp3, Casp7, CERK, ATG4D, FAS, PKN1, FADD, Casp3, RERE, UBA1, XRCC3, Casp8, IER3, BAD, FASLG, Casp7, Casp9, BOK and BAK), and down regulated (PCK2, , DHRS2, MYEOV, LAMP2, HMOX1, TMEM39A, C9orf6, MAP1LC3B, WARS, MYC, TNFAIP3, SYVN1, NACC1, PAK4, PKN1, RASSF7, BCL2A1, DHRS2, PCTK3, ATF4, MAFF, CTTN, NACC1, TRIB3 and BIRC3); some of these genes have been reported by other researchers to be effected by Boswellic acid specifically AKBA at certain concentrations but most of them have been presented for the first time in this thesis. (Roy et al., 2016, Xue et al., 2016). The transcription of genes involved in critical physiological processes, such as cell proliferation (table 5.2.5) byinhibiting the 5 lipoxgenases which inhibit cell proliferation and leads to apoptosis

(Hamidpour et al., 2016). DNA damage and repair up regulated genes included PI3, CITED4, ATP7B, HINT3, RRP7A, FKBP1A, FAM100A, STARD13, BRI3BP, UBA1, XRCC3 and MAPK12 whilst and down regulated genes includes LEMD1, ST6GALNAC3, C4orf34, GARS, NAMPT, LONP1, SLC3A2, DDIT3, UHRF1BP1, NFIL3, TARS, EAF1, SCG2, NFE2L2, RAB9A, MAFF, C7orf40, C12orf47, CEBPG, SNHG5, MOCOS, BRCA1, BRCA2; again some of these genes already been reported (Rajabian et al., 2016, Khan et al., 2016). In addition to this, cell metabolism and other pathways were altered in response to the AKBA treatment. AKBA was tested for the first time on ovarian cancer cell lines and the gene expression for OVCAR 4 cell line was presented here for the first time.

6.1.3 Cell proliferation

The transcriptomic data confirmed the cell cycle arrest identified by the *in vitro* experimental data in the four ovarian cancer cell lines. Overall, there were 22 significantly up-regulated (CCNE1, CERK, STARD13, DGCR2, HAS3, CBX6, FOSL1, PKMYT1, MCM10, TM4SF4, RRP15, CDKN1A, UBA52, UBE2E1, SHPK, ZNF207, SNRNP70, CEP152, GRB10, CDK6, TXNL4B, HSPA9 and GADD45A) and 40 down-regulated genes (HAS3, MTMR9, TXNL4B, FNBP1L, CEBPB, ZNF616, TUBE1, HSPA13, ASNS, EIF4G1, SPIRE1, RIOK2, TERF2IP, HSPA5, ZNF165, XPOT, SERPINI1, TUBE1, BBS2, LAMP2, ASNS, ZNF323, PCK2, ATF4, CTNNB1, NAMPT, BHLHB2, YWHAZ, SDCBP, MYC, ASNS, OSBPL9, YARS, IFRD1, PPFIBP1, MARS, UBXN2B, SARS, CLDN1, NCKAP1, TUBE1, SDCBP, LAMP2, HIST1H2BK, UHRF1BP1 and PAK4) after AKBA treatment highlighting the generally negative regulation of the cell cycle and of cell proliferation induced by AKBA. One notable exception was the *CDK6* gene, encoding a protein that allows the passage through the G1/S cell cycle checkpoint, which was up-regulated after 6 hours' exposure to AKBA. The up-regulation of this gene would normally allow cell cycle to progress (Fiaschi-Taesch et al., 2010), however it is interesting to note that at higher AKBA concentrations, *cdk6* is not significantly up-regulated. The up-regulation at lower AKBA concentrations may be due to a decrease in the intracellular concentration of the *cdk6* regulator, Cyclin D (Liu et al., 2006). The G0/G1 cell cycle regulator p21, encoded by the gene *CDKN1A* (Dutto et al., 2015), was up-regulated by exposure to AKBA, supporting the *in vitro* results showing that OVCAR4 (and other cell lines) shifted in a sub-G1 as the cells are daying. Many of the other up-regulated genes are annotated as having a positive

involvement in chromatin organisation and large-scale DNA transcription regulation, indicative of reduced cellular activity after AKBA treatment.

6.1.4 DNA damage and repair

The *in vitro* cell culture experiments provided compelling evidence of accumulated DNA damage through double-strand breaks that were the likely trigger for cell cycle apoptosis through either the defect in BRCA1 gene as in UWB1.289 cell lines or by the inhibition of topoisomerase I and II. However, at the transcriptomic level more genes were annotated as having a role in DNA damage and repair were down-regulated than induced by AKBA which leads to the accumulation of DNA damage and leads to cell death. It has been stated previously that AKBA induces apoptosis through the formation of DNA damage (Takada et al., 2006), and the up-regulation of genes such as *UBAI* (DNA repair) and *GADD45A* (induced by DNA damage) confirmed this hypothesis. Interestingly, two significantly down-regulated genes were *BRCA1* and *BRCA2*, which have been implicated previously as having a role in combating oxidative stress (Marks, 2013, Yi et al., 2014). As the cell culture experiments outlined in the present study have hypothesised that DNA damage in the cell did not result from a build-up of reactive oxygen species but through some other mechanisms, which was evident by both BRCA genes not being up-regulated as part of the DNA repair pathway.

6.1.5 Cell metabolism and DNA damage

In general, cellular metabolism was down-regulated in response to AKBA. This finding corroborates the experimental data that showed the OVCAR4 cells entering a period of quiescence or cell death, in which lower metabolic output would be expected. The accumulation of reactive oxygen species was expected in the cancer cells as per previous studies (Khan et al., 2014). Although the transcriptional data presented here indicated a general stress response in the DNA damage level in OVCAR 4 cells, there are few major genes involved in the DNA damage and repair mechanisms which includes up regulation of *CCNE1*, *CERK*, *STARD13*, *DGCR2*, *HAS3*, *CBX6*, *FOSL1*, *PKMYT1*, *MCM10*, *TM4SF4*, *RRP15*, *CDKN1A*, *UBA52*, *UBE2E1*, *SHPK*, *ZNF207*, *SNRNP70*, *CEP152*, *GRB10*, *CDK6*, *TXNL4B*, *HSPA9* and *GADD45A* and down regulation of *LEMD1*, *ST6GALNAC3*, *C4orf34*, *GARS*, *NAMPT*, *LONP1*, *SLC3A2*, *DDIT3*, *UHRF1BP1*, *NFIL3*, *TARS*, *EAF1*, *SCG2*, *NFE2L2*, *RAB9A*, *MAFF*, *C7orf40*, *C12orf47*, *CEBPG*, *SNHG5*, *MOCOS*, *BRCA1* and *BRCA2* which been presented for the first time. There

were no genes up or down regulated that have been identified as being involved in the formation or in the sequestering of endogenously-produced reactive oxygen species which might be the case that the DNA damage occurred through other mechanisms not via ROS production.

On the other hand Audeh et al (2010) determined that Poly(ADP-ribose) polymerase (PARP) is a critical signaling pathway for repairing single-strand breaks in DNA. When PARP is inhibited, single-strand DNA breaks accumulate, yielding double-stranded DNA breaks, Inhibition of PARP leads to accumulation of single-strand DNA breaks, and ultimately derailing replication forks (Audeh et al., 2010), which can cause formation of double-strand DNA breaks. Without PARP inhibition, double-stranded DNA is typically subject to repair by BRCA1 and BRCA2 (Audeh et al., 2010). BRCA1 and BRCA2 were the same cell line mutations identified as responsible for the ovarian cancer. They are considered the primary constructs of the homologous recombination repair pathway, and with the inhibition of topoisomerase and PARP cells proceed to apoptosis (Chashoo et al., 2011a). Audeh et al (2010) highlight that BRCA1 and BRCA2 mutations are particularly sensitive to repair interference via PARP inhibition, as it achieved via AKBA treatment in Chapter 4.

6.1.6 Apoptosis

Two major pathways have been described in the apoptosis induction mechanism: the extrinsic or the death-receptor pathway and the intrinsic or the mitochondrial pathway that is associated with activation of Bax, from the Bcl2 family, which causes disruption in the mitochondrial function and releases of the pro-apoptotic proteins like cytochrome c, which activate caspase 9 and caspase 3 and leads to cell death. The extrinsic pathway is normally defined by caspase-8 activation. This cysteinyl-aspartate protease is recruited by the adapter molecule FADD, which is associated with the death domain of death receptors such as FAS, TNF-R1 or TRAIL, upon ligand binding which then cleave caspase 8 and caspase 3 leading to cell death (Reyes-Zurita et al., 2016).

The gene expression data provided compelling evidence for caspase-induced apoptosis in the OVCAR4 cells. For example, the microarray data reveal that exposure to 50 μ M AKBA for six hours resulted in a significant up-regulation of *CASP3* and *CASP7*, encoding executor caspases directly involved in apoptosis (Lakhani et al., 2006). In addition, the initiator caspases *CASP2*, *CASP8*, *CASP9* and *CASP10* were all significantly up-regulated after exposure to AKBA, indicating apoptosis was occurring. As well as the

involvement of caspases in apoptosis there was an up-regulation in genes encoding proteins known to have a role in the recruitment of caspases for apoptosis, such as *NOD1* and *NOD2* (Caruso et al., 2014). The caspase-dependent Death-associated protein kinase gene *DAPK1* was up-regulated at concentrations of 10 μ M AKBA after six hours, indicating that the process of apoptosis signalling occurs even at low concentrations. Three genes within the TNF receptor super family (*TNFRSF21*, *TNFRSF25* and *TNFRSF1B*) were also up-regulated; these encoded proteins are known to have a role in inducing apoptosis through the interaction with the TRADD protein, which sequesters and inactivates the apoptosis inhibitor TRAF2 (Jackson-Bernitsas et al., 2006).

Although involving a complex series of cell signalling pathways, the gene expression data allow a potential mechanism for AKBA-induced apoptosis to be elucidated. The DNA damage identified through the γ -H2AX and comet *in vitro* assays causes the activation of the intrinsic apoptotic pathway via caspase-8. This hypothesis confirms an earlier study, which described boswellic acid-induced apoptosis being mediated through caspase-8 (Lu et al., 2008). A second apoptotic signalling route may occur through the so-called extrinsic pathway through which AKBA is detected in the cell culture medium by the Fas ligand, encoded by the AKBA-induced FasL gene. After internalisation into the cell, the Fas proteins bind the Fas-Associated protein with Death Domain (FADD), which is involved in the activation of caspase-8. Although the gene expression data in the current study supported the involvement of the extrinsic pathway, with FADD, FasLG and Fas all up-regulated by six hours exposure to AKBA, it should be noted that a previous study has determined that AKBA-mediated apoptosis occurred in a variety of cell lines (but not ovarian cancer cells) by a mechanism that was independent of Fas/FasL interaction (Takada et al., 2006). If this were the case in OVCAR4 cells, the possibility exists for the extrinsic apoptosis pathway to proceed through other receptors, such as the TNF super family, which would activate caspase-8 through the TRADD and FADD proteins (Ashkenazi, 2008). Previous researchers suggested that soluble Fas does not have to be produced to induce cell killing via extrinsic pathway, both intrinsic and extrinsic processes might have induced apoptosis. It is been reported that AKBA suppressed tumour metastases and cell adhesion in colorectal cancer (CRC) (Yadav et al., 2011, Park et al., 2011b) by down regulation of (PAK4 and CTTN) and up regulation of PKN1 in OVCAR4 cells as reported in Chapter 5.

6.1.7 AKBA as potential anti-cancer agent

The present study has shown that AKBA has the potential to kill ovarian cancer cells through several mechanisms. Firstly, AKBA induces DNA damage, originally hypothesised to be caused by a build-up of reactive oxygen species; but this was not the case in this project data and there is no data been published reporting that AKBA induces DNA damage by increasing ROS production up-to-date. On the other hand the results from the cell-cycle population at the sub-G1 stage and gene expression evident that AKBA induces apoptosis through the intrinsic pathway. Secondly, the transcriptomic data suggested a possible mechanism of apoptosis through the extrinsic pathway after detection, binding and internalisation of AKBA by cell-surface receptors. The multiple modes of action of AKBA against these cancer cells is a promising therapeutic trait. Additionally, the suggestion that AKBA may also be able to address cisplatin resistance to some extent is promising, for example in chemotherapy-resistant cancers (Shen et al., 2012). It might be necessary to modify the AKBA compound in a way to increase the metabolic activity of AKBA inside the human body or to increase the absorption of AKBA compound either via fat diet or direct injection to the tumour site (Kruger et al., 2008).

Despite the promising *in vitro* results, it should be noted that AKBA may not be cancer-cell specific and the cytotoxic effects of the compound might result in the death of healthy cells *in vivo* if it is been taken excessively (Xia et al., 2016). Even though this compound is been used for many years in herbal medicine, nobody knows the exact concentrations which may cause side effects in human body. Further pre-clinical studies in ovarian cancer patients should be implemented. Furthermore, the mechanism of causing DNA damage without the production of reactive oxygen species and the effect in cell metabolism instead may have some effect in health tissues (Liou and Storz, 2010). The present study tested the effect of a range of AKBA concentrations, finding that different cell lines had a different susceptibility to AKBA, as indicated by the sensitivity of A2780cis line to AKBA at low (10 μ M) concentrations.

The *in vitro* experiments performed in this study indicated that AKBA might have a cytotoxic effect in cell culture medium. Therefore, a therapeutic drug would likely be most effective if administered to the tissue surrounding a solid ovarian tumour. Because of the non-cell-specific nature of the compound, cytotoxic side effects affecting healthy

tissue are likely to be encountered if the therapy was administered orally or via injection into the bloodstream. The *in vivo* half-life of AKBA would also need to be determined before this compound could be considered for further testing in clinical trials.

6.2 Summary of the results obtained in all cell lines

6.2.1 Method of choice to assess the effect of AKBA in ovarian cancer cell line

There is a grown body of research in the different natural products, which has been used for many years as herbal medicine, and prove its effect as either a therapeutic effect or prevention for different type of diseases including cancer (Sporn MB. and N., 2000). Triterpenes are one of the biological active compounds in this field where it's been reported as major active used ingredients in traditional medicine (Fernandez-Navarro et al., 2006).

This project was carried out using four cell lines, with different characteristics. Time constraints and access to material did not permit however the testing of a suitable non-transformed cell line as a model of normal tissue.

From this project's results, the important evident clearly indicated that AKBA at certain concentrations and times effectively induces apoptosis. The work was started by testing the effect of AKBA in cell morphology using light microscope and cell growth, and cell proliferation, using a cell counter and Almar blue staining. It was concluded that AKBA was toxic to the cell and causes cell growth inhibition in a dose and time dependent manner; similar results was obtained in colorectal cancer (CRC) (Takahashi et al., 2012, Kunnumakkara et al., 2009). The study was extended to determine if this cell growth inhibition correlated with any cell cycle arrest which examined using flow cytometry using PI staining. It was evident that AKBA leads to the majority of cells to enter sub-G without noticeable cell cycle arrest, and this increased with both time points and concentrations which was similarly reported before (Noaman et al., 2009). This referred could be to the effect of AKBA in apoptosis pathway where all cells are dying. Since AKBA has been shown to inhibit topoisomerase activity (Hoernlein et al., 1999b), this may be one mechanism by which AKBA inhibits cell growth and induces apoptosis in a similar way to other anticancer therapies (Nitiss, 2009). Assessment of apoptosis from the sub-G1 cell population results was carried out using Annexin V/PI, and significantly showed that AKBA leads to early and late apoptotic in dose and time dependent manner (Toden et al., 2015). It was reported earlier that AKBA effect the mobilization of Ca^{2+}

inside the cell, which decreases its basal intracellular level (Poeckel et al., 2006). Following these findings, it was decided to study potential DNA damage formation using comet assay (Collins, 2004), to see if it has any role in AKBA-induced ovarian cancer cell death, DCFDA for ROS detection and the γ -H2AX assay as it has been demonstrated (Kinner et al., 2008) to assess any DSBs. Interestingly it was evident that AKBA causes DNA damage in a dose and time dependent manner, but without ROS production at any time point of the treatment in fact there was a reduction in ROS, which was possibly linked to the loss of the cell metabolism and DNA damage. This leads to cell death due to topoisomerase inhibition which points to the defect in DNA unwinding and repair, and ends with cell apoptosis (Hoernlein et al., 1999a, Roy et al., 2016). Apoptotic, cell cycle arrest and DNA damage protein expressions were tested using western blotting and found that cleaved caspase-3, cleaved PARP, P21 and P16 were expressed at certain time points and concentrations of AKBA. Finally, to examine in more details the mechanism of action by which AKBA leads to apoptosis, microarray gene expression technology was used.

In summary, the key points of this study are:

- **AKBA addresses resistance in cisplatin resistance cell line (A2780cis)**

Chapter 3, concluded that AKBA addresses the resistance of an established cisplatin resistant cell line. AKBA affected both the cisplatin sensitive and resistant cell line in a similar way with slightly higher sensitivity towards the cisplatin resistance cell line leading to cell death with an IC₅₀ of 21.78 μ M in A2780, compared to IC₅₀ of 18.58 μ M in A2780cis cells (fig 3.1.3). There was a significant increase in the level of DNA damage and cell apoptosis in the cisplatin resistant cell line (fig 3.4.1).

- **AKBA is cytotoxic towards both a BRCA1 mutated UWB1.289 ovarian cancer cell lines and high grade serous, OVCAR4 cell lines**

From chapter 4 it was notably significant that AKBA affected both cell lines similarly, with significant increase in the level of DNA damage and the total number of γ -H2AX foci. This may be due to the defect in the DNA repair mechanisms, which might cause the accumulations of high level of DNA damage which, leading to cell death and apoptosis through unknown mechanisms.

- **AKBA is cytotoxic towards the OVCAR4 cell line, a model cell line for high grade serous ovarian cancer**

Chapter 5, illustrates that AKBA has a major role in different pathways within the cancer cells which leads to apoptosis. From the list of genes obtained by microarray and QPCR it was very clear that AKBA has a role in DNA damage, cell cycle, metabolism and apoptosis. The possible explanation of the mechanism by which AKBA exposure leads to apoptosis may be by both the intrinsic and extrinsic pathways.

6.3 Conclusion

This project demonstrates, as with other tumour types that AKBA is worth investigating as a therapeutic agent alongside commonly used therapies for ovarian cancer and offers a proof of principle data that should be taken forward into mouse models of ovarian cancer and further translational studies in human should be consider. Despite a lot of pharmacological companies funding clinical trials research in novel anticancer agents, AKBA has not yet been assessed in human clinical trials. This lack of activity might be due to the lack of understanding in mechanistic effects of AKBA. On the other hand AKBA is an herbal medicine and consequently not patentable, which made its ability to be commercially exploited is limited. The experiments performed here add to a growing body of research into the use of naturally-produced compounds as anticancer treatments. The low toxicity and fast acting nature of AKBA suggests this compound may form the basis of a therapeutic drug to be used alongside conventional chemotherapy, although further clinical studies are required to determine compatibility with platinum-based treatments and to evaluate whether cancer cells can be resistant AKBA-mediated cell death.

6.4 Future work

Frankincense is available in the market in different forms and the correct method of administration of AKBA treatments is not been established and the most effective concentrations for different type of disease are not well known. The common ways people taken frankincense as herbal medicine and supplements is either by chew the gum resin or soak it in water over night and drink the water next day. Boswellia AKBA capsules have been available in the USA markets since 2005, as dietary supplements. Therefore, future work should serve to address three key questions:

- To address the mechanistic explanation behind the 1-5 μM and 10-15 μM threshold whereby AKBA seems to have an all or nothing induction of apoptosis. Key to this will be better understanding of the stability of the AKBA molecule in cell culture conditions. Similarly, covering a greater range of time points including 36hrs, 60hrs and 72hrs may provide a clearer picture of what is going on.
- To study in details the mechanism and the genes affected by which DNA damage is induced cell cycle arrest and cell metabolism inhibition by using full assay panel for QPCR.
- To determine whether AKBA works synergistically with other chemotherapeutic agents, to induce cell death and tumour size reduction. Most commonly utilized chemotherapeutic agents ultimately activate apoptotic pathways and cause cell death, but with unfortunate side effects and toxicities. Utilisation of optimised in-vitro methods, such as those herein presented will be an important part of addressing whether addition of AKBA to a therapeutic regimen will a) increase the efficacy of the treatment, or b) allow a lower, less toxic dose of the standard therapeutic agent(s) to be administered. It would be therefore worthwhile extending the present study to test therapeutics commonly utilized in the clinical treatment of ovarian cancer in combination with AKBA. However, the use of mice models of ovarian cancer would provide a more physiological understanding of the potential synergy between AKBA and other, commonly utilized apoptosis inducing chemotherapeutics(Ricci et al., 2013).
- Test in an ovarian cancer animal model.
- Establish preclinical *in vivo* ADME and PK studies. This is a vital first step prior to phase I clinical trial in human.
- Study the possible ways to increase the bioavailability of AKBA inside the human body.

6.5 Thesis related work:

AL-SALMANI, K. K., DON G JONES., MOSSESTHER., RAJ PATEL., BURNEY, I. A., AHMED AL-HARASSI & EVANS, M. D. Frankincense as a Potentially Novel Therapeutic Agent in Ovarian Cancer. 1-4 November 2015. (Meeting Abstract), NCRI Cancer Conference, Liverpool, A82.

AL-SALMANI, K. K., DON G JONES., BURNEY, I. A. & EVANS, M. D. The use of 3-O-acetyl-11-keto- β -boswellic acid (AKBA): Bioactive Ingredients of Omani Frankincense as a novel ovarian anticancer therapy, May 2015. (Oral presentation) international cancer conference at Sultan Qaboos University, Oman.

AL-SALMANI, K. K., DON G JONES., MOSS ESTHER., RAJ PATEL., BURNEY, I. A., & EVANS, M. D. Frankincense as a Potentially Novel Therapeutic Agent in A2780 and A2780cis Ovarian Cancer cell lines. Feb 2014. (Meeting Abstract), 27th lorne conference in Australia.

AL-SALMANI, K. K., COOKE, M. S., BURNEY, I. A. & EVANS, M. D. 2013. Evaluation of the cytotoxic effects of 3-O-acetyl-11-keto- β -boswellic acid in UWB1.289 ovarian cancer cells. *Clinical Cancer Research*, 19(Supplement), A43-A43.

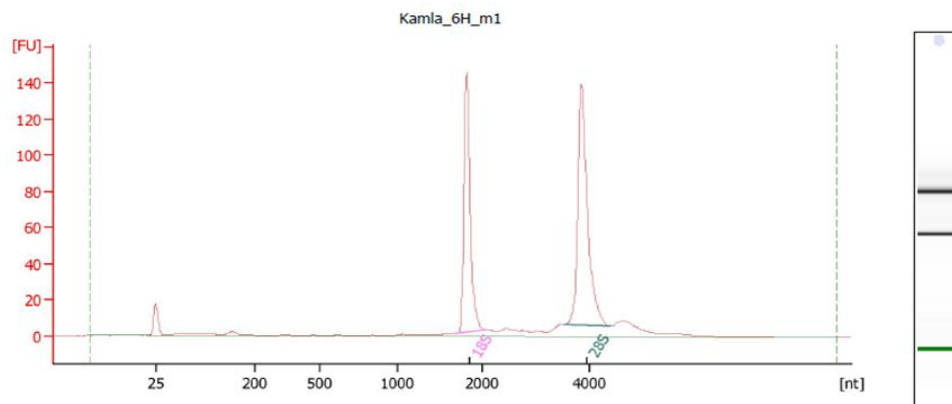
AL-SALMANI, K. K., COOKE, M. S., BURNEY, I. A. & EVANS, M. D. 2013. Examination of the cytotoxic effects of 3-O-acetyl-11-keto- β -boswellic acid in A2780 and A2780sic ovarian cancer cells. *Advances in Ovarian Cancer Research: From Concept to Clinic*, September 18-21, 2013, Miami, FL, USA

Appendix

Appendix

Microarray RNA quantifications sample examples results:

Electropherogram Summary Continued ...



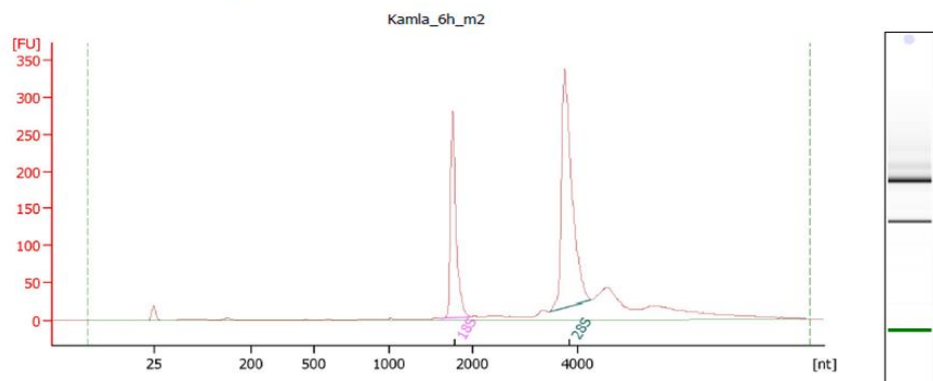
Overall Results for sample 1 : Kamla_6H_m1

RNA Area:	519.6	RNA Integrity Number (RIN):	9.9 (B.02.07)
RNA Concentration:	200 ng/μl	Result Flagging Color:	
rRNA Ratio [28s / 18s]:	1.2	Result Flagging Label:	RIN: 9.90

Fragment table for sample 1 : Kamla_6H_m1

Name	Start Size [nt]	End Size [nt]	Area	% of total Area
18S	1,665	2,071	154.5	29.7
28S	3,519	4,390	189.6	36.5

Electropherogram Summary Continued ...



Overall Results for sample 2 : Kamla_6h_m2

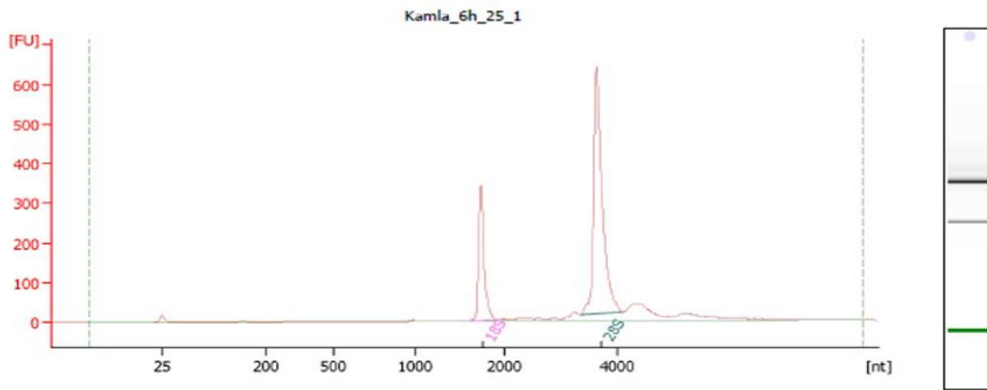
RNA Area:	1,283.3	RNA Integrity Number (RIN):	10 (B.02.07)
RNA Concentration:	495 ng/μl	Result Flagging Color:	
rRNA Ratio [28s / 18s]:	1.8	Result Flagging Label:	RIN:10

Fragment table for sample 2 : Kamla_6h_m2

Name	Start Size [nt]	End Size [nt]	Area	% of total Area
18S	1,601	1,977	278.4	21.7
28S	3,455	4,250	495.2	38.6

Figure 7. 1 RNA concentrations and purity for the control samples 1&2 using Nano DE 72901367

Electropherogram Summary Continued ...



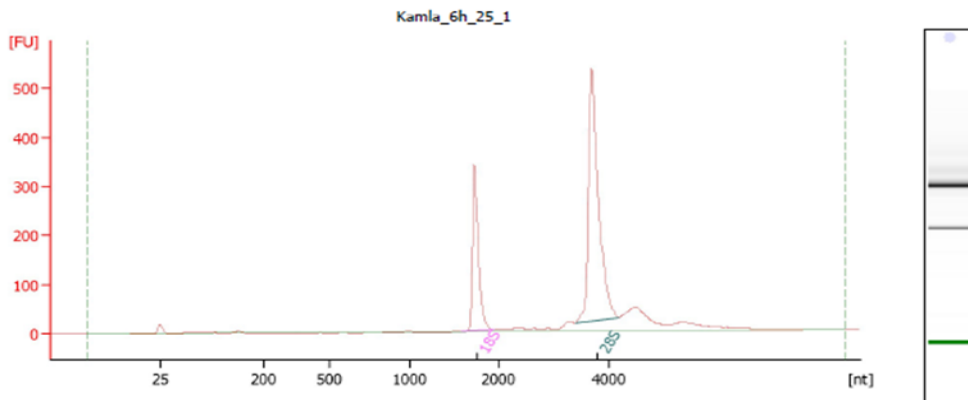
Overall Results for sample 8 : Kamla_6h_25_1

RNA Area: 1,540.9 RNA Integrity Number (RIN): 10 (B.02.07)
 RNA Concentration: 594 ng/µl Result Flagging Color:
 rRNA Ratio [28s / 18s]: 2.4 Result Flagging Label: RIN:10

Fragment table for sample 8 : Kamla_6h_25_1

Name	Start Size [nt]	End Size [nt]	Area	% of total Area
18S	1,578	1,927	328.4	21.3
28S	3,327	4,104	771.8	50.1

Electropherogram Summary Continued ...



Overall Results for sample 7 : Kamla_6h_25_1

RNA Area: 1,549.0 RNA Integrity Number (RIN): 10 (B.02.07)
 RNA Concentration: 597 ng/µl Result Flagging Color:
 rRNA Ratio [28s / 18s]: 2.2 Result Flagging Label: RIN:10

Fragment table for sample 7 : Kamla_6h_25_1

Name	Start Size [nt]	End Size [nt]	Area	% of total Area
18S	1,581	1,954	335.2	21.6
28S	3,407	4,195	733.2	47.3

Figure 7. 2 RNA concentrations and purity for the 6 h treatment with 25 µM samples 1&2 using Nano DE 72901367

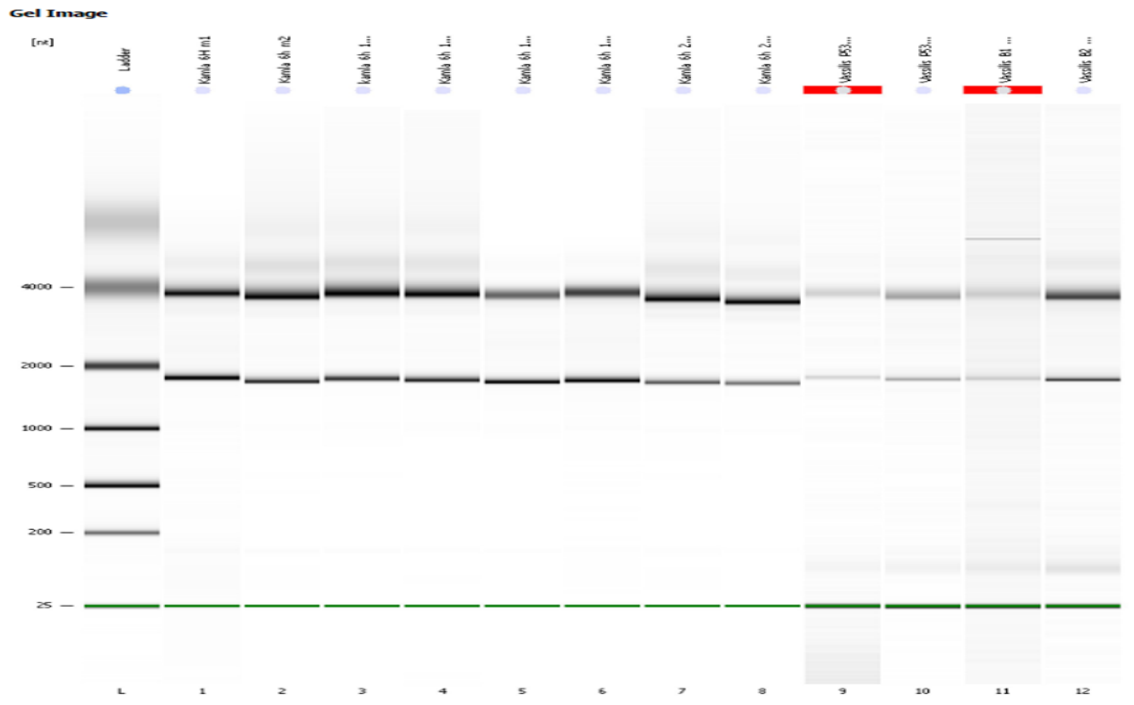


Figure 7. 3 Gel image with Total RNA concentrations using Nano DE 72901367

Standard Curve

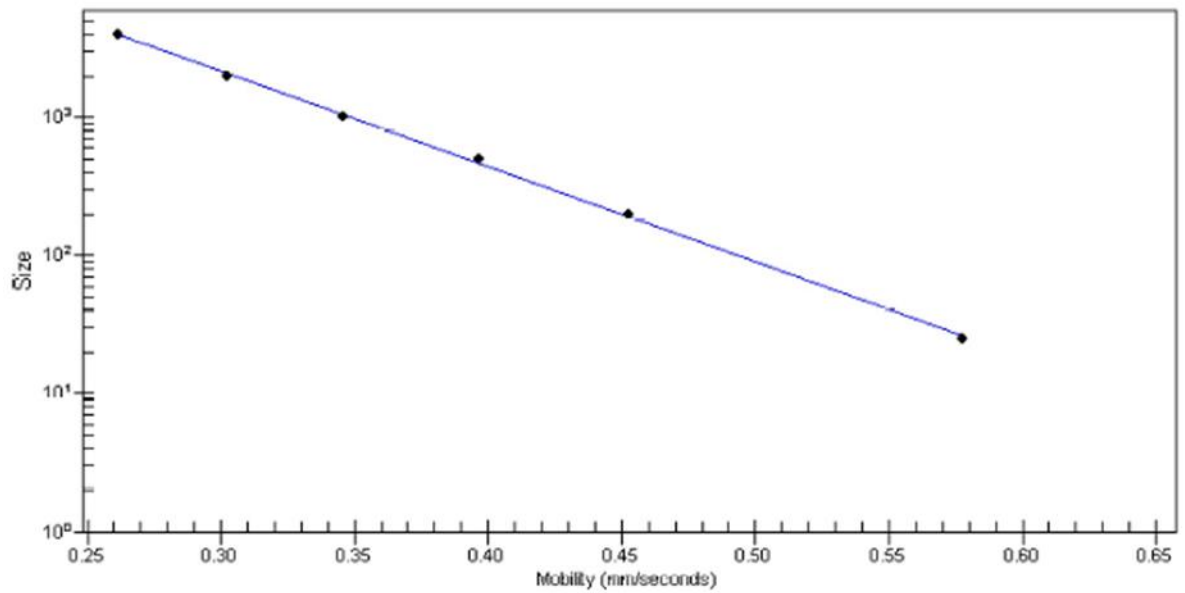


Figure 7. 4 Gel image with Total RNA concentrations using Nano DE 72901367

References

- ABDEL-TAWAB, M., WERZ, O. & SCHUBERT-ZSILAVECZ, M. 2011. Boswellia serrata an overall assessment of in vitro preclinical, pharmacokinetic and clinical data. *Clin Pharmacokinet*, 50, 349-69.
- ABOU-NASSAR, K. & BROWN, J. R. 2010. Novel agents for the treatment of chronic lymphocytic leukaemia. *Clin Adv Haematol Oncol*, 8.
- AGARWAL, A., TRESSEL, S. L., KAIMAL, R., BALLA, M., LAM, F. H., COVIC, L. & KULIOPULOS, A. 2010. Identification of a metalloprotease-chemokine signaling system in the ovarian cancer microenvironment: implications for antiangiogenic therapy. *Cancer Res*, 70, 5880-90.
- AL-SALMANI, K. K., COOKE, M. S., BURNEY, I. A. & EVANS, M. D. 2013. Evaluation of the cytotoxic effects of 3-O-acetyl-11-keto- β -boswellic acid in ovarian cancer cells. *Clinical Cancer Research*, 19(Supplement), A43-A43.
- AL-SALMI, S. 2006. Al Tasamoh book; The frankincense trading and the communications in Middle East. *sultan Qaboos university library*, 1, 248-254.
- ALAM, M., KHAN, H., SAMIULLAH, L. & SIDDIQUE, K. M. 2012. A review on Phytochemical and Pharmacological studies of Kundur (Boswellia serrata Roxb ex Colebr.)-A Unani drug. *Journal of Applied Pharmaceutical Science*, 2, 148-156.
- ALI, E. N. & MANSOUR, S. Z. 2011. Boswellic acids extract attenuates pulmonary fibrosis induced by bleomycin and oxidative stress from gamma irradiation in rats. *Chin Med*, 6, 36.
- ALTMANN, A., POECKEL, D., FISCHER, L., SCHUBERT-ZSILAVECZ, M., STEINHILBER, D. & WERZ, O. 2004. Coupling of boswellic acid-induced Ca²⁺ mobilisation and MAPK activation to lipid metabolism and peroxide formation in human leucocytes. *Br J Pharmacol*, 141, 223-32.
- AMMON P. 2006. Boswillic Acid in Chronic Inflammatory Diseases. *Planta Med* 1-17.
- ANDOTRA, S. S., HAMID, A., MONDHE, D. M., QURISHI, Y., SAXENA, A. K., SHAH, B. A., SHARMA, P. R., SINGH, S. K., TANEJA, S. C., WANI, Z. A. & ZARGAR, M. A. 2012. PARP cleavage and perturbation in mitochondrial membrane potential by 3-[α]-propionyloxy- β -boswellic acid results in

cancer cell death and tumor regression in murine models. *Future Oncology*, 8, 867+.

ARMSTRONG, D. K., BUNDY, B., WENZEL, L., HUANG, H. Q., BAERGEN, R., LELE, S., COPELAND, L. J., WALKER, J. L. & BURGER, R. A. 2006. Intraperitoneal cisplatin and paclitaxel in ovarian cancer. *N Engl J Med*, 354, 34-43.

ASHKENAZI, A. 2008. Targeting the extrinsic apoptosis pathway in cancer. *Cytokine and Growth Factor Reviews*, 19, 325-331.

AUDEH, M. W., CARMICHAEL, J., PENSON, R. T., FRIEDLANDER, M., POWELL, B., BELL-MCGUINN, K. M. & TUTT, A. 2010. Oral poly (ADP-ribose) polymerase inhibitor olaparib in patients with BRCA1 or BRCA2 mutations and recurrent ovarian cancer: a proof-of-concept trial. *The Lancet*, 376, 245-251.

BADRIA, F. A. 2015. Frankincense (Heaven's Gift) — Chemistry, Biology, and Clinical Applications.

BADRIA, F. A., ABU-KARAM, M., MIKHAEL, B. R., MAATOOQ, G. T. & AMER, M. M. 2003b. Anti-Herps Activity of isolated compounds from Frankincense. *Biosciences. Biotechnology Research Asia*, 1, 1-10.

BADRIA, F. A., HOUSSEN, W. E., EL-NASHAR, E. M. & SAAED, S. A. 2003a. Effect of glycyrrhizin and *Boswellia carterii* extract on liver injury: Biochemical and histopathological evaluation of glycyrrhizin and *Boswellia carterii* extract on rat liver injury. *Biosciences, Biotechnology Research Asia*, 1, 93-96.

BAE, I., FAN, S., MENG, Q., RIH, J. K., KIM, H. J., KANG, H. J., XU, J., GOLDBERG, I. D., JAISWAL, A. K. & ROSEN, E. M. 2004. BRCA1 induces antioxidant gene expression and resistance to oxidative stress. *Cancer Res*, 64, 7893-7909.

BARRETINA, J., CAPONIGRO, G., STRANSKY, N., VENKATESAN, K., MARGOLIN, A. A., KIM, S., WILSON, C. J., LEHAR, J., KRYUKOV, G. V., SONKIN, D., REDDY, A., LIU, M., MURRAY, L., BERGER, M. F., MONAHAN, J. E., MORAIS, P., MELTZER, J., KOREJWA, A., JANEVALBUENA, J., MAPA, F. A., THIBAUT, J., BRIC-FURLONG, E., RAMAN, P., SHIPWAY, A., ENGELS, I. H., CHENG, J., YU, G. K., YU, J., ASPESI, P., JR., DE SILVA, M., JAGTAP, K., JONES, M. D., WANG, L., HATTON, C., PALESCANDOLO, E., GUPTA, S., MAHAN, S., SOUGNEZ, C., ONOFRIO, R. C., LIEFELD, T., MACCONAILL, L., WINCKLER, W., REICH, M., LI, N., MESIROV, J. P., GABRIEL, S. B., GETZ, G., ARDLIE, K., CHAN, V., MYER,

- V. E., WEBER, B. L., PORTER, J., WARMUTH, M., FINAN, P., HARRIS, J. L., MEYERSON, M., GOLUB, T. R., MORRISSEY, M. P., SELLERS, W. R., SCHLEGEL, R. & GARRAWAY, L. A. 2012. The Cancer Cell Line Encyclopedia enables predictive modelling of anticancer drug sensitivity. *Nature*, 483, 603-7.
- BEAUFORT, C. M., HELMIJR, J. C., PISKORZ, A. M., HOOGSTRAAT, M., RUIGROK-RITSTIER, K., BESSELINK, N., MURTAZA, M., VAN, I. W. F., HEINE, A. A., SMID, M., KOUDIJS, M. J., BRENTON, J. D., BERNS, E. M. & HELLEMAN, J. 2014. Ovarian cancer cell line panel (OCCP): clinical importance of in vitro morphological subtypes. *PLoS One*, 9, e103988.
- BEHBAKHT, K., SILL, M. W., DARCY, K. M., RUBIN, S. C., MANNEL, R. S., WAGGONER, S., SCHILDER, R. J., CAI, K. Q., GODWIN, A. K. & ALPAUGH, R. K. 2011. Phase II trial of the mTOR inhibitor, temsirolimus and evaluation of circulating tumor cells and tumor biomarkers in persistent and recurrent epithelial ovarian and primary peritoneal malignancies: a Gynecologic Oncology Group study. *Gynecol Oncol*, 123, 19-26.
- BELL 2011. Integrated genomic analyses of ovarian carcinoma. *Nature*, 474, 609-15.
- BEN SAHRA, I., LE MARCHAND-BRUSTEL, Y., TANTI, J.-F. & BOST, F. 2010. Metformin in Cancer Therapy: A New Perspective for an Old Antidiabetic Drug? *Molecular Cancer Therapeutics*, 9, 1092-1099.
- BERNS, E. M. & BOWTELL, D. D. 2012. The changing view of high-grade serous ovarian cancer. *Cancer Res*, 72, 2701-4.
- BHUSHAN, S., KAKKAR, V., PAL, H. C., GURU, S. K., KUMAR, A., MONDHE, D. M., SHARMA, P. R., TANEJA, S. C., KAUR, I. P., SINGH, J. & A.K., S. 2013. Enhanced anticancer potential of encapsulated Solid Lipid Nanoparticles of TPD: a Novel triterpenediol from *Boswellia serrata*. *Mol. Pharm*, 10, 225–235.
- BONE, K. 2006. Does boswellia have a role in cancer therapy? *MediHerb*, 100, 1 – 2.
- BRATTON, S. B. & SALVESEN, G. S. 2010. Regulation of the Apaf-1–caspase-9 apoptosome *Journal of Cell Science*, 123, 3209-3214.
- BÜCHELE, B. & SIMMET, T. 2003. Analysis of 12 different pentacyclic triterpenic acids from frankincense in human plasma by high-performance liquid chromatography and photodiode array detection. *J Chromatogr B Analyt Technol Biomed Life Sci*, 795, 355-62.

- BUCHHOLZ, T. A., WEIL, M. M., STORY, M. D., STROM, E. A., BROCK, W. A. & MCNEESE, M. D. 1999. Tumor suppressor genes and breast cancer. *Radiat Oncol Investig*, 7, 55-65.
- BURLANDO, B., PARODI, A., VOLANTE, A. & BASSI, A. M. 2008 Comparison of the irritation potentials of Boswellia serrata gum resin and of acetyl-11-keto- β -boswellic acid by in vitro cytotoxicity tests on human skin-derived cell lines. . *Toxicology Letters* 177, 144-149.
- BUSH, J. A., CHEUNG, K. J., JR. & LI, G. 2001. Curcumin induces apoptosis in human melanoma cells through a Fas receptor/caspase-8 pathway independent of p53. *Exp Cell Res*, 271, 305-14.
- CANCER RESEARCH UK. 2012. Ovarian cancer survival statistics [Online]. Available: <http://www.cancerresearchuk.org/cancer-info/cancerstats/types/ovary/survival/ovarian-cancer-survival-statistics#By4>.
- CANCER RESEARCH UK. 2013. Ovarian cancer statistics. Available: <http://www.cancerresearchuk.org/cancer-info/cancerstats/types/ovary/>
- CANNISTRA, S. A. 2004. Cancer of the Ovary *N Eng J Med*, 351, 2519-2529.
- CARUSO, R., WARNER, N., INOHARA, N. & NÚÑEZ, G. 2014. NOD1 and NOD2: Signaling, Host Defense, and Inflammatory Disease. *Immunity*, 41, 898-908.
- CHAITANYA, G. V., ALEXANDER, J. S. & BABU, P. P. 2010. PARP-1 cleavage fragments: signatures of cell-death proteases in neurodegeneration. *Cell Communication and Signaling : CCS*, 831-31.
- CHASHOO, G., SINGH, S. K., SHARMA, P. R., MONDHE, D. M., HAMID, A., SAXENA, A., ANDOTRA, S. S., SHAH, B. A., QAZI, N. A., TANEJA, S. C. & AXENA, A. K. 2011. A propionyloxy derivative of 11-keto-beta-boswellic acid induces apoptosis in HL-60 cells mediated through topoisomerase I & II inhibition. *Chem Biol Interact*, 189, 60-71.
- CHEUNG, H. W., GLENN S. COWLEY., BARBARA A. WEIRB., JESSE S. BOEHMB., SCOTT RUSINB., JUSTINE A. SCOTTB., ALEXANDRA EASTB., LEVI D. ALIB., PATRICK H. LIZOTTEB., TERENCE C. WONGB., GUOZHI JIANGB., JESSICA HSIAOB., CRAIG H. MERMELA., GAD GETZB., JORDI BARRETINAA., SHUBA GOPALB., PABLO TAMAYOB., JOSHUA GOULDB., AVIAD TSHERNIAKB., NICOLAS STRANSKYB., BIAO LUOB., YIN REND., RONNY DRAPKINE., SANGEETA N. BHATIAB., JILL P. MESIROVB., LEVI A. GARRAWAYA., MATTHEW

- MEYERSONA., ERIC S. LANDERB., DAVID E. ROOTB. & WILLIAM C. HAHNA. 2011. Systematic investigation of genetic vulnerabilities across cancer cell lines reveals lineage-specific dependencies in ovarian cancer. *PNAS*, 108, 12372–12377.
- CHIVUKULA, M., NIEMEIER, L. A., EDWARDS, R., NIKIFOROVA, M., MANTHA, G., MCMANUS, K. & CARTER, G. 2011. Carcinomas of Distal Fallopian Tube and Their Association with Tubal Intraepithelial Carcinoma: Do They Share a Common "Precursor" Lesion? Loss of Heterozygosity and Immunohistochemical Analysis Using PAX 2, WT-1, and P53 Markers. *ISRN Obstet Gynecol*, 2011, 858647.
- CIOFFI, M., D'ALTERIO, C., CAMERLINGO, R., TIRINO, V., CONSALES, C., RICCIO, A., IERANO, C., CECERE, S. C., LOSITO, N. S., GREGGI, S., PIGNATA, S., PIROZZI, G. & SCALA, S. 2015. Identification of a distinct population of CD133(+)CXCR4(+) cancer stem cells in ovarian cancer. *Sci Rep*, 5, 10357.
- COLEMAN, M. P., FORMAN, D., BRYANT, H., BUTLER, J., RACHET, B., MARINGE, C., NUR, U., TRACEY, E., COORY, M., HATCHER, J., MCGAHAN, C. E., TURNER, D., MARRETT, L., GJERSTORFF, M. L., JOHANNESSEN, T. B., ADOLFSSON, J., LAMBE, M., LAWRENCE, G., MEECHAN, D., MORRIS, E. J., MIDDLETON, R., STEWARD, J. & RICHARDS, M. A. 2011. Cancer survival in Australia, Canada, Denmark, Norway, Sweden, and the UK, 1995-2007 (the International Cancer Benchmarking Partnership): an analysis of population-based cancer registry data. *Lancet*, 377, 127-38.
- COLLINS, A. 2002. The comet assay. Principles, applications, and limitations. . *Methods in Molecular Biology (Clifton, NJ)*, 203, 163.
- COLLINS, A. R. 2004. The Comet Assay for DNA Damage and Repair: Principles, Applications, and Limitations. *Molecular Biotechnology*, 26, 249–261.
- COTTON, S. 2014. What actually is in frankincense and myrrh? *Scientific American*.
- CROW, D. 2004. Frankincense *Yogi Times*.
- CULLEN, S. P. & MARTIN, S. J. 2009. Caspase activation pathways: some recent progress. *Cell Death Differ*, 16, 935-938.

- D'ANDRILLI, G., KUMAR, C., SCAMBIA, G. & GIORDANO, A. 2004. Cell cycle genes in ovarian cancer: steps toward earlier diagnosis and novel therapies. *Clin Cancer Res*, 10, 8132-41.
- DEANS, A. J. & WEST, S. C. 2011. DNA interstrand crosslink repair and cancer. *Nat Rev Cancer*, 11, 467-80.
- DECANIO, F. 2012. Analysis and synthesis of Exodus. *Bible.org*.
- DELLORUSSO, C., WELCSH, P. L., WANG, W., GARCIA, R. L., KING, M. C. & SWISHER, E. M. 2007. Functional characterization of a novel BRCA1-null ovarian cancer cell line in response to ionizing radiation. *Mol Cancer Res*, 5, 35-45.
- DELMAS, D., REBE, C., LACOUR, S., FILOMENKO, R., ATHIAS, A., GAMBERT, P., CHERKAOU-MALKI, M., JANNIN, B., DUBREZ-DALOZ, L., LATRUFFE, N. & SOLARY, E. 2003. Resveratrol-induced apoptosis is associated with Fas redistribution in the rafts and the formation of a death-inducing signaling complex in colon cancer cells. *J Biol Chem*, 278, 41482-90.
- DENG, C. X. 2003. Roles of BRCA1 in DNA damage repair: a link between development and cancer. *Human Molecular Genetics*, 12, 113R-123.
- DHARMANANDA, S. 2003. Myrrh and frankincense. *ITM Internet Journal*.
- DOMCKE, S., SINHA, R., LEVINE, D. A., SANDER, C. & SCHULTZ, N. 2013. Evaluating cell lines as tumour models by comparison of genomic profiles. *Nat Commun*, 4, 2126.
- DRIESENS, N., VERSTEYHE, S., GHADDHAB, C., BURNIAT, A., DE DEKEN, X., VAN SANDE, J., DUMONT, J. E., MIOT, F. & CORVILAIN, B. 2009. Hydrogen peroxide induces DNA single- and double-strand breaks in thyroid cells and is therefore a potential mutagen for this organ. *Endocr Relat Cancer*, 16, 845-856.
- DU BOIS, A., FLOQUET, A., KIM, J. W., RAU, J., DEL CAMPO, J. M., FRIEDLANDER, M., PIGNATA, S., FUJIWARA, K., VERGOTE, I., COLOMBO, N., MIRZA, M. R., MONK, B. J., KIMMIG, R., RAY-COQUARD, I., ZANG, R., DIAZ-PADILLA, I., BAUMANN, K. H., MOURET-REYNIER, M. A., KIM, J. H., KURZEDER, C., LESOIN, A., VASEY, P., MARTH, C., CANZLER, U., SCAMBIA, G., SHIMADA, M., CALVERT, P., PUJADE-LAURINE, E., KIM, B. G., HERZOG, T. J., MITRICA, I., SCHADEBRITTINGER, C., WANG, Q., CRESCENZO, R. & HARTER, P. 2014.

- Incorporation of pazopanib in maintenance therapy of ovarian cancer. *J Clin Oncol*, 32, 3374-3382.
- DUTTO, I., TILLHON, M., CAZZALINI, O., STIVALA, L. A. & PROSPERI, E. 2015. Biology of the cell cycle inhibitor p21(CDKN1A): molecular mechanisms and relevance in chemical toxicology. *Arch Toxicol*, 89, 155-178.
- ECKSTEIN, N., SERVAN, K., HILDEBRANDT, B., POLITZ, A., VON JONQUIERES, G., WOLF-KUMMETH, S., NAPIERSKI, I., HAMACHER, A., KASSACK, M. U., BUDCZIES, J., BEIER, M., DIETEL, M., ROYER-POKORA, B., DENKERT, C. & ROYER, H. D. 2009. Hyperactivation of the insulin-like growth factor receptor I signaling pathway is an essential event for cisplatin resistance of ovarian cancer cells. *Cancer Res*, 69, 2996-3003.
- EL-DEIRY, W. S. 2016. p21(WAF1) Mediates Cell-Cycle Inhibition, Relevant to Cancer Suppression and Therapy. *Cancer Res*, 76, 5189-91.
- ELMORE, S. W. 2007. Apoptosis: a review of programmed cell death. *Toxicol Pathol*, 35, 495-516.
- ERUSLANOV, E. & KUSMARTSEV, S. 2010. Identification of ROS using oxidized DCFDA and flow-cytometry. *Advanced Protocols in Oxidative Stress II. Springer*, 57-72.
- ETEMADMOGHADAM, D., DEFAZIO, A., BEROUKHIM, R., MERMEL, C., GEORGE, J., GETZ, G., TOTHILL, R., OKAMOTO, A., RAEDER, M. B., HARNETT, P., LADE, S., AKSLEN, L. A., TINKER, A. V., LOCANDRO, B., ALSOP, K., CHIEW, Y. E., TRAFICANTE, N., FEREDAY, S., JOHNSON, D., FOX, S., SELLERS, W., URASHIMA, M., SALVESEN, H. B., MEYERSON, M. & BOWTELL, D. 2009. Integrated genome-wide DNA copy number and expression analysis identifies distinct mechanisms of primary chemoresistance in ovarian carcinomas. *Clin Cancer Res*, 15, 1417-27.
- EVERSHED, R. P., VAN BERGEN, P. F., PEAKMAN, T. M., LEIGH-FIRBANK, E. C., HORTON, M. C., EDWARDS, D. & ROWLEY-CONWAY, P. A. 1997. Archaeological frankincense. *Nature*, 390, 667-668.
- F., B., EL-FARAHATY., A., S., S., H. & M.F., E.-B. 2004. Boswellia-curcumin Ppation for treating knee osteoarthritis: A clinical evaluation. *Alternative and Complementary Therapy*, 8, 341-8.
- FARLEY, J., BRADY, W. E., VATHIPADIEKAL, V., LANKES, H. A., COLEMAN, R., MORGAN, M. A., MANNEL, R., YAMADA, S. D., MUTCH, D.,

- RODGERS, W. H., BIRRER, M. & GERSHENSON, D. M. 2012. Selumetinib in women with recurrent low-grade serous carcinoma of the ovary or peritoneum: an open-label, single-arm, phase 2 study. *Lancet Oncol*, 14, 134-40.
- FAVALORO, B., ALLOCATI, N., GRAZIANO, V., DI ILIO, C. & DE LAURENZI, V. 2012. Role of Apoptosis in disease. *AGING*, 4, 330-349.
- FERNANDEZ-NAVARRO, M., PERAGON, J., ESTEBAN, F., DE LA HIGUERA, M. & LUPIANEZ, J. 2006. Maslinic acid as a feed additive to stimulate growth and hepatic protein-turnover rates in rainbow trout (*Onchorhynchus mykiss*). *Comp Biochem Physiol C Toxicol Pharmacol*, 144, 130-140.
- FIASCHI-TAESCH, N., BIGATEL, T. A., SICARI, B., TAKANE, K. K., SALIM, F., VELAZQUEZ-GARCIA, S., HARB, G., SELK, K., COZAR-CASTELLANO, I., & STEWART, A. F. 2010. Survey of the Human Pancreatic β -Cell G1/S Proteome Reveals a Potential Therapeutic Role for Cdk-6 and Cyclin D in Enhancing Human β -Cell Replication and Function In Vivo. *Diabetes*, 58, 882-893.
- FLEMING, J. S., BEAUGIE, C. R., HAVIV, I., CHENEVIX-TRENCH, G. & TAN, O. L. 2006. Incessant ovulation, inflammation and epithelial ovarian carcinogenesis: revisiting old hypotheses. *Mol Cell Endocrinol*, 247, 4-21.
- FONG, M. Y., MCDUNN, J. & KAKAR, S. S. 2011. Identification of metabolites in the normal ovary and their transformation in primary and metastatic ovarian cancer. *PLoS One*, 6, e19963.
- FONG, P. C., BOSS, D. S., YAP, T. A., TUTT, A., WU, P., MERGUI-ROELVINK, M., MORTIMER, P., SWAISLAND, H., LAU, A., O'CONNOR, M. J., ASHWORTH, A., CARMICHAEL, J., KAYE, S. B., SCHELLENS, J. H. & DE BONO, J. S. 2009. Inhibition of poly(ADP-ribose) polymerase in tumors from BRCA mutation carriers. *N Engl J Med*, 361, 123-34.
- FONG, P. C., YAP, T. A., BOSS, D. S., CARDEN, C. P., MERGUI-ROELVINK, M., GOURLEY, C., DE GREVE, J., LUBINSKI, J., SHANLEY, S., MESSIOU, C., A'HERN, R., TUTT, A., ASHWORTH, A., STONE, J., CARMICHAEL, J., SCHELLENS, J. H., DE BONO, J. S. & KAYE, S. B. 2010. Poly(ADP)-ribose polymerase inhibition: frequent durable responses in BRCA carrier ovarian cancer correlating with platinum-free interval. *J Clin Oncol*, 28, 2512-9.
- FRANK, A. & UNGER, M. 2006. Analysis of frankincense from various *Boswellia* species with inhibitory activity on human drug metabolising cytochrome P450

- enzymes using liquid chromatography mass spectrometry after automated on-line extraction. *J Chromatogr A*, 1112, 255-62.
- FRANK, M. B., YANG, Q., OSBAN, J., AZZARELLO, J. T., SABAN, M. R., SABAN, R., ASHLEY, R. A., WELTER, J. C., FUNG, K. M. & LIN, H. K. 2009. Frankincense oil derived from *Boswellia carteri* induces tumor cell specific cytotoxicity. *BMC Complement Altern Med*, 9, 6.
- FUNK, C. D., HOSHIKO, S., MATSUMOTO, T., RDMARK, O. & SAMUELSSON, B. 1989. Characterization of the human 5-lipoxygenase gene. *Proceedings of the National Academy of Sciences*, 86, 2587-2591.
- GARAJ-VRHOVAC, V. & KOPJAR, N. 2003. The alkaline Comet assay as biomarker in assessment of DNA damage in medical personnel occupationally exposed to ionizing radiation. *Mutagenesis*, 18, 265-271.
- GEBREHIWOT, K., MUYS, B., HAILE, M. & MITLOEHNER, R. 2003. Introducing *Boswellia papyrifera* (Del.) Hochst and its non-timber forest product, frankincense *International Forestry Review*, , 5, 348-353.
- GERHARDT, H., SEIFERT, F., BUVARI, P., VOGELANG, H. & REPGES, R. 2001. Therapy of active Crohn disease with *Boswellia serrata* extract H15Z. *Gastroenterology*, 39, 11-17.
- GERL, R. & VAUX, D. L. 2005. Apoptosis in the development and treatment of cancer. *Carcinogenesis*, 26, 263-70.
- GLASER, T., WINTER, S., GROSCURTH, P., SAFAYHI, H., SAILER, E. R., AMMON, H. P., SCHABET, M. & WELLER, M. 1999. Boswellic acids and malignant glioma: induction of apoptosis but no modulation of drug sensitivity. *Br J Cancer*, 80, 756-65.
- GODWIN, A. K., MEISTER, A., O'DWYER, P. J., HUANG, C. S., HAMILTON, T. C. & ANDERSON, M. E. 1992. High resistance to cisplatin in human ovarian cancer cell lines is associated with marked increase of glutathione synthesis. *Proc Natl Acad Sci U S A*, 89, 3070-3074.
- GORE, M. E., FRYATT, I., WILTSHAW E., DAWSON T., ROBINSON B.A. & CALVERT A.H. 1989. Cisplatin /carboplatin cross-resistance in ovarian cancer. *Br. J. Cancer*, 60, 767-769.
- GORRINI, C., HARRIS, I. S. & MAK, T. W. 2013. Modulation of oxidative stress as an anticancer strategy. *Nat Rev Drug Discov*, 12, 931-947.
- GREEN, D. R. 2005. Apoptotic pathways: ten minutes to dead. *Cell*, 121, 671-4.

- GRIEVE, M. 2014. A modern herbal: Frankincense. Botanical.com.
- GUPTA, I., GUPTA, V., PARIHAR, A., GUPTA, S., LUDTKE, R., SAFAYHI, H. & AMMON, H. P. 1998. Effects of *Boswellia serrata* gum resin in patients with bronchial asthma: results of a double-blind, placebo-controlled, 6-week clinical study. *Eur J Med Res*, 3, 511-4.
- GUPTA, I., PARIHAR, A., MALHOTRA, P., SINGH, G. B., LUDTKE, R., SAFAYHI, H. & AMMON, H. P. 1997. Effects of *Boswellia serrata* gum resin in patients with ulcerative colitis. *Eur J Med Res*, 2, 37-43.
- HAKIM, A. A., BARRY, C. P., BARNES, H. J., ANDERSON, K. E., PETITTE, J., WHITAKER, R., LANCASTER, J. M., WENHAM, R. M., CARVER, D. K., TURBOV, J., BERCHUCK, A., KOPELOVICH, L. & RODRIGUEZ, G. C. 2009. Ovarian adenocarcinomas in the laying hen and women share similar alterations in p53, ras, and HER-2/neu. *Cancer Prev Res (Phila)*, 2, 114-21.
- HAMIDPOUR, R., HAMIDPOUR, S., HAMIDPOUR, M. & HAMIDPOUR, R. 2016. frankincense (*boswellia* species): the novel phytotherapy for drug targeting in cancer. *Archives in Cancer Research*, 4 1-5.
- HAMIDPOUR, R., HAMIDPOUR, S., HAMIDPOUR, M. & SHAHLARI, M. 2013. Frankincense (ru xiang; *boswellia* species): from the selection of traditional applications to the novel phytotherapy for the prevention and treatment of serious diseases. *J Tradit Complement Med*, 3, 221-6.
- HAMILTON, T. C., YOUNG, R. C. & OZOLS, R. F. 1984. Experimental model systems of ovarian cancer: application to the design and evaluation of new treatment approaches. *Seminars in Oncology*, 11285-11298.
- HANAHAN, D. & WEINBERG, R. A. 2000. The Hallmarks Of Cancer. *Cell Cycle*, 100, 57-70.
- HANDE, K. R. 1998. Etoposide: four decades of development of a topoisomerase II inhibitor. *Eur J Cancer*, 34, 1514-1521.
- HANNAFORD, P., C., SELVARAJ, S., ELLIOT, A., M., ANGUS, V., IVERSEN, L. & LEE, A. 2007. Cancer risk among users of oral contraceptives: cohort data from the Royal College of General Practitioner's oral contraception study. *BMJ*, 335, 651-658.
- HEARN, J. M., ROMERO-CANELON, I., MUNRO, A. F., FU, Y., PIZARRO, A. M., GARNETT, M. J., MCDERMOTT, U., CARRAGHER, N. O. & SADLER, P. J.

2015. Potent organo-osmium compound shifts metabolism in epithelial ovarian cancer cells. *Proc Natl Acad Sci U S A*, 112, E3800-5.
- HENKEL, A. 2011. Novel Molecular Targets of Boswellic Acids and Characterization of Bioactive Ingredients of Frankincense. PhD, . *Eberhard Karls University of Tübingen*.
- HENKELS, K. M. & TURCHI, J. J. 1997. Induction of apoptosis in cisplatin-sensitive and -resistant human ovarian cancer cell lines. *Cancer Res*, 57, 4488-92.
- HERCEG, Z., WANG, ZHAO-QI., 2001. Functions of poly(ADP-ribose) polymerase (PARP) in DNA repair, genomic integrity and cell death. *Mutation Research*, 477, 97–110.
- HOERNLEIN, R. F., ORLIKOWSKY, T., ZEHRER, C., NIETHAMMER, D., SAILER, E., SIMMET, T., DANNECKER, G. & AMMON, H. 1999a Acetyl-11-Keto-b-Boswellic Acid Induces Apoptosis in HL-60 and CCRF-CEM Cells and Inhibits Topoisomerase I. *The American Society for Pharmacology and Experimental Therapeutics*, 288(2), 613-9.
- HONGMEI, Z. 2012. Extrinsic and Intrinsic Apoptosis Signal Pathway Review.
- HOSTANSKA, K., DAUM, G. & SALLER, R. 2002. Cytostatic and apoptosis-inducing activity of boswellic acids toward malignant cell lines in vitro. *Anticancer Research*, 22, 2853-62.
- HUANG, L. C., CLARKIN, K. C. & WAHL, G. M. 1996. Sensitivity and selectivity of the DNA damage sensor responsible for activating p53-dependent G1 arrest. *Proc Natl Acad Sci U S A*, 93, 4827-4832.
- HUI LM., ZHAO GD. & JJ., Z. 2015. δ -Cadinene inhibits the growth of ovarian cancer cells via caspase-dependent apoptosis and cell cycle arrest. *Int J Clin Exp Pathol*, 8, 6046-6056.
- HUNN, J. & RODRIGUEZ, G. C. 2012. Ovarian cancer: etiology, risk factors, and epidemiology. *Clin Obstet Gynecol*, 55, 3-23.
- JACKSON-BERNITSAS, D. G., ICHIKAWA, H., TAKADA, Y., MYERS, J. N., LIN, X. L., DARNAY, B. G., CHATURVEDI, M. M. & AGGARWAL, B. B. 2006. Evidence that TNF-TNFR1-TRADD-TRAF2-RIP-TAK1-IKK pathway mediates constitutive NF-[kappa]B activation and proliferation in human head and neck squamous cell carcinoma. *Oncogene*, 26, 1385-1397.
- JAYSON, G. C., KOHN, E. C., KITCHENER, H. C. & LEDERMANN, J. A. 2014. Ovarian cancer. *Lancet*, 384, 1376-88.

- JEMAL A, SIEGEL R & AL., X. J. E. 2010. Cancer statistics 2010. *CA Cancer J Clin*, 60, 277-300.
- JING, Y., XIA, L. & HAN, R. 1992. Growth inhibition and differentiation of promyelocytic cells (HL-60) induced by BC-4, an active principle from *Boswellia carterii* Birdw. *Chin Med Sci J*, 7, 12-15.
- KALAYDA, G. V. & JAEHDE, U. 2008. Altered localisation of the copper efflux transporters ATP7A and ATP7B associated with cisplatin resistance in human ovarian carcinoma cells. *BMC Cancer* 8, 175.
- KAMINSKI, M., KIESSLING, M., SUSS, D., KRAMMER, P. H. & GULOW, K. 2007. Novel role for mitochondria: protein kinase C θ -dependent oxidative signaling organelles in activation-induced T-cell death. *Mol Cell Biol*, 27, 3625-39.
- KAMPAN, N. C., MADONDO, M. T., MCNALLY, O. M., QUINN, M. & PLEBANSKI, M. 2015. Paclitaxel and Its Evolving Role in the Management of Ovarian Cancer. *Biomed Res Int*, 2015, 413076.
- KARIHTALA, P., SOINI, Y., VASKIVUO, L., BLOIGU, R. & PUISTOLA, U. 2009. DNA adduct 8-hydroxydeoxyguanosine, a novel putative marker of prognostic significance in ovarian carcinoma. *Int J Gynecol Cancer*, 19, 1047-51.
- KHAKOO, S. S. & BANERJEE, S. 2015. Neoadjuvant and Adjuvant Chemotherapy for Advanced Ovarian Cancer, Including Biological Agents. *Pelvic Cancer Surgery*, 441-453.
- KHAN, M. A., ALI, R., PARVEEN, R., NAJMI, A. K. & AHMAD, S. 2016. Pharmacological evidences for cytotoxic and antitumor properties of Boswellic acids from *Boswellia serrata*. *J Ethnopharmacol*, 191, 315-23.
- KHAN, M. A., SINGH, M., KHAN, M. S., NAJMI, A. K. & AHMAD, S. 2014. Caspase mediated synergistic effect of *Boswellia serrata* extract in combination with doxorubicin against human hepatocellular carcinoma. *Biomed Res Int*, 2014, 294143.
- KIELA, P. R., MIDURA, A. J., KUSCUOGLU, N., JOLAD, S. D., SOLYOM, A. M., BESSELSSEN, D. G., TIMMERMANN, B. N. & GHISHAN, F. K. 2005. Effects of *Boswellia serrata* in mouse models of chemically induced colitis. *Am J Physiol Gastrointest Liver Physiol*, 288, G798-808.
- KIMMATKAR, N., THAWANI, V., HINGORANI, L., KHIYANI, R. 2003. Efficacy and tolerability of *Boswellia serrata* extract in treatment of osteoarthritis of knee--a randomized double blind placebo controlled trial. *Phytomedicine*.

- KING, M. C., MARKS, J. H. & MANDELL, J. B. 2003. Breast and ovarian cancer risks due to inherited mutations in BRCA1 and BRCA2. . *Science*, 302, 643-6.
- KINNER, A., WU, W., STAUDT, C. & ILIAKIS, G. 2008. Gamma-H2AX in recognition and signaling of DNA double-strand breaks in the context of chromatin. *Nucleic Acids Res*, 36, 5678-94.
- KIRSTE, S., TREIER, M., WEHRLE, S. J., BECKER, G., ABDEL-TAWAB, M., GERBETH, K., HUG, M. J., LUBRICH, B., GROSU, A. L. & MOMM, F. 2011. Boswellia serrata acts on cerebral edema in patients irradiated for brain tumors: a prospective, randomized, placebo-controlled, double-blind pilot trial. *Cancer*, 117, 3788-95.
- KOSHIYAMA, M., MATSUMURA, N. & KONISHI, I. 2017. Subtypes of Ovarian Cancer and Ovarian Cancer Screening. *Diagnostics (Basel)*, 7.
- KOTSOPOULOS, J., SHEN, H., RAO, A. V., POLL, A., AINSWORTH, P., FLESHNER, N. & NAROD, S. A. 2008. A BRCA1 mutation is not associated with increased indicators of oxidative stress. *Clin Breast Cancer*, 8, 506-510.
- KRUGER, P., DANESHFAR, R., ECKERT, G. P., KLEIN, J., VOLMER, D. A., BAHR, U., MULLER, W. E., KARAS, M., SCHUBERT-ZSILAVECZ, M. & ABDEL-TAWAB, M. 2008. Metabolism of boswellic acids in vitro and in vivo. *Drug Metab Dispos*, 36, 1135-42.
- KUMARAVEL, T. & JHA, A. N. 2006. Reliable Comet assay measurements for detecting DNA damage induced by ionising radiation and chemicals *Mutation Research/Genetic Toxicology and Environmental Mutagenesis*, 605, 7-16.
- KUNNUMAKKARA, A. B., NAIR, A. S., SUNG, B., PANDEY, M. K. & AGGARWAL, B. B. 2009. Boswellic acid blocks signal transducers and activators of transcription 3 signaling, proliferation, and survival of multiple myeloma via the protein tyrosine phosphatase SHP-1. *Mol Cancer Res*, 7, 118-28.
- KURMAN, R. J. & SHIH IE, M. 2010. The origin and pathogenesis of epithelial ovarian cancer: a proposed unifying theory. *Am J Surg Pathol*, 34, 433-43.
- LA, O. R., TAI, L., LEE, L., KRUSE, E. A., GRABOW, S., FAIRLIE, W. D., HAYNES, N. M., TARLINTON, D. M., ZHANG, J. G., BELZ, G. T., SMYTH, M. J., BOUILLET, P., ROBB, L. & STRASSER, A. 2009. Membrane-bound Fas ligand only is essential for Fas-induced apoptosis. *Nature*, 461, 659-63.

- LAKHANI, S. A., MASUD, A., KUIDA, K., PORTER, G. A., BOOTH, C. J., MEHAL, W. Z., INAYAT, I. & FLAVELL, R. A. 2006. Caspases 3 and 7: Key Mediators of Mitochondrial Events of Apoptosis. *Science*, 311, 847-851.
- LALITHAKUMARI, K., KRISHNARAJU, A. V., SENGUPTA, K., SUBBARAJU, G. V. & CHATTERJEE, A. 2006. Safety and Toxicological Evaluation of a Novel, Standardized 3-O-Acetyl-11-keto-beta-Boswellic Acid (AKBA)-Enriched *Boswellia serrata* Extract (5-Loxin(R)). *Toxicol Mech Methods*, 16, 199-226.
- LAMBROS, M. B., FIEGLER, H., JONES, A., GORMAN, P., ROYLANCE, R. R., CARTER, N. P. & TOMLINSON, I. P. 2005. Analysis of ovarian cancer cell lines using array-based comparative genomic hybridization. *J Pathol*, 205, 29-40.
- LANDEN, C. N., JR., BIRRER, M. J. & SOOD, A. K. 2008. Early events in the pathogenesis of epithelial ovarian cancer. *J Clin Oncol*, 26, 995-1005.
- LAU, M. T., SO, W. K. & LEUNG, P. C. 2013. Fibroblast growth factor 2 induces E-cadherin down-regulation via PI3K/Akt/mTOR and MAPK/ERK signaling in ovarian cancer cells. *PLoS One*, 8, e59083.
- LEDERMANN, J. A. 2010. Optimal treatment for relapsing ovarian cancer.
- LIU, G.-Y. & STORZ, P. 2010. Reactive oxygen species in cancer. *Free radical research*, 44, 479-496.
- LIU, J., NILSSON, A., OREDSSON, S., BADMAEV, V. & DUAN, R. 2002a. Keto- and acetyl-keto-boswellic acids inhibit proliferation and induce apoptosis in Hep G2 cells via a caspase-8 dependent pathway. *International Journal of Molecular Medicine*, 10, 501-505.
- LIU, J. J., HUANG, B. & HOOI, S. C. 2006. Acetyl-keto-beta-boswellic acid inhibits cellular proliferation through a p21-dependent pathway in colon cancer cells. *Br J Pharmacol*, 148, 1099-107.
- LIU, J. J., NILSSON, Å., OREDSSON, S., BADMAEV, V., ZHAO, W. Z. & DUAN, R. D. 2002b. Boswellic acids trigger apoptosis via a pathway dependent on caspase-8 activation but independent on Fas/Fas ligand interaction in colon cancer HT-29 cells. *Carcinogenesis*, 23, 2087-2093.
- LIU, Y. Q., HU, X. Y., LU, T., CHENG, Y. N., YOUNG, C. Y., YUAN, H. Q. & LOU, H. X. 2012. Retigeric acid B exhibits antitumor activity through suppression of nuclear factor-kappaB signaling in prostate cancer cells in vitro and in vivo. *PLoS One*, 7, e38000.

- LOS, M., MOZOLUK, M., FERRARI, D., STEPCZYNSKA, A., STROH, C., RENZ, A., HERCEG, Z., WANG, Z. Q. & SCHULZE-OSTHOFF, K. 2002. Activation and caspase-mediated inhibition of PARP: a molecular switch between fibroblast necrosis and apoptosis in death receptor signaling. *Mol Biol Cell*, 13, 978-88.
- LOUIE, K. G., BEHRENS, B. C., KINSELLA, T. J., HAMILTON, T. C., GROTZINGER, K. R., MCKOY, W. M., WINKER, M. A. & OZOLS, R. F. 1985. Radiation survival parameters of antineoplastic drug-sensitive and -resistant human ovarian cancer cell lines and their modification by buthionine sulfoximine. *Cancer Res*, 45, 2110-5.
- LOW, L. S. & LIN, W. A. 2000. Apoptosis in cancer.pdf. *Carcinogenesis*, 21, 485-495.
- LU, M., XIA, L., HUA, H. & JING, Y. 2008. Acetyl-keto-beta-boswellic acid induces apoptosis through a death receptor 5-mediated pathway in prostate cancer cells. *Cancer Res*, 68, 1180-6.
- MABUCHI, S., ALTOMARE, D. A., CHEUNG, M., ZHANG, L., POULIKAKOS, P. I., HENSLEY, H. H., SCHILDER, R. J., OZOLS, R. F. & TESTA, J. R. 2007. RAD001 inhibits human ovarian cancer cell proliferation, enhances cisplatin-induced apoptosis, and prolongs survival in an ovarian cancer model. *Clin Cancer Res*, 13, 4261-70.
- MADISCH, A., MIEHLKE, S., EICHELE, O., MRWA, J., BETHKE, B., KUHLSCH, E., BASTLEIN, E., WILHELMS, G., MORGNER, A., WIGGINGHAUS, B. & STOLTE, M. 2007. Boswellia serrata extract for the treatment of collagenous colitis. A double-blind, randomized, placebo-controlled, multicenter trial. *Int J Colorectal Dis*, 22, 1445-51.
- MAH, L., EL-OSTA, A. & KARAGIANNIS, T. 2010. γ H2AX: a sensitive molecular marker of DNA damage and repair. *Leukemia*, 24, 679-686.
- MAHMOOD T. & P-C., Y. 2012. Western Blot: Technique, Theory, and Trouble Shooting. *North American Journal of Medical Sciences*, 4, 429-434.
- MALEK, M., AGHILI, R., EMAMI, Z. & KHAMSEH, M. E. 2013. Risk of cancer in diabetes: the effect of metformin. *ISRN Endocrinol*, 2013636927.
- MARKMAN, M. & BOOKMAN, M. A. 2000. Second-line treatment of ovarian cancer. *Oncologist*, 5, 26-35.
- MARKS, J. R. 2013. Refining the role of BRCA1 in combating oxidative stress. *Breast Cancer Res*, 15, 320.

- MARTINEZ-OUTSCHOORN, U. E., BALLIET, R., LIN, Z., WHITAKER-MENEZES, D., BIRBE, R. C., BOMBONATI, A., PAVLIDES, S., LAMB, R., SNEDDON, S., HOWELL, A., SOTGIA, F. & LISANTI, M. P. 2012a. BRCA1 mutations drive oxidative stress and glycolysis in the tumor microenvironment: implications for breast cancer prevention with antioxidant therapies. *Cell Cycle*, 11, 4402-4413.
- MARTINEZ-OUTSCHOORN, U. E., BALLIET, R. M., LIN, Z., WHITAKER-MENEZES, D., HOWELL, A., SOTGIA, F. & LISANTI, M. P. 2012b. Hereditary ovarian cancer and two-compartment tumor metabolism: epithelial loss of BRCA1 induces hydrogen peroxide production, driving oxidative stress and NFkappaB activation in the tumor stroma. *Cell Cycle*, 11, 4152-66.
- MARULLO, R., WERNER, E., DEGTYAREVA, N., MOORE, B., ALTAVILLA, G., RAMALINGAM, S. S. & DOETSCH, P. W. 2013. Cisplatin induces a mitochondrial-ROS response that contributes to cytotoxicity depending on mitochondrial redox status and bioenergetic functions. *PLoS One*, 8, e81162.
- MASS, W. 2017. TESARO Announces Availability of Zejula™ (Niraparib) for Patients With Recurrent. *GLOBE NEWSWIRE*.
- MASUDA, H., OZOLS, R. F., LAI, G. M., FOJO, A., ROTHENBERG, M. & HAMILTON, T. C. 1988. Increased DNA repair as a mechanism of acquired resistance to cis-diamminedichloroplatinum (II) in human ovarian cancer cell lines. *Cancer Res*, 48, 5713-6.
- MCILWAIN, D. R., BERGER, T. & MAK, T. W. 2013. Caspase Functions in Cell Death and Disease. *Cold Spring Harbor Perspectives in Biology*, 5.
- MENON, U., GRIFFIN, M. & GENTRY-MAHARAJ, A. 2014. Ovarian cancer screening--current status, future directions. *Gynecol Oncol*, 132, 490-5.
- MIKHAEIL, B. R., MAATOOQ, G. T., BADRIA, F. A. & AMER, M. M. 2003. Chemistry and immunomodulatory activity of frankincense oil. *Journal of Biosciences* 58, 230-238.
- MILLS, K. & FUH, K. 2017. Recent Advances in Understanding, Diagnosing, and Treating Ovarian Cancer. *F1000Res*, 6, 84.
- MIRZA, M. R., MONK, B. J., HERRSTEDT, J., OZA, A. M., MAHNER, S., REDONDO, A., FABBRO, M., LEDERMANN, J. A., LORUSSO, D., VERGOTE, I., BEN-BARUCH, N. E., MARTH, C., MADRY, R., CHRISTENSEN, R. D., BEREK, J. S., DORUM, A., TINKER, A. V., DU BOIS,

- A., GONZALEZ-MARTIN, A., FOLLANA, P., BENIGNO, B., ROSENBERG, P., GILBERT, L., RIMEL, B. J., BUSCEMA, J., BALSER, J. P., AGARWAL, S., MATULONIS, U. A. & INVESTIGATORS., E.-O. N. 2016. Niraparib Maintenance Therapy in Platinum-Sensitive, Recurrent Ovarian Cancer. *N Engl J Med*, 375, 2154-2164.
- MITRA, A. K., DAVIS, D. A., TOMAR, S., ROY, L., GURLER, H., XIE, J., LANTVIT, D. D., CARDENAS, H., FANG, F., LIU, Y., LOUGHRAN, E., YANG, J., SHARON STACK, M., EMERSON, R. E., COWDEN DAHL, K. D., M, V. B., NEPHEW, K. P., MATEI, D. & BURDETTE, J. E. 2015. In vivo tumor growth of high-grade serous ovarian cancer cell lines. *Gynecol Oncol*, 138, 372-7.
- MONK, B. J., MINION, L. E. & COLEMAN, R. L. 2016. Anti-angiogenic agents in ovarian cancer: past, present, and future. *Ann Oncol*, 27 Suppl 1, i33-i39.
- MOREY, J. S., RYAN, J. C. & VAN DOLAH, F. M. 2006. Microarray validation: factors influencing correlation between oligonucleotide microarrays and real-time PCR. *Biological Procedures Online*, 8175-8193.
- MOSS, E., P PEARMAIN., S ASKEW., K SINGH., KK CHAN., L HIRSCHOWITZ. & GANESAN., R. 2015. Should high-grade serous ovarian, tubal and primary peritoneal carcinoma be classed as a single disease? *International journal of gynecological cancer*.
- MOUSSAIEFF A. & MECHOULAM R. 2009. Boswellia resin: from religious ceremonies to medical uses; a review of in-vitro, in-vivo and clinical trials. *Journal of Pharmacy and Pharmacology* 61, 1281–1293
- MULLARD, A. 2016. Pioneering apoptosis-targeted cancer drug poised for FDA approval. *Nat Rev Drug Discov*, 15, 147-9.
- MUSCOLINI, M., CIANFROCCA, R., SAJEVA, A., MOZZETTI, S., FERRANDINA, G., COSTANZO, A. & TUOSTO, L. 2008. Trichostatin A up-regulates p73 and induces Bax-dependent apoptosis in cisplatin-resistant ovarian cancer cells. *Mol Cancer Ther*, 7, 1410-9.
- NAM, E. J. & KIM, Y. T. 2008. Alteration of cell-cycle regulation in epithelial ovarian cancer. *Int J Gynecol Cancer*, 18, 1169-82.
- NI, X., SUHAIL, M. M., YANG, Q., CAO, A., FUNG, K. M., POSTIER, R. G. & LIN, H. K. 2012. Frankincense essential oil prepared from hydrodistillation of *Boswellia sacra* gum resins induces human pancreatic cancer cell death in cultures

- and in a xenograft murine model. *BMC Complementary and Alternative Medicine*, 12, 1 – 14.
- NITISS, J. L. 2009. Targeting DNA topoisomerase II in cancer chemotherapy. *Nat Rev Cancer*, 9, 338-50.
- NOAMAN, E. & KANDIL, E. 2009. Boswellic Acid Fractions Induces Apoptosis And Cell Cycle Arrest In Hepatocellular Carcinoma Cell Line (HEP-G2) Through P53 Accumulation. *Egyptian Journal of Biochemistry and Molecular Biology*, 27, 101.
- NUR, E. K. A., LI, T. K., ZHANG, A., QI, H., HARS, E. S. & LIU, L. F. 2003. Single-stranded DNA induces ataxia telangiectasia mutant (ATM)/p53-dependent DNA damage and apoptotic signals. *J Biol Chem*, 278, 12475-12481.
- OECKINGHAUS, A., HAYDEN, M. S. & GHOSH, S. 2011. Crosstalk in NF-[kappa]B signaling pathways. *Nat Immunol*, 12, 695-708.
- OYADOMARI, S. & MORI, M. 2004. Roles of CHOP GADD153 in endoplasmic reticulum stress. *Cell Death and Differentiation. nature*, 11, 381–389.
- OZOLS, R. F., BUNDY, B. N., GREER, B. E., FOWLER, J. M., CLARKE-PEARSON, D., BURGER, R. A., MANNEL, R. S., DEGEEST, K., HARTENBACH, E. M. & BAERGEN, R. 2003. Phase III trial of carboplatin and paclitaxel compared with cisplatin and paclitaxel in patients with optimally resected stage III ovarian cancer: a Gynecologic Oncology Group study. *J Clin Oncol*, 21, 3194-200.
- PAN B., KANG-SHEN YAO., BRETT P. MONIA., NICHOLAS M. DEAN., ROBERT A. MCKAY., THOMAS C HAMILTON. & O'DWYER., P. J. 2002. Reversal of cisplatin resistance in human ovarian cancer cell lines by a c-jun antisense Oligodeoxynucleotide (ISIS 10582): evidence for the role of transcription factor overexpression in determining resistant phenotype. *Biochemical Pharmacology* 63 1699-1707.
- PANG, X., YI, Z., ZHANG, X., SUNG, B., QU, W., LIAN, X., AGGARWAL, B. B. & LIU, M. 2009. Acetyl-11-keto-beta-boswellic acid inhibits prostate tumor growth by suppressing vascular endothelial growth factor receptor 2-mediated angiogenesis. *Cancer Res*, 69, 5893-900.
- PARK, B., PRASAD, S., YADAV, V., SUNG, B. & AGGARWAL, B. B. 2011b. Boswellic acid suppresses growth and metastasis of human pancreatic tumors in an orthotopic nude mouse model through modulation of multiple targets. *PLoS One*, 6, e26943.

- PARK, B., SUNG, B., YADAV, V. R., CHO, S. G., LIU, M. & AGGARWAL, B. B. 2011a. Acetyl-11-keto-beta-boswellic acid suppresses invasion of pancreatic cancer cells through the downregulation of CXCR4 chemokine receptor expression. *Int J Cancer*, 129, 23-33.
- PARK, Y. S., LEE, J. H., BONDAR, J., HARWALKAR, J. A., SAFAYHI, H. & GOLUBIC, M. 2002a. Cytotoxic action of acetyl-11-keto-beta-boswellic acid (AKBA) on meningioma cells. *Planta Medica*, 68 397-401.
- PARK, Y. S., LEE, J. H., BONDAR, J., HARWALKAR, J. A., SAFAYHI, H., AND GOLUBIC, M. 2002b. Acetyl-11-keto-beta-boswellic acid (AKBA) is cytotoxic for meningioma cells and inhibits phosphorylation of the extracellular-signal regulated kinase 1 and 2. . *Advanced Experimental Medical Biology*, 507, 387-93.
- PAYET, D., GAUCHERON, F., SIP, M. & LENG, M. 1993. Instability of the monofunctional adducts in cis-[Pt(NH₃)₂(N7-N-methyl-2-diazapyrenium)Cl](2+)-modified DNA: rates of cross-linking reactions in cis-platinum-modified DNA. *Nucleic Acids Res*, 21, 5846-51.
- PETRILLO, M., NERO, C., AMADIO, G., GALLO, D., FAGOTTI, A. & SCAMBIA, G. 2016. Targeting the hallmarks of ovarian cancer: The big picture. *Gynecol Oncol*, 142, 176-83.
- PICCOLO, M. T. & CRISPI, S. 2012. The Dual Role Played by p21 May Influence the Apoptotic or Anti-Apoptotic Fate in Cancer. *Journal of Cancer Research Updates*, 1, 189-202.
- PLAXE, S. C., DELIGDISCH, L., DOTTINO, P. R. & COHEN, C. J. 1990. Ovarian intraepithelial neoplasia demonstrated in patients with stage I ovarian carcinoma. *Gynecol Oncol*, 38, 367-72.
- POECKEL, D., TAUSCH, L., GEORGE, S., JAUCH, J. & WERZ, O. 2006. 3-O-acetyl-11-keto-boswellic acid decreases basal intracellular Ca²⁺ levels and inhibits agonist-induced Ca²⁺ mobilization and mitogen-activated protein kinase activation in human monocytic cells. *J Pharmacol Exp Ther*, 316, 224-32.
- PRASAD, M., BERNARDINI, M., TSALENKO, A., MARRANO, P., PADEROVA, J., LEE, C. H., BEN-DOR, A., BARRETT, M. T. & SQUIRE, J. A. 2008. High definition cytogenetics and oligonucleotide aCGH analyses of cisplatin-resistant ovarian cancer cells. *Genes Chromosomes Cancer*, 47, 427-36.
- QIN, Y., JINGYAO XU., K. A., GABRIELA OPREA., AVINASH REDDY., ROLAND MATTHEWS., JOEL OKOLI., ALAN CANTOR., WILLIAM E GRIZZLE.,

- EDWARD E PARTRIDGE., E SHYAM P REDDY., CHARLES LANDEN. & N.RAO., V. 2012. BRCA1 proteins regulate growth of ovarian cancer cells by tethering Ubc9.pdf. *Am J Cancer Res* 2, 540-548.
- QURISHI, Y., HAMID, A., SHARMA, P. R., WANI, Z. A., MONDHE, D. M., SINGH, S. K., ZARGAR, M. A., ANDOTRA, S. S., SHAH, B. A., TANEJA, S. C. & SAXENA A.K. 2013. NF- κ B down-regulation and PARP cleavage by novel 3- α -butyryloxy- β -boswellic acid results in cancer cell specific apoptosis and in vivo tumor regression. *Anticancer Agents Med. Chem*, 13 777–790.
- RAJA, A. F., ALI, F., KHAN, I. A., SHAWL, A. S. & ARORA, D. S. 2011. Acetyl-11-keto-beta-boswellic acid (AKBA); targeting oral cavity pathogens. *BMC Res Notes*, 4, 406.
- RAJABIAN, A., BOROUSHAKI, M. T., HAYATDAVOUDI, P. & SADEGHNIA, H. R. 2016. Boswellia serrata Protects Against Glutamate-Induced Oxidative Stress and Apoptosis in PC12 and N2a Cells. *DNA and Cell Biology*.
- RAMPERSAD, S. N. 2012. Multiple Applications of Alamar Blue as an Indicator of Metabolic Function and Cellular Health in Cell Viability Bioassays. *Sensors* 12, 12347-12360.
- REYES-ZURITA, F. J., RUFINO-PALOMARES, E. E., GARCIA-SALGUERO, L., PERAGON, J., MEDINA, P. P., PARRA, A., CASCANTE, M. & LUPIANEZ, J. A. 2016. Maslinic Acid, a Natural Triterpene, Induces a Death Receptor-Mediated Apoptotic Mechanism in Caco-2 p53-Deficient Colon Adenocarcinoma Cells. *PLoS One*, 11, e0146178.
- RICCI, F., BROGGINI, M. & DAMIA, G. 2013. Revisiting ovarian cancer preclinical models: implications for a better management of the disease. *Cancer Treat Rev*, 39, 561-568.
- RICHARDSON, N. & DORR, M. 2015. The story of frankincense. *Middle East Institute*.
- RIEDL, S. J. & SHI, Y. 2004. Molecular mechanisms of caspase regulation during apoptosis. *Nat Rev Mol Cell Biol*, 5, 897-907.
- RIEGER, A. M., NELSON, K. L., KONOWALCHUK, J. D. & BARREDA, D. R. 2011. Modified annexin V/propidium iodide apoptosis assay for accurate assessment of cell death. *J Vis Exp*.
- ROTHKAMM, K., BARNARD, S., MOQUET, J., ELLENDER, M., RANA, Z. & BURDAK-ROTHKAMM, S. 2015. DNA damage foci: Meaning and significance. *Environmental and Molecular Mutagenesis*, 56, 491-504.

- ROY, N. K., DEKA, A., BORDOLOI, D., MISHRA, S., KUMAR, A. P., SETHI, G. & KUNNUMAKKARA, A. B. 2016. The potential role of boswellic acids in cancer prevention and treatment. *Cancer Lett*, 377, 74-86.
- SAFAYHI, H., MACK, T., SABIJERAJ, J., ANAZODO, M. I., SUBRAMANIAN, L. R. & AMMON, H. P. 1992. Boswellic acids novel specific nonredox inhibitors of 5 lipoxygenase. *J Pharmacol Exp Ther*, 261, 1143-1146.
- SAFAYHI, H. & SAILER, E. R. 1997. Anti-inflammatory actions of pentacyclic triterpenes. *Planta Med*, 63, 487-93.
- SAFAYHI, H., SAILER, E. R. & AMMON, H. P. T. 1996. 5-Lipoxygenase inhibition by acetyl-11-keto- β -boswellic acid (AKBA) by a novel mechanism. *Phytomedicine*, 3, 71-72.
- SAILER, E. R., SUBRAMANIAN, L. R., RALL, B., HOERNLEIN, R. F., AMMON, H. P. & SAFAYHI, H. 1996. Acetyl-11-keto-beta-boswellic acid (AKBA): structure requirements for binding and 5-lipoxygenase inhibitory activity. *Br J Pharmacol*, 117, 615-8.
- SALIM E, MOORE M, AL-LAWATI J, AL-SAYYADJ, BAWAZIR A, BAZARBASHI S, BENER A, CORBEX M, EL-SAGHIR N, HABIB O, MAZIAK W, SEIF-ELDIN E & T., S. 2009. Cancer Epidemiology and control in Arab World-Past, Present and Future. *Asian Pacific Journal of Cancer Prevention*, 10, 3-16.
- SAMIMI G., KATANO K., HOLZER AK., SAFAEI R. & SB., H. 2004. Modulation of the cellular pharmacology of cisplatin and its analogs by the copper exporters ATP7A and ATP7B. *Mol Pharmacol*, 66, 25-32.
- SAPIEZYNSKI, J., TARATULA, O., RODRIGUEZ-RODRIGUEZ, L. & MINKO, T. 2016. Precision targeted therapy of ovarian cancer. *J Control Release*, 243, 250-268.
- SAYED, A. S. & EL SAYED, N. S. 2016. Co-administration of 3-Acetyl-11-Keto-Beta-Boswellic Acid Potentiates the Protective Effect of Celecoxib in Lipopolysaccharide-Induced Cognitive Impairment in Mice: Possible Implication of Anti-inflammatory and Antiglutamatergic Pathways. *J Mol Neurosci*, 59, 58-67.
- SCHILDER, R. J., HALL, L., MONKS, A., HANDEL, L. M., FORNACE, A. J., JR., OZOLS, R. F., FOJO, A. T. & HAMILTON, T. C. 1990. Metallothionein gene expression and resistance to cisplatin in human ovarian cancer. *Int J Cancer*, 45, 416-22.

- SCHILDKRAUT, J. M., BASTOS, E. & BERCHUCK, A. 1997. Relationship between lifetime ovulatory cycles and overexpression of mutant p53 in epithelial ovarian cancer. *J Natl Cancer Inst*, 89, 932-8.
- SELVAKUMARAN, M., PISARCIK, D. A., BAO, R., YEUNG, A. T. & HAMILTON, T. C. 2003b. Enhanced cisplatin cytotoxicity by disturbing the nucleotide excision repair pathway in ovarian cancer cell lines. *Cancer Res*, 63, 1311-6.
- SHANKAR, S. & SRIVASTAVA, R. K. 2007. Bax and Bak genes are essential for maximum apoptotic response by curcumin, a polyphenolic compound and cancer chemopreventive agent derived from turmeric. *Curcuma longa*. *Carcinogenesis*, 28, 1277-86.
- SHAO, R.-G., CAO, C.-X., NIEVES-NEIRA, W., DIMANCHE-BOITREL, M.-T., ERIC, S. & YVES, P. 2001. Activation of the Fas pathway independently of Fas ligand during apoptosis induced by camptothecin in p53 mutant human colon carcinoma cells. *Oncogene*, 20, 1852 - 1859.
- SHAO, Y., HO, C. T., CHIN, C. K., BADMAEV, V., MA, W. & HUANG, M. T. 1998. Inhibitory activity of boswellic acids from *Boswellia serrata* against human leukemia HL-60 cells in culture. *Planta Med*, 64, 328-331.
- SHARMA, R. 2010. Recommendations on herbs and herbal formula in cancer prevention. *Open Nutraceuticals Journal*, 3, 129-140.
- SHEN, Y., TAKAHASHI, M., BYUN, H. M., LINK, A., SHARMA, N., BALAGUER, F., LEUNG, H. C., BOLAND, C. R. & GOEL, A. 2012. Boswellic acid induces epigenetic alterations by modulating DNA methylation in colorectal cancer cells. *Cancer Biol Ther*, 13, 542-52.
- SIEMONEIT, U., KOEBERLE, A., ROSSI, A., DEHM, F., VERHOFF, M., RECKEL, S., MAIER, T. J., JAUCH, J., NORTHOFF, H., BERNHARD, F., DOETSCH, V., SAUTEBIN, L. & WERZ, O. 2011. Inhibition of microsomal prostaglandin E2 synthase-1 as a molecular basis for the anti-inflammatory actions of boswellic acids from frankincense. *Br J Pharmacol*, 162, 147-62.
- SINGH, G. B. & ATAL, C. K. 1986. Pharmacology of an extract of salai guggal ex-
Boswellia serrata, a new non-steroidal anti-inflammatory agent. *Agents Actions*, 18, 407-12.
- SINGH, N. P., MCCOY, M. T., TICE, R. R. & SCHNEIDER, E. L. 1988. A simple technique for quantitation of low levels of DNA damage in individual cells. *Experimental Cell Research*, 175, 184-191.

- SINGH, S. K., BHUSARI, S., SINGH, R., SAXENA, A., MONDHE, D. & QAZI, G. N. 2007. Effect of acetyl 11-keto beta-boswellic acid on metastatic growth factor responsible for angiogenesis. *Vascul Pharmacol*, 46, 333-7.
- SPORN MB. & N., S. 2000. Chemoprevention of cancer. *Carcinogenesis*, 21, 525–530.
- STEWART, J. J., WHITE, J. T., YAN, X., COLLINS, S., DRESCHER, C. W., URBAN, N. D., HOOD, L. & LIN, B. 2006. Proteins associated with Cisplatin resistance in ovarian cancer cells identified by quantitative proteomic technology and integrated with mRNA expression levels. *Mol Cell Proteomics*, 5, 433-43.
- STIFF, T., O'DRISCOLL, M., RIEF, N., IWABUCHI, K., LÖBRICH, M. & JEGGO, P. A. 2004. ATM and DNA-PK Function Redundantly to Phosphorylate H2AX after Exposure to Ionizing Radiation. *Cancer Research*, 64, 2390-2396.
- STORDAL, B., TIMMS, K., FARRELLY, A., GALLAGHER, D., BUSSCHOTS, S., RENAUD, M., THERY, J., WILLIAMS, D., POTTER, J., TRAN, T., KORPANTY, G., CREMONA, M., CAREY, M., LI, J., LI, Y., ASLAN, O., O'LEARY, J. J., MILLS, G. B. & HENNESSY, B. T. 2013. BRCA1/2 mutation analysis in 41 ovarian cell lines reveals only one functionally deleterious BRCA1 mutation. *Mol Oncol*, 7, 567-79.
- SUHAIL, M. M., WU, W., CAO, A., MONDALEK, F. G., FUNG, K. M., SHIH, P. T., FANG, Y. T., WOOLLEY, C., YOUNG, G. & LIN, H. K. 2011. Boswellia sacra essential oil induces tumor cell-specific apoptosis and suppresses tumor aggressiveness in cultured human breast cancer cells. *BMC Complement Altern Med*, 11, 129.
- SYROVETS, T., BUCHELE, B., GEDIG, E., SLUPSKY, J. R. & SIMMET, T. 2000. Acetyl-boswellic acids are novel catalytic inhibitors of human topoisomerases I and IIalpha. *Mol Pharmacol*, 58, 71-81.
- SYROVETS, T., GSCHWEND, J. E., BUCHELE, B., LAUMONNIER, Y., ZUGMAIER, W., GENZE, F. & SIMMET, T. 2005. Inhibition of IkappaB kinase activity by acetyl-boswellic acids promotes apoptosis in androgen-independent PC-3 prostate cancer cells in vitro and in vivo. *J Biol Chem*, 280, 6170-80.
- TAKADA, Y., ICHIKAWA, H., BADMAEV, V. & AGGARWAL, B. B. 2006. Acetyl-11-Keto- -Boswellic Acid Potentiates Apoptosis, Inhibits Invasion, and Abolishes Osteoclastogenesis by Suppressing NF- B and NF- B-Regulated Gene Expression. *The Journal of Immunology*, 176, 3127-3140.

- TAKAHASHI, M., SUNG, B., SHEN, Y., HUR, K., LINK, A., BOLAND, C. R., AGGARWAL, B. B. & GOEL, A. 2012. Boswellic acid exerts antitumor effects in colorectal cancer cells by modulating expression of the let-7 and miR-200 microRNA family. *Carcinogenesis*, 33, 2441-9.
- TEWARY, P., GUNATILAKA, A. A. & SAYERS, T. J. 2016. Using natural products to promote caspase-8-dependent cancer cell death. *Cancer Immunol Immunother*.
- TODEN, S., OKUGAWA, Y., BUHRMANN, C., NATTAMAI, D., ANGUIANO, E., BALDWIN, N., SHAKIBAEI, M., BOLAND, C. R. & GOEL, A. 2015. Novel Evidence for Curcumin and Boswellic Acid-Induced Chemoprevention through Regulation of miR-34a and miR-27a in Colorectal Cancer. *Cancer Prev Res (Phila)*, 8, 431-43.
- UPAGANLAWAR, A. & GHULE, B. 2009. Pharmacological Activities of *Boswellia serrata* Roxb. - Mini Review.pdf. *Ethnobotanical Leaflets*, 13, 766-774.
- VAKIFAHMETOGLU, H., OLSSON, M., ORRENIUS, S. & ZHIVOTOVSKY, B. 2006. Functional connection between p53 and caspase-2 is essential for apoptosis induced by DNA damage. *Oncogene*, 25, 5683-5692.
- VASEY, P. A. 2003. Resistance to chemotherapy in advanced ovarian cancer: mechanisms and current strategies. *Br J Cancer*, 89 Suppl 3, S23-8.
- VASKIVUO, L., RYSA, J., KOIVUPERA, J., MYLLYNEN, P., VASKIVUO, T., CHVALOVA, K., SERPI, R., SAVOLAINEN, E. R., PUISTOLA, U. & VAHAKANGAS, K. 2006. Azidothymidine and cisplatin increase p14ARF expression in OVCAR-3 ovarian cancer cell line. *Toxicol Appl Pharmacol*, 216, 89-97.
- WAJANT, H. 2002. The Fas Signaling Pathway: More Than a Paradigm. *SCIENCE* 296, 31.
- WANG, J. & YI, J. 2014. Cancer cell killing via ROS: To increase or decrease, that is the question. *Cancer Biology & Therapy*, 7, 1875-1884.
- WANG, Q., ZHENG, X. L., YANG, L., SHI, F., GAO, L. B., ZHONG, Y. J., SUN, H., HE, F., LIN, Y. & WANG, X. 2010. Reactive oxygen species-mediated apoptosis contributes to chemosensitization effect of saikosaponins on cisplatin-induced cytotoxicity in cancer cells. *J Exp Clin Cancer Res*, 29159.
- WANG, Y., TANG, X., YU, B., GU, Y., YUAN, Y., YAO, D., DING, F. & GU, X. 2012. Gene network revealed involvements of Birc2, Birc3 and Tnfrsf1a in anti-apoptosis of injured peripheral nerves. *PLoS One*, 7, e43436.

- WEBERPALS, J., BRIEN, A. M. O., NIKNEJAD, N., GARBUIO, K. D., CLARK-KNOWLES, K. V. & DIMITROULAKOS, J. 2011a. The effect of the histone deacetylase inhibitor M344 on BRCA1 expression in breast and ovarian cancer cells. *Cancer Cell International*, 11:29.
- WONG, R. S. 2011. Apoptosis in cancer from pathogenesis to treatment. *Wong Journal of Experimental & Clinical Cancer Research* 30, 1-14.
- WOOD, J. P., SMITH, A. J., BOWMAN, K. J., THOMAS, A. L. & JONES, G. D. 2015. Comet assay measures of DNA damage as biomarkers of irinotecan response in colorectal cancer in vitro and in vivo. *Cancer Med*, 4, 1309-21.
- XIA, C., MENG, Q., LIU, L. Z., ROJANASAKUL, Y., WANG, X. R. & JIANG, B. H. 2007. Reactive oxygen species regulate angiogenesis and tumor growth through vascular endothelial growth factor. *Cancer Res*, 67, 10823-30.
- XIA, D., LOU, W., FUNG, K. M., WOLLEY, C. L., SUHAIL, M. M. & LIN, H. K. 2016. Cancer Chemopreventive Effects of Boswellia sacra Gum Resin Hydrodistillates on Invasive Urothelial Cell Carcinoma: Report of a Case. *Integr Cancer Ther*.
- XIA, L., CHEN, D., HAN, R., FANG, Q., WAXMAN, S. & JING, Y. 2005. Boswellic acid acetate induces apoptosis through caspase-mediated pathways in myeloid leukemia cells. *Mol Cancer Ther*, 4, 381-388.
- XUE, X., CHEN, F., LIU, A., SUN, D., WU, J., KONG, F., LUAN, Y., QU, X. & WANG, R. 2016. Reversal of the multidrug resistance of human ileocecal adenocarcinoma cells by acetyl-11-keto-beta-boswellic acid via downregulation of P-glycoprotein signals. *Biosci Trends*.
- YADAV, V. R., PRASAD, S., SUNG, B., GELOVANI, J. G., GUHA, S., KRISHNAN, S. & AGGARWAL, B. B. 2011. Boswellic acid inhibits growth and metastasis of human colorectal cancer in orthotopic mouse model by downregulating inflammatory, proliferative, invasive and angiogenic biomarkers. *Int J Cancer*, 130, 2176-84.
- YADAV, V. R., PRASAD, S., SUNG, B., GELOVANI, J. G., GUHA, S., KRISHNAN, S. & AGGARWAL, B. B. 2012. Boswellic acid inhibits growth and metastasis of human colorectal cancer in orthotopic mouse model by downregulating inflammatory, proliferative, invasive and angiogenic biomarkers. *Int J Cancer*, 130, 2176-84.
- YAN, N., CHAI, J., LEE, E. S., GU, L., LIU, Q., HE, J., WU, J.-W., KOKEL, D., LI, H., HAO, Q., XUE, D. & SHI, Y. 2005. Structure of the CED-4-CED-9 complex

- provides insights into programmed cell death in *Caenorhabditis elegans*. *Nature*, 437, 831-837.
- YANG, D. H., SMITH, E. R., COHEN, C., WU, H., PATRIOTIS, C., GODWIN, A. K., HAMILTON, T. C. & XU, X. X. 2002. Molecular events associated with dysplastic morphologic transformation and initiation of ovarian tumorigenicity. *Cancer Biol Ther*, 94, 2380-92.
- YASMEEN, A., BEAUCHAMP, M. C., PIURA, E., SEGAL, E., POLLAK, M. & GOTLIEB, W. H. 2011. Induction of apoptosis by metformin in epithelial ovarian cancer: involvement of the Bcl-2 family proteins. *Gynecol Oncol*, 121, 492-8.
- YI, Y. W., KANG, H. J. & BAE, I. 2014. BRCA1 and Oxidative Stress. *Cancers (Basel)*, 6, 771-795.
- YOULE, R. J. & STRASSER, A. 2008. The BCL-2 protein family: opposing activities that mediate cell death. *Nat Rev Mol Cell Biol*, 9, 47-59.
- YUAN, J. S., REED, A., CHEN, F. & STEWART, C. N., JR. 2006. Statistical analysis of real-time PCR data. *BMC Bioinformatics*, 7, 85.
- ZHAN, Q. 2005. Gadd45a, a p53- and BRCA1-regulated stress protein, in cellular response to DNA damage. *Mutat Res*, 569, 133-43.
- ZHANG, Y. S., XIE, J. Z., ZHONG, J. L., LI, Y. Y., WANG, R. Q., QIN, Y. Z., LOU, H. X., GAO, Z. H. & QU, X. J. 2013. Acetyl-11-keto-beta-boswellic acid (AKBA) inhibits human gastric carcinoma growth through modulation of the Wnt/beta-catenin signaling pathway. *Biochim Biophys Acta*, 1830, 3604-15.
- ZHAO, W., ENTSCHLADEN, F., LIU, H., NIGGEMANN, B., FANG, Q., ZAENKER, K. S. & HAN, R. 2003. Boswellic acid acetate induces differentiation and apoptosis in highly metastatic melanoma and fibrosarcoma cells. *Cancer Detection and Prevention*, 27, 67-75.
- ZHU, K., FUKASAWA, I., FUJINOKI, M., FURUNO, M., INABA, F., YAMAZAKI, T., KAMEMORI, T., KOUSAKA, N., OTA, Y., HAYASHI, M., MAEHAMA, T. & INABA, N. 2005. Profiling of proteins associated with cisplatin resistance in ovarian cancer cells. *Int J Gynecol Cancer*, 15, 747-54.